Skolkovo Institute of Science and Technology

UBR-UBIQUITIN LIGASES OF THE ARG/N-DEGRON PATHWAY AS NEW TARGETS FOR THERAPY: IMPLICATIONS IN CANCER AND INFLAMMATION

Doctoral Thesis

by

DOMINIQUE LEBOEUF

DOCTORAL PROGRAM IN LIFE SCIENCES

Supervisors:
Adjunct Professor Konstantin Piatkov
Associate Professor Timofei Zatsepin

Moscow – 2020

I hereby declare that the work presented in this thesis was carried out by myself at Skolkovo Institute of Science and Technology, Moscow, except where due acknowledgement is made, and has not been submitted for any other degree.

Candidate (Dominique Leboeuf)
Supervisors (Adjunct Prof. Konstantin Piatkov
and Associate Prof. Timofei Zatsepin)

Skolkovo Institute of Science and Technology

THESIS DEFENSE COMMITTEE:

Chair: Professor Yuri Kotelevtsev, PhD, Skoltech, Russia

Professor Emmanuelle Graciet, PhD, Maynooth University, Ireland
Friedrich Felix Hoyer, PhD, University Hospital of Cologne, Germany
Professor Petr Sergiev, PhD, Skoltech, Russia
Professor Konstantin Lukyanov, PhD, Skoltech, Russia

Moscow – 2020

À Joseph,
En profond remerciement

« Que tes œuvres sont grandes,
Seigneur!
Combien sont profondes
tes pensées! »

Ps 91, 6

Abstract

Despite significant advances in development of new therapies, cancer is still the second leading cause of death and the incidence of some cancers such as hepatocellular carcinoma remains on the rise. The current focus of anticancer drug development involves targeted therapies, where specific molecular pathways are identified and used to inhibit cancer proliferation or increase cancer cell death. The Agr/N-degron pathway has been identified as a modulator of many hallmarks of cancer through degradation of proteins that influence various cellular mechanisms. Thus, the central aim of this project was the validation of the Arg/N-degron pathway as a new target for the development of cancer therapy. Using an RNA interference approach to downregulate UBR1, UBR2, UBR4 and UBR5 in mice, we investigated the role of these proteins in the normal liver and in the context of hepatocellular carcinoma. General physiological processes such as inflammation or toxicity to the liver were also investigated. Our results demonstrate that downregulation of the four Arg/N-degron-dependent ubiquitin ligases decreases cell migration and proliferation and increases spontaneous apoptosis in cancer cells. Chronic treatment with lipid nanoparticles (LNPs) loaded with siRNA in mice efficiently downregulates the expression of UBR-ubiquitin ligases in the liver without any significant toxic effects but engages the immune system and causes inflammation. As chronic inflammation is a main driver of liver cancer progression, we discovered that repeated administration of LNPs containing siRNA against the Arg/N-degron pathway in hepatocelllular carcinoma (HCC) favors cancer growth. However, when the dose of siRNA was lowered, and the LNPs were co-administered with a chemotherapeutic drug, downregulation of the Arg/N-degron pathway successfully reduced tumor load by decreasing proliferation and increasing apoptosis in a mouse model of HCC. As the N-degron pathway is involved in proliferation, migration, apoptosis and DNA damage repair, any drug or treatment that interferes with these pathways could be boosted by prior or concomitant downregulation of the N-degron pathway. Additionally, the inflammation observed with long-term downregulation of the Arg/N-degron pathway in the liver using high doses of LNP-siRNA led us to uncover the role of this pathway in the regulation of inflammation. We propose that the Arg/N-degron pathway participates in the control of inflammation through selective degradation of inflammatory mediators or proinflammatory fragments. In this function, the Arg/N-degron pathway becomes an "off switch" through which resolution of inflammation is possible. Finally, we identified potential partners for co-therapy along with downregulation of the Arg/N-degron pathway. These proteins could further increase the sensitivity to apoptosis, and/or participate in the control of inflammation. Thus, downregulation of the N-degron pathway has the potential to contribute in the development of combinatorial therapy for cancer and inflammatory diseases.

Publications

1. Leboeuf, D., T. Abakumova, T. Prikazchikova, L. Rhym, Anderson, DG., Zatsepin TS. and Piatkov KI. 2020. Downregulation of the Arg/N-degron Pathway Sensitizes Cancer Cells to Chemotherapy In Vivo. Mol Ther, 28: 1092-104.

2. Gubina, N.*, Leboeuf, D.*, Piatkov, K. and Pyatkov, M. 2020. Novel Apoptotic Mediators Identified by Conservation of Vertebrate Caspase Targets. Biomolecules, 10: 612. *Both authors contributed equally to this work.

3. Leboeuf, D., Pyatkov, M., Zatsepin, TS. and Piatkov, KI. 2020. The Arg/N-degron Pathway – a Potential Running Back in Fine-Tuning the Inflammatory Response? Biomolecules, 10, 6: 903.

Patent application

Leboeuf, D., T. Abakumova, T. Prikazchikova, L. Rhym, Anderson, DG., Zatsepin TS. and Piatkov KI. Композиции и способы для ингибирования протеолитическово пути аргинин/н-дегрона. Composition and methods for downregulation of the Arg/N-degron pathway. Russian patent application W20019459

Thank you

> *You can't connect the dots looking forward; you can only connect them looking backwards. So you have to trust that the dots will somehow connect in your future* –Steve Jobs

Never in a million years did I expect to one day defend a PhD thesis and yet, here I am. As I look back on the journey that brought me here, I am grateful for all the turns and unexpected adventures. Without them, I would not have met the fantastic people that mentored, guided, taught, encouraged and shaped me into the person I am now. God, I thank You for the joys, the tears, the laughter, the trials and tribulations, the journey, Your love, and I entrust my future to Your Providence.

I want to take this opportunity to thank everyone who played a role in my PhD journey. Words on a page at the beginning of this thesis will never be sufficient, but trust that they are accompanied with abundant gratitude.

First and foremost, thank you, Konstantin Piatkov and Timofei Zatsepin. Your mentorship, guidance, support and patience helped me immensely. Thank you for pushing me beyond what I thought I was capable of. Thank you for sharing with me your never-ending fountains of information ☺ Thank you for your generosity, your positivity, your drive and your willingness to share it all. It was a great privilege and pleasure to work under your supervision.

Tatiana Abakumova, thank you for your friendship, and for always making me feel welcome. Thank you for your many gestures of kindness, your help in all sorts of things, at any hour of the day. Thank you for your passion, your work ethic and your honesty.

Thank you to all of my colleagues from Skoltech and MIT, who helped me along the way: Arsen Mikaelyan, Tatiana Prikazchikova, Mikhail Nesterchuk, Elena Smekalova, Olga Sergeeva, Natalia Logvina, Crystal Chu, Benjamin Hawks, Marion Paolini, Piotr Kowalski, Joshua Doloff, Kaitlyn Sadtler and Luke Rhym.

A special thank you to Natalia Malkova, Dominik Knoll, John Blake, Anna Dubovic, Anna Fefilova, Evgeny Sviridov, Noemi Marco, Katy Newlin and Aliya Khayrullina for your friendship and support.

Pavel Averyanov, thank you for my first job at Skoltech, the opportunity that allowed for this whole adventure to begin!

I cannot speak about my journey in research without mentioning and thanking Martin Guimond. Thank you for reigniting my love of biology. I wasn't thinking about a career in research but the time spent in your lab made me understand that my place is here. Thank you for the opportunities you gave me, for your trust in me and for your mentorship.

Finally, last but by no means the least, thank you to my parents, Suzanne-Marie and Christian, for the stones you laid out upon which to build my foundation, for the choices you made that impacted mine, for your constant example in life and for your never ending love and support. Thank you to my brother, Jean-François, and to Rachel. Thank you to all my wonderful and beloved community sisters and brothers. Thank you for your prayers and your continual support.

My time in Russia and my PhD journey have been life changing. I am immensely grateful for the people I've met, for the encounters, the experiences, the moments and for all the "dots" that I've collected and connected during these years. Without a doubt, these are seeds for the future!

Table of Contents

List of Symbols and Abbreviations

AFP: Alpha fetoprotein
AMP: adenosine monophosphate
ANOVA: Analysis of variance
ASO: Antisense oligonucleotide
ATP: adenosine triphosphate
Arg: Arginine
CAR-T: Chimeric antigen receptor T cell
CDK: cyclin-dependent kinase
Ctrl: control
DNA: deoxyribonucleic acid
Dox: Doxorubicin
DUB: Deubiquitylating enzyme
HCC: Hepatocellular carcinoma
HECT: Homologous to the E6AP carboxyl terminus
JBS: Johanson-Blizzard syndrome
IFN: Interferon
IL: Interleukin
LNP: Lipid nanoparticle
NAFLD: Non-alcoholic fatty liver disease
Nt-Ac: N-terminal acetylation
PEG: Poly-ethylene glycol
qPCR: quantitative polymerase chain reaction
RING: Really interesting new gene
RISC: RNA-induced silencing complex
RNA: ribonucleic acid
siRNA: small interfering RNA
TNF: Tumor necrosis factor
Ub: ubiquitin
UPS: Ubiquitin proteasome system
URT: Ubiquitin reference technique

List of Figures

List of Tables

Chapter 1
Introduction

Cancer is the second leading cause of death globally (G. B. D. Causes of Death Collaborators, 2018), and finding new treatment strategies remains the focus of many research groups around the world. In the last decade, vaccines, CAR-T cells and checkpoint inhibitors have redefined cancer therapy, offering promising solutions for previously untreatable diseases. However, some cancers, such as hepatocellular carcinoma (HCC), remain refractory to current therapies (Cheng et al. 2020; Vogel and Saborowski 2020). Hepatocellular carcinoma is the fourth most common cancer worldwide, and incidence of the disease has more than tripled since 1980 (Yang et al. 2019; Global Burden of Disease Liver Cancer et al. 2017). Representing 75-85% of all malignant liver tumors, HCC is the third leading cause of cancer-related deaths in the world with nearly 782,000 diseased in 2018 alone (Rawla et al. 2018). This high fatality rate reflects the extreme aggressiveness of advanced stage HCC and its resistance to all conventional chemotherapies. Risk factors include chronic viral hepatitis C, hepatitis B (HBV infections), liver cirrhosis, non-alcoholic fatty liver disease (NAFLD), diabetes (El-Serag, Hampel, and Javadi 2006), risk factors associated with genetic defects and chronic exposure to environmental factors such as alcohol or aflatoxin B (Rawla et al. 2018; Altekruse, McGlynn, and Reichman 2009; Alter

2007). The high functional capacity of the liver and the absence of pathological symptoms complicate early diagnosis of HCC (Bialecki and Di Bisceglie 2005), resulting in a high occurrence of inoperable patients. The present standard-of-care for HCC includes multikinase inhibitors sorafenib and regorafenib, which inhibit cancer growth directly by causing tumor cell apoptosis, and indirectly by preventing angiogenesis in tumors. However, many patients respond poorly or develop resistance to sorafenib and only recently, multiple kinase-inhibitor lenvatinib and two different immune check-point inhibitors were approved as first-line treatment for unresectable HCC or for patients who progress after sorafenib. The FDA also approved the use of Vascular endothelial growth factor receptor (VEGFR) inhibitors ramucirumab and cabozantinib (Vogel and Saborowski 2020). Despite this, the median survival following diagnostic for inoperable patients is 6 to 8 months (Weledji et al. 2014), and the use of regorafenib increased the overall survival by only 3 months (Personeni et al. 2018), highlighting the need to develop novel medications based on newly identified vulnerable molecular pathways and targets.

According to the National Cancer Institute, targeted cancer therapies are the current focus of anticancer drug development. Otherwise known as 'molecularly targeted therapies' or 'precision medicine', targeted cancer therapies interfere with specific molecular pathways or molecules that are involved with cancer growth and cellular proliferation, and differ from chemotherapy in the following manner: (1) they act on molecular targets that are associated or amplified in cancer; (2) they are specific to a pathway, rather than generally causing cell death; (3) they target cancer cells versus all rapidly proliferating cells. In this work, we identified the Arg/N-degron pathway and its molecular recognition components as new targets for cancer therapy, and demonstrated that interfering with this pathway reduces cancer cell proliferation and increases apoptosis while sensitizing to chemotherapy (Leboeuf et al. 2020).

The N-degron pathway is part of the Ubiquitin Proteasome System (UPS), and regulates the half-life of proteins that contain specific degradation signals (degrons) by polyubiquitylating and targeting these substrates for degradation via the 26S proteasome (Bachmair and Varshavsky 1989; Mogk, Schmidt, and Bukau 2007; Sriram, Kim, and Kwon 2011; Tasaki and Kwon 2007). Through proteolysis, the N-degron pathway has been shown to influence several cancer hallmarks, including sustained cell proliferation, activated

migration and resisting cell death (Hanahan and Weinberg 2011; Varshavsky 2011, 2019). Many components of the Arg/N-degron pathway are highly expressed in proliferating cells and developing tissues, and are essential during embryogenesis (Kwon et al. 2001; Kwon et al. 2002; Kwon et al. 2003; Saunders et al. 2004; An et al. 2010; Tasaki et al. 2013; Kim, Lee, Tasaki, Hwang, et al. 2018). These same enzymes are often overexpressed in different types of cancers, suggesting the reliance of cancer cells on the Arg/N-degron pathway. Finally, work from several groups revealed a major anti-apoptotic function of the Arg/N-degron pathway through its ability to selectively degrade specific proapoptotic protein fragments (Piatkov, Brower, and Varshavsky 2012; Xu, Payoe, and Fahlman 2012). Apoptosis is critical for removing unneeded or diseased cells, therefore blocking apoptosis is vital to cancer cell survival. Conversely, promoting cell death is a key aspect of most cancer therapies. The anti-apoptotic activity of the Arg/N-degron pathway suggests that its up-regulation may suppress apoptosis and thus promote malignant phenotypes. Therefore, inhibition of the N-degron pathway has the potential to be a new effective cancer therapy, and could be extrapolated to many types of malignancies due to the ubiquitous expression of the Arg/N-degron pathway.

Strategy and Objectives

The central aim of this project was the validation of the Arg/N-degron pathway as a new therapeutic target for the treatment of cancer. Using an RNA interference approach in animal models, we investigated the role of the four E3 UBR-ubiquitin ligases of the pathway, UBR1, UBR2, UBR4 and UBR5 (Sriram and Kwon 2010; Tasaki et al. 2009), in the normal liver and in the context of hepatocellular carcinoma, in order to distinguish the effects of ablating the Arg/N-degron pathway on normal versus cancer cells. General physiological processes such as inflammation or toxicity to the liver were also investigated.

Inhibition or suppression of the Arg/N-degron pathway has been attempted in the past with small molecule inhibitors. However, toxicity issues and poor delivery to target organs prevented the usage of these inhibitors in vivo to study the role of the Arg/N-degron pathway in normal tissue as well as in the context of cancer. We chose the siRNA approach, coupled with lipid nanoparticle (LNP) technology for the many advantages this method

brings. First, we can simultaneously downregulate the four E3 ligases of the Arg/N-degron pathway without affecting other UBR-box containing E3 ligases in the cell, something which is not possible to do with small inhibitors targeting this very domain. Second, since the lipid nanoparticles deliver siRNA only in the liver, we can study the role of the target proteins in this organ specifically, and we can also examine the consequences of downregulation of the entire Arg/N-degron pathway in adult tissue, which has never been done before. Finally, we can look at the role of individual UBR-ubiquitin-ligase, or a combination of some, or all E3 ligases, on the development and maintenance of liver cancer. The siRNA-LNP tool developed in the context of this study gives us the flexibility to adapt and modify the dose, regime and target protein, according to the goal of the experiment or to adjust rapidly to previously obtained results.

Four main goals were addressed during this research project:

1. To study the consequences of long-term downregulation of UBR1, UBR2, UBR4 and UBR5 in the normal adult liver
2. To evaluate long-term partial ablation of the Arg/N-degron pathway in the development and maintenance of hepatocellular carcinoma using an oncogene driven model of HCC
3. To investigate the modulation of the Arg/N-degron pathway *in vivo*, with or without chemotherapy, as a new therapy for HCC, by downregulating the expression of UBR1, UBR2, UBR4 and UBR5 using siRNAs delivered directly to the liver via lipid nanoparticles
4. To propose additional target proteins that can be used as co-therapy in combination with downregulation of the Arg/N-degron pathway, to increase sensitivity to apoptosis inducing drugs

The next section of the thesis is dedicated to a thorough review of the literature concerning the N-degron pathway and its various roles in the cell, followed by siRNA-mediated downregulation of mRNA expression. Different means of delivery of the siRNA will also be covered.

Chapter 2
Literature Review

Targeted protein degradation; the N-degron pathway, part of the ubiquitin/proteasome system

The ubiquitin system of protein regulation

Decades of pioneering biochemical research performed by Nobel Prize winners Avram Hershko, Aaron Ciechanover, and Irwin A. Rose led to the discovery of one of the most important control mechanisms in the cell: the ubiquitin system (reviewed in (Hershko 1991; Hershko and Ciechanover 1998)). Originally thought to be only a mechanism of protein degradation, the ubiquitin system is now understood to be a cornerstone in signaling pathways. Through ubiquitylation, the attachment of a ubiquitin molecule to a target protein by a ubiquitin ligase, the ubiquitin system regulates pathways involved in cell cycle progression, proliferation, transcription regulation, endocytosis, misfolded protein degradation, to name only a few. Perturbations of any participant of the system leads to disease. For instance, ubiquitin-dependent protein degradation of cyclins, cyclin-dependent kinases (CDK) and CDK inhibitors strictly controls the progression of each step of the cell cycle and disregulation of many of these proteins can be found in cancer (Nakayama and Nakayama 2006). Proteolysis-independent functions of ubiquitylation include cytokine

signaling control through polyubiquitylation of TRAF6 and IKK activation, as well as DNA repair, by ubiquitylation of PCNA and FANCD2 proteins (Sun and Chen 2004). Prevention of monoubiquitylation of FNACD2 is partially responsible for Fanconi Anemia (Meetei et al. 2003). Thus, uncovering the participants in the ubiquitin system is vital for the understanding of disease and development of new treatments.

The transfer of a ubiquitin molecule to a target protein requires the sequential action of three enzymes (Figure 1). First, an E1 enzyme activates the C-terminal Gly residue of ubiquitin using ATP. This step involves binding of ubiquitin to the Cys residue of E1, releasing AMP. The second step is the transfer of the activated ubiquitin to the Cys residue of the active site of an E2 enzyme. Finally, in the third step, ubiquitin is catalytically linked by an E3 enzyme or an E2/E3 complex to the lysine of the substrate protein, or the lysine of a previously attached ubiquitin, by the Gly on the C-terminal end of ubiquitin (reviewed in (Ciechanover 1994)). In the human genome, there are two E1, 38 E2 and 600-1000 E3 proteins (Li et al. 2008; Ye and Rape 2009), which can be classified into three families, based on their protein domains: HECT (homologous to the E6AP carboxyl terminus), RING (really interesting new gene) and RBR (RING between RING) (Berndsen and Wolberger 2014; Metzger, Hristova, and Weissman 2012). The mechanism of transfer of the ubiquitin molecule onto the target protein is dependent on the type of E3, and this also affects the role of the E2 enzyme. For instance, if working with a HECT E3, the E2 enzyme will transfer the ubiquitin to the active site Cys of the E3, which will then transfer it to the target substrate. However for RING E3s, which function as co-factors for E2s, the E2 enzyme is responsible for determining which of the seven lysines of ubiquitin will serve for polyubiquitylation and catalytically transfers the ubiquitin molecule on the target protein (Stewart et al. 2016). Nonetheless, in all cases, the E3 enzyme is responsible for the specificity of the system by recognizing their own specific and unique substrates, and determining the identity of the lysine on the target protein (David et al. 2011; Mattiroli and Sixma 2014).

Ubiquitin may be attached to substrate proteins as a monomer or in the form of polymeric chains in which ubiquitin molecules are linked through specific isopeptide bonds to one of their seven internal lysines, K6, K11, K27, K29, K33, K48 and K63. The position of the linkage, as well as the length and the composition of the chain, will determine if the

substrate will be degraded through the proteasome or will be activated and serve in signaling pathways (Komander and Rape 2012). For instance, the canonical chain of more than four ubiquitin molecules linked through their Lys48 or the atypical Lys11 chain sends the target protein to degradation through the 26S proteasome (Chau et al. 1989; Baboshina and Haas 1996) whereas Lys63-linked ubiquitin targets the protein for lysosomal degradation (Mukhopadhyay and Riezman 2007). Ubiquitin monomers and poly-branched chains generally lead to nonproteolytic signaling (Komander and Rape 2012).

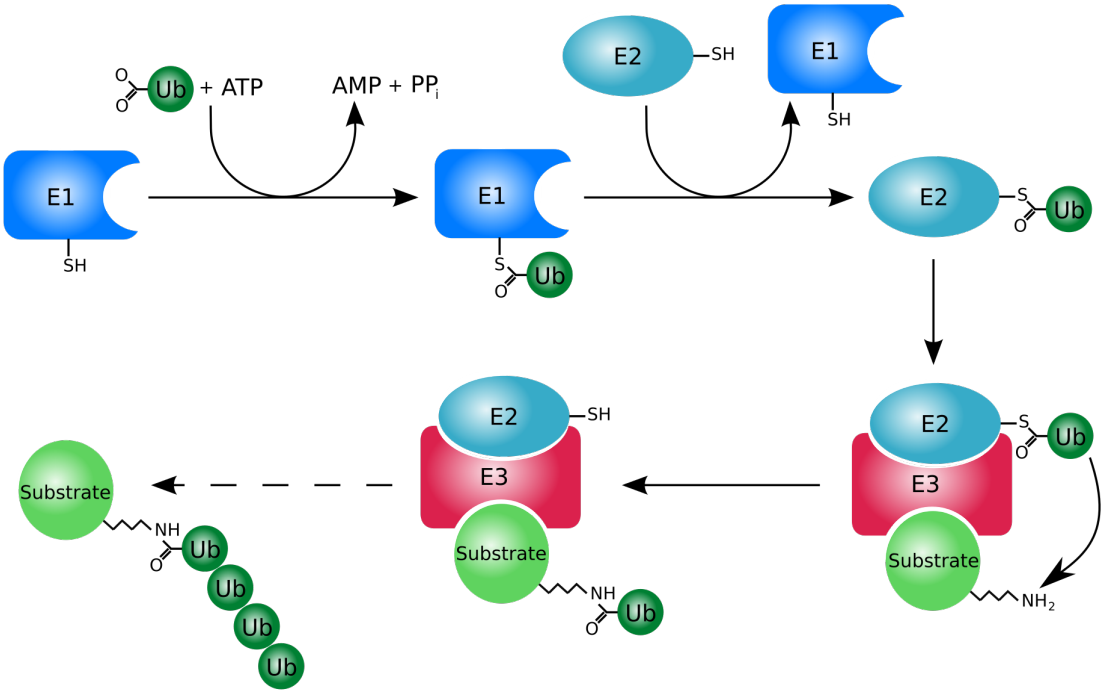

Figure 1: **The ubiquitin system.** Activation of ubiquitin requires an E1 enzyme, which transfers ubiquitin to an E2 enzyme, which then, with the help of an E3 enzyme, catalytically links the ubiquitin to the substrate protein. Ubiquitin molecules are linked by their C-terminal Gly residue, to Lys residues of substrates. Image created by Roger B. Dodd (https://en.wikipedia.org/wiki/File:Ubiquitylation.svg).

An important part of protein regulation through the ubiquitin system is the capability of removing the ubiquitin molecule if the signal is no longer needed. Enzymes responsible for this process are called deubiquitylating enzymes (DUBs) and function by cleaving the amide bond between the ubiquitin and its substrate or the isopeptide bond between ubiquitin molecules. Through their biochemical activities, DUBs participate in ubiquitin precursor processing, editing or rescue of ubiquitin conjugates, protein trafficking, and are

essential for developmental processes, for proper functioning of the cell cycle and various signaling events in the cell (Amerik and Hochstrasser 2004).

Post-translational modifications such as phosphorylation can signal proteins for ubiquitylation and degradation through the proteasome (Hunter 2007). Other signals, such as internal degrons or N- or C-terminal degrons that become exposed after proteolytic processing, are inherent to the structure of the protein. One of the most characterized of these signals is the N-degron, which confers metabolic instability to the protein, relating the half-life of the protein to the identity of its N-terminal amino acid. This pathway is described in detail in the next section.

N-degron Pathway

The N-degron pathway (previously known as the N-end rule pathway) was first discovered by A. Bachmair, D Finley and A. Varshavsky upon the observation that proteins bearing certain N-terminal amino acids were degraded more rapidly than others (Bachmair, Finley, and Varshavsky 1986). Studies performed in *S. cerevisiae* using a fusion construction between ubiquitin and the reporter protein β-galactosidase, Ub-X-βgal, where X is any amino acid, revealed that the various X-β-gal proteins produced after deubiquitylase processing had very different half-lives in vitro, ranging from 3 minutes to 20 hours depending on the identity of the N-terminal amino acid. The processing by the deubiquitylases takes place for all residues at the C-terminal side of the cleavage site, proline being the single exception, indicating that the nature of the new N-terminal amino acid was the determining factor for degradation of these X-βgal proteins. The first known destabilizing residues, or N-degrons were uncovered: Arg, Lys, Phe, Leu, Trp and Tyr (Bachmair, Finley, and Varshavsky 1986; Varshavsky 1996).

Studies over the next three decades identified distinct classes or branches of N-degrons where all 20 universal amino acids can act as destabilizing N-terminal residues of an N-degron (Figure 2) (Shemorry, Hwang, and Varshavsky 2013; Hwang, Shemorry, and Varshavsky 2010; Kim et al. 2014; Kim, Seok, et al. 2018; Chen et al. 2017; Davydov and Varshavsky 2000). The fundamental and required structure of the N-degron was also characterized: N-degrons comprise (1) a N-terminal destabilizing residue, which can be recognized by an E3 ubiquitin ligase, (2) an internal lysine that acts as the polyubiquitylation

site, and (3) an unstructured segment required by the proteasome to initiate proteolysis (Bachmair and Varshavsky 1989; Inobe et al. 2011; Varshavsky 2011). The N-degron pathway is ubiquitously expressed across all kingdoms of life, although there are variations in components, degrons, and hierarchical structures of these pathways in eukaryotes and prokaryotes examined to date (Varshavsky 2011; Graciet and Wellmer 2010; Bachmair, Finley, and Varshavsky 1986; Tobias et al. 1991). For the sake of simplicity and clarity, only the eukaryotic N-degron pathway will be addressed in this review.

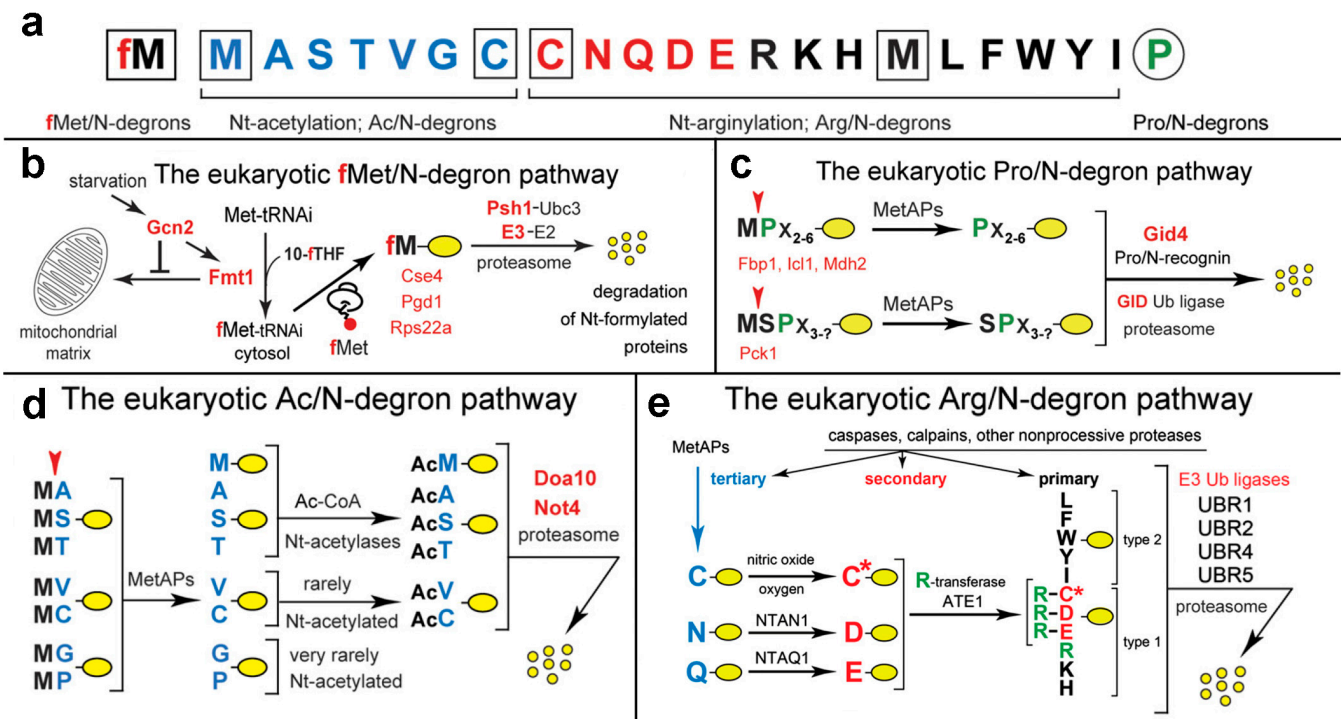

Figure 2. **The different branches of the eukaryote N-degron pathway.** Adapted from (Varshavsky 2011, 2019; Piatkov, Brower, and Varshavsky 2012). Nt-residues are indicated by single-letter abbreviations. A yellow oval denotes the rest of a protein substrate. (a) The 20 universal amino acids can act as destabilizing N-terminal residue of an N-degron. (b) The eukaryotic fMet/N-degron pathway (Kim, Seok, et al. 2018); 10-fTHF: 10-formyltetrahydrofolate; Fmt1: Formyltransferase 1. (c) The eukaryotic Pro/ N-degron pathway (Chen et al. 2017). (d) The eukaryotic Ac/N-degron pathway (Hwang, Shemorry, and Varshavsky 2010). (e) The eukaryotic Arg/N-degron pathway (Tasaki et al. 2012). Proteins marked in red are further described in the text.

The different branches of the N-degron pathway

In eukaryotes, the N-degron pathway consists of four branches: the **fMet/N-degron** pathway, the **Pro/N-degron** pathway, the **Ac/N-degron** pathway and the **Arg/N-degron** pathway, where the prefixes fMet, Pro, Ac and Arg highlight the specific features of the pathways, such as the step of N-terminal (Nt) arginylation found in the Arg/N-degron pathway.

- The **fMet/N-degron** pathway is specific to only one degron, the N-terminal formylated Methionine on nascent proteins. First discovered in bacteria, where all nascent proteins begin with fMet (formyltransferases formylate the Met moiety of all initiator Met-tRNAs) (Piatkov et al. 2015), the fMet/N-degron pathway is also present in eukaryotes, notably in *S. cerevisiae* (Kim, Seok, et al. 2018). This pathway is particularly involved in the response to certain cellular stress such as undernutrition or formation of misfolded proteins. In these conditions, the Gnc2 kinase increases the cytosolic location of Formyltransferase 1 (Fmt1), thereby augmenting the quantity of fMet-tRNA in the cytosol and the levels of N-terminaly formylated proteins in the cell. Substrates of this pathway include Cse4, Pgd1 and Rps22a, and are recognized by the E3/E2 complex Psh1/Ubc3.
- The **Pro/N-degron** pathway was discovered in the context of yeast gluconeogenesis, and refers to the specific degradation of gluconeogenesis cytosolic enzymes that contain a Nt-Pro residue or a Pro at position 2, in the presence of distinct (but non-unique) adjoining sequence motifs (Chen et al. 2017; Dong et al. 2018). Substrates of this pathway include the gluconeogenic enzymes Fbp1, Icl1, Mdh2 and Pck1 and are recognized by the N-recognin Gid4, a subunit of the GID ubiquitin ligase, targeting these proteins for degradation through the proteasome.
- The **Ac/N-degron** pathway refers to the targeted degradation of proteins which are N-terminally acetylated (Hwang, Shemorry, and Varshavsky 2010). Although more than 80% of human proteins and 60% of yeast proteins are irreversibly N-terminally acetylated (Ree, Varland, and Arnesen 2018) few Nt-acetylated proteins are actually short-lived. This discrepancy could be explained by steric shielding provided by the protein itself or rapid sequestration within cognate protein complexes, especially

since Nt-Ac is known to increase thermodynamic stability of the complex (Nguyen et al. 2018; Scott et al. 2011; Shemorry, Hwang, and Varshavsky 2013). Through degradation of Nt-Ac-protein fragments, the Ac/N-degron pathway is involved in the regulation of protein quality (Shemorry, Hwang, and Varshavsky 2013), in the regulation of blood pressure (Park et al. 2015), circadian rhythms (Wadas et al. 2016) and in the formation of lipid droplets (Nguyen et al. 2019). The N-recognins of the eukaryotic Ac/N-degron pathway are Doa10 and Not4.

- Recently, **glycine** was discovered using a Global Protein Stability system as a new type of primary N-degron, which does not require N-terminal acetylation to be recognized. Glycine-specific N-terminal recognition and degradation is mediated by two Cul2 Cullin-RING E3 ligase complexes defined by the substrate adaptors ZYG11B and ZER1 and serves as a quality control mechanism for protein N-myristoylation (Timms et al. 2019). Protein myristoylation is an essential co- and post-translational modification that occurs only on N-terminal glycine and tags proteins for membrane localization, protein-protein interactions and functions in a variety of signal transduction pathways (Thinon et al. 2014).
- The final branch of the N-degron pathway deals with targeting of unacetylated amino acid residues (Bachmair, Finley, and Varshavsky 1986; Kwon et al. 2002; Lee et al. 2005; Piatkov, Brower, and Varshavsky 2012; Brower, Piatkov, and Varshavsky 2013). The **Arg/N-degron** pathway is organized hierarchically into "primary" destabilizing N-terminal residues Arg, Lys, His, Leu, Phe, Tyr, Trp, and Ile, which are directly recognized by specific E3 ligases called N-recognins; "secondary" destabilizing N-terminal residues Asp, Glu and oxidized Cys, which require Nt arginylation for recognition; and "tertiary" destabilizing N-terminal residue Cys, and residues Asn and Gln, which require Nt-deamidation (Varshavsky 1996). Further, these unacetylated residues are divided into two groups: type 1 positively charged residues (Arg, Lys and His) and type 2 bulky hydrophobic residues (Leu, Ile, Trp, Tyr and Phe) (Gonda et al. 1989; Reiss, Kaim, and Hershko 1988). The Arg/N-degron pathway is the main focus of this thesis, and will therefore be elaborated upon in the following section.

Arg/N-degron pathway

The Arginine branch of the N-degron pathway is undoubtedly the most studied and characterized due to its vast array of functions (Figure 3). Since the discovery of nsP4 as the first physiological substrate of the Arg/N-degron pathway (Shirako and Strauss 1998) (the pathway was discovered on engineered substrates), new roles for the pathway are continuously emerging.

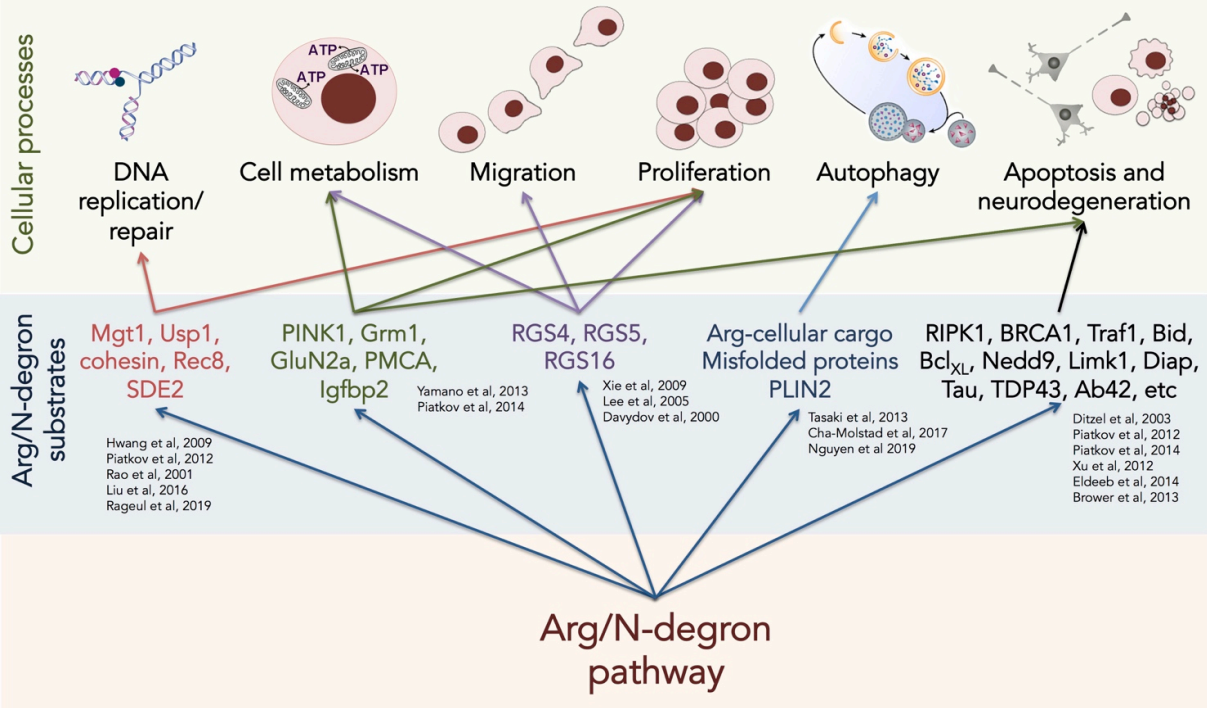

Figure 3: **Regulation of various cellular processes by the Arg/N-degron pathway through targeted degradation of proteins or protein fragments.** Selected substrates are listed here to illustrate the variety and breadth of general cellular processes affected by the Arg/N-degron pathway. Phenotypes observed after knockout of Arg/Ndegron pathway components are not included, because specific substrates causing these phenotypes are still unknown.

The Arg/N-degron is known to regulate various cellular processes such as proliferation (Brower and Varshavsky 2009; Lee et al. 2012); apoptosis (Piatkov, Brower, and Varshavsky 2012; Piatkov et al. 2014; Eldeeb and Fahlman 2014; Xu, Payoe, and Fahlman 2012; Ditzel et al. 2003); DNA replication (Rageul et al. 2019); DNA repair (Hwang, Shemorry, and Varshavsky 2009); chromosome cohesion/segregation (meiosis) (Rao et al. 2001); migration (Xie et al. 2009) and regulation of G proteins (Lee et al. 2005; Davydov and

Varshavsky 2000). Knockouts of various components of the pathway illustrated roles of the Arg/N-degron pathway in sensing of oxygen, nitric oxide (NO), heme, and short peptides (Hu et al. 2008a; Hu et al. 2005); repression of neurodegeneration (Brower, Piatkov, and Varshavsky 2013; Kechko et al. 2019); autophagy (Cha-Molstad et al. 2017; Kim, Lee, Tasaki, Mun, et al. 2018; Tasaki et al. 2013; Yoo et al. 2018); cardiovascular development, spermatogenesis and neurogenesis (Kwon et al. 2002; An et al. 2006; Brower and Varshavsky 2009; An et al. 2010) and the formation of fat and muscle tissue (Kwon et al. 2001).

N-terminal arginylation by Ate1

Secondary destabilizing N-degrons of the Arg/N-degron pathway require N-terminal (Nt) arginylation for recognition by N-recognins of this pathway, and this post-translational modification is provided by the arginyltransferase Ate1 (Soffer 1980; Kwon, Kashina, and Varshavsky 1999; Kwon et al. 2002). The *Ate1* gene is highly conserved throughout evolution and is present in all eukaryote cells; in lower eukaryotes, the gene encodes for a single protein while higher species express multiple isoforms differentially across various cell types (Kwon, Kashina, and Varshavsky 1999; Hu et al. 2006; Saha and Kashina 2011). Although a non-essential protein in yeast and nematodes, knock-out of Ate1 is lethal in all organisms from Drosophila to humans, indicating the high physiological importance of protein arginylation. Indeed, mice lacking Ate1 die at embryonic day 15, with defects in heart and cardiovascular development (Kwon et al. 2002) and post-natal deletion of Ate1 leads to loss of visceral fat, higher metabolism, neurological defects and diminished spermatogenesis (Brower and Varshavsky 2009). Nt-Arginylated proteins that are subsequently targeted for degradation via the Arg/N-degron pathway include the GTPase-activating proteins RGS4, RGS5 and RGS16 (Davydov and Varshavsky 2000), some proapoptotic fragments such as Cys-Ripk1, Cys-Traf1, Asp-Brca1, Asp-Bcl_{XL}, Asp-Epha4, Glu-Bak (Piatkov, Brower, and Varshavsky 2012; Piatkov et al. 2014), the genomic stability regulator Gln-Usp1 (Piatkov et al. 2012), neurodegenerative fragments Asp-TDP43, Gln-synuclein, Glu-Tau and Asp-Aβ (Brower, Piatkov, and Varshavsky 2013). Finally, N-terminal arginylation functions as a bimodal switch, directing targeted proteins either to proteasomal

degradation through ubiquitylation or to macroautophagy through binding to the ZZ domain of the autophagic adaptor p62/STQSM/Sequestosome-1, depending on the physiological state (Yoo et al. 2018).

E3 ubiquitin ligases of the Arg/N-degron pathway

In eukaryotes, the recognition components of the N-degron pathways, called N-recognins, are E3 ligases that recognize N-degron pathway substrates and target them for degradation through the 26S proteasome (Varshavsky 2011). Some publications in the literature refer to N-recognins as the E3 ubiquitin ligases and/or the E2-E3 complexes that mediate recognition of substrates and ubiquitylation. For simplicity, I will refer to N-recognins as E3 ligases only. The yeast Arg/N-degron pathway is mediated by the N-recognin UBR1 (Bartel, Wünning, and Varshavsky 1990), while the mammalian system has four: UBR1, UBR2, UBR4 and UBR5 (Figure 4) (Tasaki et al. 2005). These E3 ligases recognize Type 1 N-degrons through their UBR box (Choi et al. 2010) and Type 2 N-degrons through their N-domain (Matta-Camacho et al. 2010). The study by Tasaki et al (2005) revealed seven E3 ligases bearing the UBR box (Figure 4), although only four of them are capable of degrading Arg/N-degron pathway substrates. These proteins will be discussed in detail below.

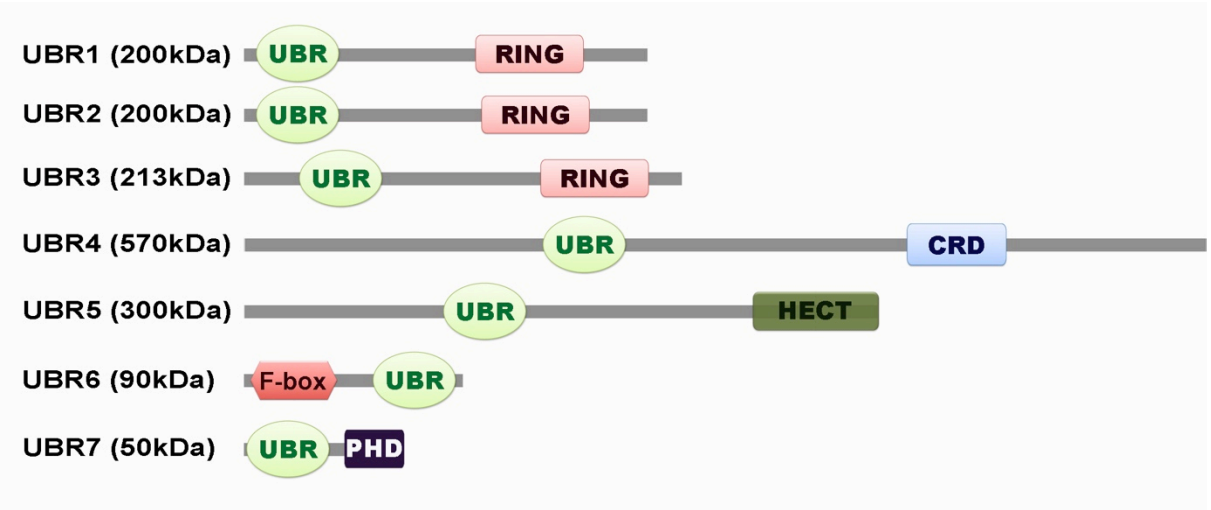

Figure 4. **E3 ligases containing the UBR box**. Only UBR1, UBR2, UBR4 and UBR5 are N-recognins of the Arg/N-degron pathway. Adapted from Tasaki et al, 2005.

UBR1

UBR1 was not only the first Arg/N-recognin to be characterized, but was the first E3 ubiquitin ligase to be discovered. When the N-degron pathway was identified in 1986, it was strongly suspected that one or more specialized E3 ubiquitin ligases could recognize specific N-terminal amino acids and target the proteins bearing these N-degrons for degradation. Further studies determined that this ubiquitin ligase contains two different types of binding sites that correspond to the two different types of N-degrons: type 1 (positively charged) and type 2 (bulky hydrophobic) (Reiss, Kaim, and Hershko 1988; Gonda et al. 1989). Mutations in these sites have shown that both sites can be inactivated without perturbing the other, and both sites are situated within the 50kDa N-terminal region of the protein (Xia et al. 2008). One year later, Bartel, Wünning and Varshavsky (1990) identified the sequence of the only N-recognin in yeast, corresponding to a 225 kDa protein, and responsible for the degradation of all Arg/N-degrons. This protein was named UBR1 (Bartel, Wünning, and Varshavsky 1990). UBR1 was later shown to physically bind the E2 Ubc2/Rad6 and that this interaction is necessary for the degradation of Arg/N-degron substrates, as RING domain E3 ligases generally function through catalyzing the direct transfer of ubiquitin from the E2 to the substrate (Dohmen et al. 1991; Xie and Varshavsky 1999; Deshaies and Joazeiro 2009).

The mammalian UBR1 (200 kDa) was identified in rabbit reticulocytes and furthermore characterized in the mouse and human, where it was shown to contain a RING domain and a Cys-His region, later to be revealed as the UBR box (Reiss and Hershko 1990; Kwon et al. 1998; Tasaki et al. 2005). These two regions are the only sequences to be highly conserved between species, and are now known to be the drivers of Arg/N-degron substrate recognition and ubiquitylation (Kwon et al. 1998; Xie and Varshavsky 1999). UBR1$^{-/-}$ mice revealed roles of this protein in the formation of skeletal muscle and adipose tissue (Kwon et al. 2001). Another interesting observation from this knock-out mouse is that the contribution of UBR1 to the degradation of N-degron substrates is not equal in all tissue, some tissues having completely lost the activity of the N-degron pathway while it persisted in others, revealing the presence of other UBR-ubiquitin ligases involved in the Arg/N-degron pathway. Finally, mutations in the UBR1 gene in humans are associated to the Johanson-Blizzard Syndrome (JBS). Symptoms of JBS include an exocrine pancreatic

insufficiency and inflammation, multiple malformations as well as mental retardation and deafness (Zenker et al. 2005; Zenker et al. 2006; Kruger et al. 2009; Hwang et al. 2011). UBR1$^{-/-}$ mice exhibit JBS symptoms in a milder form, illustrating differences between mice and human UBR1 not only in sequence but also in function.

UBR2

Mammalian UBR2 is a functional homolog of UBR1, sharing 47% identity and 68% similarity of the UBR1 sequence. It also possesses a UBR box and a RING domain, and was shown to bind to type 1 and type 2 Arg/N-degron substrates (Kwon et al. 2003). Female UBR2$^{-/-}$ mice are non viable in most strains, while males are viable only on the mixed C57Bl6/129 background, but they are not fertile due to postnatal degeneration of testes. This indicates roles for UBR2 in female embryogenesis and male meiosis and spermatogenesis (Kwon et al. 2003). UBR2 was also shown to be important in chromosome stability through histone ubiquitylation (An et al. 2012), and more recently, was discovered to be vital in the immune response against anthrax lethal factor (Chui et al. 2019; Xu et al. 2019).

UBR4

UBR4 (p600, Big) is the largest Arg/N-recognin (570 kDa), and one of the most characterized due to its important and multiple functions, including roles in autophagy. The sequence homology between UBR1 and UBR4 is restricted to the UBR domain, as the cysteine rich domain (CRD) of UBR4 differs substantially from the RING domain of UBR1. UBR4 also does not contain a known ubiquitylation domain, suggesting a different mechanism in N-degron degradation compared to other N-recognins (Tasaki et al. 2005). UBR4$^{-/-}$ mice die during embryogenesis due to impaired development of yolk sac endoderm and vasculature. Loss of UBR4 leads to multiple disregulations in the autophagy pathway, particularly in the formation of autophagosomes destined to professionally enlarged lysosomes. This implies that regeneration of the amino acid pool, which normally occurs in part through autophagy, is impaired in the absence of UBR4 (Tasaki et al. 2013). Further analysis of UBR4$^{-/-}$ mice revealed roles for this enzyme in early endosome formation, formation of multivesicular bodies, homeostasis of cell surface proteins and thus, cell

adhesion, integrity and migration (Kim, Lee, Tasaki, Hwang, et al. 2018; Kim, Lee, Tasaki, Mun, et al. 2018). The relation between these functions of the UBR4 protein and its ability to recognize Arg/N-degron pathway substrates remains to be understood.

UBR5

The mammalian UBR5 (EDD) Arg/N-recognin belongs to the family of HECT domain E3 ligases, and it is through this particular region that the interaction with the E2 enzyme takes place. The HECT domain, situated at the C-terminal end of UBR5, consists of a N-terminal N-lobe, which interacts with the E2 enzyme, and a C-terminal C-lobe that contains the active site that forms the thioester bond with the ubiquitin (Huang et al. 1999). This important enzyme also contains a UBR domain at the N-terminal end, which allows for recognition of Arg/N-degron pathway substrates, as well as a RING-like zinc finger domain, a UBA domain and a poly(A)-binding protein (PABP)-like domain near the C terminus, all of which serve for protein-protein interactions (Saunders et al. 2004). UBR5 is highly conserved and is essential for mammalian development (Callaghan et al. 1998; Saunders et al. 2004). The known substrates of UBR5 as an Arg/N-recognin include huntingtin (Koyuncu et al. 2018), hPXR (Ong et al. 2014), Gkn1 (Yang et al. 2016), Groucho/TLE (Flack et al. 2017), MOAP-1 (Matsuura et al. 2017) and many more. Through protein-protein interactions, UBR5 also influences DNA replication, (Cipolla et al. 2019), progesterone signaling (Henderson et al. 2002), p53 phosphorylation (Ling and Lin 2011) and cell cycle through CHK2 phosphorylation (Henderson 2006), to name only a few. This confers to UBR5 roles in maintenance of proteostasis in pluripotent stem cells, sensing of toxins, cell growth, β-catenin signaling, hedgehog signaling, hormone signaling, DNA damage response, as well as oncoprotein and tumor suppressor functions (Shearer et al. 2015). As for UBR4, the ties between all the various functions of UBR5 and the Arg/N-degron pathway are still subject of research.

Arg/N-degron pathway and apoptosis

Involvement of the Arg/N-degron pathway in the regulation of apoptosis became evident with the discovery of the first known metazoan substrate of the pathway, Diap1 (Ditzel et al. 2003). In *Drosophila*, Diap1 is essential for cell survival, directly repressing

caspase activity and preventing unrestrained caspase-mediated damage. Activated caspases cleave Diap1, revealing a destabilizing residue at its N-terminus and targeting the shorter fragment for degradation through the 26S proteasome. This confers to Diap1 an antiapoptotic function, and a proapoptotic activity to the Arg/N-degron pathway. However, results are not so straightforward, as inhibition experiments revealed that the Arg/N-degron pathway can be both pro- or anti-apoptotic in *Drosophila*, depending on the apoptotic conditions.

Apoptosis, a form of programmed cell death, occurs naturally in all multicellular eukaryotes and is essential for proper embryonic development, homeostatic maintenance of cell populations in tissues and elimination of infected or diseased cells (Koonin and Aravind 2002; Elmore 2007). Initiation of apoptosis can occur from three different pathways: extrinsic (death receptor), intrinsic (mitochondrial pathway) and granzyme-dependent pathway. Although the initiating mechanisms differ, all three pathways converge on the same execution pathway: activation of apoptosis effector caspases (-3 and -7), which results in DNA fragmentation, formation of apoptotic bodies and eventually phagocytosis (Elmore 2007). Therefore, in all apoptotic programs, one of the main outcomes in the beginning of the effector phase is the generation of thousands of cleaved caspase substrates. The cleavage site of caspase targets is generally situated in a "turn" secondary structure, and comprises eight amino acids: P4-P1 and P1'-P4', the cut occurring after P1 (Schechter and Berger 1967; Timmer et al. 2009). Caspases have an almost absolute requirement for an Asp residue at the position P1, Glu being the only other residue that can occupy this position, in very few cases (Seaman et al. 2016). The P1' position is a small residue in around 70% of the substrates, with glycine, serine and alanine being the most common residues observed. Of the other residues found in position P1', 18-21% are destabilizing according to the Arg/N-degron pathway (Mahrus et al. 2008; Stennicke et al. 2000).

At the onset of apoptosis, activated effector caspases cleave more than 1200 different proteins in mammalian cells, although very few of these possess actual proven proapoptotic activities (Piatkov, Brower, and Varshavsky 2012; Crawford et al. 2013). Of these 20 or so protein fragments that increase the probability of apoptosis when cleaved, 80% were found to bear Nt-destabilizing residues according to the Arg/N-degron pathway, and 50% contain natural experimentally proven N-degrons (Cys-Ripk1, Cys-Traf1, Asp-

Brca1, Leu-Limk1, Tyr-Nedd9, Arg-Bid, Asp-BclXL, Arg-BimEL, Asp-Epha4, and Tyr-Met) (Piatkov, Brower, and Varshavsky 2012; Xu, Payoe, and Fahlman 2012). Additionally, using knock-out cell lines and the Ate1$^{-/flox}$ mouse, Piatkov and colleagues demonstrated that a partial ablation of the Arg/N-degron pathway is sufficient to cause accumulation of the proapoptotic fragments containing N-degrons and sensitize cells to spontaneous apoptosis. These results indicate that the Arg/N-degron pathway regulates apoptosis through selective degradation of proapoptotic fragments (Figure 5), contributing to the maintenance of proapoptotic fragment levels below thresholds that would otherwise lead cells beyond the point of no return in the apoptotic program.

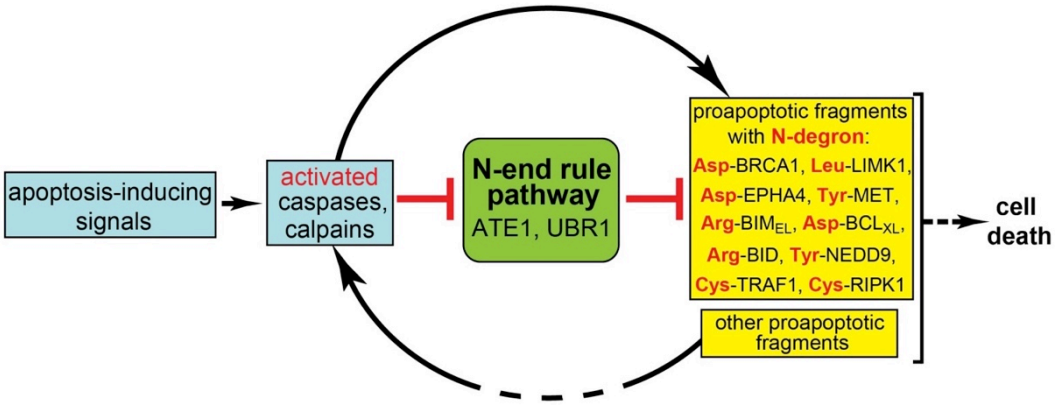

Figure 5. **The Arg/N-degron pathway as a regulator of apoptosis.** Apoptosis inducing signals activate caspases, which cleave proteins into proapoptotic fragments. The Arg/N-degron pathway acts on the apoptotic program by degrading N-degron bearing proapoptotic fragments (Asp-BRCA1, Leu-LIMK1, Tyr-NEDD9, Arg-BID, Asp- BCLXL, Arg-BIMEL, Asp-EPHA4, Tyr-MET, Cys-TRAF1, and Cys-RIPK1) by the Arg/N-degron pathway, keeping the levels of these fragments below thresholds that would otherwise fully commit cells towards apoptosis. Activated caspases can also counteract the anti-apoptotic activity of the N-degron pathway by cleaving UBR-ubiquitin ligases of the pathway as well as Ate1. (Piatkov, Brower, and Varshavsky 2012)

The Arg/N-degron pathway and cancer

Due to their roles in cell proliferation, migration, development and more, it would not be surprising if the UBR-ubiquitin ligases of the Arg/N-degron pathway were particularly important in the development and maintenance of cancer. In fact, two of the four proteins are upregulated in many types of cancer. UBR2 is upregulated in gastric cancer and its

expression in tumor cells is strongly induced by cachetic stimuli including proinflammatory cytokines (Mao et al. 2017; Zhang et al. 2013). UBR5 is upregulated in mantle cell lymphoma, triple-negative breast, ovarian, colorectal and gastric cancers, and has been shown to enhance cancer cell survival and proliferation, de novo angiogenesis, is involved in degradation of tumor suppressors and drives resistance to chemotherapy (Meissner et al. 2013; Bradley et al. 2014; Eblen and Bradley 2017; Liao et al. 2017; Wang et al. 2017; Xie et al. 2017; Yang et al. 2016). Additionally, the degradation of specific oncoproteins like c-Fos, as well as tumor suppressors such as PTPN14 in cervical cancer, is attributed to UBR1 and UBR4 (Szalmas et al. 2017; Sasaki et al. 2006). These and other data support the idea that the N-degron pathway plays an important role in the positive regulation of cancer cell proliferation, motility, and survival and that inhibition of this pathway offers the potential to be a highly effective anti-tumor treatment.

Inhibition of the Arg/N-degron pathway

Several attempts have been made to inhibit the Arg/N-degron pathway. Indeed, because of its implication in many cellular processes, the Arg/N-degron pathway is an attractive candidate to manipulate in order to impact these same processes in target cells. Knockouts of the various components of the Arg/N-degron pathway are embryonically lethal (Kwon et al. 2001; Kwon et al. 2002; Kwon et al. 2003; Saunders et al. 2004; An et al. 2006; Tasaki et al. 2013), therefore only post-natal deletion or inhibition of the pathway is possible. Listed below are the different strategies used to inhibit one or more of the components of the Arg/N-degron pathway.

Dipeptides and monomer inhibitors

The recognizable element of an Arg/N-degron substrate is the N-degron, which is composed of a destabilizing N-terminal residue along with an internal lysine and an unspecified N-terminal structure, the most critical element of these three being the identity of the N-terminal amino acid (Bachmair and Varshavsky 1989). This ensures recognition by N-recognins, ubiquitylation and subsequent degradation by the 26S proteasome. Dipeptides were developed to mimic type 1 or type 2 N-degrons and inhibit proteolysis by

the N-degron pathway through competitive binding of the N-recognins (Figure 6a). These dipeptides are characterized by their L-form conformation, and the presence of an unmodified α-amino group, hydrophobic side chain of the N-terminal amino acid and a peptide bond (Baker and Varshavsky 1991; Kitamura 2016). Successful inhibition of proteolysis of N-degron pathway substrates was achieved in *S. cerevisiae*, *S. pombe* and rabbit reticulocytes although this occurred only at high concentrations, which could be toxic in vivo, and the effect was lost after a few hours due to hydrolysis of the dipeptides (Baker and Varshavsky 1991; Davydov and Varshavsky 2000). Additionally, use of these dipeptides in animals or humans would be further complicated by lack of delivery vehicles for targeted inhibition of the pathway. Later variants of these inhibitors are monomers, which conserve the L-form conformation and the unmodified α-amino group, but have minimal interacting motifs (Figure 6b). These molecules show better endopeptidase resistance and are effective at lower doses than dipeptides (Sriram et al. 2013).

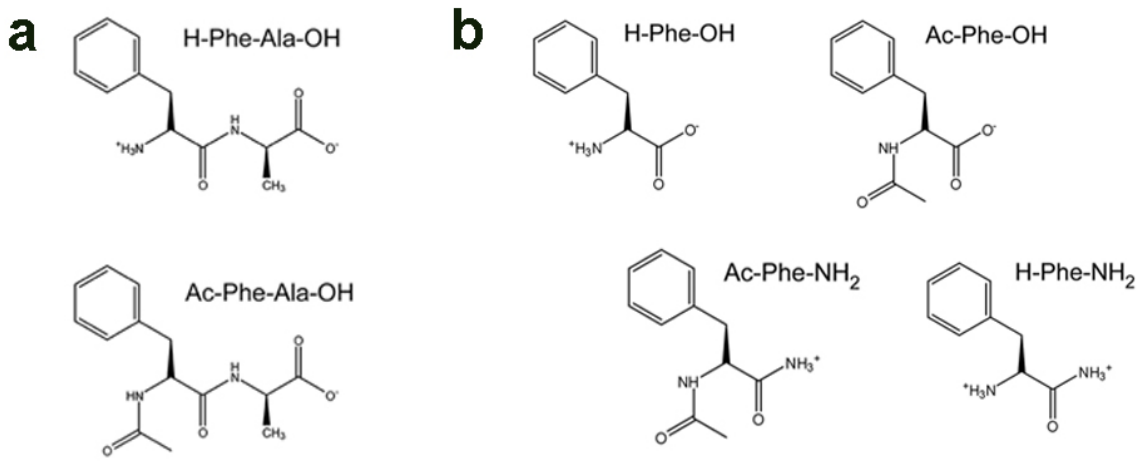

Figure 6. **Dipeptide (a) and monomer (b) inhibitors of the N-degron pathway.** Phe is a type 2 Arg/N-degron substrate while Ala is a substrate of the Ac/N-degron pathway. These examples were used in the study by Sriram et al, 2013.

Heterovalent inhibitors

Another approach is the development of multivalent inhibitors that contain two carbon chains attached to destabilizing residues, linked by a lysine (Figure 7). These N-degron "mimics" can bind N-recognins and prevent binding to their natural substrates, effectively stopping degradation (Kwon, Levy, and Varshavsky 1999; Lee et al. 2008; Jiang et al. 2013). The heterovalent inhibitors take advantage of their double chains to target both

the UBR-box and the N-domain of the E3 ligases of the Arg/N-degron pathway (Figure 7a). Compared to dipeptides, multivalent inhibitors provide enhanced binding affinity and more stability. The model Arg-Phe-C11 compound used in the study by Lee et al (2008), was shown to inhibit type 1 and type 2 N-degron degradation through cooperative simultaneous binding to multiple sites on different N-recognins, namely UBR1 and UBR5. The same compound, entrapped in liposomes, was used to inhibit the Arg/N-degron pathway in a colon cancer mouse model (Agarwalla and Banerjee 2016). Successful inhibition was achieved in all cases, nonetheless with the same drawbacks observed with dipeptide molecules. Additionally, targeting the UBR-box implies binding of the inhibitors to other UBR-ubiquitin ligases that are not part of the N-degron pathway.

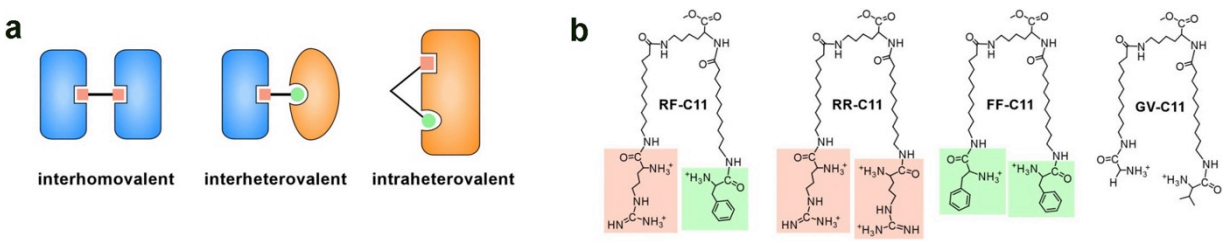

Figure 7. **Heterovalent inhibitors can successfully compete with type 1 and type 2 Arg/N-degron substrates.** (a) Models of homo or heterovalent inhibitors, inhibiting the UBR (type 1) or N (type 2) domains on one or two E3 ligases. (b) Heterovalent inhibitors developed in Lee et al, 2008, where Phe (green) is used as a type 2 substrate and Arg (orange) is used as a type 1 substrate. Figure adapted from Lee et al, 2013.

Natural compounds

Finally, the last strategy is to target upstream components of the N-degron pathway. Natural compounds such as the tri-peptide Glu-Val-Phe, heparin or hemin were found to inhibit the Arg-tRNA-transferase Ate1, however none of these compounds have high specificity to Ate1 or are able to inhibit the activity of Ate1 in cells (Kato 1983; Ciechanover et al. 1988; Hu et al. 2008b). More recently, tannic acid and merbromin were found to inhibit Ate1 and its activities, albeit with differential effects on cell motility, actin skeleton and angiogenesis, despite having the same specificity for Ate1 (Saha et al. 2012). Different mechanisms of action could explain the different effects observed, but this could also be caused by binding to other effectors. Nonetheless, the phenotypes observed after inhibition

of Ate1 by tannic acid or merbromin recapitulated known consequences of Ate1 deletion in the mouse, indicating proper inhibition of Ate1.

In this work, we chose to use a RNA interference approach in order to target all four N-recognins of the Arg/N-degron pathway, individually or all at once, effectively ablating the complete pathway. This gave us flexibility in the investigation, as the same technology can be used *in vitro* or *in vivo*. Coupled with lipid nanoparticles, our siRNA approach enables us to study downregulation of the Arg/N-degron pathway in the liver of healthy adult mice and in the context of hepatocellular carcinoma, something that has never been done before. The next section discusses the mechanism of RNA interference using small interfering RNA, and will illustrate the advantages of the technology and how it is currently applied in the clinic.

Targeted mRNA downregulation: siRNA and methods of delivery

The powerful technology of siRNA developed for gene downregulation is based on the naturally occurring process of targeted RNA interference (RNAi) and uses the machinery already present in all eukaryote cells in order to control the expression of specific genes. Indeed, small non-coding RNA such as microRNA (miRNA), small interfering RNA (siRNA) and Piwi-interacting RNA (piRNA) are encoded in the eukaryote genome and regulate more than 60% of transcribed genes (Friedman et al. 2009; Kozomara and Griffiths-Jones 2014). The modes of interference of these three types of small-RNAs differ in the source of RNA and the mechanisms of silencing but the outcome remains the same: through transcriptional gene silencing, mRNA degradation or translational repression, expression of the target is reduced. The beauty of the system lies in its versatility, programmability and potency, and these three reasons explain why RNAi is on the rise in clinical studies and targeted therapy development (Hu et al. 2019).

In the late 1990s, Andrew Fire and Craig Mello, with the help of talented post-docs Mary Montgomery and Si Qun Xu, discovered that double-stranded RNA, when injected into cells, could prevent the expression of the gene bearing the matching anti-sense sequence, by binding to mRNA and causing its degradation (Fire et al. 1998; Montgomery, Xu, and Fire 1998). The molecular machinery enabling the process as well as the specific

requirements for the double-stranded RNA were discovered in the following years by various different groups, in a race to understand and develop what was already foreseen as the future of pharmacopeia for undruggable targets (Gewirtz 2007). However, once the molecular mechanisms of RNAi were identified, how to deliver the dsRNA into targeted organs and cells became the immediate challenge, and remains a difficulty today, although much progress has been made (Zatsepin, Kotelevtsev, and Koteliansky 2016; Singh, Trivedi, and Jain 2018). The mechanisms of RNA interference as well as the means of delivery will be addressed and described in the sections below.

RNA interference by siRNA

Small interfering RNAs (siRNA) generally derive from exogenous sources such as viruses or synthetically made oligonucleotides, although some endogenous siRNA can originate from transcription of hairpins, inverted repeats, transposons or convergent transcription (Golden, Gerbasi, and Sontheimer 2008). Experiments performed in plants and later in mammalian cells revealed that the dsRNA mediating the interference are typically 20-25nt long (Hamilton and Baulcombe 1999; Elbashir, Harborth, et al. 2001; Elbashir, Lendeckel, and Tuschl 2001), and are processed into these small effectors in the cytoplasm by the Dicer enzyme (Tuschl et al. 1999; Hammond et al. 2000; Zamore et al. 2000; Bernstein et al. 2001).

Dicer

The Dicer family of RNase III enzymes is extremely conserved throughout evolution, although not all organisms have the same number of Dicer enzymes. For instance, mammals and nematodes have only one Dicer (Dicer and rde-1, respectively) while *Drosophila* expresses two (Dcr-1 and Dcr-2) and the model plant *Arabidopsis* possesses four (DCL1, DCL2, DCL3 and DCL4) (Hammond et al. 2000; Bernstein et al. 2001; Schauer et al. 2002). In organisms with more than one Dicer enzyme such as *Drosophila*, the functions are typically distinct for each protein: Dcr-1 is necessary for miRNA processing while Dcr-2 is specific to the anti-viral response (Lee et al. 2004). Dicer contains a series of domains organized in a specific order: a DExD/H-box RNA helicase domain, a DUF283 domain, a

PAZ domain, two tandem RNase III domains and a dsRNA binding domain (Figure 8) (Zhang et al. 2002; Macrae et al. 2006; Carthew and Sontheimer 2009; Lau et al. 2012).

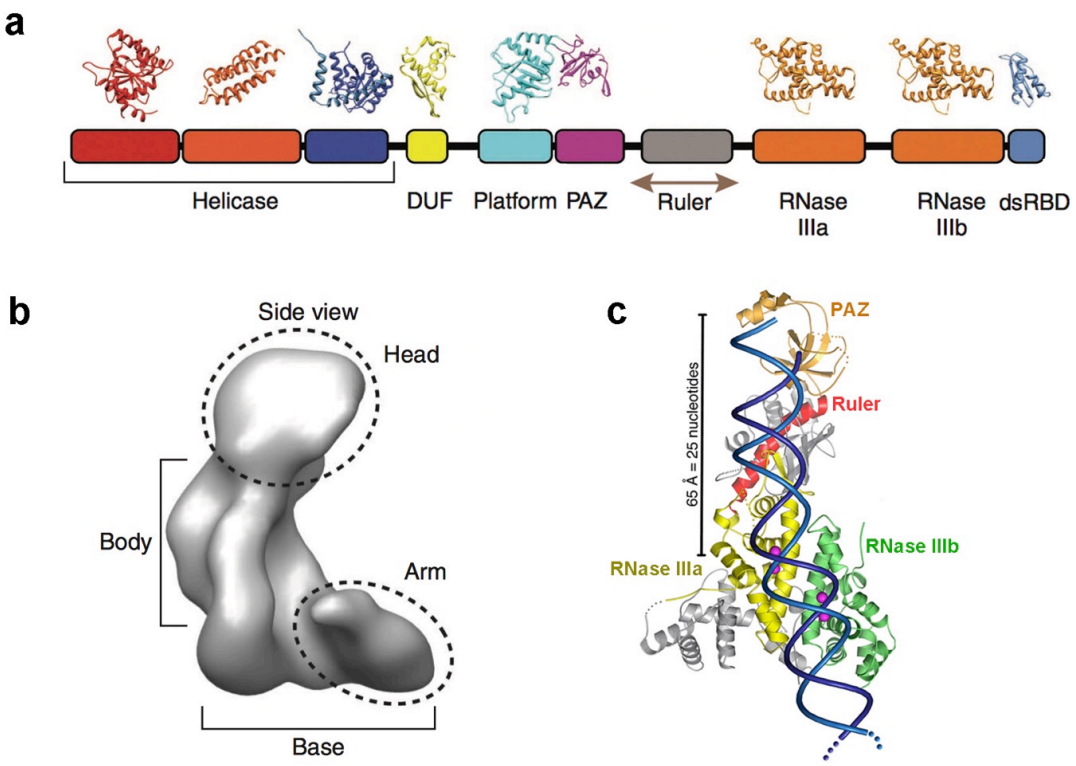

Figure 8. **The Dicer enzyme.** (a) The conserved domains of the metazoan Dicer enzyme. (b) electronic microscope reconstruction of Dicer in 3D form. (c) structure of human Dicer bound to dsRNA, as revealed by X-ray crystallography. Figures modified from (Lau et al. 2012; MacRae, Zhou, and Doudna 2007)

The PAZ and the RNase III domains of Dicer play a critical role in excising siRNA, preferentially from the ends of long dsRNA: the PAZ domain directly binds the dsRNA at the 3' end of one strand, while the two RNAse domains each cleave one of the RNA strands, generating 2-nt 3' overhangs (Zhang et al. 2004; Macrae et al. 2006; MacRae, Zhou, and Doudna 2007). The distance between the PAZ domain and the active sites of the RNase domains allows the RNA to wrap around the protein and extend approximately two helical turns, which confers the length of 20-25nt to the short dsRNA products of Dicer (MacRae, Zhou, and Doudna 2007) (Figure 8c). The requirement for ATP during RNA processing by Dicer varies among different species, as it was demonstrated that ATP promotes dsRNA

cleavage by Dicer in *Drosophila* and *C. elegans* while the human variant of Dicer does not require ATP for the same function (Bernstein et al. 2001; Carmell and Hannon 2004; Zhang et al. 2002). Nevertheless, for all species studied, removal of Dicer abolishes processing of long dsRNA into short 20-25nt dsRNA that mediate RNA interference, indicating that Dicer is the sole enzyme responsible for the generation of endogenous siRNA.

Argonaute

Once the double-stranded RNA is processed by Dicer (is 20-25nt long and has 2nt 3'-end overhangs), the ds-siRNA is loaded onto Argonaute (AGO) proteins and together they form large ribonucleoprotein complexes termed RNA-Induced Silencing Complex (RISC) (Hammond et al. 2000; Nakanishi 2016). In the case of naturally processed siRNA, transfer of the short dsRNA from Dicer to AGO proteins most often requires the help of dsRNA binding proteins (dsRBP) such as TRBP and PACT in mammals (Wang et al. 2009; Lee, Zhou, et al. 2013) as well as the molecular chaperones Hsc70/Hsp90, which mediate the ATP-consuming conformational change of the AGO protein needed to accept the bulky, rigid siRNA (Iwasaki et al. 2010). As was the case for Dicer, members of the Argonaute protein family are varied: not all species express the same AGO proteins, and not all biological roles are identical between them. For instance, in humans, of the four variants of AGO (hAGO1-4), only hAGO2 possesses slicing activities, whereas in Drosophila, Ago1 is responsible for miRNA silencing activities while Ago2 acts with siRNA (Liu et al. 2004; Meister et al. 2004; Song et al. 2004; Forstemann et al. 2007). AGO proteins are bi-lobed and contain the following domains: N-terminal, linker 1, and PAZ, which form the N-lobe, and linker 2, MID and PIWI domains forming the C-lobe (Hock and Meister 2008). The MID domain is responsible for firmly holding the 5' end of the guide siRNA strand, while the PAZ domain binds to the 3' end of the same strand. Abundant interactions between the guide strand (2'-OH ribose) and the core of the AGO protein provide RNA specificity and confer stability to the complex (Yan et al. 2003; Song et al. 2004). The PIWI domain contains the catalytic center of the AGO proteins: the DEDH active tetrad (in humans, this sequence varies in other species), which requires Mg^{2+} for RNA slicing activity (Rivas et al. 2005). However, the catalytic tetrad DEDH is not the only crucial element needed for slicer

activities since restoring the corresponding amino acids in catalytically inactive AGO protein hAGO1 does not confer slicing capacity. Indeed, interactions between specific amino acids in the N-terminal domain with the catalytic tetrad are essential for optimal slicing of dsRNA (Faehnle et al. 2013).

RISC assembly and siRNA strand selection

The assembly of the RISC complex is a two-step process: (1) loading of the siRNA onto Argonaute (Figure 9) and (2) unwinding and removal of one of the RNA strands, named the passenger strand (Figure 10). Selection of the passenger strand in mammals is an asymmetrical non-random process, which occurs during loading and is purely dictated by the relative thermodynamic properties of the two duplex ends. This is demonstrated by the fact that the strand with the least stably based-paired 5′ end, with a high prevalence of U or A, is preferentially chosen as the guide strand, and that siRNAs with equal stability at both ends will be incorporated into RISCs at equal frequency (Figure 9) (Khvorova, Reynolds, and Jayasena 2003; Frank, Sonenberg, and Nagar 2010; Suzuki et al. 2015). For endogenous siRNA, the proteins that load the oligonucleotide onto AGO determine the polarity of the asymmetry. In flies, the tandem Dcr2/R2D2 senses the thermodynamic stability of the dsRNA, fixing the more stable end onto R2D2 and having Dcr2 hold the opposite end before transferring the siRNA onto Ago (Tomari et al. 2004). In mammals, Dicer and TRBP perform the same function, organizing the siRNA in the correct orientation so that the less stable 5′ end, preferentially starting with a Uracil or Adenine, sits in the MID domain of AGO, assuring that this strand will be retained in the RISC (Gredell et al. 2010; Noland, Ma, and Doudna 2011; Frank, Sonenberg, and Nagar 2010; Suzuki et al. 2015). In contrast to these results, many studies have proven that Dicer is dispensable for processing, RISC loading and siRNA mediated cleavage of mRNA targets when synthetic exogenous siRNA are used for RNA interference (Martinez et al. 2002; Kanellopoulou et al. 2005; Murchison et al. 2005; Betancur and Tomari 2012). In this case, the presence of U or A at the 5′ end of one strand, or the addition of chemical modifications such as methylation of the 5′-OH of the future passenger strand can help in the selection of the guide strand (Chen et al. 2008). Indeed, siRNA or miRNA naturally processed by Dicer carry 5′ phosphate and 3′ hydroxyl

groups while synthetic siRNA carry 5′-hydroxyl ends, which are rapidly phosphorylated by the kinase Clp1, enabling loading onto AGO (Elbashir, Harborth, et al. 2001; Weitzer and Martinez 2007). Methylation, or any blocking of the 5′-OH group, prevents phosphorylation and reduces the chances of occupancy of RISC by the methylated strand (Chen et al. 2008). Binding of the 5′ end of the siRNA to the AGO protein is the first step in the formation of the RISC complex and is common to all Argonaute proteins.

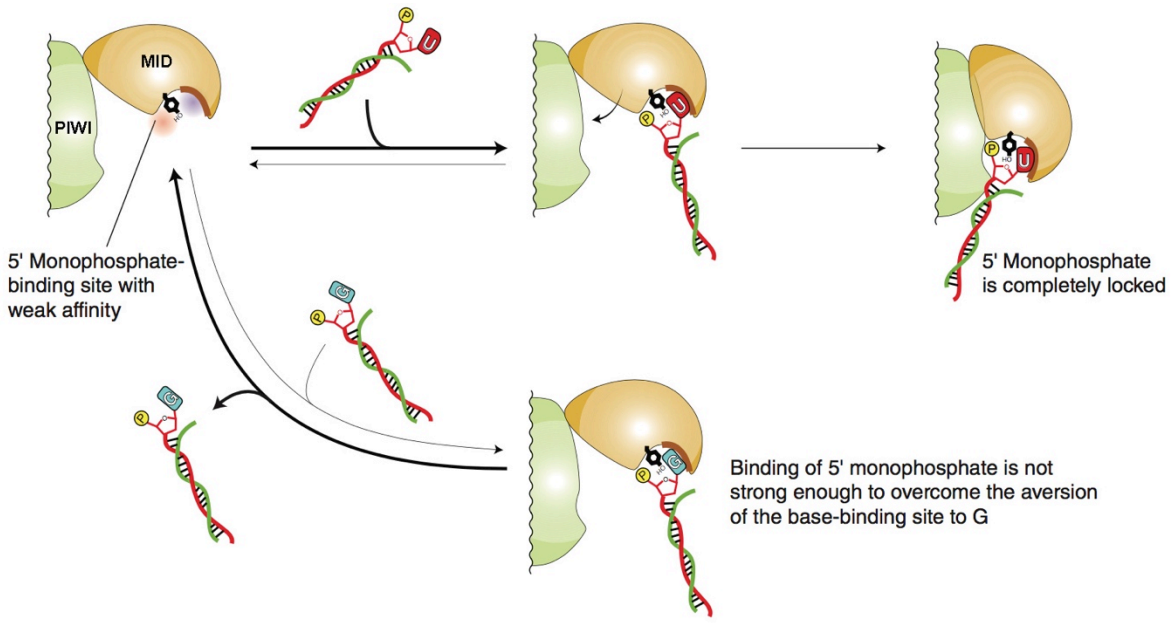

Figure 9. **Duplex loading onto Argonaute.** The guide strand is selected by the affinity of the MID domain to the 5′ base. If the 5′ base is a uracil or adenine, the interaction is stable enough and conformational change occurs to form the composite pocket with the PIWI domain. Owing to the aversion of the nucleotide specificity loop to cytosine and guanine, if a guanine (or cytosine) binds to the 5′ base-binding pocket, most of the complexes are dissociated before they form the composite pocket with PIWI domain. Therefore, duplexes starting with guanine (or cytosine) are easily released from the AGO proteins. Adapted from Nakanishi, 2016.

When the 5′ base of the guide strand binds to the MID domain of AGO, this induces a conformational change in AGO from an open state to a closed conformation where the PIWI domain shifts close to MID and forms the composite pocket, locking the 5′ monophosphate in place (Parker, Roe, and Barford 2005; Elkayam et al. 2012) (Figure 9). The change in conformation pushes the N and L1/L2 domains outwards, wedging the RNA duplex in the nucleic acid-binding channel of AGO and destabilizing the base pairs between

the 3′ end of the guide and the 5′ end of the passenger strand (Kwak and Tomari 2012). The next step of the passenger strand ejection process is divided into two types of mechanisms: slicer-dependent or slicer-independent, and is determined by the cleavage capability of the Argonaute protein and the perfect or mismatch pairing of the RNA duplex (Figure 10). In the slicer-dependent ejection mechanism, the PIWI domain of AGO2 (in mammals, only AGO2 has slicer properties) slices the perfectly complementary passenger strand in two parts. Since the guide strand is firmly anchored in the MID domain of AGO2, only the passenger strand will be squeezed out of RISC due to increased structural pressure (Schirle, Sheu-Gruttadauria, and MacRae 2014; Leuschner et al. 2006). On the other hand, the slicer-independent ejection mechanism (in mammals, this involves AGO1, AGO3 and AGO4) relies on the intrinsic instability of the RNA duplex, where mismatches in the stem region promote passenger strand ejection (Gu et al. 2011). Finally, the PAZ domain of AGO proteins participates in the release of the passenger strand, in both mechanisms, by binding to the 3′ end of the guide strand and vigorously shaking it, causing the passenger strand to detach itself from the guide strand (Park and Shin 2015).

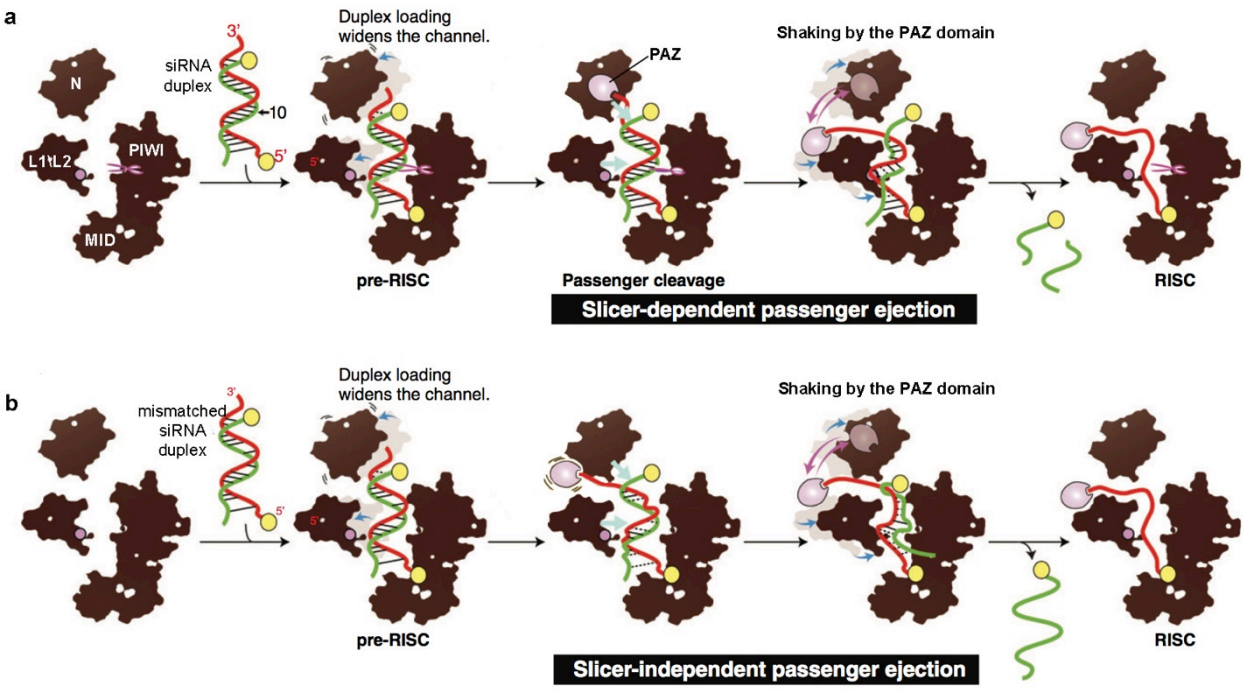

Figure 10. **siRNA loading onto Argonaute and passenger strand ejection.** (a) Slicer-dependent passenger ejection. The siRNA duplex (guide (red) and passenger (green), 5′ phosphates shown as yellow spheres) is loaded onto AGO2 to form the pre-RISC. This

causes the N and L1/L2 domains to move outwards to expand the width of the nucleic acid-binding channel. The MID domain anchors the guide RNA at its 5′ phosphate and then the loaded siRNA duplex is squeezed by the N and L1/L2 domains (cyan arrows), which also expels the passenger strand after cleavage. The PAZ domain shakes the 3′ end of the guide strand (pink arrows), which facilitates the ejection of the cleaved passenger strand. (b) Slicer-independent passenger ejection. Because of its thermodynamic instability, the mismatched siRNA duplex is heavily distorted by inward pressure. All other steps are similar to slicer-dependent ejection. Modified from Nakanishi, 2016.

Silencing by slicer

The canonical pathway of RNA interference involves the guide siRNA loaded onto Argonaute, directing the RISC to the target mRNA for cleavage by the catalytic tetrad of the AGO2 PIWI domain (Figure 11, left panel) (Liu et al. 2004; Song et al. 2004). A few key principles need to be respected for efficient and specific cleavage. First, the cleavage of the target mRNA requires perfect Watson-Crick base pairing between the seed region of the guide strand of the siRNA (positions 2-8) and the target mRNA and extensive pairing in the remaining regions (Elbashir, Martinez, et al. 2001; Llave et al. 2002; Wilson and Doudna 2013). Structural studies revealed that positions 2-6 of the guide siRNA are situated outside the RNA groove of AGO, suggesting that these bases are used to scan for target mRNA (Nakanishi et al. 2012). The mechanisms by which the AGO protein ensures that there is perfect complementarity between the guide siRNA and the target mRNA are still unclear, however it is known that both lobes of the AGO protein participate in this activity since absence or mutations in the N-lobe prevent cleavage of mismatched target mRNA (Hur et al. 2013; Dayeh, Kruithoff, and Nakanishi 2018). Second, base-pairing is necessary at the site of cleavage, between bases 10 and 11 (Elbashir, Martinez, et al. 2001; Haley and Zamore 2004). Lastly, the position of the siRNA target sequence needs to be in an accessible region of the mRNA (Holen et al. 2002).

The Mg^{2+}-dependent RISC slicing of mRNA generates a 3′-OH group and a 5′-phosphate group on the termini of the mRNA (Figure 11) (Martinez et al. 2002; Schwarz, Tomari, and Zamore 2004). Since the mRNA is cleaved by an endonuclease, decay occurs via two pathways: the 3′ fragment is degraded by major cellular 5′-to-3′ exonucleases such as Xrn1 while the 5′ fragment is degraded by the exosome and/or the associated SKI

complex (Orban and Izaurralde 2005; Garneau, Wilusz, and Wilusz 2007). Alternatively, a poly-U tail can be added to the 5' product in order to enhance degradation of small RNA exosome substrates (Shen and Goodman 2004).

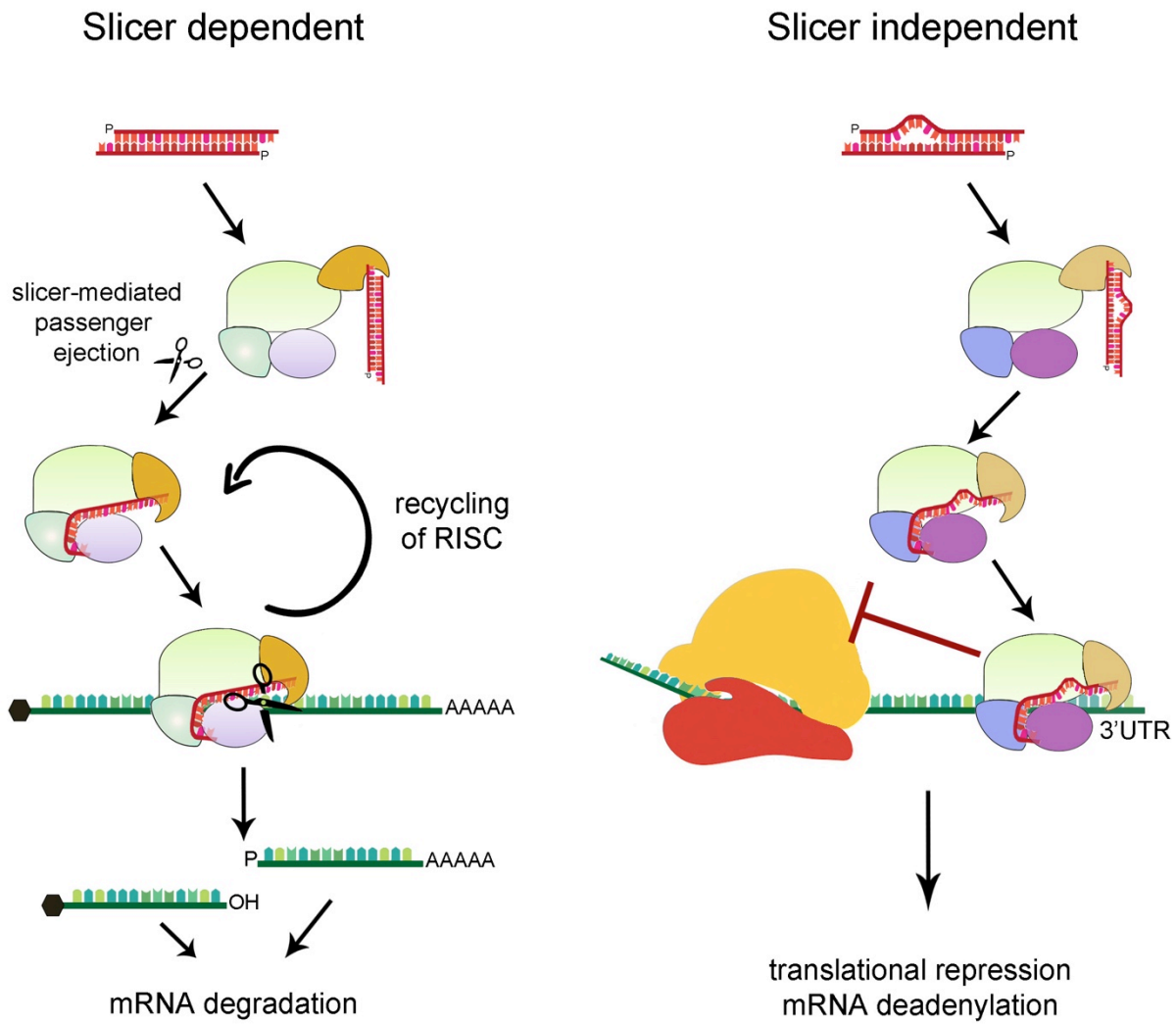

Figure 11: **RNA interference.** Slicer dependent RNA interference (left) is based on perfect Watson-Crick base pairing between the guide strand of the siRNA and the mRNA and generates two mRNA fragments that will be degraded via major cellular mRNA degradation mechanisms. Recycling of the RISC complex allows for multiple rounds of mRNA cleavage. Slicer independent RNA interference (right) occurs when mismatches in the guide-mRNA pair exist. Silencing involves translational repression and mRNA deadenylation.

Another interesting fact about RISC mediated silencing is the multi-turnover property of this mechanism (Figure 11). Indeed, once a siRNA is loaded onto Argonaute, the RISC

complex can proceed to multiple rounds of target binding, cleavage and dissociation, while retaining its original configuration (Hutvagner and Zamore 2002; Martinez et al. 2002; Haley and Zamore 2004). This, combined to the fact that RISC complexes are generally long-lived, suggests that few siRNA molecules per cell can achieve long-term target mRNA downregulation. However, factors such as mRNA relative abundance and turnover rates strongly influence efficacy and potency of each specific siRNA (Olejniczak et al. 2013; Arvey et al. 2010; Larsson, Sander, and Marks 2010).

Silencing via non-slicer mechanisms

RISC complexes involving catalytically inactive AGO proteins or partially mismatched siRNA guide-target mRNA pairs can also mediate mRNA silencing, generally through translational repression or exonucleolytic degradation (Figure 11, right panel) (Ruda et al. 2014). Non-slicer siRNA mediated RNA interference is reminiscent of miRNA-mediated silencing mechanisms and involves interactions between RISC and GW182 family proteins, which, upon relocation to P-bodies, mediate interactions with additional silencing partners such as deadenylases, the decapping complex and RNA helicases and induce RNA degradation through the general translational control machinery (Eulalio, Huntzinger, and Izaurralde 2008; Fabian and Sonenberg 2012).

Anti-Sense Oligonucleotides

Another important strategy for interfering with RNA metabolism is the use of DNA anti-sense oligonucleotides (ASO). ASOs can be classified into two main categories according to their mechanism of action: (1) RNase H dependent cleavage of mRNA and (2) steric blockage of mRNA, which prevents translation (Dias and Stein 2002). The majority of the anti-sense oligonucleotides presently in the clinic are based on cleavage of the mRNA. This requires the processive exonuclease RNase H, which recognizes RNA/DNA duplexes and cleaves the phosphodiester bonds of RNA, leaving 3′ hydroxyl and 5′ phosphate groups on the ends of the mRNA, targeting it for exonucleolytic degradation (Moelling, Broecker, and Kerrigan 2014; Zamaratski, Pradeepkumar, and Chattopadhyaya 2001). As RNase H is present in the nucleus as well as the cytoplasm, ASOs are active in both cellular

compartments of the cell, contrarily to siRNA, which can only act in the cytoplasm due to absence of the RISC complex in the nucleus.

Chemical modifications of siRNA to improve stability and on-target effects

RNA interference off target effects refers to unintended mRNA downregulation caused by non-target sequence recognition by the RISC complex. The main driving mechanism for siRNA off target effects is through slicer-independent "miRNA-like" target recognition and translational repression. This is caused by the fact that the seed region, positions 2-7 in the 5' end of the siRNA where target recognition occurs, is only 6 nucleotides long, with statistically probable recognition sites in every 4kb RNA sequence ($(1/4)^6$=1/4096 base pairs). Additionally, the recognition requirements for slicer-independent RNA interference allows for disparities in the seed region, implying that one miRNA (or mismatched siRNA) will naturally have multiple targets (Lewis et al. 2003). Therefore, many strategies have been developed to optimize the siRNA molecule and avoid off-target effects. Specialized algorithms are used to improve specificity by eliminating candidate siRNA with near perfect pairing with non-target mRNA. These algorithms also input target site accessibility, low GC content, A/U-rich 5' ends, specific nucleotides at certain positions in the sense strand, lack of internal repeats and thermodynamic stability, to eliminate off-target binding and favor proper strand selection, improve target binding and general efficacy of the siRNA (Gong and Ferrell 2004; Amarzguioui and Prydz 2004; Schubert et al. 2005; Baranova et al. 2011; Han et al. 2017) as these parameters strongly correlate with functional siRNA (Reynolds et al. 2004; Kamola et al. 2015).

Another measure to avoid off-target effects and to improve many features of the siRNA such as stability or proper strand loading is to use chemically modified oligonucleotides. The chemical modifications made to the dsRNA molecule can also serve to avoid triggering an immune response by activation of TLR receptors that react to ssRNA, dsDNA and CpG motifs. Indeed, innate immune cells have been shown to produce IFNα and TNFα in an endosomal intra-cellular TLR7/8 dependent manner in response to the presence of siRNA (Sioud 2005; Zamanian-Daryoush et al. 2008). Chemical modifications to

the ribose backbone of the siRNA can prevent TLR stimulation and immune activation (Manoharan et al. 2011; Broering et al. 2014).

The most common chemical modifications made to siRNA oligonucleotides involve modifying single molecules on the phosphate or the ribose moiety. These include replacing one or two non-bridging oxygen by sulphur on the phosphate moiety, creating phosphorothioates or phosphorodithioates, or replacing the 2'OH on the ribose moiety by a 2'-O-methyl group or 2'-Fluoro (Figure 12a) (Manoharan 2004; Choung et al. 2006; Eckstein 2014; Selvam et al. 2017). These modifications increase efficacy and potency of the siRNA by preventing nuclease degradation (Lubini, Zurcher, and Egli 1994; Layzer et al. 2004; Yang et al. 2012), increasing loading onto the RISC complex (Wu et al. 2014), suppressing off-target effects (Jackson et al. 2006; Iribe et al. 2017) and facilitating cellular uptake (Geary et al. 2001).

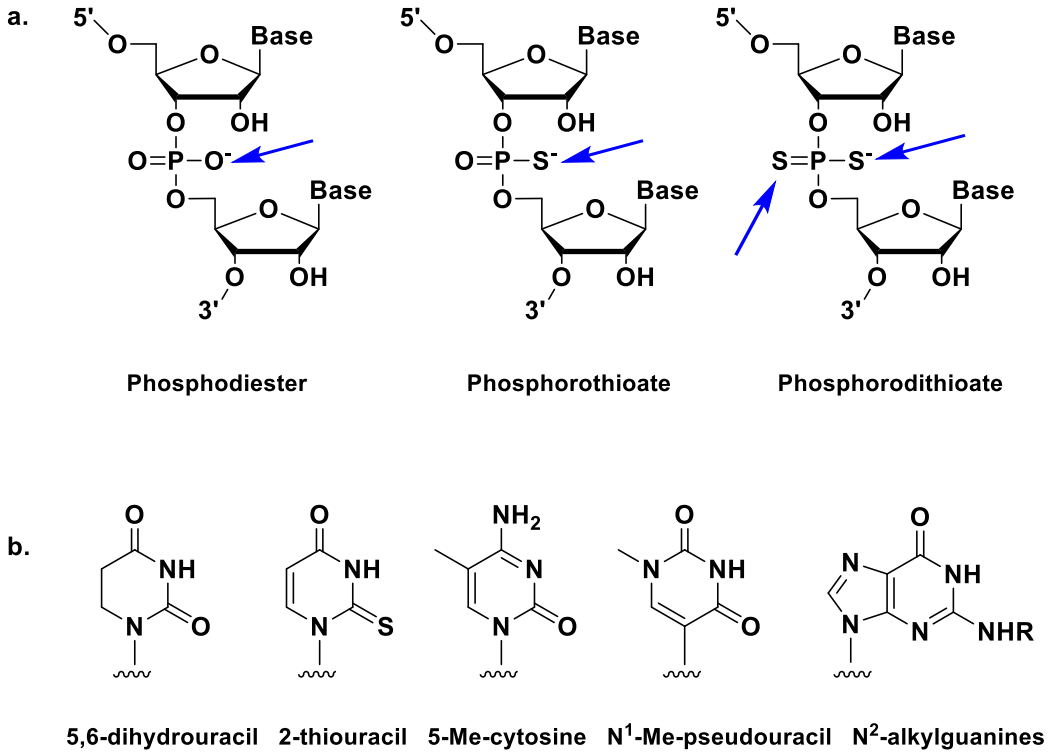

Figure 12. Chemical modifications to the backbone of RNA oligonucleotides (a) or to RNA bases (b).

Other less common modifications are the use of modified RNA bases such as dihydrouracil, thiouracil, 5-Me-cytosine and others illustrated in Figure 12b (Peacock, Kannan, et al. 2011). These modified bases influence on the activity of the siRNA by enhancing thermodynamic asymmetry of the siRNA duplex and favouring passenger strand

dissociation (Sipa et al. 2007; Terrazas and Kool 2009), improving sequence selectivity (Xia et al. 2006; Somoza et al. 2008) and by avoiding the immune response (Peacock, Fucini, et al. 2011).

Not all chemical modifications have a positive impact on the activity of siRNA, and most studies agree to demonstrate the position and sequence specificity of quality enhancing chemical modifications. Therefore, extensive experimental work must be performed to ensure on-target efficient and potent siRNA-mediated mRNA downregulation (see Box 1 for definitions of efficacy and potency). Additionally, although chemical modifications increase siRNA stability, they do not dramatically affect delivery in vivo, and special carriers or conjugates are needed to ensure that the siRNA reaches proper target organs. These will be discussed in the following section.

Box 1: Efficacy vs Potency and the measure of IC50

The **efficacy** of a siRNA is described as the maximum effect regardless of dose.

Potency is measured by the amount of the siRNA required to produce an effect of a given intensity. The IC50 (half maximal inhibitory concentration) is a measure of potency: it is the concentration at which 50% inhibition is reached.

Therefore, a highly **efficient** siRNA will almost reach 100% downregulation of a target, and a highly **potent** siRNA will reach 50% downregulation of the target gene at the lowest concentration.

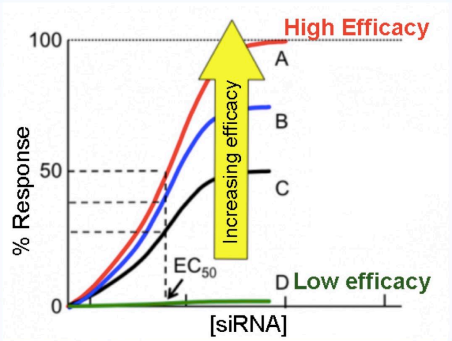

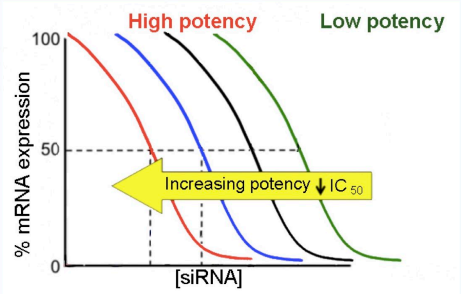

http://tmedweb.tulane.edu/pharmwiki/doku.php/basic_principles_of_pharm

Targeted delivery of siRNA

One major road block that must be addressed before a siRNA based therapy can reach the clinic is the delivery method: how to properly deliver these rather large negatively charged molecules into the cell of interest in vivo without triggering side effects? First, in order to reach the tissue of interest, the siRNA must cross several physiological barriers. If the siRNA is injected intravenously, degradation from nucleases in the serum or capture by phagocytic cells of the reticuloendothelial system will be the first obstacle to overcome (Shannahan, Bai, and Brown 2015). Then, the siRNA must cross the vascular endothelial wall, which can easily be done in any vessel by transcytosis for molecules smaller than 70nm, or will occur in the liver and spleen for larger particles, where fenestrations between endothelial cells allow their egress (Komarova and Malik 2010). The siRNA must also avoid clearance by the renal system, which filters molecules with sizes of 3-6nm, a typical size for oligonucleotides (Haraldsson, Nystrom, and Deen 2008). Additional challenges include targeted delivery to the proper organ, cell penetrance and endosomal escape (Whitehead, Langer, and Anderson 2009). Selective carriers are the best solution to protect the siRNA during delivery, to direct the oligonucleotide to the proper organ, to help with cell penetrance and promote endosomal escape. A variety of strategies have been developed over the years, and will be elaborated below.

Peptides

Cationic cell-penetrating peptides (CPP), endosome-disrupting peptides, noncovalent multifunctional peptide complexes, functionalized peptides and several alternative versatile peptide/protein strategies have been explored to overcome the barriers to siRNA delivery (Cummings, Zhang, and Jakymiw 2019). Peptides can be covalently or non-covalently attached to siRNA, due to high positively charged residue density enabling interactions with the negatively charged backbone of the siRNA (Deshayes et al. 2008). Cell penetrance usually occurs through direct crossing of the cell membrane via pore formation or clathrin/caveolae mediated endocytosis (Singh et al. 2018; McClorey and Banerjee 2018). Limitations of peptide carriers are their non-specificity to particular cells or tissues and their

propensity to remain entrapped in the endosomes, preventing the siRNA from reaching the RISC complex. To address this, dual-complexes of tissue specific peptides with endosome-disruptive subunits and peptide-based nanostructures were developed, however these led to poor siRNA activity in vivo, most likely due to interference with RISC loading or steric hindrance (Alexander-Bryant et al. 2017; Panigrahi et al. 2018).

Polymeric particles

Many different polymer-based delivery systems have been developed specifically for oligonucleotide delivery. These nanoparticles assemble through multivalent interactions, and their physical properties will vary according to their composition. Synthetic polyamines such as Polyethylenimine (PEI) were chosen for their high aqueous solubility and pH buffering capacity in acidic conditions, which make them ideal for maintaining their integrity in the endosome (Islam et al. 2014). However, their strong cationic charge density and non-degradable properties make them toxic for cells, unless low-molecular weight PEI polymers are functionalized with lipids, lipidoids or polyethylene glycol chains (Dahlman et al. 2014; Luten et al. 2008). PEI-based nanoparticles were used to successfully deliver siRNA to the vascular epithelium and to the lung (Dahlman et al. 2014). Polysaccharide based (for example chitosan) and polyaminoacid based materials (such as poly(N-2-hydroxyethyl)-d,l-aspartamide or PHEA) are also attractive candidates as they are water soluble, biocompatible, non immunogenic nor antigenic, and easily functionalized with a variety of small molecules or polymeric chains. However, minimal solubility and low buffering capacity at physiological pH confer only weak delivery efficiency to polysaccharides (Barba et al. 2015). Finally, and perhaps the most famous polymer: poly (lactic-co-glycolic acid), or PLGA. This polymer has received FDA approval and is currently used in many nanoparticle formulations due to its low toxicity, high biodegradability and that it can easily be manipulated to render particles of various shapes and sizes (Rezvantalab et al. 2018). Targeting molecules must be attached to their surface for delivery to specific organs, and with these modifications, successful delivery of PLGA nanoparticles was achieved to the brain vasculature (Chen et al. 2013), in joints (Scheinman et al. 2011), in the liver (Khan et al. 2019)and in prostate tumors (Cheng et al. 2007).

Viral particles

Recombinant Adeno-Associated Virus (AAV) particles are currently the most used therapy vectors, because they naturally infect primates, are nonpathogenic and remain almost completely episomal with a very low integration rate in humans (Kaeppel et al. 2013). Although the FDA has approved three gene therapy drugs delivered with AAV (Keeler and Flotte 2019), this vehicle still comprises many risks due to the immunogenicity of AAV vectors, perturbation of cell signaling and persistence of the AAV in host cells (Colella, Ronzitti, and Mingozzi 2018). Repeated injections using AAV vectors are successful only by changing the serotype of the virus (Majowicz et al. 2017), which greatly increases the cost of production of the treatment. Further challenges are related to AAV's tropism that lacks cell type selectivity, resulting in uncontrolled genome editing in unrelated organs. Improvement of delivery specificity is possible by engineering of the AAV capsid, but this also complexifies the development of a treatment strategy (Buning et al. 2015). Therefore, other solutions, such as lipid nanoparticles, are needed to palliate to these problems.

Lipid nanoparticles

Composition

Self-assembled lipid nanoparticles formed of cationic and helper lipids (Figure 13) are the most commonly used nonviral vectors for RNA delivery, primarily to the liver, but also in the spleen, peripheral macrophages and lungs, both in academic studies and clinical trials (Barba et al. 2019). Since their first use in non-human primates (Zimmermann et al. 2006), a number of different lipids and lipid-like materials (lipidoids) have been developed to improve transfer efficiency and stability and decrease the immune response as well as renal escape. Original cationic lipids, selected for their positive charge, were replaced by or used in combination with ionizable lipids, which change their charge according to the pH of the surrounding environment. This enhances the stability of the LNP inside the endosome and ensures release of the cargo only in the cytosol (Habrant et al. 2016). The helper lipids, or fusogenic lipids such as phospholipids (like Dioleoyl phosphatidylethanolamine (DOPE) or Distearoyl phosphatidylcholine (DSPC)), polyethylene glycol (PEG) lipids and cholesterol (Kumar, Qin, et al. 2014; Li et al. 2015) are necessary to decrease toxicity, increase

endosomal escape and protect from activating the immune system. They also allow for enhanced particle stability, transfection and blood compatibility (Cheng and Lee 2016). Lipid-anchored PEG serves many additional purposes: reduction of particle size, minimization of serum protein binding, increase of circulation time and shielding from macrophages (Kanasty et al. 2013). Finally, significant progress has been made to develop lipids or lipidoids that are better suited to the type of oligonucleotide that is encapsulated (Guimaraes et al. 2019; Fenton et al. 2017; Kauffman et al. 2015; Dong et al. 2014; Love et al. 2010).

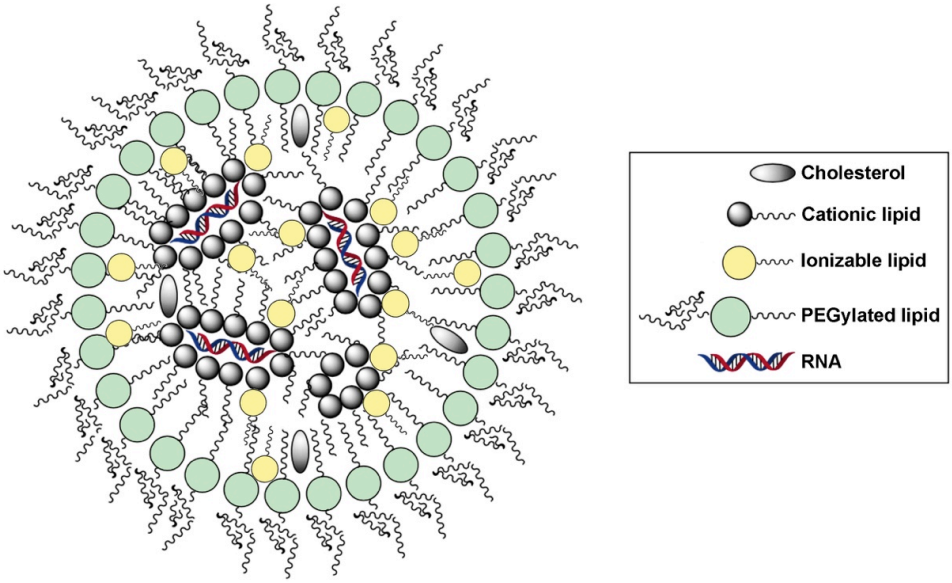

Figure 13: **Lipid nanoparticles used in this study.** The ionizable lipid used in the formulation is C12-200 (Love et al, 2010). Adapted from Zatsepin et al, 2016.

Nonetheless, despite significant advances in making LNPs less reactive to the immune system, repeated injections of LNPs, especially if they are coated in pegylated lipids, may cause rejection due to recognition by the immune system. This is caused in part by the Accelerated Blood Clearance phenomenon first characterized by Dams et al. (Dams et al. 2000) when they showed that the first dose of PEGylated liposomes, injected into rats and rhesus monkeys, caused enhanced clearance of the second dose of PEGylated liposomes, injected one week later. Accelerated Blood Clearance phenomenon occurs via two mechanisms: production of IgM against the PEGylated surface and acquisition of T

lymphocyte mediated immunity (Besin et al. 2019; Mohamed et al. 2019). Since polyethylene glycol is present in a range of products starting from toothpaste to chemotherapeutic drugs, many humans already have developed immunity against this polymer (Schellekens, Hennink, and Brinks 2013). Therefore, a great deal of effort has been expended on improving the PEG coating, not only for a decreased immune reaction, but also not to hinder uptake by hepatocytes.

Uptake

Clearance of the lipid nanoparticles from the blood stream into hepatocytes is mediated by the serum protein apolipoprotein E, which covers LNPs while in circulation, and binds to the low-density lipoprotein receptor (LDLR), other LDLR family members or scavenger receptors on the surface of hepatocytes (Akinc et al. 2010; Yan et al. 2005). The precise mechanism by which cells uptake nanoparticles is still under investigation, and can involve clathrin-dependent endocytosis, followed by macropinocytosis (Gilleron et al. 2013) or clathrin-calveolin-independent endocytosis mechanisms such as flotillin-mediated, Arf6-mediated or Graf1-mediated endocytosis (Juliano 2018). A recent study demonstrated that each cell type has a preferred endocytosis mechanism, and that the way in which the nanoparticle enters the cell influences the molecular composition of the endosome, the intracellular trafficking and the actual processing of the cargo (Vocelle, Chan, and Walton 2020). Therefore, one way to increase specificity and efficacy is to design lipid nanoparticles that favor the preferred endocytosis mechanism, ensuring better uptake. Once inside the endosome, the cationic and ionizable lipids of the particle interact with the membrane lipids to form a non-bilayer lipid phase that disrupts the endosomal membrane and releases the content including the siRNA to the cytosol (Zelphati and Szoka 1996). However, this is a very inefficient process, since only 1-2% of the entrapped siRNA actually reaches the cytoplasm (Gilleron et al, 2013). Nevertheless, this is sufficient to reach significant downregulation of target genes.

While most cationic and ionizable lipid-based nanoparticle formulations deliver siRNA to the liver at more than 90% (Akinc et al. 2009; Love et al. 2010; Dong et al. 2014), some delivery to the kidney, spleen and lungs has been demonstrated. Additionally, professional phagocytic cells such as monocytes, macrophages and neutrophils can

internalize nanoparticles while they are in circulation or in the spleen. In the case of the C12-200 ionizable lipid, delivery to cells of the immune system was demonstrated, and optimization of chemical composition of the LNPs increases this, although much higher doses are required compared to hepatocytes and less target gene downregulation is observed, indicating possible issues with accumulation in tissues without uptake or endosomal escape (Novobrantseva et al. 2012; Leuschner et al. 2011). Indeed, if nanoparticles are phagocytosed, the internalized vesicles will fuse with lysosomes, leading to oligonucleotide destruction due to low pH (Gustafson et al. 2015). Therefore, fine-tuning of the lipid nanoparticle components, including the selection of cationic or ionizable lipids, is needed for non-hepatic delivery, especially to myeloid cells (Whitehead et al. 2014).

Conjugates

Conjugation of oligonucleotides to a biomolecule capable of binding to a receptor present in sufficient quantities on the cells of a particular organ is another efficient mean of specific targeted delivery. Examples of these conjugated biomolecules include folate; cholesterol; antibodies; aptamers (for example, the A10 aptamer specific for PSMA expressed on prostate cancer cells); peptides (the cRGD peptide that binds to αVβ3/5 integrins that are expressed at a high level in tumor cells and vascular endothelium cells; the SPACE peptide, which promotes penetration of the siRNA through the epidermis and dermis following application on the skin surface); and receptor ligands (N-acetylgalactosamine) (reviewed in (Chernikov, Vlassov, and Chernolovskaya 2019)). Oligonucleotide conjugates with a trimer of N-acetylgalactosamine (GalNAc) (Nair et al. 2014; Prakash et al. 2014), avidly binds to the asialoglycoprotein receptor (ASGPR) that is predominantly expressed on liver hepatocytes. Indeed, the sinusoidal surface of the hepatocyte expresses 25,000-50,000 ASGPR molecules at any given time, which represents 5-10% of the actual amount of ASGP receptors in the cell (Steer and Ashwell 1980). Since the first iterations of the GalNAc conjugate, many new structures of the GalNAc trimer as well as linkers connecting the different moieties of the molecule have been explored to improve penetrance, endosomal escape and reduce inhibition of the biological activity of the oligonucleotide (Sharma et al. 2018; Cedillo et al. 2017). GalNAc-mediated delivery revolutionized RNA therapeutics due to selective delivery to hepatocytes in vivo through the

ASGP receptors, which resulted in outstanding safety profiles (Huang 2017). However, because the oligonucleotides are unshielded during transport to the liver, conjugated nucleic acid oligos must be chemically modified to sustain ribonucleases present in the blood, avoid immune detection and decrease toxicity.

RNA interference in the clinic

In the last decade, many new treatments based on RNA interference have hit the market (Table 1) and more than 12 are in ongoing or completed clinical trials, for cancer treatment alone (clinicaltrials.org). The FDA approved the first LNP-siRNA based treatment for herediraty transthyretin amyloidosis (Onpattro, (Akinc et al. 2019)) in 2018 and Givosiran, the first chemically modified siRNA conjugated to GalNAc, in 2019 (Scott 2020), for the treatment of acute hepatic porphyria. A second conjugate, Inclisiran, which targets the protein PCSK9 for the treatment of familial hypercholesterolaemia has successfully passed Phase III clinical trials (Ray et al. 2020). Most of the approved RNAi treatments are based on antisense oligonucleotides (ASO), probably due to the fact that they are more universal and can be injected without a delivery platform, as they can penetrate cells in a clathrin-independent manner (Koller et al. 2011). However, ASOs are prone to off-target effects because the RNase H activity can be initiated by a DNA/RNA duplex as small as 5 nucleotides (Dias and Stein 2002). Additionally, owing to the requirements of the RNase H for recognition of the duplex, ASOs are less tolerant to chemical modifications, especially those made to the 2'OH group, which could interfere with the efficacy of the anti-sense oligonucleotide (Moelling, Broecker, and Kerrigan 2014; Crooke et al. 2018). This gives a significant advantage to siRNA, as they can be heavily modified to avoid nuclease-mediated destruction and improve on-target activity. The simplicity of the design, the flexibility of the platform and the efficient delivery of the siRNA technology will most likely encourage the development of many therapies using this strategy, especially in cases where inhibitors against the protein are impossible to create.

RNA interference and derived technologies have been extensively used to interrogate molecular pathways in both normal physiology and disease and are now a cornerstone in the development of new treatments for cancer. Additionally, many studies

show promising results using a combination of targeted gene downregulation with immune checkpoint inhibitors (Ganesh et al. 2018; Matsuda et al. 2019), with chemotherapy (Tang et al. 2019; Van Woensel et al. 2017), or with small molecule anti-cancer drugs, particularly those which can be used as carriers for siRNA (Saraswathy and Gong 2014; Steinborn et al. 2018). In this work, we used the power of siRNA as a tool to explore the biology of the UBR ubiquitin ligases of the Arg/N-degron pathway, in the normal liver as well as in a cancer setting, to determine if these proteins could become targets in therapy against cancer.

Table 1: RNAi drugs approved by the FDA

Name	Company	Date FDA approval	Target	Disease	Type of drug and delivery system	ref
Vitravene (Fomivirsen)	Iris Pharmaceuticals Novartis	1998	CMV-IE-2	CMV retinitis	ASO Intravitreal injection	[1]
Kynamro (Mipomersen)	Ionis Pharmaceuticals Kastle Therapeutics	2013	apoB	Homozygous familial hypercholesterolemia	ASO Subcutaneous injection	[2-4]
Exondys 51 (Eteplirsen)	Sarepta Therapeutics	2016	dystrophin	Duschene muscular dystrophy	ASO IV solution	[5]
Spinraza (Nusinersen)	Ionis Pharmaceuticals Biogen	2016	SMN1 and SMN2	Spinal Muscular Atrophy	ASO Intrathecal injection	[6]
Onpattro (Patisiran)	Alnylam	2018	TTR	Hereditary transthyretin amyloidosis	siRNA in LNP IV injection	[7]
Givlaari (Givosiran)	Alnylam	2019	ALAS1	Acute Hepatic Porphyria	siRNA-GalNAc SC injection	[8]

ASO: antisense oligonucleotide; IV: intra venous; SC: subcutaneous

1. Vitravene Study G (2002) Am J Ophthalmol 133(4):467-474.
2. McGowan MP, et al. (2012) PLoS One 7(11):e49006.
3. Stein EA, et al. (2012) Circulation 126(19):2283-2292.
4. Thomas GS, et al. (2013) J Am Coll Cardiol 62(23):2178-2184.
5. Mendell JR, et al. (2016) Ann Neurol 79(2):257-271.
6. Wurster CD & Ludolph AC (2018) Ther Adv Neurol Disord 11:1756285618754459.
7. Akinc A, et al. (2019) Nat Nanotechnol 14(12):1084-1087.
8. Scott LJ (2020) Drugs 80(3):335-339.

Chapter 3
Materials and Methods

siRNA description and LNP formulation

We designed chemically modified siRNAs targeting mouse Ubr1, Ubr2, Ubr4 or Ubr5 (10 siRNA per gene) (NCBI Genbank accession codes NM_009461.2, NM_001177374.1, NM_001160319.1, NM_001081359.3) (Table 2). siRNA were selected to avoid off-target activity based on several known criteria (Reynolds et al. 2004; Anderson et al. 2008; Pei and Tuschl 2006). Candidate 19-mer sequences were aligned against RefSeq mRNA database and estimated for their off-target binding capability. In particular, siRNA were ranked based on the number/positions of the mismatches in the seed region, mismatches in the non-seed region, and mismatches in the cleavage site position. The resulted sequences were further filtered to avoid known miRNA motifs and immune stimulatory sequence motifs (Pei and Tuschl 2006; Frank-Kamenetsky et al. 2008). Introduction of 2'-OMe pyrimidine nucleotides in siRNA further reduces immune response and off-target effects (Jackson et al. 2006; Pei and Tuschl 2006) and together with the use of 3'-internucleotide phosphorothioates increases stability against nucleases. Potency and efficacy of siRNA targeting Ubr1, Ubr2, Ubr4 and Ubr5 were studied by transfection in Hepa1–6 cells followed by quantitative PCR (qPCR) analysis after 24h. siRNA with the lowest IC50 and highest downregulation of the target were selected for further studies (Table 2, siRNA in bold). The control siRNA targets the Firefly Luciferase gene (si-Ctrl).

Table 2:Selected siRNA used in the study

		Sense	Anti-sense
si-Ctrl	si-LUC	cuuAcGcuGAGuAcuucGATsT	UCGAAGuACUcAGCGuAAGTsT
si-Ubr1	si-1-1	caAAGuAGuGuucauAAAAdTsdT	UUUuAUGAAcACuACUUUGdTsdT
	si-1-2	ccuucGGuGAuAAaAuAcAdTsdT	UGuAUUUuAUcACCGAAGGdTsdT
	si-1-3	gguuAuGGcucAccAGAAAdTsdT	UUUCUGGUGAGCcAuAACCdTsdT
	si-1-4	gacuuuAGAcAGAuAuuuudTsdT	AAAAuAUCUGUCuAAAGUCdTsdT
	si-1-5	gacAGGAAcAAuAaAuucAdTsdT	UGAAUUuAUUGUUCCUGUCdTsdT
	si-1-6	**caGAcuAGGuGcuauuucAdTsdT**	**UGAAAuAGcACCuAGUCUGdTsdT**
	si-1-7	gauuAAAcAGuAuaAuAcAdTsdT	UGuAUuAuACUGUUuAAUCdTsdT
	si-1-8	gcuuAGAGAAuGucAuAAAdTsdT	UUuAUGAcAUUCUCuAAGCdTsdT
	si-1-9	ggcccGGcuGuuAcuGAAAdTsdT	UUUcAGuAAcAGCCGGGCCdTsdT
	si-1-10	caGAAuAucGGGuuAuAAudTsdT	AUuAuAACCCGAuAUUCUGdTsdT
si-Ubr2	si-2-1	gauGGuGAAcAGccAAucAdTsdT	UGAUUGGCUGUUcACcAUCdTsdT
	si-2-2	ccAAGAAAAAGuuaGcAuudTsdT	AAUGCuAACUUUUUCUUGGdTsdT
	si-2-3	auuGuuAAGcAAAaGuGAAdTsdT	UUcACUUUUGCUuAAcAAUdTsdT
	si-2-4	aaGuGAAGuGGcAuAuAAAdTsdT	UUuAuAUGCcACUUcACUUdTsdT
	si-2-5	aguGAAGuGGcAuauAAAudTsdT	AUUuAuAUGCcACUUcACUdTsdT
	si-2-6	aguGGcAuAuAAAuuuccAdTsdT	UGGAAAUUuAuAUGCcACUdTsdT
	si-2-7	gcuccuAccucuAaGuGAAdTsdT	UUcACUuAGAGGuAGGAGCdTsdT
	si-2-8	gauAGAAcAuccucuuAGAdTsdT	UCuAAGAGGAUGUUCuAUCdTsdT
	si-2-9	**ggcGAGAGAuGuucGAcAAdTsdT**	**UUGUCGAAcAUCUCUCGCCdTsdT**
	si-2-10	gacuAuGGGAAGAgAuucAdTsdT	UGAAUCUCUUCCcAuAGUCdTsdT
si-Ubr4	si-4-1	caAAGAAGAuGAcuAcGAAdTsdT	UUCGuAGUcAUCUUCUUUGdTsdT
	si-4-2	gcAAGuGuAGuucaGuGAAdTsdT	UUcACUGAACuAcACUUGCdTsdT
	si-4-3	gaAccuAGGGuuuccGAAAdTsdT	UUUCGGAAACCCuAGGUUCdTsdT
	si-4-4	gcAuuuGGcuGuuaGccAudTsdT	AUGGCuAAcAGCcAAAUGCdTsdT
	si-4-5	cgAucAAccuGuAcuAcAAdTsdT	UUGuAGuAcAGGUUGAUCGdTsdT
	si-4-6	cacGGAGcAuuGuauuAcAdTsdT	UGuAAuAcAAUGCUCCGUGdTsdT
	si-4-7	**ggAcAuGAccAcAgGuAcAdTsdT**	**UGuACCUGUGGUcAUGUCCdTsdT**
	si-4-8	gccGGuAucAAGAacAAcAdTsdT	UGUUGUUCUUGAuACCGGCdTsdT
	si-4-9	ccAuGGAAAuGAGauuGAAdTsdT	UUcAAUCUcAUUUCcAUGGdTsdT
	si-4-10	gcuuGAGuGuGuAcAucuudTsdT	AAGAUGuAcAcACUcAAGCdTsdT
si-Ubr5	si-5-1	agcuGAAcAAGuAcAAuuudTsdT	AAAUUGuACUUGUUcAGCUdTsdT
	si-5-2	ggAGcAGGcuAcuauuAAAdTsdT	UUuAAuAGuAGCCUGCUCCdTsdT
	si-5-3	ggcAcAAGuuGuucuAcAAdTsdT	UUGuAGAAcAACUUGUGCCdTsdT
	si-5-4	**ugAuAAGGAuGGAacAAAAdTsdT**	**UUUUGUUCcAUCCUuAUcAdTsdT**
	si-5-5	guAGcuAcuGAAAauAAcAdTsdT	UGUuAUUUUcAGuAGCuACdTsdT
	si-5-6	ccGAGAAGAcuGAaAuAcudTsdT	AGuAUUUcAGUCUUCUCGGdTsdT
	si-5-7	gcGcucAGAAAGAaAuAcAdTsdT	UGuAUUUCUUUCUGAGCGCdTsdT
	si-5-8	gaAucAGGGAGGAucGcAAdTsdT	UUGCGAUCCUCCCUGAUUCdTsdT
	si-5-9	ggcuucGuccAAAaAGAAAdTsdT	UUUCUUUUUGGACGAAGCCdTsdT
	si-5-10	caGccAAuuGGAAaAuGcAdTsdT	UGcAUUUUCcAAUUGGCUGdTsdT

Uppercase letters: ribonucleotides; Lowercase letters: 2′-O-Methyl nucleotides; s: phosphorothioate

The siRNA were formulated in Lipid nanoparticles (LNP) as previously described (Bogorad et al. 2014). Briefly, LNPs were formed by mixing solutions of siRNA in acidic water buffer and lipids in ethanol (3:1, v:v) using the microfluidic NanoAssemblr device (Precision NanoSystems) as described earlier (Whitehead et al. 2014). siRNA (0.4 mg/ml for individual siRNA or 0.1 mg/ml of each for a mix of four ones) are first diluted in a 10 mM citrate buffer (pH 3.0) while lipids (C12-200 (Love et al. 2010):DSPC (850365, Avanti Polar Lipids):cholesterol (C8667, Sigma-Aldrich):PEG-lipid (880150, Avanti Polar Lipids) are prepared at a 50:10:38.5:1.5 mol:mol ratio in ethanol (8.83 mg/ml total). siRNA and lipid solutions were mixed at a 10 ml/min rate according to the manufacturer's protocol. The final ratio of siRNA:C12-200 after mixing is 1:5, w:w. The LNP suspension was diluted in PBS buffer, dialyzed against 500 volumes of PBS at pH7.4 in 20,000 MW cutoff dialysis cassettes (66012, Thermo Fisher Scientific) overnight and filtered through a PES syringe filter (0.2 µm pores) (3915, Corning). Particle size and zeta potential measurements were performed using a Zetasizer Nano ZSP (Malvern Panalytical) according to the manufacturer's protocol (Table 3). Zeta potential measurements were conducted under neutral pH conditions. Reported values are the average of 10–25 runs. siRNA entrapment efficiency was determined using the Quant-iT™ RiboGreen® reagent (R11491, Thermo Fisher Scientific) as described earlier (Walsh et al. 2014).

Table 3: Characteristics of lipid nanoparticles used in our study.

LNP-siRNA	Particle size, nm	Polydispersity index, PdI	Zeta potential
LNP si-Ubr1	84.5 ± 1.1	0.093	3.2 ± 1.7
LNP si-Ubr2	85.9 ± 0.6	0.1	3.7 ± 1.7
LNP si-Ubr4	85.4 ± 0.7	0.094	3.4 ± 1.4
LNP si-Ubr5	92.1 ± 2.0	0.1	3.2 ± 1.2
LNP si-Ubrs	94.8 ± 3.7	0.13	2.9 ± 1.5
LNP si-Ctrl	80.0 ± 0.8	0.062	3.9 ± 1.5

Cell culture and transfections

Mouse Hepa1-6, AML-12 and J774A.1 cell lines (ATCC #CRL-1830, CRL-2254, TIB-67 VA) were grown in DMEM supplemented with 10% FBS (Gibco #161400) and 2 mM L-glutamine (Gibco #250300) without antibiotics. Cells were split when they reached 80% confluency. Plasmids were transfected using Lipofectamine 2000 (Invitrogen, #11668), and siRNA were transfected using Lipofectamine RNAiMAX (Invitrogen, #13778), according to

the manufacturer's instructions. Hepa 1-6 cells were treated with doxorubicin (Millipore-Sigma #D2975000) for 48h or Staurosporine (Millipore-Sigma, #S6942) at concentrations mentioned in the text. J774A.1 cells were stimulated with LPS (O11:B4, Sigma #L4391) at 1, 10 or 50 ng/ml for 6h or 24h, with ATP (5mM) added during the last hour, or with staurosporine at 500nM for 24h (Sigma, #S6942) in DMEM with 2% FBS.

cDNA synthesis and qPCR

RNA was prepared by disrupting cells or liver tissue in TRIzol (Invitrogen, #15596), using the MP FastPrep-24 instrument and Lysing Matrix D (MP Biomedicals, SKU116913050-CF), followed by precipitation with isopropanol, according to the manufacturer's instructions. cDNA was generated using the High Capacity cDNA Reverse Transcription Kit (Applied Biosystems, 4368814). Levels of mRNA were assessed by qPCR using SYBR Green (ThermoFisher, A25778), in the QuantStudio 5 thermocycler (Applied Biosystems). The mRNA levels were normalized to the level of the mouse housekeeping gene (mGAPDH) and to the average value of the control group. Specific primers are listed in Table 4.

Cell or tissue extracts and immunoblotting

Cells or tissue were lysed in RIPA buffer (Thermo Scientific, #8990) containing complete protease inhibitor cocktail (Roche, 5892791001) using the MP FastPrep-24 instrument and Lysing Matrix D. The extracts were centrifuged at 12,000×g for 10 min at 4°C. Media samples were concentrated ~6x using ultra-centrifugation filtration units with a MWCO of 3kDa (Amicon, UFC8003). Total protein concentrations in the lysates and supernatants were determined using the BCA assay (Pierce, #2322). Samples were diluted in LDS sample buffer (Thermo, #NP0008) supplemented with 25 mM DTT and heated at 95°C for 10 min, except for detection of UBR4, where samples were heated at 56°C for 30 minutes. Protein analysis was performed in SDS 5–12% PAGE, with 10-100 μg of total protein loaded per lane. PAGE-fractionated proteins were transferred onto nitrocellulose membrane and analyzed by immunoblotting using the following antibodies: anti-UBR1 (Abcam #156436), anti-UBR2 (Abcam #191505), anti-UBR4 (Abcam #86738), anti-EDD (Santa Cruz #515494), anti-GAPDH (Santa Cruz #sc32233), anti-IL-1β (Cell Signaling #12507), anti-

cleaved-caspase-1 (Cell Signaling #4199), anti-caspase-3 (Cell Signaling #14220). Immunoblots were visualized using the SuperSignal West Femto reagent (Pierce #34095) according to manufacturer's instructions, in the Fusion Solo S Imager (Vilber Lourmat).

Table 4: Primers used in this study

Number	Sequence, 5'→3'
1414	AAAAACCGCGGAGGAAACCCAGCTATGCCCACATCCT
1415	AAAAACCGCGGAGGAGTTCCAGCTATGCCCACATCCT
1416	TTTTAATCGATATCTTTAAACCACACCACACCAGG
1417	AAAAACCGCGGAGGACAAATATCCCCCAATAAAAAAGCTC
1418	AAAAACCGCGGAGGAGTTATATCCCCCAATAAAAAAGCTC
1419	TTTTAATCGATGTCTCTGACCCACAGTTCCCC
1420	AAAAACCGCGGAGGACAAAAGATCACCAGTGTAAAACCTCTTC
1421	AAAAACCGCGGAGGAGTTAAGATCACCAGTGTAAAACCTCTTC
1422	TTTTAATCGATGTCTCTGACCCAGAGTTCCCCA
1438	AAAACCGCGGAGGAGATGTTGAAATACAGGGACATACTAGCTT
1439	AAAACCGCGGAGGAGTTGTTGAAATACAGGGACATACTAGCTT
1440	TTTTAATCGATATCATTGGAGTCTTGTGGCTCAC
1447	GGGAATTCCTCGAGATCGATATCGACTACAAAGACGATGACGACAAAGGTTAAT
1448	CTAGATTAACCTTTGTCGTCATCGTCTTTGTAGTCGATATCGATCTCGAGGAATTCCCGC
1451	AAAAACCGCGGAGGATGTGGAATGAAGTACATAGAGACCTCAGCC
1452	AAAAACCGCGGAGGAGTTGGAATGAAGTACATAGAGACCTCAGCC
1453	TTTTAATCGATCATAGCCATACAGAAGCACTCTTTTCTGGGCTT
1530	AAAAACCGCGGAGGAGACGCCGTGCCCATCCAGTCCA
1531	AAAAACCGCGGAGGAGTTGCCGTGCCCATCCAGTCCA
1532	TTTTAATCGATCTGCACAGCGGCGTCCGGG
1964	AAAAACCGCGGAGGAATCATTGGAGGAGACACGGTTGTTCCTC
1965	AAAAACCGCGGAGGAGTTAAGGGAGGAGACACGGTTGTTCCTC
1968	TTTTTATCGATCACAGAACCCTTCATAATCTTCTTTATCC
1979	AAAAACCGCGGAGGAATCATTGGGGGTCGAGAGGCAGTCCCGC
1980	AAAAACCGCGGAGGAGTTAAGGGGGGTCGAGAGGCAGTCCCGC
1983	TTTTTATCGATGACCAAAGATTGGGGTGACCAGCGACCAAT
mGAPDH dir	AGGTCGGTGTGAACGGATTTG
mGAPDH rev	TGTAGACCATGTAGTTGAGGTCA
mUbr1up	CCCAGCAGTTCCTGTCTTGT
mUbr1lo	ATCAGGAGGCACTTTCAGGC
mUbr2up	AGAGTTTTCAGTCGCAGACCT
mUbr2lo	TGATCGGGTCCATTCCCTGC
mUbr4up	GCAGGGAGGGGTACAAGTTC
mUbr4lo	GGCCTCTAGCCAACCTGAC
mUbr5up	AGAACCATTACCACCACGGC
mUbr5lo	CCACCTCAACCTCTTCCACG

Functional assay of the N-degron pathway and immunoblotting

Hepa 1-6 cells were plated at 40% confluency in 24-well plates, and transfected using Lipofectamine 2000 with plasmids encoding native (^{f}DHFR-Ub^{R48}-Asp^{1119}-BRCA1^{f}) or stable (^{f}DHFR-Ub^{R48}-Val^{1119}-BRCA1^{f}) versions of the flag-tagged proapoptotic BRCA1 fragment (Piatkov, Brower, and Varshavsky 2012), with or without siRNA at 2.5 nM. After 72h, cells were lysed with 1% SDS, 5 mM DTT, containing complete protease-inhibitor mixture followed by heating at 95°C for 10 min. Samples were diluted in LDS sample buffer, heated at 95°C for 10 min and followed by SDS 10% PAGE. Membranes were incubated with anti-FLAG M2 antibody (Sigma, F1804) and visualized using SuperSignal West Femto reagents according to manufacturer's instructions, on a Fusion Solo S (Vilber Lourmat) imager.

Cell proliferation, Migration and Apoptosis assays

Hepa 1-6 cells were plated at a density required to reach 80% confluency in 72 or 96h, transfected with siRNA against Luciferase (control) or Ubrs for 72h, at concentrations mentioned in the text, and treated or not with doxorubicin (Millipore-Sigma #D2975000) for 48h or Staurosporine (Millipore-Sigma, #S6942) for 24h. The Neutral Red assay (adapted from Fautz et al (Fautz, Husein, and Hechenberger 1991)) was used to assess proliferation in Hepa 1-6 cells. After treatment, culture media was replaced by a solution of 50 ug/ml Neutral Red (Millipore-Sigma, #N2889) in DMEM supplemented with 10% FBS, for 3h at 37°C, 5% CO_2. Cells were then washed once with PBS and the dye was extracted from the cells by adding elution buffer (50% EtOH, 1% acetic acid). After 5 minutes of incubation, the elution buffer was transferred onto a new plate and absorbance read at 540 nm.

Migration was assessed using a scratch assay, where a monolayer of cells was scraped using a pipette tip. Photos were taken after the initial scratch and 24h later. Migration was evaluated by calculating the distance between the edges of the scratch.

Apoptosis was measured using the fluorescein-based In Situ Cell Death Detection Kit TMR red (Roche, #12156792910). Treated cells were fixed with 4% paraformaldehyde, permeabilized with 0,25% Triton-X-100/0,25% Tween-20 for 7 minutes on ice, and assayed

according to the manufacturer's protocol. Cells were counterstained using Hoechst 33342 (Thermo Scientific, #62249), and analyzed by fluorescence microscopy using the EVOS FL imaging system (Thermo Fisher).

Plasmids

DH5α *Escherichia coli* strain (Invitrogen, #EC0111) was used for cloning and production of plasmids. Phusion High-Fidelity DNA polymerase (New England Biolabs, #M0530) was used for PCR. Sequences of all constructed plasmids were verified by Sanger sequencing. The plasmid pKP496 was constructed by ligation of annealed primers 1447 and 1448 into SacII/XbaI-cut pcDNA3^{f}DHFRUb^{R48}Xpr (Sheng et al. 2002). The resulting plasmid, which encoded the ^{f}DHFR-Ub^{K48R}-MCS (SacII-EcoRI-XhoI-ClaI-EcoRV)-flag fusion, was used to construct the following plasmids for the ubiquitin reference technique (Varshavsky 2005). All plasmids generated in this study are available from the Lead Contact upon request.

hCASP-1. The human Caspase-1 ORF was amplified using cDNA from OpenBiosystems (5583549) and primers 1414 and 1416 for Asn^{120}-hCASP-1 or 1415 and 1416 for Val^{120}-hCASP-1. The resulting fragments were cut with SacII and ClaI and cloned into SacII/ ClaI-cut pKP496, generating the plasmids pKP502 and pKP503, respectively.

hCASP-4. The human Caspase-4 ORF was amplified using cDNA from OpenBiosystems (6276763) and primers 1417 and 1419 for Gln^{81}-hCASP-4 or 1418 and 1419 for Val^{81}-hCASP-4. The resulting fragments were cut with SacII and ClaI and cloned into SacII/ ClaI-cut pKP496, generating the plasmids pKP504 and pKP505, respectively.

hCASP-5. The human Caspase-5 ORF was amplified using cDNA from OpenBiosystems (30915395) and primers 1,420 and 1,422 for Gln^{138}-hCASP-5 or 1421 and 1422 for Val^{138}-hCASP-5. The resulting fragments were cut with SacII and ClaI and cloned into SacII/ ClaI-cut pKP496, generating the plasmids pKP506 and pKP507, respectively.

hRab39a. The human Rab39a ORF was amplified using cDNA from OpenBiosystems (5583549) and primers 1451 and 1453 for Cys^{149}-hRab39a or 1452 and 1453 for Val^{149}-hRab39a. The resulting fragments were cut with SacII and ClaI and cloned into SacII/ ClaI-cut pKP496, generating the plasmids pKP510 and pKP511, respectively.

hPDK1. The human Pdpk1 ORF was amplified using cDNA from OpenBiosystems (4830546) and primers 1530 and 1532 for Asp^{10}-hPdk1 or 1531 and 1532 for Val^{10}-hPDK1. The resulting fragments were cut with SacII and ClaI and cloned into SacII/ ClaI-cut pKP496, generating the plasmids pKP538 and pKP539, respectively.

mGRZA. The mouse GrzA ORF was amplified using a cDNA library derived from the C57Bl/6J mouse RNA and primers 1964 and 1968 for Ile^{29}-mGRZA or 1965 and 1968 for Val^{29}-mGRZA. The resulting fragments were cut with SacII and ClaI and cloned into SacII/ ClaI-cut pKP496, generating the plasmids pDL1 and pDL2, respectively.

mGRZM. The mouse GrzM ORF was amplified using cDNA from C57Bl/6J mouse and primers 1979 and 1983 for Ile^{29}-mGRZM or 1980 and 1983 for Val^{29}-mGRZM. The resulting fragments were cut with SacII and ClaI and cloned into SacII/ ClaI-cut pKP496, generating the plasmids pDL7 and pDL8, respectively.

hBRCA1. The mouse Brca1 ORF was amplified using cDNA from OpenBiosystems (30431022) and primers 1,438 and 1,440 for Asp^{1119}-BRCA1 or 1,439 and 1,440 for Val^{1119}-BRCA1. The resulting DNA fragments were cut with SacII and ClaI and cloned into SacII/ClaI-cut pKP496, generating the plasmids pKP528 and pKP529, respectively.

In Vitro Transcription–Translation–Degradation Assay.

The TNT T7 Coupled Transcription/Translation System (Promega, #L1170), was used to carry out transcription–translation–degradation assays. Reaction samples were prepared according to the manufacturer's instructions. Newly formed proteins in reticulocyte extract were pulse-labeled with L-[^{35}S]methionine (0.55 mCi/mL, 1'000 Ci/mmol; MP Biomedicals)

for 5 min in total volume of 30 μL. The labeling was quenched by the addition of cycloheximide (Sigma, #C4859) and unlabeled methionine to the final concentrations of 0.1 mg/mL and 5 mM, respectively. Unless stated otherwise, the reactions were carried out at 30°C and terminated by the addition of an equal volume of TDS (Tris-dodecylsulfate) buffer (1% SDS, 5 mM DTT, 50 mM Tris·HCl, pH 7.4, also containing complete protease inhibitor mixture) followed by heating at 95°C for 10 min. The resulting samples were diluted with 10 volumes of TNN (Tris-Nonidet-NaCl) buffer (0.5% Nonidet P-40, 0.25 M NaCl, 5 mM EDTA, 50 mM Tris·HCl, pH 7.4, also containing complete protease-inhibitor mixture), and the amounts of ^{35}S were measured by precipitating an aliquot with 10% trichloroacetic acid, followed by counting in a Liquid Scintillation counter (Beckman Coulter LS6000). For immunoprecipitation, samples were adjusted to contain equal amounts of total ^{35}S and were added to 10 μL beads with an immobilized antibody, anti-FLAG M2. The samples were incubated with rocking at 4°C for 4h, followed by four washes with TNN buffer, resuspension in 20 μL SDS sample buffer, and heating at 95°C for 10 min followed by SDS 4–15% PAGE and autoradiography. Quantification of autoradiograms was carried out using PhosphorImager and ImageQuant software (Molecular Dynamics).

Caspase-1 activity assay

Caspase-1 activity was measured using the bioluminescent Caspase-Glo 1 Inflammasome Assay (Promega, #G9951) in cell supernatants from J774A.1 cells stimulated with 100ng/ml LPS (O11:B4) or 500 nM staurosporine for 24h, following the manufacturer's instructions using Ac-YVAD-CHO as a specific caspase-1 inhibitor.

Animal care and treatments

All animal care and procedures were carried out according to the relevant National Institutes of Health guidelines, and were approved by the Institutional Animal Care and Use Committee and the Office of Laboratory Animal Research at the Massachusetts Institute of Technology (MA, USA) and the Institute of Developmental Biology (Moscow, Russia), where the present study was performed. C57BL/6 or FVB/N mice of 6-8 weeks of age were

purchased from Charles River or bred in house. Mice were housed at 22 °C using a 12 h light to 12 h dark cycle, fed *ad libitum* with regular rodent chow. Lipid nanoparticles and doxorubicin were diluted in sterile saline and injected via tail vein (i.v.) at doses and regime specified in the text. Hepatocellular carcinoma was induced in FVB/N mice as previously described (Bogorad et al. 2014), using plasmids encoding human ΔN90-β-catenin, human MET and Sleeping Beauty transposase (Tward et al. 2007). α-fetoprotein levels in the serum were tested by Western Blot at day 35 (anti-AFP, R&D systems, #BAF5369). Animals were euthanized on days 66-68 post tumor induction unless otherwise mentioned. Serum for analysis and liver samples for histology and immunohistochemistry were collected, the rest of the liver was snap frozen and ground. Aliquots of homogenized liver were used for mRNA and protein analysis.

Histological and immunohistochemical analysis of liver samples

Liver samples were fixed in 4% buffered paraformaldehyde and embedded with paraffin using standard procedures. 5-µm-thick sections were subjected to hematoxylin-eosin (H&E) staining or immunohistochemistry. H&E staining was performed using a ThermoShandon Gemini automated stainer (Eosin and Hematoxylin from Leica Biosystems). The envision system (Dako) was used for indirect peroxidase reaction using DAB to detect Ki67 (BioCare Medical). TUNEL staining was performed on liver sections treated with proteinase K using the In Situ Cell Death Detection Kit, TMR red. The sections were counterstained with Hoechst 33342 and analyzed by fluorescence microscopy using the EVOS FL imaging system.

Blood biochemistry

Serum was collected by cardiac puncture followed by centrifugation at 1700g for 20 minutes. Biochemical analysis was performed by IDEXX Laboratories, Inc., Westbrook, Maine, U.S.A.

Flow cytometry

Spleens were disrupted manually using the blunt end of a syringe plunger, while livers were incubated in Collagenase Type IV (Worthington, #LS004188) (0.5mg/ml in HBSS with Ca^{2+}, 5mM HEPES, 0.5mM EDTA) for 30 minutes before manual disruption and gradient separation using Optiprep (Cosmo Bio, #NC1059560). Cells were resuspended at a density of $1x10^7$ cells/mL in DMEM with 2% FBS, and were incubated 15 minutes at room temperature with diluted monoclonal antibodies and then washed and resuspended in PBS with 2% FBS for immediate analysis. The following monoclonal antibodies were used from BioLegend (San Diego, CA): FITC-anti-CD11b (M1/70); PE-anti-F4/80 (BM8); PerCPCy5.5-anti-CD11c (N418), PeCy7-anti-B220 (RA3-6B2); BV421-anti-Ly6G (1A8); BV510-anti-CD45 (30-F11); APC-anti-IA/IE (M5/114.15.2); APCFire-anti-Ly6C (HK1.4). Annexin V/7AAD staining was performed according to the manufacturer (Biolegend). Data was acquired using a BD LSRFortessa™ and analysis of flow cytometry data was performed using FlowJo software (BD Bioscience, San Jose, CA).

Cytokine Bead Assay (CBA)

Cytokine levels were measured by the Cytokine Bead Assay (BD Bioscience, Flex Set #560232) according to the manufacturer's instructions. Briefly, cell culture media was concentrated 5-6x using ultra-centrifugation filtration units with a MWCO of 3kDa (Amicon, UFC8003), following manufacturer's instructions. Total protein concentrations in the supernatants were determined using the BCA assay, and 160μg of protein was assessed in each sample. Data was acquired using a BD LSRFortessa™ and analysis of flow cytometry data was performed using FlowJo software (BD Bioscience).

Bioinformatic analysis of caspase substrates

Human inflammation caspase cleavage sites were collected from the MEROPS database (Rawlings, Barrett, and Finn 2016). The search for orthologous sites was produced using pBLAST (Altschul et al. 1997) with an e-value cutoff of $1e^{-16}$. The database subset was obtained from a non-redundant database restricted by taxon Vertebrates (txid: 7742). Input

sequences for pBLAST including human octamer (P4-P4') +/- 26 surrounding amino acids, 60 amino acids in total, were retrieved from the Uniprot database (The UniProt Consortium 2017). Subsequent data analysis was performed using an in-house package R language (R Core Team 2013).

For apoptotic caspase substrates, all data analysis, statistical treatment, and visualization were completed using the R free software (version 3.6.2) (R Foundation for Statistical Computing, Vienna, Austria), package "Tidyverse" (Wickham 2017). Scripts are available online at Github. URL https://github.com/mpyatkov/caspases.

1. Gathering human apoptotic caspase cleavage sites

Human apoptotic caspase cleavage sites were collected from existing databases: MEROPS (Rawlings, Barrett, and Finn 2016), CutDB (Igarashi et al. 2007), Degrabase (Crawford et al. 2013), CaspDB (Kumar, van Raam, et al. 2014), and from the literature. Only experimentally approved sites obtained after direct activation of apoptosis by any caspase were considered; predicted targets and results of machine learning were excluded. Although caspases can cleave after glutamate (Seaman et al. 2016), only P1 D-cut sites were kept for later analysis, because the functional significance of P1 E-cut sites is still unclear. Obsolete Uniprot IDs, duplicates, and readthroughs were filtered out. Pseudogenes were kept if they had Uniprot evidence at the protein level.

2. Search for vertebrate orthologs of human apoptotic caspase cleavage sites, selection of species with a well-represented proteome

The search for orthologs of human apoptotic caspase cleavage sites was done using pBLAST (Altschul et al. 1997), with default parameters and an e-value cut-off of $1e^{-16}$, and on the vertebrate subset of a non-redundant (NR) protein database. Input sequences for pBLAST, including the human octamer cleavage sites +/- 26 surrounding amino acids for a total of 60 amino acids (Figure 14a), were retrieved from the Uniprot database (The UniProt 2017) using an R script (Team 2013). In similar studies, the authors used whole proteins as a query sequence to search for orthologs. We chose partial sequences (60-amino acids) because they help to locate orthologs more precisely while being representative for the

search of structure similarity. When pBLAST found a batch of orthologs within a single species, we kept only one hit sequence per species with the highest e-value, to avoid duplicates. Selection of the threshold for proteome representation was based on the distribution of species by total number of proteins in the vertebrate subset of a non-redundant database and the number of matches with 3363 human caspase targets (Figure 14b); 328 species with a well-represented proteome (N proteins per species > 8000) were selected for the following analyses.

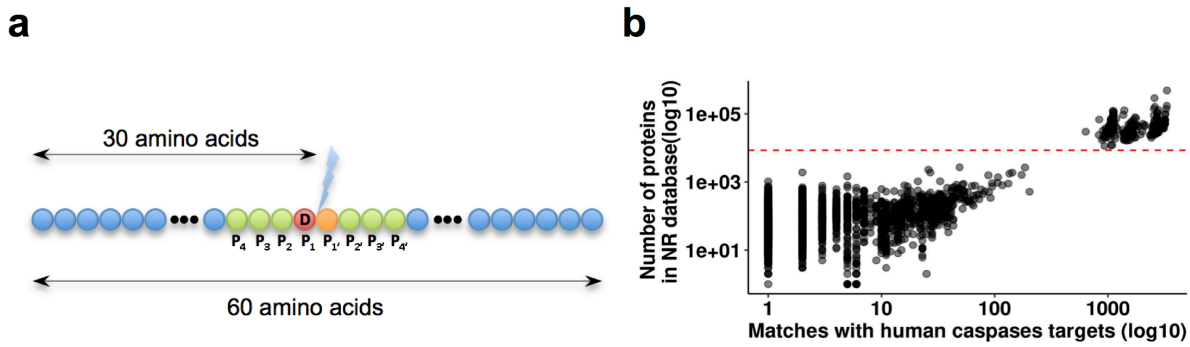

Figure 14. **Identification of human caspase substrates and search for orthologs.** (a) The 60-amino-acid sequences surrounding the human caspase substrates were retrieved from the Uniprot database and used as a query to identify the orthologs for each substrate. (b) Only the species with a well-represented proteome were conserved for future analysis (top right corner).

3. Identification of the caspase cleavage site and P1 Aspartate in orthologs, prediction and analysis of the secondary structure and estimation of hydrophobicity indices

Orthologous cleavage sites and P1 amino acids were located using Hamming distance estimation (Hamming 1950) between human and orthologous 60-amino acids sequences with P1 aspartate as an anchor. This approach is algorithmically simpler and faster than using any type of alignment. For eight-amino acid sequences, Hamming distances range from 0 to 8, 0 meaning that there are no differing amino acids and that the sequences are identical, 8 meaning that all eight amino acids are different.

Secondary structure prediction was performed using the web-service MUFOLD (Fang, Shang, and Xu 2018). As a query, we used the same human 60-amino acid sequences that were used to search for orthologs. The results of prediction were described in Q3 accuracy terms: helix (H), strand (E), and coil (C).

Hydrophobicity indices are defined as the free energy required to transfer amino acid side-

chains from cyclohexane to water and are expressed as kilo-calories per mole. The indices for each of the 20 amino acids, in a distribution from non-polar to polar at pH = 7, were taken from Radzicka & Wolfenden (Radzicka and Wolfenden 2002).

4. Pathway Analysis

The final list of 99 proteins containing 107 conserved apoptotic caspase targets was submitted to the DAVID free online software (Huang da, Sherman, and Lempicki 2009). Pathway enrichment was performed for two sets of annotation terms: Gene Ontology (Thomas et al. 2019) and Uniprot (The UniProt Consortium 2017), with post-hoc adjustment by Benjamini–Hochberg correction. Adjusted p-values less than 0.05 were taken as significance threshold for enrichment.

RNA sequencing and analysis

RNA was extracted from mouse liver using Trizol (Invitrogen), as per the manufacturer's protocol. The concentration of RNA samples was measured with a Qubit fluorometer (Thermo Fisher) and RNA length distribution and integrity was assessed with Bioanalyzer2100 (Agilent). RNA library preparation was performed on 1μg of RNA. PolyA mRNA was selected using magnetic beads with oligo-dT oligonucleotides according to the manufacturer (NEBNext Poly(A) mRNA Magnetic Isolation Module, Cat# E7490). RNA fragmentation, annealing to random hexamer primers, synthesis of cDNA strands, ligation of adapters and PCR were done using the NEBNext Ultra II RNA kit (Cat# E7770), according to the manufacturer's protocol. Sequencing was performed on Nextseq500 (Illumina) with a read length of 84 nt.

Analysis: To map the samples, genome annotations were obtained from Ensembl, release 93. Paired-end reads were mapped using STAR v2.5.3a (Dobin et al. 2013) with default settings except for: –quantMode GeneCounts. The resulting gene counts were further processed with R using the package DESeq2 (Love, Huber, and Anders 2014), and normalized using the RLE method. Moreover, in order to take into account unwanted variation in the data, we introduced into the design matrix additional variables, obtained by the sva package (Leek 2014), that capture the unwanted variation. The DESeq2 package was

used to perform differential expression analysis based on Wald test. We defined genes as differentially expressed if they passed the thresholds: FDR < 0.05 and |log2foldChange| > 0.5. Additionally, we used SAJR R package (Mazin et al. 2013) to estimate the splicing events for each gene. This package allows to calculate the inclusion ratio for each exon.

Statistical analysis

Prism 7 (GraphPad Software, La Jolla, CA) was used for statistical analyses. 2-tailed, unpaired Mann-Whitney tests with 95% confidence bounds, or one-way or two-way ANOVAs were used for statistical analysis unless otherwise indicated. A P value < 0.05 was considered significant.

Chapter 4
Results

Study of UBR-ubiquitin ligases of the Arg/N-degron pathway in normal and HCC liver

Knockdown of UBR-ubiquitin ligases in vitro

To target and silence the mouse UBR1, UBR2, UBR4 and UBR5 mRNA, we designed 19-mer siRNA sequences for each gene and ranked them based on their possible off target recognition and known miRNA and immune stimulatory sequence motifs (see Materials and Methods for the detailed design strategy) (Reynolds et al. 2004; Anderson et al. 2008; Pei and Tuschl 2006). The 10 best scored siRNA against each UBR ubiquitin ligase (Table 2) were screened in Hepa 1-6 cells by transfection and subsequent qPCR analysis (Figure 15). The two most highly potent and effective siRNA probes for each UBR ubiquitin ligase were chosen and used in further studies (Table 5). The low IC50 allows using low concentrations of siRNA, which additionally decreases the possibility of off-target effects. A concentration of 0.25 nM of each siRNA was found to be sufficient to reach 70-80% downregulation of the protein after 72h (Figure 16) in Hepa1-6 and AML-12 cells.

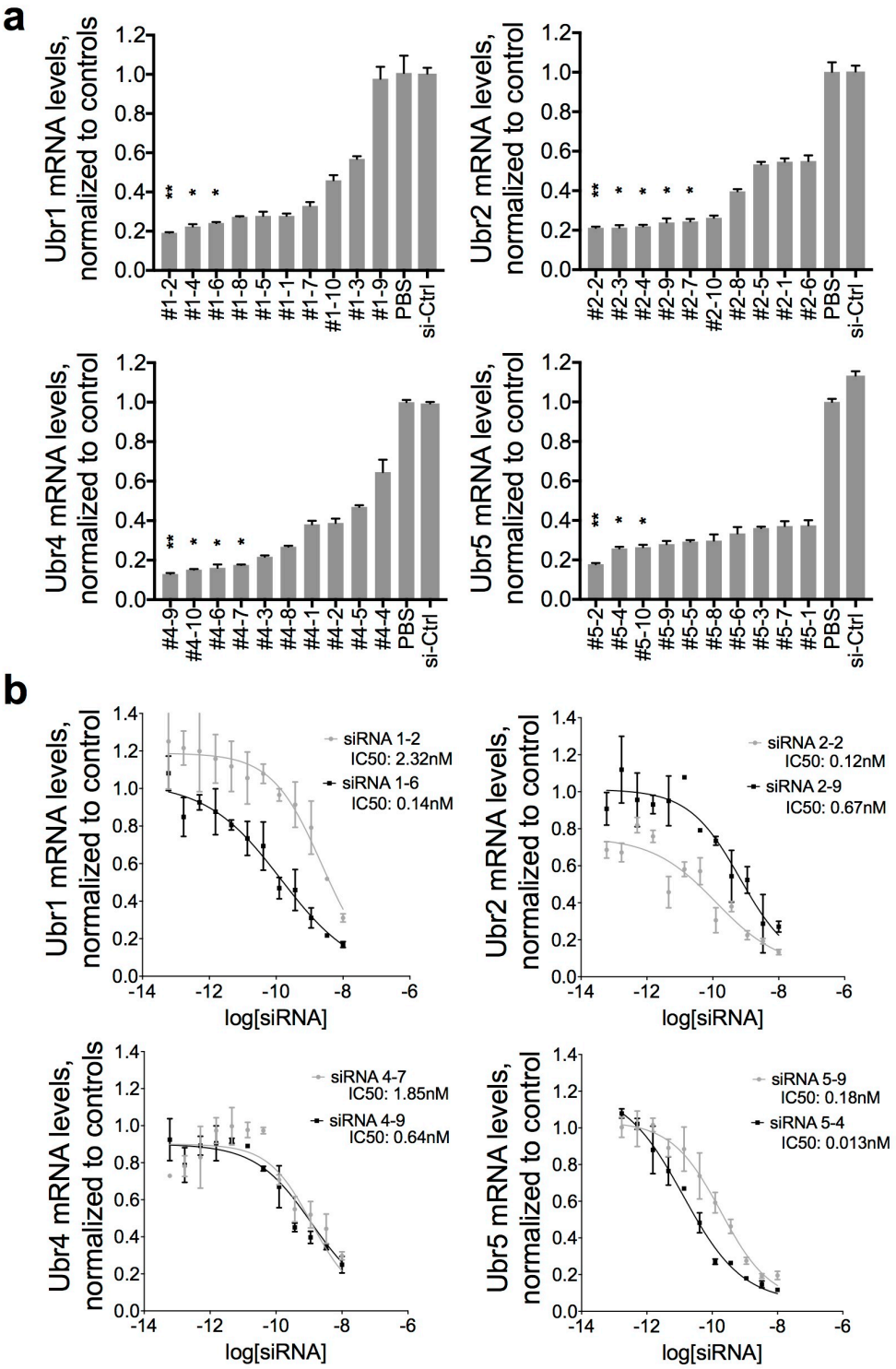

Figure 15. Selection of siRNA, in vitro. (a) mRNA downregulation in Hepa 1-6 cells by 1nM of specific siRNA against UBR1, UBR2, UBR4 or UBR5. mRNA levels were analyzed 24h post transfection. (b) Dose-dependence of mRNA downregulation in Hepa 1-6 cells. mRNA levels were analyzed 24h post transfection (mean ± SD). n=3 biological replicates per condition. P values were obtained using a one-way ANOVA, comparing to controls. (*P <0.05, **P< 0.005)

Table 5: Characteristics of selected siRNA. The numbers in bold are the siRNA formulated into nanoparticles and used throughout the study

	Name	% downregulation at 1nM, 24h	IC50 (95% CI)	Set*
UBR1	si-1-2	81 ± 0.5	2.33 nM (0.04 to 132.9)	(2)
	si-1-6	76 ± 1.0	0.14 nM (0.01 to 1.37)	(1)
UBR2	si-2-2	79 ± 1.0	0.13 nM (0.01 to 1.73)	(2)
	si-2-9	76 ± 1.0	0.67 nM (0.04 to 11.6)	(1)
UBR4	**si-4-7**	82 ± 0.5	1.86 nM (0.20 to 176.4)	(1)
	si-4-9	87 ± 1.0	0.64 nM (0.07 to 5.58)	(2)
UBR5	**si-5-4**	74 ± 1.0	0.01 nM (0.01 to 0.03)	(1)
	si-5-9	72 ± 2.0	0.18 nM (0.08 to 0.44)	(2)

* In vitro experiments were performed using the set of siUbrs (1), unless specified otherwise

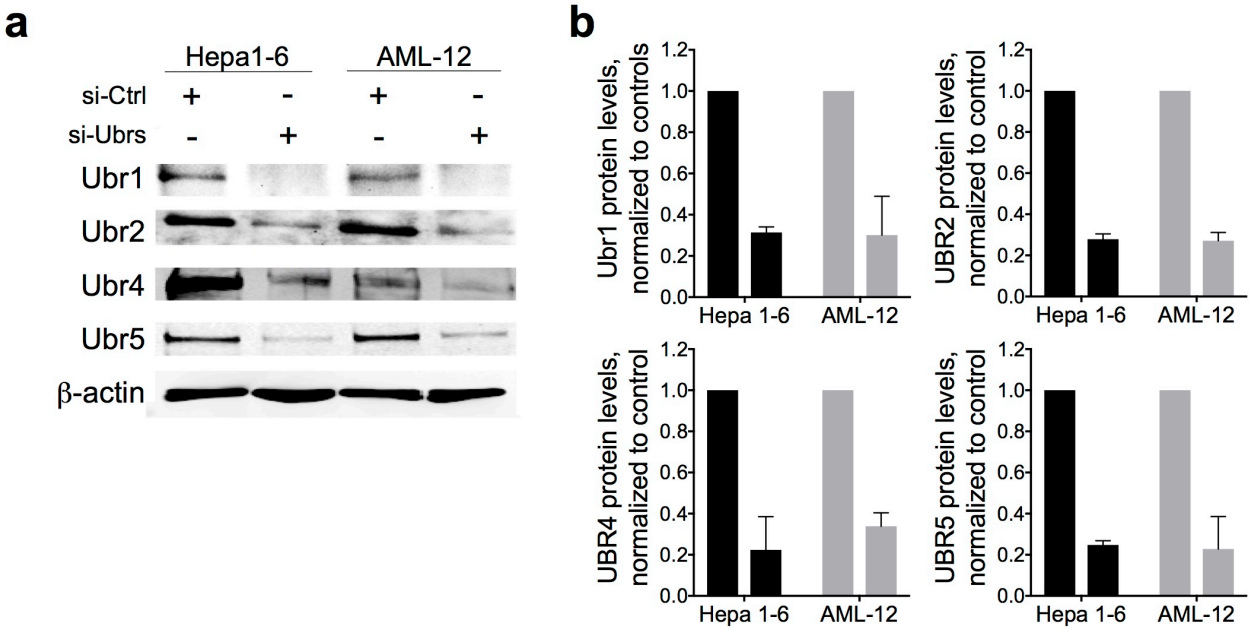

Figure 16. Downregulation of UBR-Ubiquitin ligases of the N-degron pathway, in vitro. (a) Western Blot analysis of UBR1, UBR2, UBR4 and UBR5 proteins in Hepa 1-6 and AML-12 cells after 72h of exposure to 1nM siRNA. b) Quantification of protein UBR expression in Hepa 1-6 and AML-12 cells after 72h of exposure to 1nM siRNA. n=3-5 biological replicates per condition.

Next, the Asp^{1119}-BRCA1 degradation reporter was used to prove that the observed downregulation of Arg/N-degron ubiquitin ligases is sufficient to decrease the functional activity of the pathway (Piatkov, Brower, and Varshavsky 2012). This reporter system is comprised of a ubiquitin molecule fused to the N-terminus of a reference FLAG-tagged derivative of the mouse dihydrofolate reductase (^{f}DHFR-Ub^{R48}) coupled to FLAG-tagged BRCA1, a known target of the Arg/N-degron pathway (Figure 17a). Cotranslational cleavage by deubiquitylases produces both the DHFR fragment and BRCA1 with a desired N-terminal residue, at the initial equimolar ratio. In normal conditions, the proapoptotic fragment of the BRCA-1 protein (Asp-BRCA1) is degraded by the Arg/N-degron pathway and should therefore accumulate if the pathway is impaired. Similarly, Val-BRCA1, which is not recognized by the N-degron pathway will not be degraded and serves as a control. Indeed, less degradation of the proapoptotic fragment of BRCA1 containing the Aspartate residue at its N-terminus was observed when Hepa 1-6 cells were treated with siRNA against UBRs than in the controls (Figure 17b-c), indicating that the functional activity of the N-degron pathway is inhibited in our system.

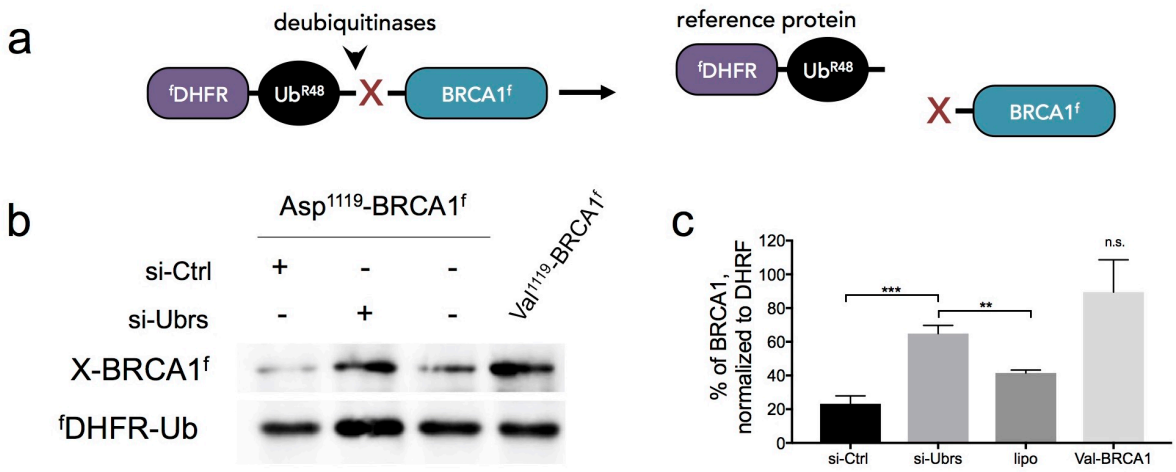

Figure 17. siRNA-mediated down-regulation of UBR-ubiquitin ligases prevents degradation of N-degron pathway target. (a) Schematic representation of the protein construct used in the present assay. (b) Asp^{1119}-BRCA1^{f} (produced from ^{f}DHFR-Ub^{R48}-Asp^{1119}-BRCA1^{f}) and Val^{1119}-BRCA1^{f} were expressed in Hepa 1-6 cells transfected with siRNA. Protein extracts were analyzed by SDS/PAGE and Western Blot against FLAG. (c) Quantification of (a). n=3 biological replicates per condition. P values were determined by a Student test (**P<0.005, ***P<0.001)

The Arg/N-degron pathway is known to positively regulate cell proliferation and migration (Kwon et al. 2002; An et al. 2006). Therefore, we evaluated these biological processes using Neutral Red and Scratch assays in Hepa 1-6 cells after 72h of exposure to siRNA to confirm that downregulation of UBR1, UBR2, UBR4 and UBR5 negatively affected cell proliferation and migration. Indeed, we observed a decrease of both cell proliferation and migration after transfection with si-UBRs compared to si-Ctrl although the effect on migration was not statistically significant (Figure 18).

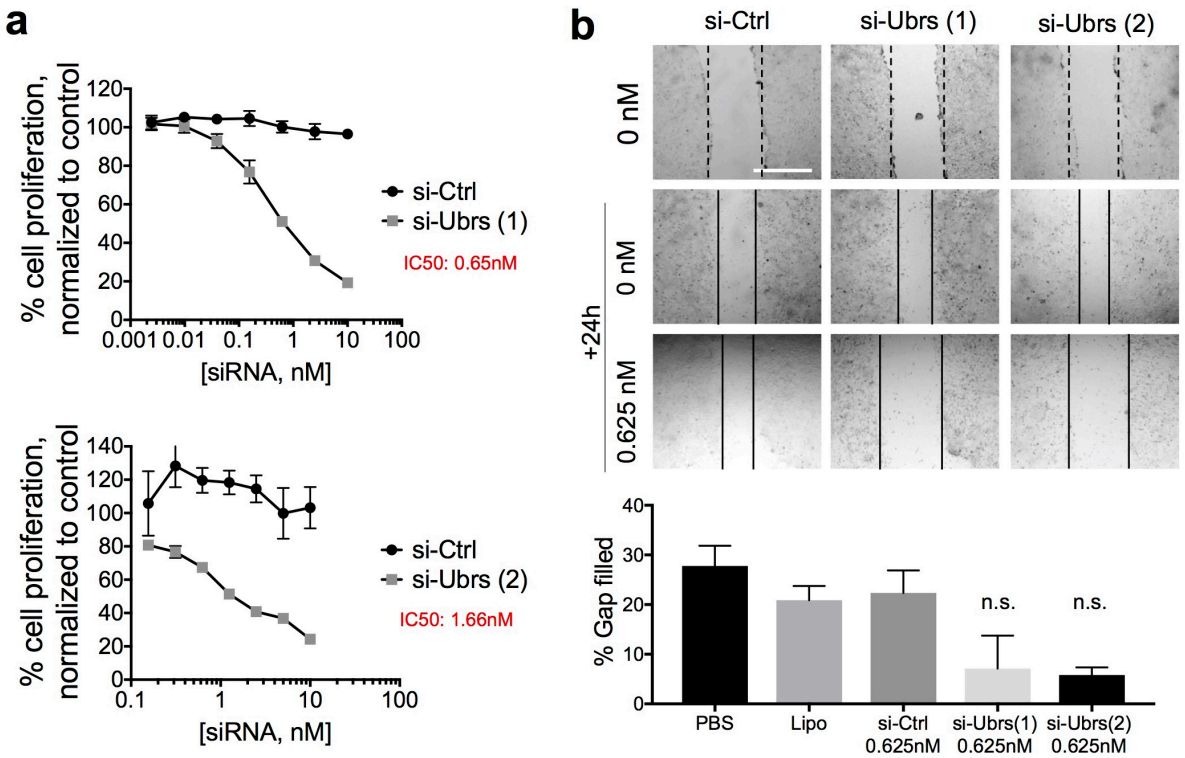

Figure 18. Downregulation of UBR-Ubiquitin ligases of the N-degron pathway decreases proliferation and migration of Hepa 1-6 cells. Two different sets of siRNA against UBRs (si-Ubrs (1) and si-Ubrs (2)) were used to assess on-target effects. See Table 5 for set descriptions. (a) Analysis of cell proliferation by the Neutral Red assay on Hepa 1-6 cells after 72h of exposure to siRNA. (b) Migration assay performed on Hepa 1-6 cells after 72h of exposure to siRNA against UBRs. Results show mean ± SD. n=3 biological replicates per condition. P values were determined by a Student test (*P<0.01)

On the other hand, the Arg/N-degron pathway is responsible for the degradation of proapoptotic fragments (Piatkov, Brower, and Varshavsky 2012). Therefore, downregulation of the UBR-ubiquitin ligases should translate into an increase of spontaneous apoptosis in siRNA-transfected cells, and this was observed as an increase of 3-8% TUNEL positive cells

compared to controls (Figure 19a-b) and Annexin V staining (Figure 19c-d). We observed no positive 7AAD cells, indicating that cells were in the early apoptotic phase at the moment of the assay. Indeed, 7AAD is excluded from viable cells, whereas membranes of dead cells are permeable to the dye. The in vitro results were also validated using a second set of highly potent UBR siRNAs (Figures 18 and 19), confirming the on-target effect of siRNA mediated downregulation of UBR-ubiquitin ligases on cell proliferation, migration and apoptosis.

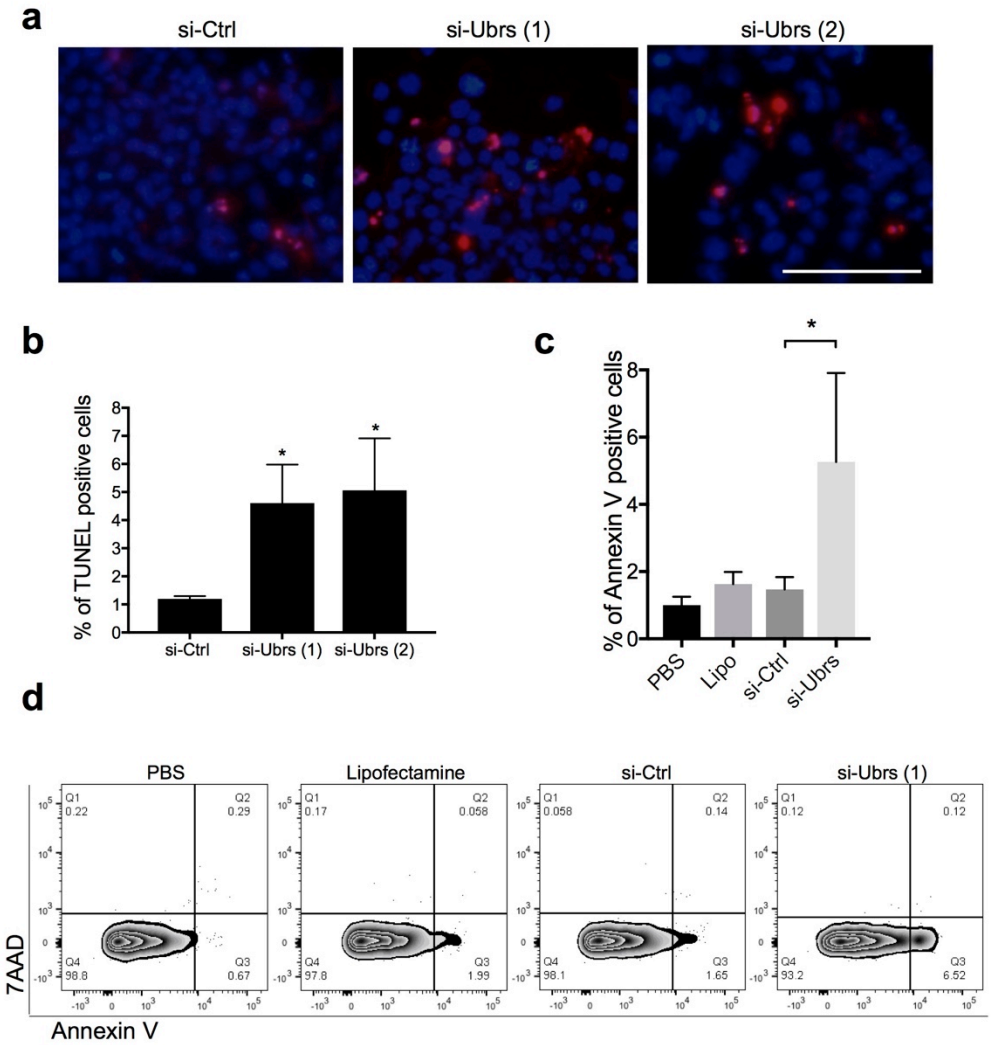

Figure 19. UBR downregulation causes an increase in apoptosis. Two different sets of siRNA against UBRs (si-Ubrs (1) and si-Ubrs (2)) were used to assess on-target effects. Analysis of cell death by (a-b) TUNEL and (c-d) Annexin V / 7AAD staining, evaluated by flow cytometry, in Hepa 1-6 cells, after 72h of exposure to siRNA against UBRs, at 1nM. Scale bar: 100μm. Results show mean ± SD. n=2-3 biological replicates per condition. A minimum of 2,000 cells per condition were counted for the TUNEL assay. P values were determined by Mann Whitney tests (*P <0.05)

UBR-ubiquitin ligase knockdown in healthy mouse liver

The selected siRNA against UBR1, UBR2, UBR4 and UBR5 were individually formulated into C12-200 lipid nanoparticles previously validated in mice and nonhuman primates (Love et al. 2010), and evaluated 72 h post treatment for activity in vivo at a dose of 0.25 mg/kg each (Figure 20). Due to their size (80-90 nm) and almost neutral charge, C12-200 siRNA-LNP easily pass through the fenestrae of the endothelium layer separating hepatocytes from blood, and are further internalized by hepatocytes via macropinocytosis (Love et al. 2010). The biological distribution of C12-200 siRNA LNP after IV injection in mice has been thoroughly assessed in previous studies, confirming RNAi-mediated silencing specifically in the liver (Bogorad et al. 2014).

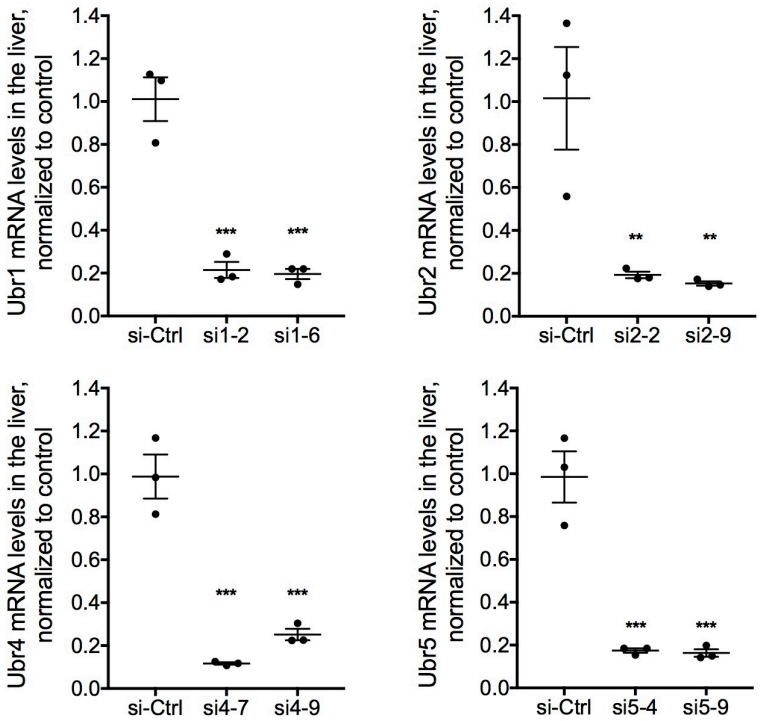

Figure 20. Downregulation of UBR1, UBR2, UBR4 and UBR5 in mouse liver. UBR mRNA levels in the total liver 3 days post injection of one of two specific LNP-siRNA for each UBR (Table 5) at 0.25mg/kg. n=3. (*P <0.05, **P< 0.005, ***P< 0.0005, ****P 0.0001)

The most efficient LNP-siRNA (si1-6, si2-9, si4-7 and si5-4, Table 5) were selected to perform dose-response (Figure 21a), target recovery (Figure 21b) and tissue biodistribution experiments (Figure 21c), as well as all further experiments in this study.

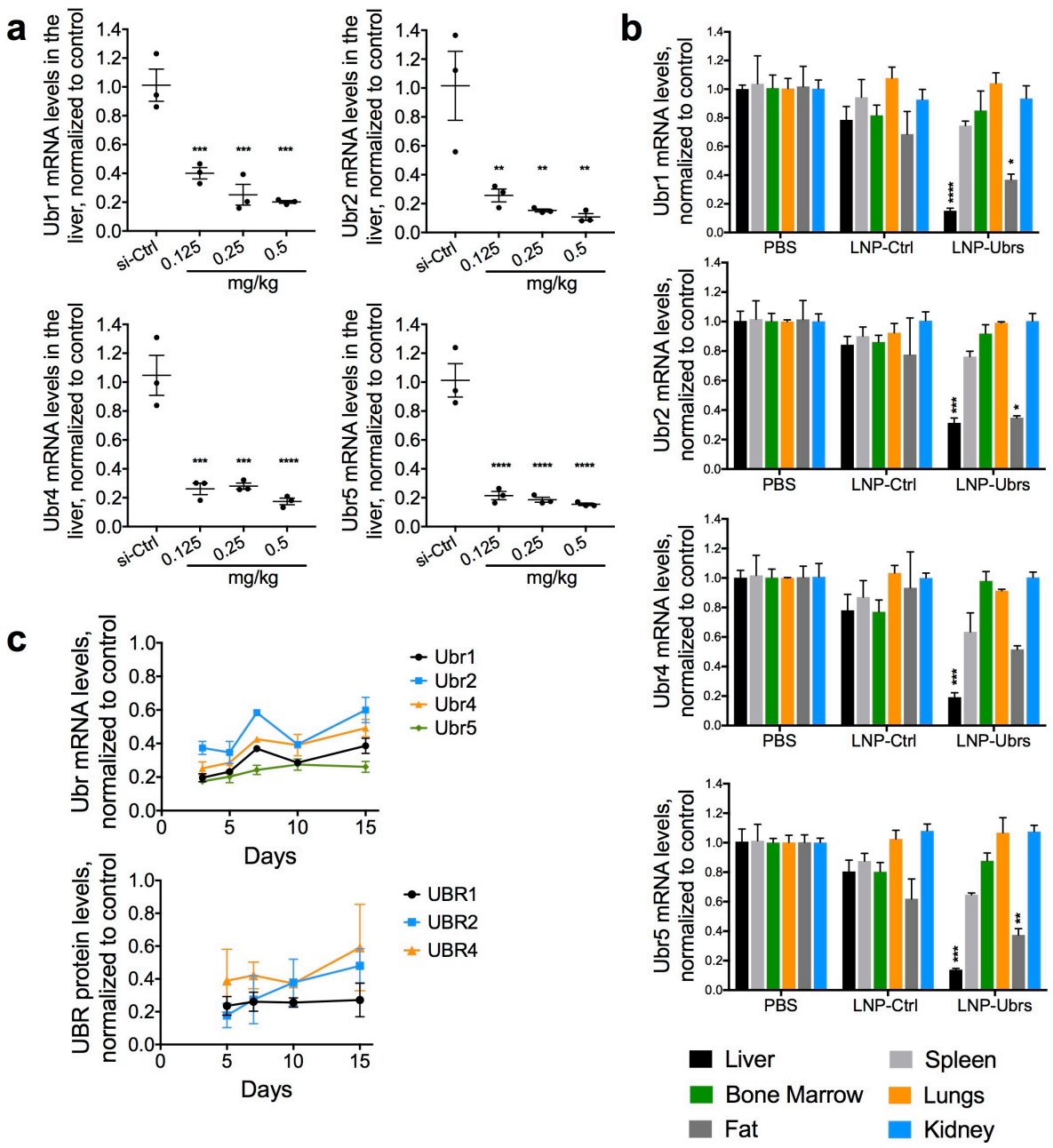

Figure 21. Liver specific delivery of Lipid Nanoparticles containing siRNA. (a) Dose dependence downregulation of mRNA levels in total liver 3 days post injection. n=3, results presented as mean ± SEM. P values were obtained by one-way ANOVA, comparing to controls. (b) Tissue-specific activity of systemically delivered siRNA formulated into LNPs 3 days post injection. (c) Recovery of UBR mRNA and protein levels of UBR1, UBR2, UBR4 and UBR5, in the mouse liver, at 3, 5, 7, 10 or 15 days after single-dose injections of LNP-siRNA. n=3 and results presented as mean ± SEM. P values were obtained using a one-way ANOVA, comparing to controls. (*P <0.05, **P< 0.005, ***P< 0.0005, ****P 0.0001)

Single administration of LNP-siUBR at doses ranging from 0.125 – 0.5 mg/kg resulted in profound knockdown of UBR mRNA levels (80–85%) in the liver of naive animals,

72 hours post injection (Figure 21a). None of the doses tested resulted in death of the animals, indicating that we did not reach the maximum tolerated dose. No significant target downregulation was detected in the spleen, kidney, lungs and bone marrow. However, 50-60% knockdown of UBRs was observed in the visceral adipose tissue (Figure 21b), possibly due to delivery to peripheral macrophages (Novobrantseva et al. 2012). The maximal observed mRNA and protein downregulation in the liver occurred at the first time point examined (72h), (Figure 21c), and silencing to more than 60% lasted at least 10 days, which allows a convenient once-per-week regimen for multiple dosing.

Chronic treatment with LNPs revealed that long-term downregulation of UBR-ubiquitin ligases can be achieved in the liver of healthy mice without inducing significant toxicity to this organ. C57Bl/6 female mice received bi-weekly injections of LNPs loaded with siRNA (1.4mg/kg total) for 4 weeks. Levels of alanine aminotransferase (ALT), aspartate aminotransferase (AST) and alkaline phosphatase (ALP) were evaluated as indicators of liver toxicity. Although the levels of ALT, AST and ALP were increased in the mice receiving LNP-siUBRs, albumin, total protein and total bilirubin remained stable (Table 6), and no significant weight change or differences in the behaviour of the mice was observed between the groups (Figure 22c), indicating that long-term administration of LNP-siUBRs was well tolerated.

Table 6: Effect of long-term knockdown of UBR-ubiquitin ligases of the N-degron pathway in mouse liver on parameters of serum chemistry.

	PBS	LNP-siCtrl	LNP-siUBRs	ANOVA P-values
ALP (U/L)	102 ± 11	88 ± 10	212 ± 54[§,¶]	0.0001
AST (U/L)	102 ± 34	106 ± 35	207 ± 59[§,¶]	0.0038
ALT (U/L)	19 ± 4	23 ± 3	62 ± 21[§,¶]	0.0006
BUN (mg/dL)	32 ± 5	31 ± 2	27 ± 4	0.1830
Albumin (g/dL)	2.9 ± 0.1	2.9 ± 0.1	2.6 ± 0.2[§,¶]	0.0007
Total bilirubin (mg/dL)	0.16 ± 0.05	0.10 ± 0.00	0.20 ± 0.07[¶]	0.0302
Total protein (g/dL)	4.7 ± 0.1	5.0 ± 0.1[v]	4.3 ± 0.3[§,¶]	0.0001
Globulin (g/dL)	1.7 ± 0.1	2.1 ± 0.1[v]	1.7 ± 0.1[¶]	<0.0001
Cholesterol (mg/dL)	75 ± 4	86 ± 10	32 ± 3[§,¶]	<0.0001

ALP: Alkaline Phosphatase ; AST: Aspartate Aminotransferase; ALT: Alanine Aminotransferase ; BUN: Blood Urea Nitrogen

§: Tukey post hoc comparison of PBS vs LNP-siUBRs, P< 0.01, P< 0.001

¶: Tukey post hoc comparison of LNP-siCtrl vs LNP-siUBRs, P< 0.01, P< 0.001

v: Tukey post hoc comparison of PBS vs LNP-siCtrl, P< 0.01

75-90% downregulation of UBR1, UBR2, UBR4 and UBR5 mRNA in the liver was achieved, compared to the PBS control group (Figure 22a). A decrease of UBR mRNA was also seen in the control siRNA group, however, this was not observed in other long-term treatments with LNPs loaded with the siRNA against luciferase at a less or equal dose (Figure 25), and no phenotypical differences were observed between healthy and LNP-siCtrl treated animals. Treatment with the control LNP slightly decreased the level of UBR4 protein, which could be the result of accelerated lysosomal degradation of UBR4. Indeed, multiple injections with LNPs can lead to significant lipid accumulation in liver cells and increased autophagy (Yang, Zhang, and Ren 2018). During the autophagy process, UBR4 delivers its substrates into autophagic lysosomes and can become trapped and degraded along with the cargo inside the autophagosomes (Kim et al. 2013).

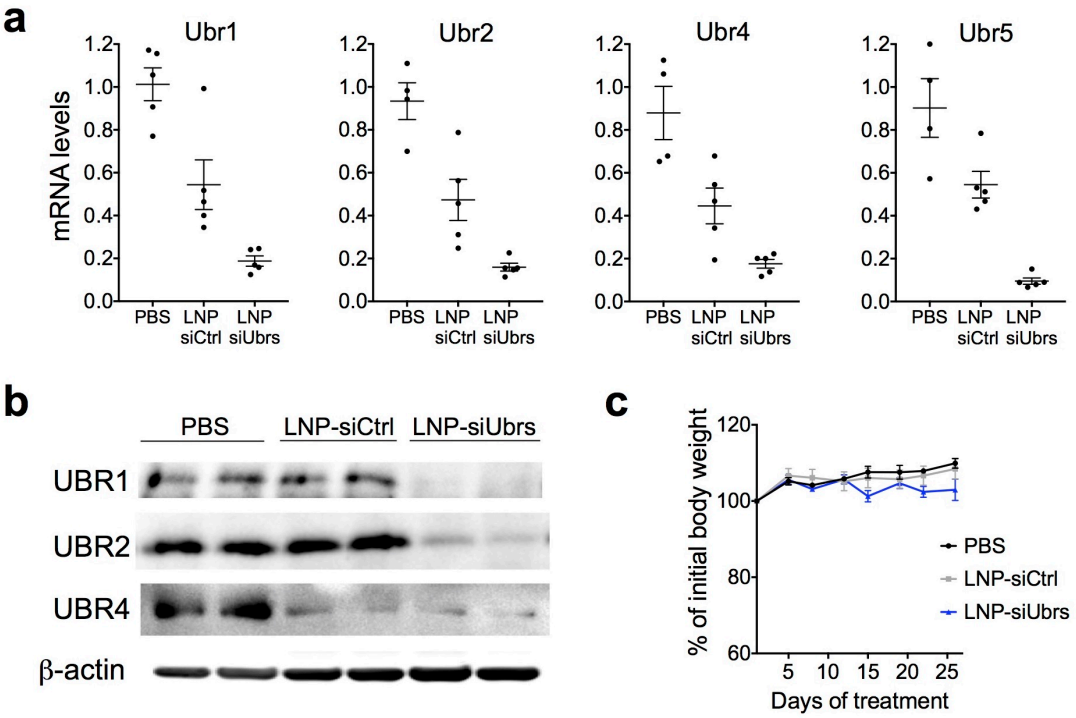

Figure 22. Chronic downregulation of UBR-Ubiquitin ligases in the liver. Mice were treated with LNP-siRNA for 4 weeks, 2x/week. The combined dose of LNP-siUBR siRNA was 0.3mg/kg for UBR1, 2 and 5, and 0.5mg/kg for UBR4, for a total of 1.4mg/kg. Mice treated with LNP-siCtrl (Luciferase) received 1.4mg/kg. (a) mRNA and (b) protein levels of UBR1, UBR2, UBR4 and UBR5 in the liver of LNP-treated mice. Protein levels of UBR5 are undetectable in the liver. (c) Weight curve of animals treated with LNPs, measured before each injection and averaged for the group. Measures were compared as a percentage of change from day 0. n=5. P values were determined by a Mann-Whitney test (*P 0.02)

Chronic downregulation of UBR-ubiquitin ligases led to a slight but significant increase of apoptotic cells and enlarged intercellular space in the liver (Figure 23a), confirming that the function of the Arg/N-degron pathway is diminished in this organ. However, one noticeable consequence is the infiltration of mononuclear cells in the livers of mice treated with LNPs containing siRNA against UBRs (Figure 23b). The infiltrating cells were identified by flow cytometry as neutrophils, $CD11b^{+}Ly6C^{high}$ infiltrating differentiating macrophages, and eosinophils (Figure 23c-d), indicating the presence of chronic inflammation in the liver. These cell populations were also increased in the spleens of the same animals (Figure 24b-c), however this seems to be a consequence of the inflammation present in the liver rather than the influence of the Arg/N-degron pathway in the spleen since no downregulation of UBR mRNA was observed in this organ (Figure 24a).

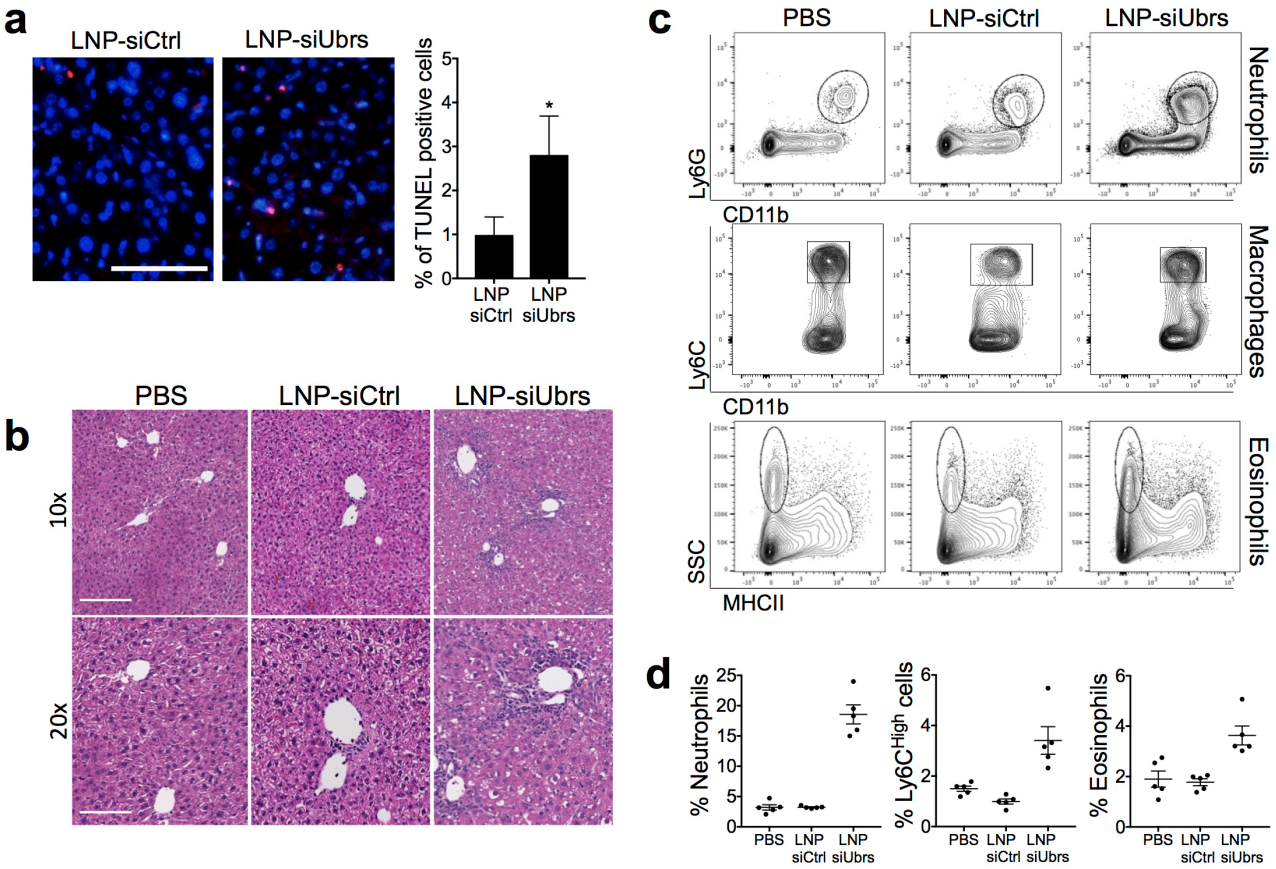

Figure 23. Long-term downregulation of UBR-Ubiquitin ligases in the liver induces inflammation. Mice were treated with LNP-siRNA for 4 weeks, 2x/week. The combined dose of LNP-siUBR siRNA was 0.3mg/kg for UBR1, 2 and 5, and 0.5mg/kg for UBR4, for a total of 1.4mg/kg. Mice treated with LNP-siCtrl (Luciferase) received 1.4mg/kg. (a) Analysis of cell death by TUNEL assay, in livers of LNP-treated mice. Red nuclei represent

TUNEL-positive cells. Scale bar, 100μm. A minimum of 2,000 cells were counted per condition. (b) H&E stain of mice treated with LNPs or vehicle. Scale bar, 200μm (10x) and 100μm (20x) (c) Representative flow cytometry analysis of neutrophil, Ly6C^{high} macrophage and eosinophil populations in the liver of mice treated with LNPs. (d) % of neutrophil, Ly6C^{high} macrophage or eosinophil populations in the livers of LNP or vehicle treated mice, gated on CD45^{+} cells. Results show mean ± SEM. n=5 mice per group.

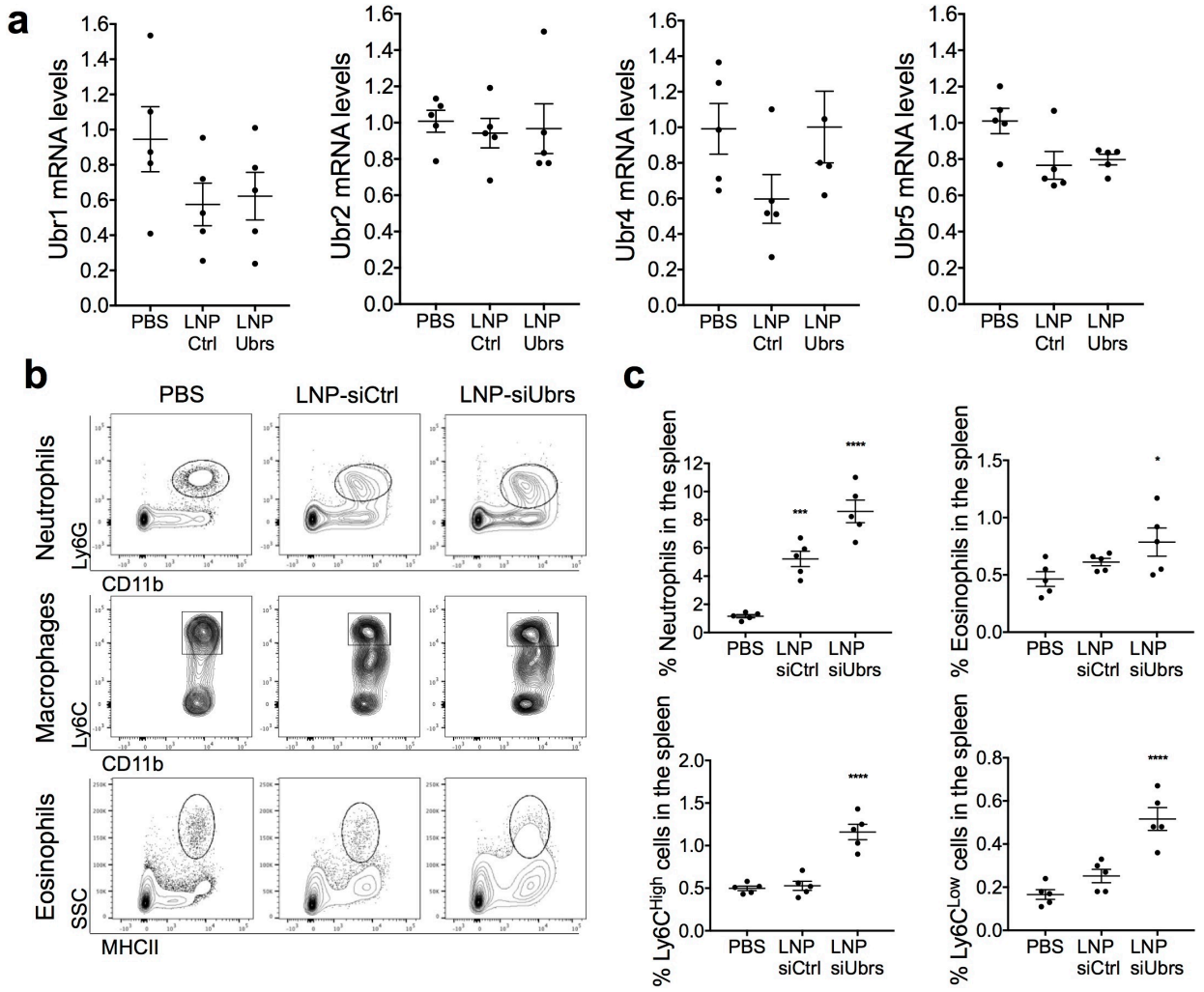

Figure 24. Effect of chronic downregulation of UBR-Ubiquitin ligases in the spleen. (a) mRNA levels of UBR1, UBR2, UBR4 and UBR5 in the spleen of LNP-treated mice. (b) Representative flow cytometry analysis of neutrophil, macrophage and eosinophil populations in the spleen of mice treated with LNPs. (c) % of neutrophil, Ly6C^{high} macrophage or eosinophil populations in the spleen of LNP or vehicle treated mice, gated on CD45^{+} cells. Results show mean ± SEM. n=5 mice per group.

Knockdown of the N-degron pathway in an oncogene driven model of HCC

Before studying the role of UBR-ubiquitin ligases of the Arg/N-degron pathway in liver cancer, we needed to establish the optimal mouse model of hepatocellular carcinoma for our laboratory. We evaluated three different models: (1) a chemical model, where diethylnitrosamine (DENA) is injected into 14-day old mice, and tumors develop in 12-14 months; (2) an orthotopic model, where Hepa 1-6 cells are injected directly into the liver of healthy mice, using matrigel, and the tumors are allowed to grow for 21-28 days; (3) an oncogene-driven model of HCC developed by Tward et al (Tward et al. 2007) and routinely used by our collaborators in MIT (laboratory of Daniel Anderson), where plasmids containing human MET and ΔN90-β−catenin and the transposase Sleeping Beauty are delivered to hepatocytes by hydrodynamic injection and the oncogenes are stably integrated into the genome by the Sleeping Beauty transposase. The chemical model was eliminated because of the time needed for tumor development and treatment, which would have required several months of LNP-siRNA injections. With the orthotopic model, we experienced very quick rejection of the tumors by the immune system of the C57BL/6 mice, and this would not have given a large enough treatment window to observe the effects of downregulation of the Arg/N-degron pathway in the tumor cells. Therefore, we chose the oncogene-driven model of HCC, in the FVB/N mouse recommended for this model. As confirmed by our own experiments, the FVB/N mouse is the strain with the highest success rate in hydrodynamic delivery models (Chen and Calvisi 2014). Once the plasmids are integrated in the hepatocytes, α-fetoprotein becomes detectable in the serum of tumor-bearing mice by the fifth week after injection, and by the end of the tenth week, the liver is greatly enlarged up to a liver-to-body mass ratio of 15 to 40% versus 4-5% in non-tumour control animals. The Anderson laboratory has also previously demonstrated efficient delivery of siRNA to the tumor nodules that develop in the plasmid-injected mice (Bogorad et al. 2014).

As UBR5 and UBR2 have been reported to be overexpressed in some types of cancer (O'Brien et al. 2008; Zhang et al. 2013), we began by assessing the levels of mRNA expression of all four UBR ubiquitin ligases and found that none were upregulated in our specific HCC model (Figure 25).

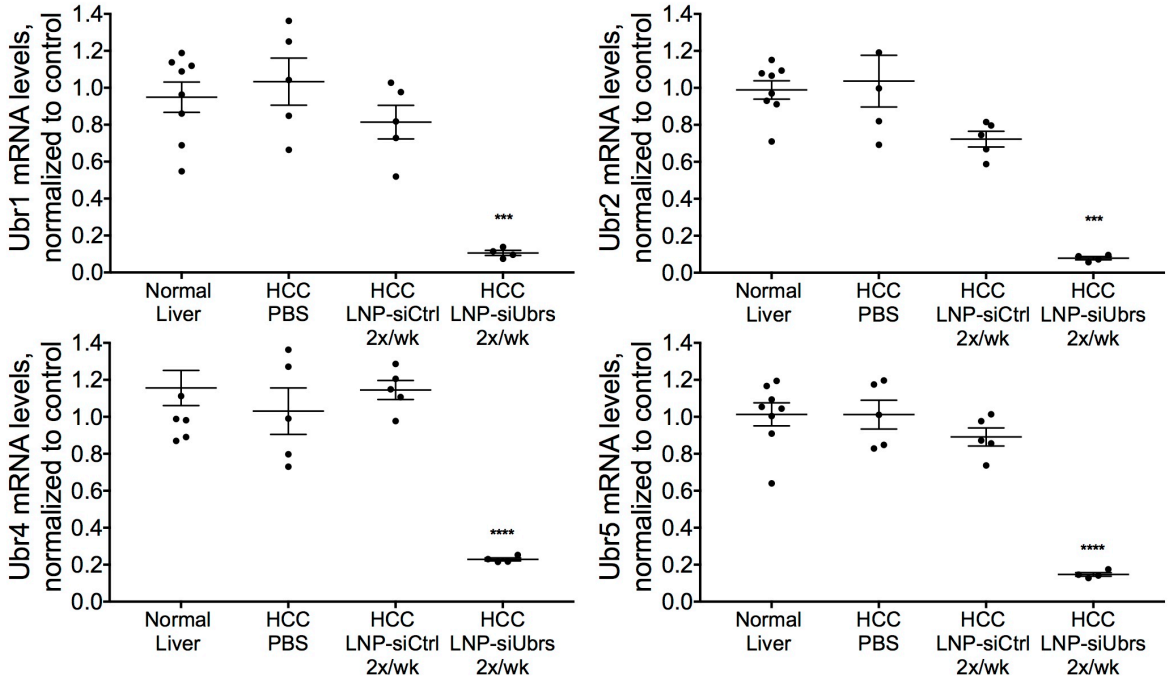

Figure 25. Expression and downregulation of UBR-Ubiquitin ligases in the liver of HCC mice. mRNA levels of UBR1, UBR2, UBR4 and UBR5 in the liver of healthy and HCC mice was measured after 5 weeks of bi-weekly i.v. injections of a total of 1.4mg/kg of LNPs. n=5-8 (***P< 0.0005, ****P< 0.0001)

The impact of downregulating the Arg/N-degron pathway on tumor load was evaluated by injecting lipid nanoparticles containing siRNA against UBRs or the control siRNA at a total dose of 1.4mg/kg into tumor bearing mice for four or five weeks, once or twice per week (Figure 26a-b). Successful downregulation of all four UBR-ubiquitin ligases was achieved in the hepatocellular carcinoma bearing mice (Figure 25), as seen by significantly decreased mRNA levels. In all regimens tested, downregulation of the targeted UBR ubiquitin ligases with high LNP doses led to an increase in liver/body weight ratio and tumor load (Figure 26c-d). The gross morphology of the cancer was also changed in the mice treated with LNP-siUbrs: increased angiogenesis and accumulation of tumor interstitial fluid caused distancing between hepatocytes and more tumor nodules could be observed in the liver of these mice (Figure 26e).

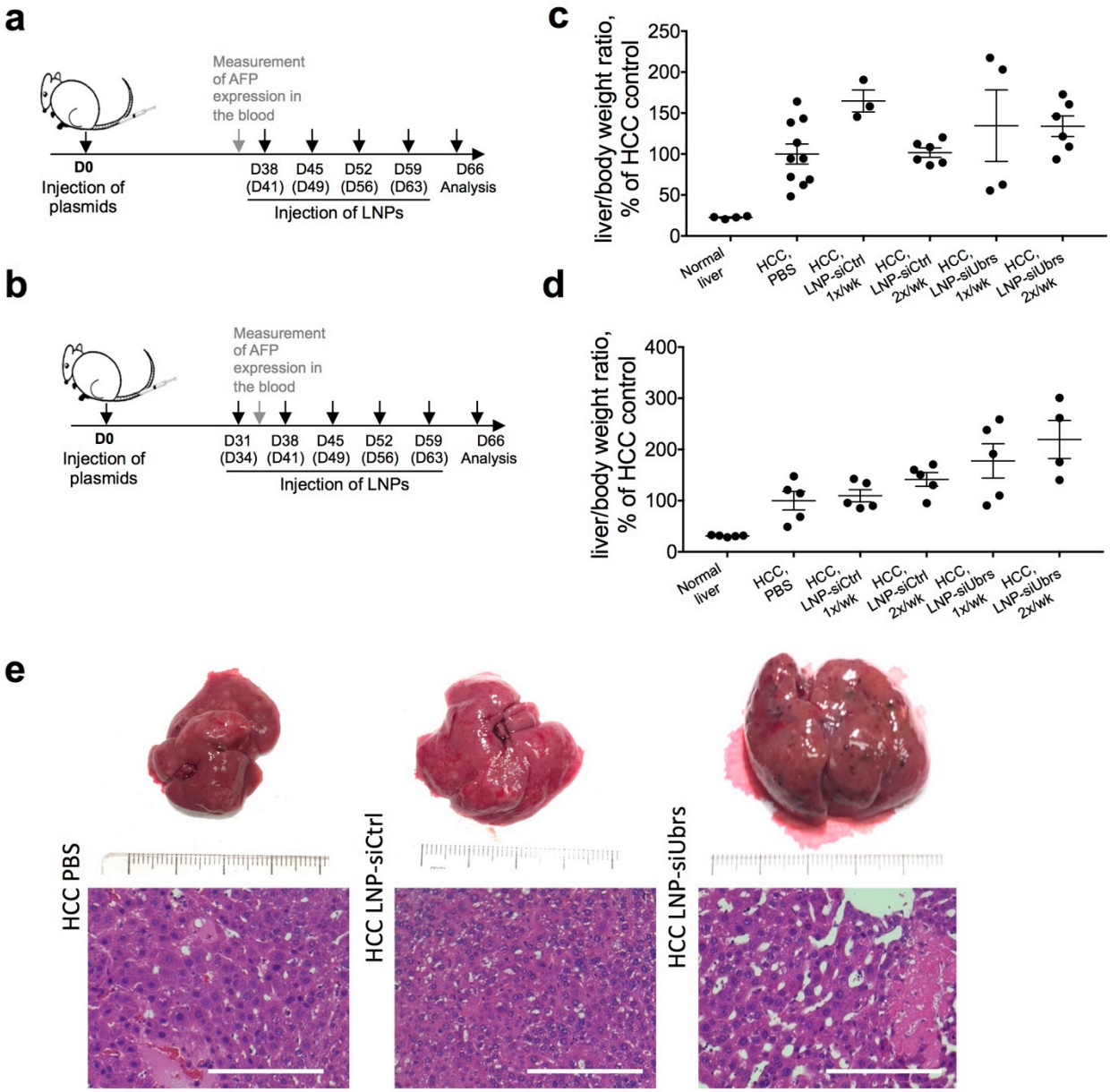

Figure 26. Downregulation of UBR-Ubiquitin ligases in HCC aggravates tumor load. (a-b) Schematic representation of the experiment: timeline of tumor induction (injection of oncogene-encoding plasmids) and repeated injections of LNP-formulated siRNA. LNPs were injected for 4 weeks (a) or 5 weeks (b), once or twice a week. Tissues were collected for analysis on day 66 after tumor induction. (c-d) Liver/body mass ratio analysis of mice bearing HCC treated for 4 weeks (c) or 5 weeks (d) with LNPs. Ratios were calculated to the ratios of the HCC control group. (e) Representative livers and histology of HCC mice treated with PBS, LNP-siCtrl or LNP-siUBRs for 4 weeks, twice per week. Ruler=cm, scale bar: 200μm. Results show mean ± SEM. n=3-10 mice per group. P values were determined by a Mann-Whitney test (*P <0.05)

Increased populations of neutrophils and Ly6C^{high} cells were also observed in the spleens of HCC animals treated with LNP-siUBRs twice a week (Figure 27), as seen in the normal animals (Figure 24), indicating increased inflammation in these animals, a well known driver of HCC development and progression. As a consequence, we re-evaluated the regimen of LNP injections and chose a lower dose and frequency for the ensuing experiments to mitigate the observed inflammation.

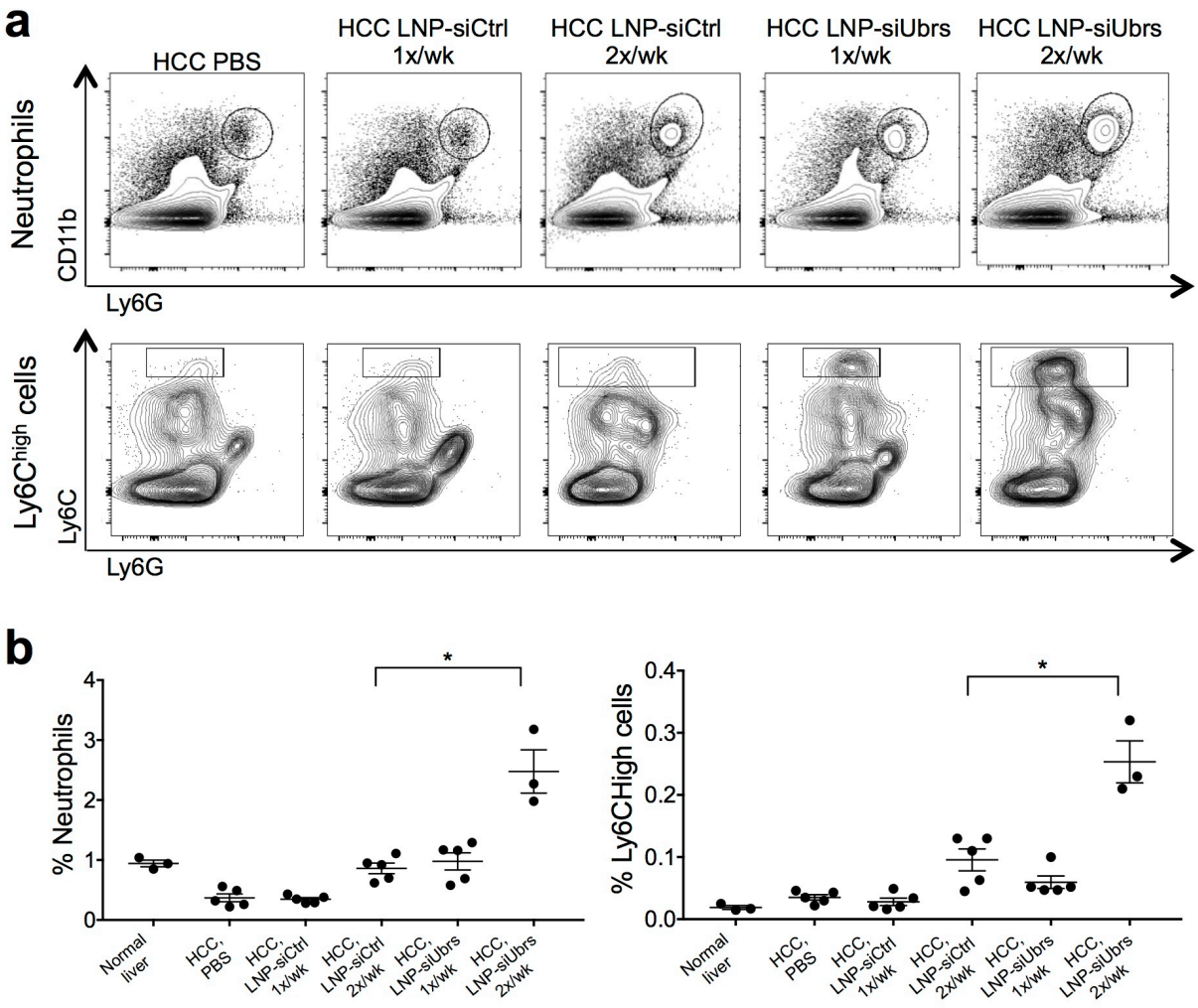

Figure 27. Downregulation of UBR-Ubiquitin ligases in HCC induces inflammation. (a) Representative flow cytometry analysis of neutrophil and Ly6C^{high} populations in the spleen of HCC mice treated with LNPs. (f) % of neutrophil and Ly6C^{high} macrophage populations in the spleen of HCC mice treated with LNP, gated on CD45^{+} cells. Results show mean ± SEM. n=3-10 mice per group. P values were determined by a Mann-Whitney test (*P <0.05)

Study of the Arg/N-degron pathway as a regulator of inflammation

The presence of inflammation in mice treated with high doses of lipid nanoparticles containing siRNA against UBR-ubiquitin ligases of the N-degron pathway, either in the normal context or during hepatocellular carcinoma, lead us to hypothesize that the Arg/N-degron pathway could be involved in the regulation of this process. Indeed, similarly to apoptosis, initiation and progression of inflammation involves activation of specific proteases that drive and amplify inflammatory signalling by cleaving their protein targets. We reasoned that just as the Arg/N-degron pathway degrades proapoptotic fragments generated by caspases, some protein fragments resulting from processing by activated inflammatory caspases or endopeptidases could be potential Arg/N-degron substrates.

Recognition of a danger signal such as foreign lipids in lipid nanoparticles, or double-stranded RNA in siRNA, triggers a coordinated cascade of events initiating the inflammatory response. In cells of the innate immune system such as neutrophils, granulocytes or macrophages, danger signals lead to activation of inflammatory caspases (caspases-1, -4, -5, -11 and -12) (Martinon, Burns, and Tschopp 2002; Jimenez Fernandez and Lamkanfi 2015) and subsequent proteolysis of a multitude of proinflammatory targets including IL-1β and various activators of inflammation (Denes, Lopez-Castejon, and Brough 2012; Wang et al. 2016). In the adaptive immune system, cytotoxic T lymphocytes (CTL) and natural killer (NK) cells influence on proinflammatory cytokine secretion through the action of granzymes (Hildebrand et al. 2014; Anthony et al. 2010). In a more general manner, inflammation can also be initiated through activation of the NF-κB pathway, mediating transcription of numerous proinflammatory genes and inducing the production of cytokines, chemokines and additional proinflammatory mediators (Liu et al. 2017). All of these events lead to the generation of proinflammatory protein fragments that could be degraded by the N-degron pathway, provided that they contain built-in degrons, contributing to the control of the inflammatory response.

Proinflammatory fragments contain destabilizing residues at their N-terminus

In order to determine if proinflammatory protein fragments could contain destabilizing residues at their N-terminus, we searched online databases for human and orthologous proteins containing caspase-1 cleavage sites. More than 120 substrates were found, 21% of which bear a destabilizing residue according to the Arg/N-degron pathway at their P1' position (the first residue after the cleavage site) (Table 7). From the shorter list of experimentally confirmed caspase-1 substrates with inflammatory functions, we identified ten fragments with possible N-degrons: Asn^{120}-CASP1 (caspase-1), Gln^{81}-CASP4 (caspase-4), Gln^{138}-CASP5 (caspase-5), Cys^{149}Rab39α, Tyr^{37}-IL-18 (interleukin-18), Tyr^{49}-CCL3 (macrophage inflammatory protein 1-alpha), Glu^{245} and Leu^{249}-Ataxin-3, Cys^{50}-hnRNPA2 (Heterogeneous nuclear ribonucleoproteins A2/B1) and Leu^{680}-Matrin-3 (Table 7). We also identified proinflammatory fragments containing destabilizing residues at their N-terminus that are generated by other endopeptidases such as PILSAP, DPP1 and Proteinase-3. These fragments include Asn^{10}-PDK1, Ile^{29}-GRZA (granzyme A), Ile^{27}-GRZM (granzyme M), Ile^{26}-GRZK (granzyme K), Glu^{6}-IL-36β and Tyr^{16}-IL36γ (interleukin 36β and γ) (Table 7). 3-phosphoinositide-dependent protein kinase 1 (PDK1) has been associated to inflammation by its involvement in the signalling pathways of NF-κB and TGF-β (Seong et al. 2005; Seong et al. 2007; Sun et al. 2017). Additionally, PDK1 is required, although not exclusive, for IL-1β induced NF-κB activation through activation of the IKK complex and phosphorylation of IκB (Parhar et al. 2007). Activation of NF-κB leads to transcription of a multitude of proinflammatory genes including chemokines, cytokines, inflammasomes, genes implicating in activation, proliferation and survival of T lymphocytes, etc (Liu et al. 2017). PDK1 is cleaved by the endopeptidase PILSAP at position 9, leaving an Asp at the P1' position (Yamazaki et al. 2004). Interestingly, all of the destabilizing N-terminal residues studied are conserved through evolution, with few exceptions such as caspase-1 (see Figure 28). Tellingly however, all of the changes in the P1' residues remain destabilizing in the Arg/N-degron pathway.

Table 7: Proinflammatory fragments with destabilizing N-terminal residues

Protein	Cleavage site	C-terminal fragment
	Experimentally confirmed N-degron pathway substrates (in this study)	
hCASP-1	115 ↓ 297 QAVQD**N**PAM…M	Proinflammatory fragment, generated by auto-cleavage. Asn-CASP1 is an N-degron pathway substrate.
hCASP-4	76 ↓ 377 FFNID**Q**ISP…N	Proinflammatory fragment, generated by auto-cleavage. Gln-CASP4 is an N-degron pathway substrate.
hCASP-5	133 ↓ 376 LLMND**Q**KIT…N	Proinflammatory fragment, generated by auto-cleavage. Gln-CASP5 is an N-degron pathway substrate.
hRAB39a	144 ↓ 217 KLSAD**C**GMK…C	Proinflammatory fragment, generated by caspase-1 mediated cleavage. Cys-RAB39a is an N-degron pathway substrate.
hPDK1	5 ↓ 556 TSQLY**D**AVP…Q	Proinflammatory fragment, generated by endopeptidase PILSAP mediated cleavage. Asp-PDK1 is an N-degron pathway substrate.
mGRZA	25 ↓ 260 GCER**I**IGGD…V	Proinflammatory fragment, generated by endopeptidase DPP1 mediated cleavage. Ile-GRZA is an N-degron pathway substrate.
mGRZM	22 ↓ 264 SFGTQ**I**IGGD…V	Proinflammatory fragment, generated by endopeptidase DPP1 mediated cleavage. Ile-GRZM is an N-degron pathway substrate.
	Proposed N-degron pathway substrates (in this study)	
mGRZK	21 ↓ 263 CFHTE**I**IGCR…H	Proinflammatory fragment, generated by endopeptidase DPP1 mediated cleavage. Ile-GRZK is a likely N-degron pathway substrate.
hIL-18	32 ↓ 193 NLESD**Y**FGK…D	Proinflammatory fragment, generated by caspase-1, of the cytokine IL-18. Tyr-IL-18 is a likely N-degron pathway substrate.
hCCL3	44 ↓ 92 NFIAD**Y**FETS…A	Proinflammatory fragment, generated by caspase-1, of the chemokine CCL3. Tyr-CCL3 is a likely N-degron pathway substrate.
hAtaxin-3	242 ↓ ↓ 361 MED**E**EAD**L**…K	Proinflammatory fragments of the protein Ataxin-3, generated by caspase-1. Likely N-degron pathway substrates.
hhnRNPA2	45 ↓ 353 GKLTD**C**VVM…Y	Proinflammatory fragment, generated by caspase-1, of the protein hnRNPA2. Cys-hnRNPA2 is a likely N-degron pathway substrate.
hMatrin-3	675 ↓ 847 GDETD**L**ANL…T	Proinflammatory fragment, generated by caspase-5, of the protein Matrin-3. Leu-Matrin-3 is a likely N-degron pathway substrate.
hIL-36b	1 ↓ 164 MNPQR**E**AAP…M	Proinflammatory fragment, generated by Cathepsin-G or Proteinase-3, of the cytokine IL-36b. Likely N-degron pathway substrate.
hIL36g	11 ↓ 169 GGRAV**Y**QSM…D	Proinflammatory fragment, generated by Elastase or Proteinase-3, of the cytokine IL-36g. Likely N-degron pathway substrate.
	Caspase-1 substrates containing possible N-degrons (no experimentally confirmed proinflammatory role)	
hICAL	^{56}ALDD**L**IDT	Calpastatin
hAT2B4	^{1077}DEID**H**AEM	plasma membrane calcium-transporting ATPase 1
hRL4	^{32}IRPD**I**VNF	60S ribosomal protein L4
hPA24A	^{465}YQSD**N**QAS	cytosolic phospholipase A2
hARFG2	^{379}WGMD**R**VEE	ADP-ribosylation factor GTPase-activating protein 2
hACTB	^{8}LVVD**N**GSG	Actin, cytoplasmic-1
hRS7	^{129}ILED**L**VFP	40S ribosomal protein S7
hEF1A1	^{359}PVLD**C**HTA	elongation factor 1 alpha
hVLDLR	^{378}YECD**C**AAG	Very low-density lipoprotein receptor
hAT2B2	^{1114}EEID**H**AER	plasma membrane calcium-transporting ATPase 2
hSQSTM	^{326}MESD**N**CSG	Sequestosome-1
hTHOC4	^{87}WQHD**L**FDS	THO complex subunit 4
hTWSG1	^{69}ECCD**C**VGM	twisted gastrulation protein homolog 1
hIL37	^{17}WEKD**E**PQC	Interleukin 37

Knowing that more than 90% of the mapped caspase cleavage sites in cellular proteins contain small residues such as Gly, Ser, Thr, and Ala at their P1′ positions (Crawford and Wells 2011), residues which are not recognised by the Arg/N-degron pathway, the change for a destabilizing residue in these proinflammatory fragments in higher mammals is significant and could indicate a fitness-increasing property that was later maintained by selection during evolution, demonstrating the importance of the N-degron pathway in the regulation and degradation of these fragments.

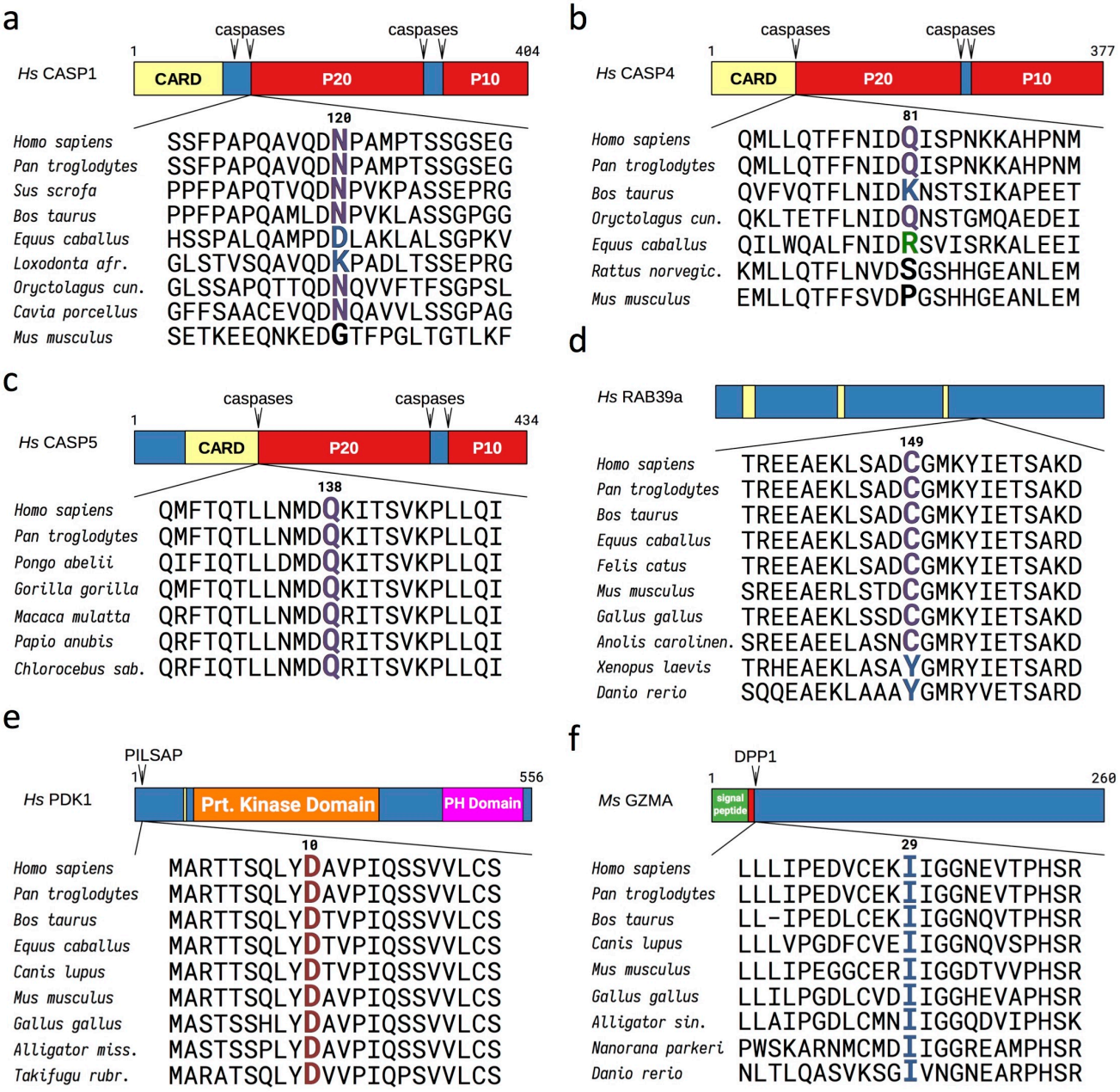

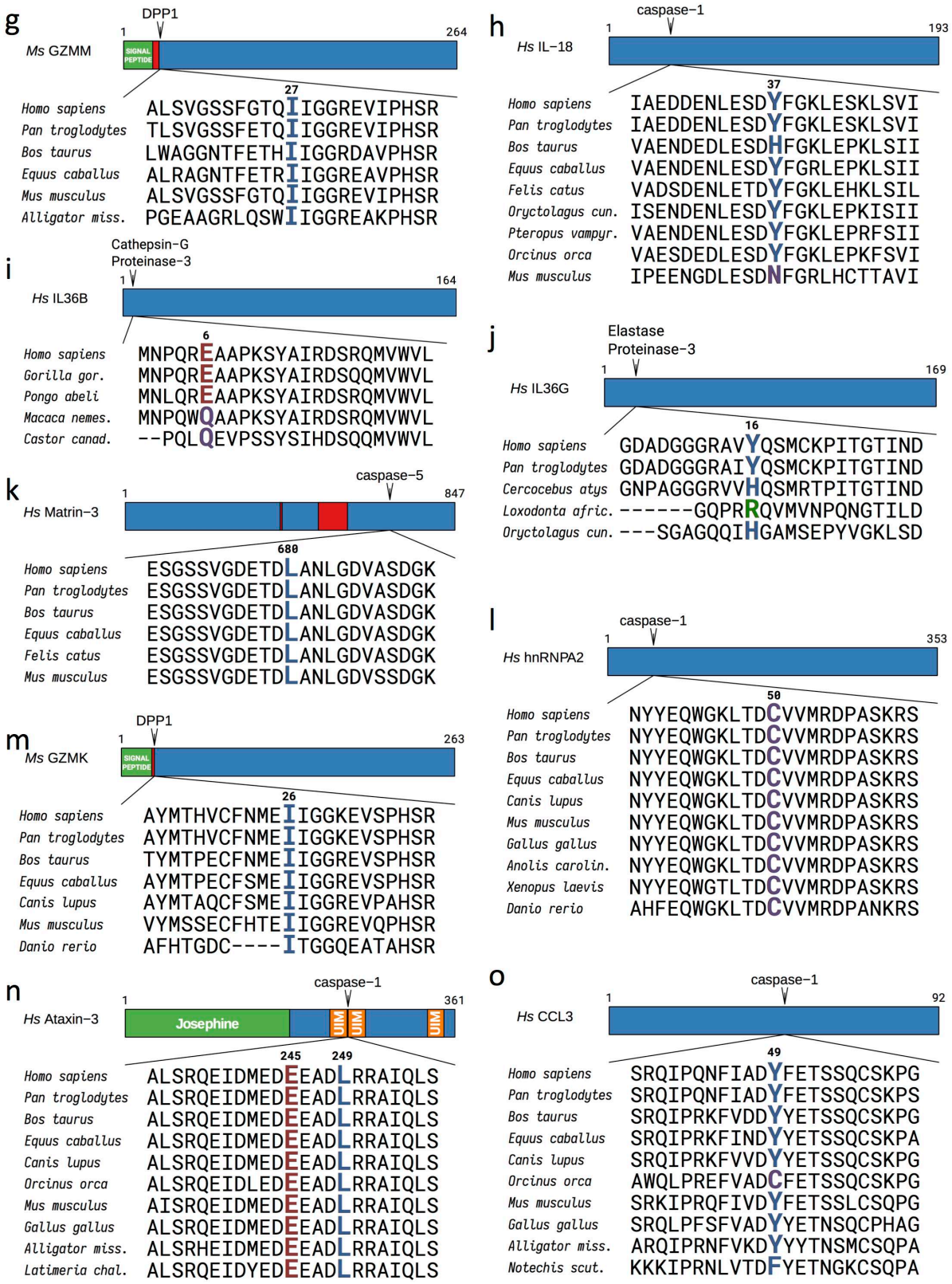

Figure 28. Evolutionary conservation of the cleavage sites and destabilizing P1' residues of putative proinflammatory Arg/N-degron pathway substrates. These substrates include (a) Asn-CASP1, (b) Gln-CASP4, (c) Gln-CASP5, (d) Cys-RAB39a, (e) Asp-PDK1, (f) Ile-GRZA, (g) and Ile-GRZM, have been shown, in the present work, to be short-lived substrates of the Arg/N-degron pathway (Fig. 30 and 31). Other fragments: (h) Tyr-IL-18, (i)

Glu-IL-36β, (j)Tyr-IL-36γ, (k) Leu-MATRIN-3 (l) Cys-hnRNPA2, (m) Ile-GRZK, (n) Glu-ATXN-3 and (o) Tyr-CCL3, are generated by inflammatory caspases-1 and -5 (-11), elastase, proteinase-3 or other endopeptidases. Cleavage sites are indicated by arrowheads. The indicated residue numbers, including the numbers of P1' residues (larger letters), are of the human or mouse versions of the cited proteins. Approximate locations and names of specific protein domains are indicated as well. UIM: ubiquitin interacting motif. Josephine: deubiquitination domain.

Proinflammatory fragments described.

As explained earlier, we focused our search on experimentally confirmed caspase-1- or endopeptidase-generated substrates with inflammatory functions. The following section briefly describes the proinflammatory roles of the fragments with confirmed or proposed N-degrons listed in Table 7.

^{120}Asn-CASP1. Originally discovered for its role in the secretion of IL-1β (Cerretti et al. 1992), caspase-1 is the most studied and best characterized caspase, and is known to cleave many proinflammatory and pro-pyroptosis fragments, including other members of the IL-1 family (Afonina et al. 2015; Denes, Lopez-Castejon, and Brough 2012; Lamkanfi et al. 2008; Shao et al. 2007; Shen et al. 2010; Wang et al. 2016). Caspase-1 is initially translated as a zymogen and requires interaction with the inflammasome for dimerization and activation. Self-cleavage of caspase-1 generates a more stable active form of the proteolytic enzyme and even serves to terminate inflammasome activity (Boucher et al. 2018). In all cases, activation of caspase-1 results in cleavage of proinflammatory peptides, leading to IL-1β secretion and pyroptosis of the infected cells. Pyroptosis is a unique cell death mechanism where rapid plasma-membrane rupture releases proinflammatory cellular contents into the extracellular space. It is caspase-1 dependant, and occurs after canonical or non-canonical inflammasome activation (Bergsbaken, Fink, and Cookson 2009). Caspase-1 is also capable of activating the NF-κB pathway through interaction of its CARD domain with RIP2 (Lamkanfi et al. 2004).

^{80}Gln-CASP4. Caspase-4 is an inflammation initiator caspase with 53% homology to caspase-1. Similarly, caspase-4 is initially produced as a zymogen and requires dimerization,

interdomain processing and cleavage for activation (Karki, Dahal, and Park 2007). Caspase-4 is required for the activation of caspase-1 through non-canonical inflammasomes, which involves detection and direct binding of intracellular LPS (Shi et al. 2014). It is also an essential effector of NLRP3 inflammasome dependent IL-1β and IL-18 secretion in response to non-canonical activators, such as UVB radiation and cholera enterotoxin subunit B, which leads to pyroptosis through Gasdermin D cleavage and activation (Sollberger et al. 2012; Knodler et al. 2014; Vigano et al. 2015). It does not process IL-1β directly.

^{138}Gln-CASP5. Human caspase-5, with caspase-4, have been suggested to originate from a duplication of the murine caspase-11. Caspase-5 was originally cloned from human THP-1 cells and placenta tissue and was named ICErelIII and TY, respectively (Munday et al. 1995). It shares 51% sequence homology with caspase-1 and 74% with caspase-4. However, contrarily to caspase-4, the expression of caspase-5 is restricted to the placenta, lung, liver, spleen, small intestine, colon, and peripheral blood lymphocytes (Lin, Choi, and Porter 2000). The roles, functions and activation mechanisms of caspase-5 are similar to caspase-4, and it is involved in many skin conditions such as psoriasis and lupus through activation by the NLRP1 inflammasome (Zwicker et al. 2017).

^{149}Cys-RAB39a. Rab39a is a member of the Rab-GTPase family of proteins, which are responsible for vesicle trafficking in pathways such as secretion and endocytosis (Zerial and McBride 2001). Rab39a is a necessary caspase-1 binding partner for the secretion of IL-1β. Cleavage of Rab39a by caspase-1 at the conserved cleavage site allows the release of the active form of IL-1β from cells, thereby propagation of the inflammatory reaction (Becker, Creagh, and O'Neill 2009).

^{29}Ile-GRZA. Activated granzyme A has the ability to process IL-1β into its active form, in a caspase-1 independent manner, in the context of a *Pasteurella multocida* infection (Hildebrand et al. 2014). Both mouse and human granzyme A could induce pro-inflammatory cytokine secretion (IL-1β, IL-6, IL-8 and TNFα) from peripheral blood monocytes, once internalized into the cells (Metkar et al. 2008). Additionally, granzyme A is

capable of activating TLR9 in the endosomes of plasmacytoid dendritic cells, switching on their maturation program and inducing type I interferon production (Shimizu et al. 2019).

^{26}Ile-GRZK. In the context of LCMV infection, activated granzyme K was shown to induce active IL-1β release from macrophages. This is specific to granzyme K as neither granzyme A or B were able to induce cytokine production after LCMV challenge (Joeckel et al. 2011).

^{27}Ile-GRZM. A role for granzyme M in the secretion of proinflammatory cytokines such as IL-1α, IL-1β, TNFα and IFNg was discovered when mice KO for this granzyme failed to secrete these cytokines in comparable levels to controls following LPS stimulation (Anthony et al. 2010). However, the mechanism of how granzyme M increases the signaling cascade and cytokine production downstream of the LPS/TLR4 activation remains unknown. Granzyme M is also required for maximal secretion of MIP-1α following *Listeria monocytogenes* infection (Baschuk et al. 2014).

^{37}Tyr-IL-18, ^{6}Glu-IL-36β and ^{16}Tyr-IL-36γ. IL-18 and IL-36 belong to the IL-1 family of cytokines, which is closely linked to inflammation and non-specific response to infection and foreign antigens (reviewed in (Dinarello 2018)). Both IL-18 and IL-36 are proinflammatory cytokines, and are involved in INF-γ and TNFα production, chemokine secretion, expression of vascular cell adhesion molecules and have a role in auto-immune skin conditions such as psoriasis ((Gracie, Robertson, and McInnes 2003; Gresnigt and van de Veerdonk 2013) and references therein). proIL-18 is processed by caspase-1 after Asp^{36} into its active form, however processing of this cytokine can also occur by mast cell chymase (after Phe^{57}), or by elastase (after Val^{98}, Leu^{143} and Val^{159}) (Robertson et al. 2006). Interestingly, all these cuts by proteases generate destabilising N-termini, suggesting that this processing destines the IL-18 peptides for degradation, a hypothesis that is corroborated by the loss of activity post-processing by elastase. IL-36 is not cleaved by caspase-1, but has multiple cleavage sites for neutrophil-derived proteases such as cathepsin-G, elastase and proteinase-3 (Henry et al. 2016). The ^{37}Tyr-IL-18, ^{6}Glu-IL-36β and ^{16}Tyr-IL-36γ fragments are likely Arg/N-degron pathway substrates.

^{49}Tyr-CCL3. Macrophage inflammatory protein 1a, (MIP-1α) also known as CCL3, is a proinflammatory chemoattractant for monocyte-lineage cells and lymphocytes into inflammatory tissue (Cook 1996). CCL3 has a caspase-1 cleavage site at Asp^{48}, revealing a destabilising residue at position 49, and making this newly formed peptide a likely Arg/N-degron pathway substrate. However, it is unclear whether or not cleavage by caspase-1 is necessary for the proinflammatory action of CCL3. Mutational analysis of the amino acids composing CCL3 revealed that the Asp^{48} is critical for aggregation of MIP-1α (Czaplewski et al. 1999), and that aggregation is necessary for the chemokine activity of this protein (Ren et al. 2010). This implies the importance of the caspase-1 cleavage site for optimal activity of CCL3.

^{245}Glu-Ataxin-3 and ^{249}Leu-Ataxin-3. Polyglutamine tract protein defective in spinocerebrellar ataxia type 3 (Ataxin-3) is a deubiquitinating enzyme involved in protein homeostasis maintenance, transcription, cytoskeleton regulation, myogenesis and degradation of misfolded chaperone substrates. It is processed by caspase-1 at the Asp^{244} and Asp^{248} sites, generating two likely Arg/N-degron pathway substrates, although this remains to be experimentally proven. Cleavage by caspase-1 causes the protein fragments to aggregate, which could lead to neurodegeneration, inflammation and apoptosis (Wellington et al. 1998; Jadhav, Zilka, and Novak 2013).

^{50}Cys-hnRNPA2. The Heterogeneous nuclear ribonucleoprotein 2 (hnRNPA2) associates with nascent pre-mRNAs, packaging them into hnRNP particles. Packaging plays a role in various processes such as transcription, pre-mRNA processing, RNA nuclear export, subcellular location, mRNA translation and stability of mature mRNAs. hnRNPA2 is crucial for embryonic development (Kwon et al. 2019), however, direct roles in inflammation have yet to be uncovered. hnRNPA2 is cleaved by caspase-1 at the Asp^{49} site, and is a likely Arg/N-degron pathway substrate.

^{681}Leu-Matrin-3. Matrin 3 is a Ca^{2+}/calmodulin-binding protein cleaved by caspase-5 at the Asp^{680} position (Valencia, Ju, and Liu 2007), and is a likely Arg/N-degron pathway substrate. Cleavage by caspases modulates the activity of the protein. Matrin-3 has recently

been involved in the DNA-mediated innate immune response, along with long-noncoding RNAs HEXIM1 and NEAT1 (Morchikh et al. 2017).

Proinflammatory fragments generated by proteases are targeted for degradation by the Arg/N-degron pathway

To determine whether proinflammatory fragments such as those listed in the first part of Table 7 are degraded by the Arg/N-degron pathway, we used the Ubiquitin reference technique (URT) where the degradation of a desired test protein is evaluated by a pulse-chase assay (Piatkov, Brower, and Varshavsky 2012; Lévy, Johnston, and Varshavsky 1999). First, a series of reporters are constructed containing the test protein (with a N-degron or not) fused to a reference ^{f}DHFR-Ub^{R48}, a FLAG-tagged derivative of the mouse dihydrofolate reductase (Figure 29). In the pulse phase of the assay, co-translational cleavage of the fusion protein by deubiquitylases produces the test protein and the reference polypeptide at an initial equimolar ratio, both labelled with radioactive methionine. Following a cycloheximide chase in the absence of ^{35}S-methionine, relative degradation rates of the test protein can be quantified by normalization to the level of the ^{f}DHFR stable reference at the same time point.

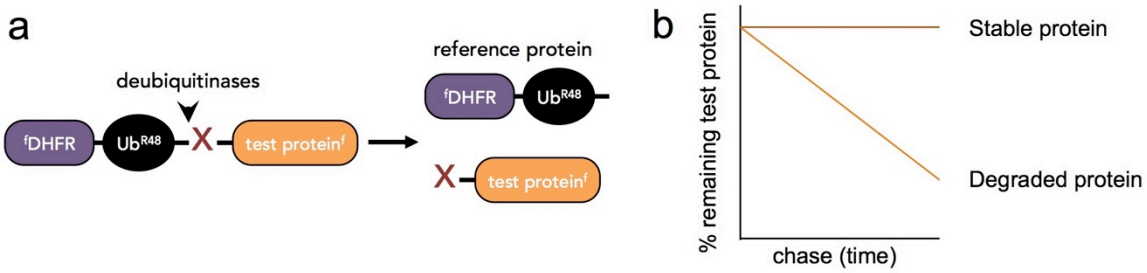

Figure 29. The URT assay (Lévy et al. 1996). (a) Schematic representation of the protein construct used in the URT assay. Co-translational cleavage of the fusion protein by deubiquitinases produces both the test protein and the reference polypeptide at an initial equimolar ratio. (b) Graphical representation of the degradation rate of an unstable protein fragment recognised and degraded by the N-degron pathway, as seen in a pulse-chase assay.

We first examined the degradation of inflammatory caspases. To demonstrate that after self-cleavage, the remaining C-terminal protein fragments are targets of the Arg/N-degron pathway, caspase-URT fusions tagged with the flag epitope at the C-terminus were labeled with ^{35}S-Met/Cys, followed by a chase, immuno-precipitation with a monoclonal anti-FLAG antibody, SDS/PAGE separation and quantification by autoradiography (Figure 30). Indeed, Asn^{120}-CASP1, Gln^{81}-CASP4 and Gln^{138}-CASP5 were degraded quickly in reticulocyte extract, whereas the otherwise identical fragments bearing the N-terminal Val residue were either stable or nearly stable (Figure 30). These results indicate that the three human inflammatory caspases contain Arg/N-degrons and are targeted for degradation by this pathway.

Next, we examined whether proinflammatory fragments generated by inflammatory caspase proteolysis or other proteases contained N-degrons. We confirmed experimentally that the Cys^{149}-Rab39a fragment generated after caspase-1 mediated cleavage was indeed a substrate of the Arg/N-degron pathway using the Ubiquitin-reference technique described above (Figure 31a-b). We also assessed 3-phosphoinositide-dependent protein kinase 1 (PDK1), as this protein has been associated to inflammation by its involvement in the signalling pathways of NF-κB and TGF-β (Seong et al. 2007; Sun et al. 2017). PDK1 is cleaved by the endopeptidase PILSAP at position 9, leaving an Asp at the P1′ position (Yamazaki et al. 2004). Mutating the Asp for a Val stabilized the protein in the URT assay, indicating that the C-terminal portion of PDK1 generated after cleavage by PILSAP is targeted by the Arg/N-degron pathway for degradation through the proteasome (Figure 31c-d). Finally, we examined the degradation of activated granzymes A and M, which are known to increase production and release of inflammatory cytokines. Processing of the granzyme activation peptide by the protease DPP1 exposes an Ile, which can be recognized by the N-degron pathway. Indeed, both granzyme A and granzyme N were short lived in the URT assay compared to identical fragments bearing a Val residue at the N-terminus (Figure 31e-h). However, changing the Ile to a Val did not completely stabilize the activated granzymes, suggesting multiple pathways for the degradation of these enzymes.

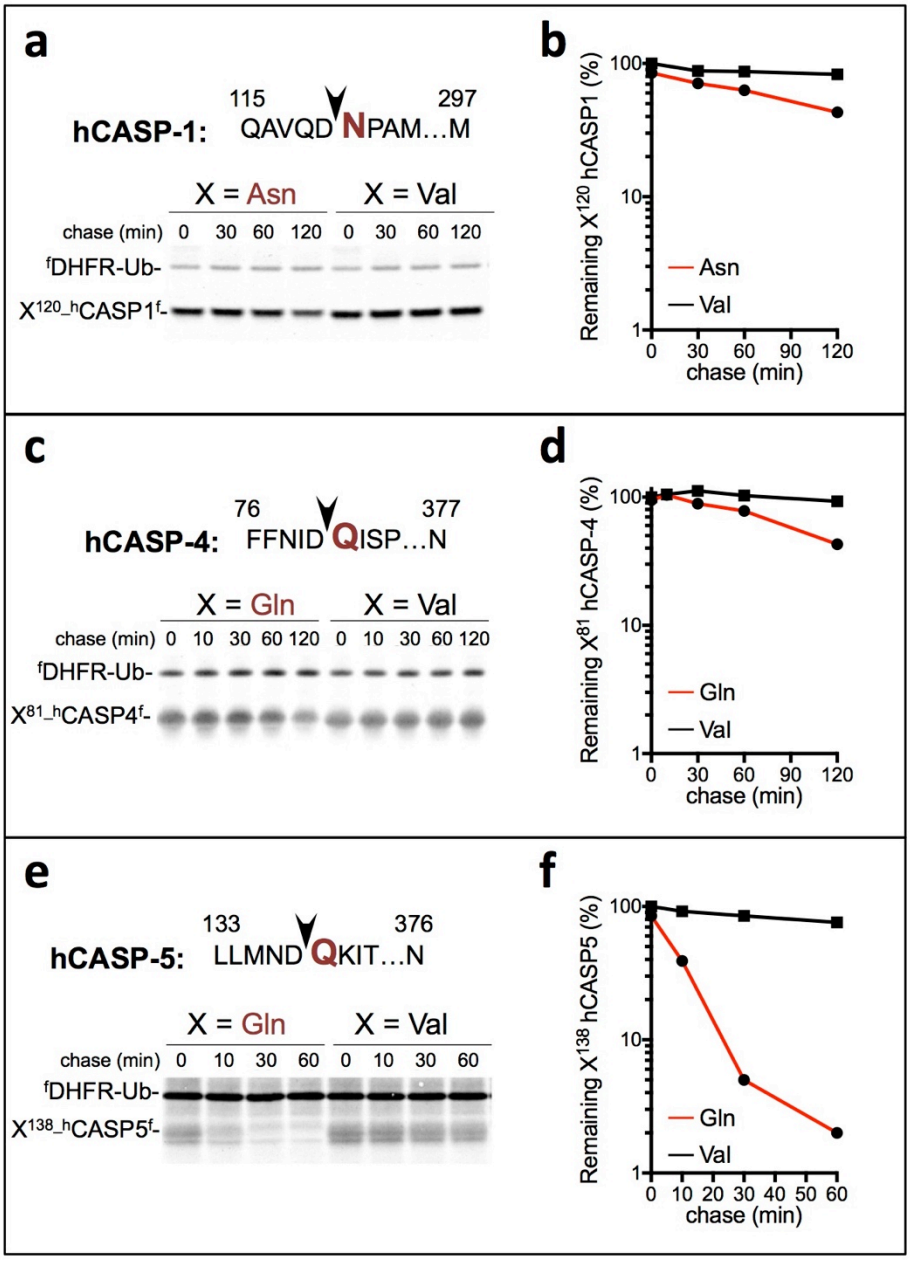

Figure 30: Proinflammatory caspases are short-lived N-degron pathway substrates. (a) The cleavage site in human CASPASE-1 is indicated by an arrowhead, with the destabilizing residue shown in red. Asn^{120}-hCASP-1 (produced from ^{f}DHFR-UBR^{48}-Asn^{120}-hCASP-1^{f}) and Val^{120}-hCASP-1 were expressed in reticulocyte extract and labeled with ^{35}S-Met/Cys for 10 min at 30°C, followed by a chase, immuno-precipitation with anti-flag antibody SDS/PAGE, and autoradiography. (b) Quantification of A using the reference protein ^{f}DHFR-UBR^{48}. (c) Same as a, but with human X^{81}-CASP-4^{f} (X=Gln and Val). (d) Quantification of c. (e) Same as a, but with human X^{138}-CASP-5^{f} (X=Gln and Val). (f) Quantification of e. Results are representative of at least 2 independent experiments.

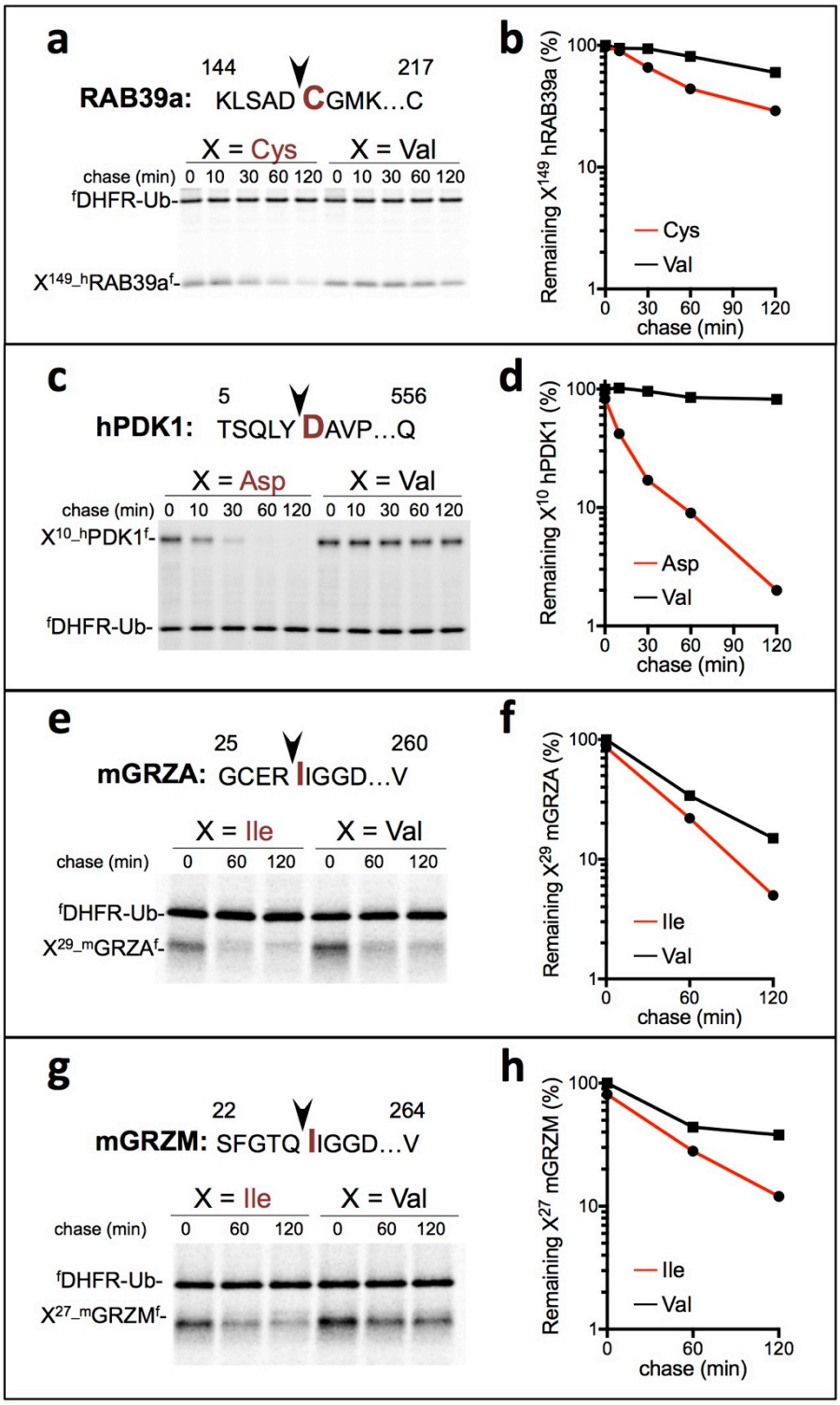

Figure 31: Proinflammatory fragments are short-lived N-degron pathway substrates. (a) The cleavage site in human Rab39a is indicated by an arrowhead, with the destabilizing residue shown in red. Cys^{149}-hRab39a and Val^{149}-hRab39a were expressed in reticulocyte extract and labeled with ^{35}S-Met/Cys for 10 min at 30°C, followed by a chase. (b) Quantification of a using the reference protein ^{f}DHFR-UBR^{48}. (c) Same as a, but with human X^{10}-PDK1 (X=Asp and Val). (d) Quantification of c. (e) Same as a, but with mouse X^{29}-

GRZA (X=Ile and Val). (f) Quantification of e. (g) Same as a, but with mouse X^{27}-GRZM (X=Ile and Val). (h) Quantification of g. Results are representative of at least 2 independent experiments.

In summary, we examined 7 of 15 proinflammatory fragments with potential N-degrons (Figure 28) and found that all of them are degraded by the Arg/N-degron pathway (Figures 30 and 31). For all fragments except granzymes, the Arg/N-degron pathway is the main mechanism of degradation, at least in reticulocyte extracts.

Partial downregulation of the Arg/N-degron pathway leads to an enhanced inflammatory response

Since inflammatory caspases and some of their substrates are targets of the Arg/N-degron pathway, even a partial ablation of this pathway should stabilize proinflammatory fragments in the cell and enhance the inflammatory response. Rab39a is a necessary binding partner to caspase-1 for the cleavage and secretion of IL-1β (Becker, Creagh, and O'Neill 2009; Monteith et al. 2018). As a result, the most straightforward consequence of stabilization of caspase-1 or Rab39a in the cell would be the increased secretion of IL-1β.

We used an RNAi approach to downregulate all four UBR-ubiquitin ligases of the Arg/N-degron pathway in the J774A.1 mouse macrophage cell line. 40-60% downregulation of mRNA and 50-90% downregulation of the proteins was achieved in J774A.1 cells after 72h of exposure to siRNA (Figure 32). Higher concentrations of siRNA led to cell death, therefore we chose to use the lower concentration of siRNA even though we could not achieve full downregulation of the Arg/N-degron pathway. This result also indicates that macrophages are sensitive to levels of activity of the N-degron pathway to a higher extent than hepatocytes, which could be related to their higher rates of proliferation. Indeed, the more a cell proliferates, the more dependent it is on the N-degron pathway (Brower and Varshavsky 2009; Leu, Kurosaka, and Kashina 2009).

To evaluate the levels of IL-1β production in macrophages with downregulated UBR-ubiquitin ligases of the Arg/N-degron pathway, we first incubated J774A.1 cells with siRNA,

then stimulated the cells with 1, 10 or 50 ng/ml of LPS, in the presence of 5 mM ATP for the last hour.

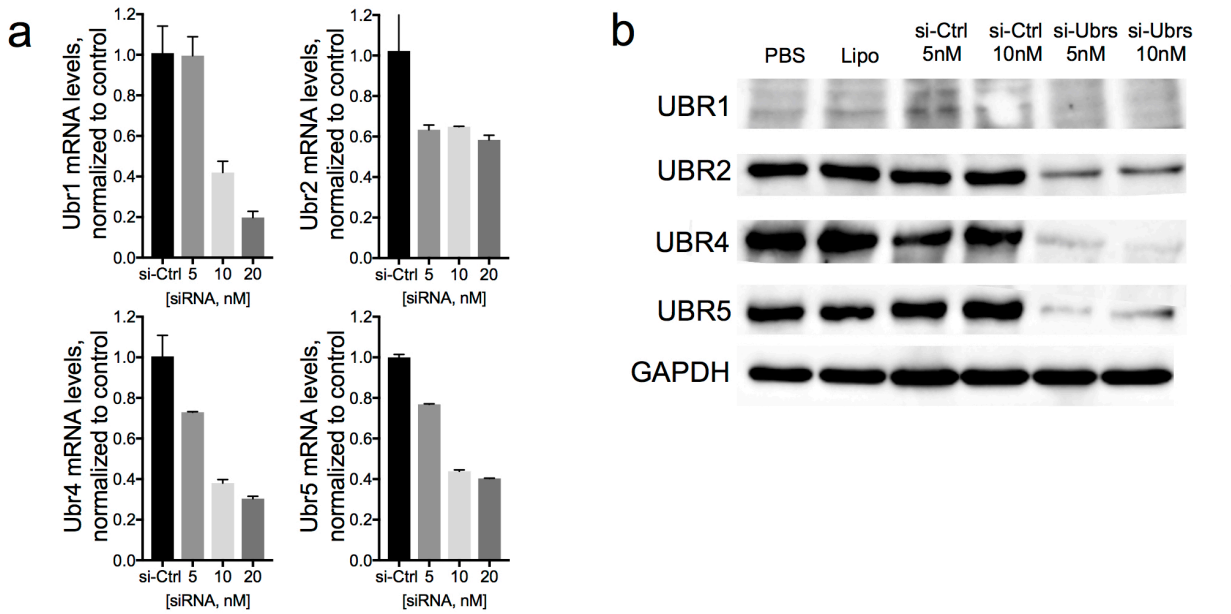

Figure 32. siRNA mediated downregulation of UBR-ubiquitin ligases of the Arg/N-degron pathway in mouse macrophages. (a) mRNA and (b) protein levels of UBR1,UBR2, UBR4 and UBR5 in J774A.1 cells after 72h of exposure to 5 or 10nM siRNA. Results are representative of 3 biological replicates.

Western blot (Figure 33a) and Cytokine Bead Assay (Figure 33b) analysis revealed a significant increase in the secretion of IL-1β in the media of cells with a downregulated Arg/N-degron pathway. The assays recognize both pro- and cleaved IL-1β but the Western Blot assay clearly demonstrates the dramatic increase of the cleaved portion of IL-1β in the media of UBR knockdown cells compared to control, especially at the lower LPS concentration. Macrophages in culture stimulated with LPS are known to commit pyroptosis, a form of cell death induced by inflammatory caspases (Hirano et al. 2017). Additionally, macrophages can secrete GAPDH under certain physiological stresses including extracellular ATP, which is also used in this assay (Chauhan et al. 2019; Takenouchi et al. 2015). Therefore, we assessed the presence of GAPDH in the media both as a loading control and to indicate that the amount of pyroptosis is the same in all conditions, indicating that the increase of IL-1β secretion is not due to an increase in cell death. Predictably, the

amounts of cleaved caspase-1 were not changed in UBR KD macrophages, since the mouse cleaved caspase-1 is not a substrate of the Arg/N-degron pathway (Figure 33a). Importantly, there was no secretion of IL-1β without LPS stimulation, indicating that downregulation of UBR-ubiquitin ligases did not induce inflammation in itself. Additionally, there was no increase in the production of pro-IL-1β in the J774A.1 cells, implying that only the cleavage and export of IL-1β was increased in the Arg/N-degron pathway knockdown cells. These results indicate that downregulation of the Arg/N-degron pathway only sensitises cells to inflammation, and requires a proinflammatory signal such as LPS to induce cytokine response. Together with the URT assays, these results demonstrate that the Arg/N-degron pathway is capable of regulating the level of IL-1β secretion, through its ability to degrade proinflammatory fragments.

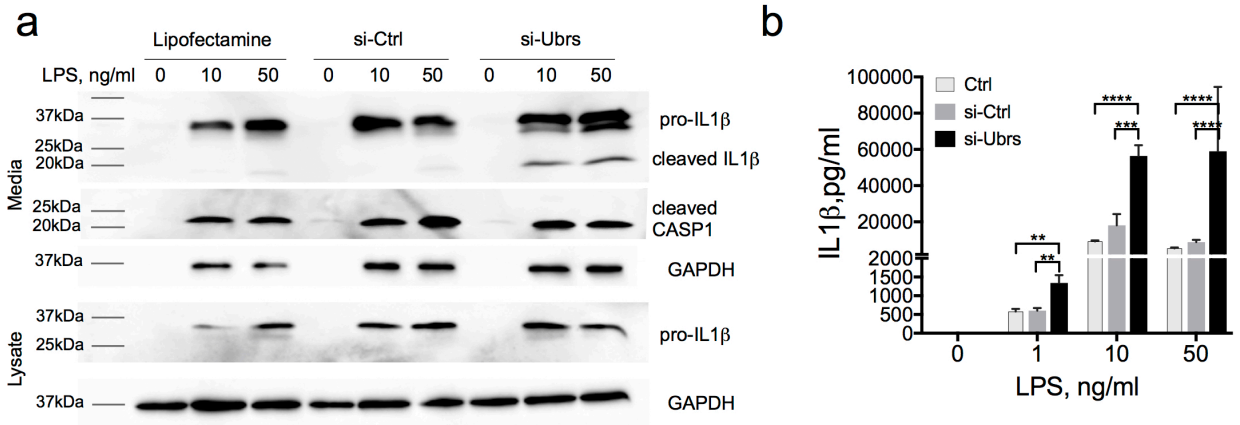

Figure 33. Increased IL-1β secretion after downregulation of UBR-ubiquitin ligases of the Arg/N-degron pathway. (a) Western Blot analysis of pro- and cleaved IL-1β and cleaved Caspase-1 from media and lysates of cells treated with 10nM of si-Ctrl or siRNA against UBRs for 72h, followed by 1, 10 or 50ng/ml of LPS for 6h in the presence of 5mM ATP for the last hour. (b) Quantification of the secreted pro- and cleaved IL-1β from the media of J774A.1 cells treated as in (a) by the Cytokine Bead Assay (CBA). n=2-3 biological replicates per condition. P values were determined by a two-way ANOVA (***P 0.001, ****P 0.0001).

N-recognins are not degraded during inflammatory response

Apoptotic caspases can cleave N-recognins of the Arg/N-degron pathway during late apoptosis, once the proapoptotic signalling exceeds the antiapoptotic activity of the Arg/N-degron pathway, pushing the cells beyond the point of no return (Piatkov, Brower, and Varshavsky 2012). Unlike apoptosis, cells can recover from a robust proinflammatory signal, and would require a functional Arg/N-degron pathway in order to degrade proinflammatory proteins. Therefore, if we are correct in assuming that the Arg/N-degron pathway participates in the regulation of inflammation, it is important that the inflammatory response does not induce the degradation of the UBR-ubiquitin ligases of this very pathway. To test this hypothesis, we used LPS to generate an inflammatory response and staurosporine to cause apoptosis in the murine macrophage cell line J774A.1. We examined protein levels of N-recognins of the Arg/N-degron pathway after stimulation and found that these levels were comparable to controls in cells treated with LPS or LPS and ATP while they are significantly decreased in cells treated with staurosporine (Figure 34). This indicates that contrarily to apoptotic conditions, UBR1, UBR2, UBR4 and UBR5 are not cleaved or degraded during inflammation.

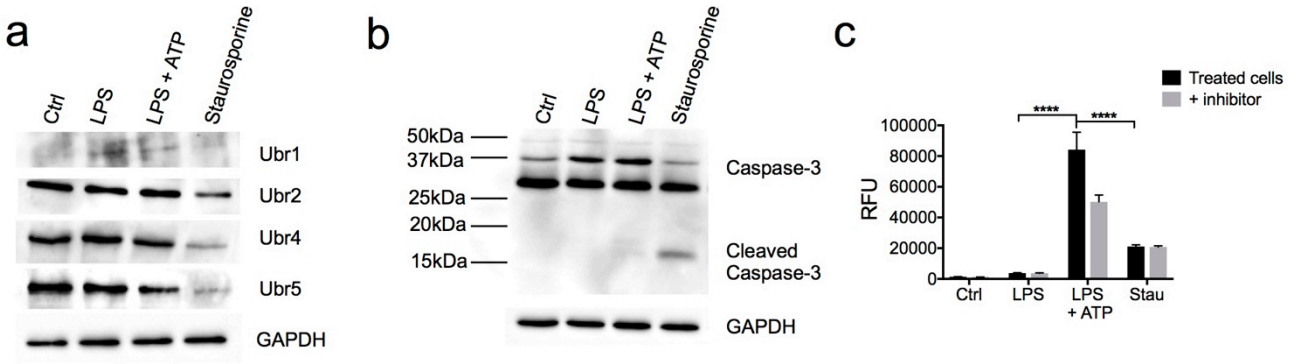

Figure 34. UBR-ub-ligases of the Arg/N-degron pathway are not targeted by caspases -1 and -3. (a) Western Blot analysis of UBR-ub ligases of the Arg/N-degron pathway after caspase-1 or caspase-3 activation. Cells were treated with LPS (100ng/ml) or staurosporine (500nM) for 24h and assessed for the 4 UBR ub-ligases, for caspase-3 (b) and for caspase-1 activity (c) Caspase-1 activity was measured in the media of cells treated as in (a), in presence of the caspase-1-specific inhibitor YVAD-CHO in half of the wells. Results are representative of two independent experiments. P values were determined by a two-way ANOVA (***P 0.001, ****P 0.0001).

In light of our new understanding that the Arg/N-degron pathway is involved in the regulation of inflammation, and that the siRNA-mediated downregulation of the pathway caused increased inflammation by accumulation of proinflammatory fragments generated by repeated inflammatory stimuli, in our case the lipid nanoparticles, we decided to adopt the following strategy in the cancer model: reduce the LNP dose and concomitantly administer chemotherapy (Figure 35).

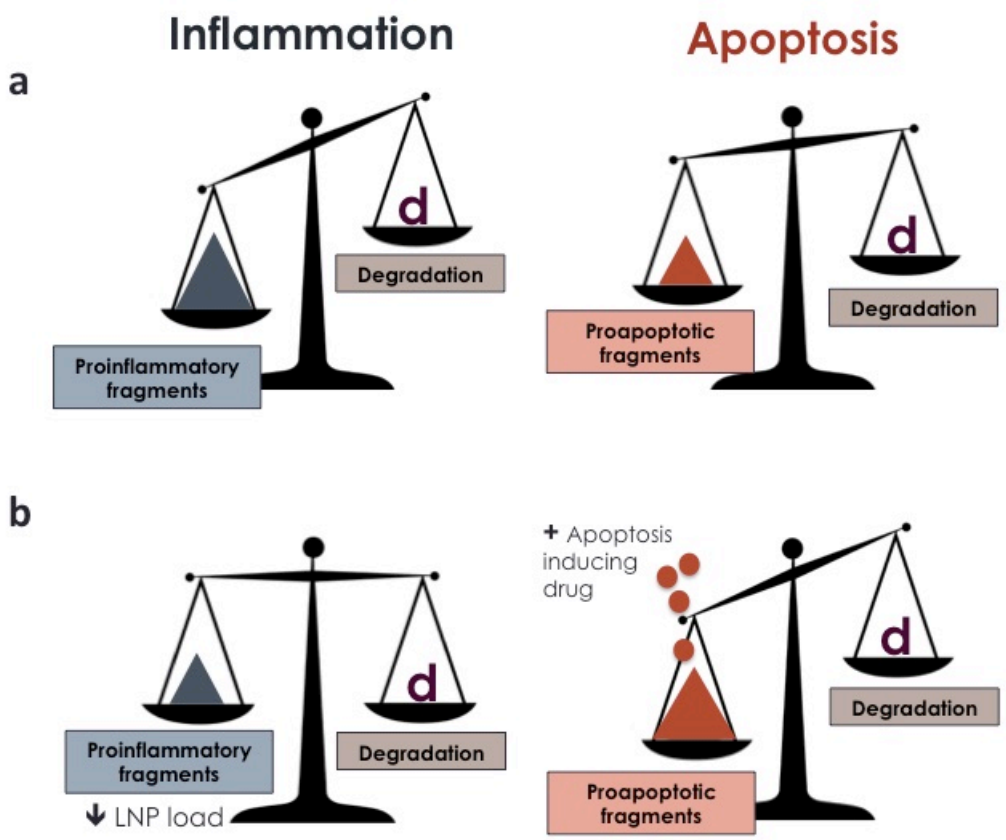

Figure 35: Schematic representation of the strategy used in this study to avoid inflammation and increase apoptosis in the HCC model. In both scenarios, the Arg/N-degron pathway is downregulated by siRNA, so the degradation of N-degron-bearing fragments is the same. (a) Repeated inflammatory stimuli causes greater accumulation of proinflammatory fragments than proapoptotic fragments. (b) Decreasing the LNP load and using apoptosis inducing drugs such as chemotherapy reduces the production of proinflammatory fragments while generating more proapoptotic fragments in the cell.

Lowering the LNP dose decreases the inflammatory stimuli given to liver cells, while administrating chemotherapy produces proapoptotic fragments in the cell, which the

downregulated N-degron pathway cannot degrade, tipping the balance towards apoptosis instead of inflammation (Figure 35). This strategy allows to capitalize on the effects of the Arg/N-degron pathway downregulation on proliferation and apoptosis in cancer cells while avoiding increased inflammation

Development of a combinatorial treatment based on downregulation of the Arg/N-degron pathway and apoptosis inducing drugs

Knockdown of the Arg/N-degron pathway potentiates the action of apoptosis inducing drugs

The combinatorial treatment with apoptosis inducing drugs combined with a reduced dose of siRNA against UBR1, UBR2, UBR4 and UBR5 was first tested *in vitro* to assess the impact of downregulating UBRs in the presence of staurosporine or doxorubicin, on proliferation and apoptosis. Hepa 1-6 cells were transfected with siRNA for 72h before the addition of low doses of doxorubicin (Figure 36a) or staurosporine (Figure 36b) for an additional 48 or 24h respectively. Using the Neutral Red assay, we determined that proliferation was inhibited at lower doses of siRNA against UBRs when doxorubicin is added to the cells (Figure 36a). Indeed, at 0.156nM of UBR-siRNA, when proliferation of the cells is inhibited by 15-25%, addition of doxorubicin at doses that do not affect proliferation (right graph) accentuates this phenotype by another 15-20%. The effect is milder on proliferation if staurosporine is used in combination with siRNA (Figure 36b), most likely because of the mode of action of staurosporine, which causes apoptosis through protein kinase inhibition and caspase-3 activation (Feng and Kaplowitz 2002), compared to doxorubicin which causes DNA damage through intercalation in the double helix, and can have an effect on proliferation as well as apoptosis (Thorn et al. 2011).

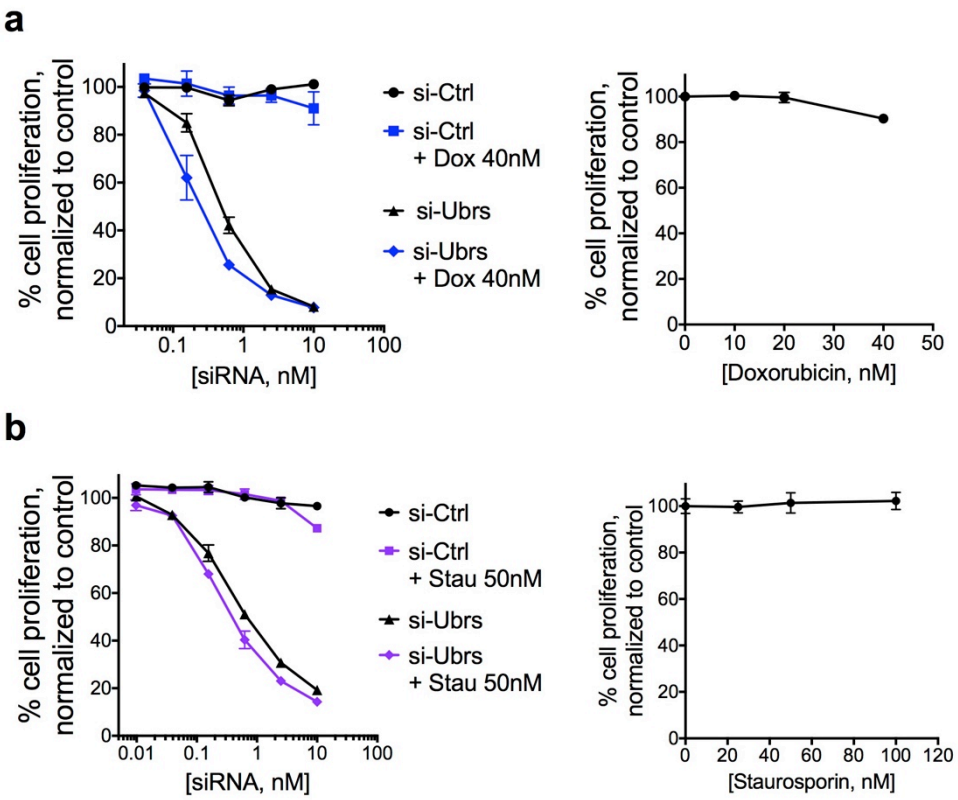

Figure 36. Knockdown of UBR-Ubiquitin ligases of the N-degron pathway potentiates the action of apoptosis inducing drugs on proliferation of cells in vitro. (a) Proliferation of Hepa 1-6 cells after exposure to siRNA and doxorubicin (left) or doxorubicin alone (right). (b) Proliferation of Hepa 1-6 cells after exposure to siRNA and staurosporine (left) or staurosposine alone (right). Results are representative of 2 independent experiments with 3 biological replicates per condition.

As for apoptosis, when cells are treated with siRNA against UBR-ubiquitin ligases alone, we see an increase of 4-5% of apoptotic cells compared to controls. However, when the siRNA are used in combination with apoptosis inducing drugs, apoptosis increases by 11.5-13.5% compared to controls (Figure 37a). The same effects on apoptosis are observed with staurosporine when coadministered with siRNA (Figure 37b). Therefore, the combinatorial approach decreases proliferation and increases apoptosis at lower doses of siRNA and apoptosis inducing drugs that would otherwise be inefficient alone, demonstrating that both treatments act in synergy to kill cancer cells.

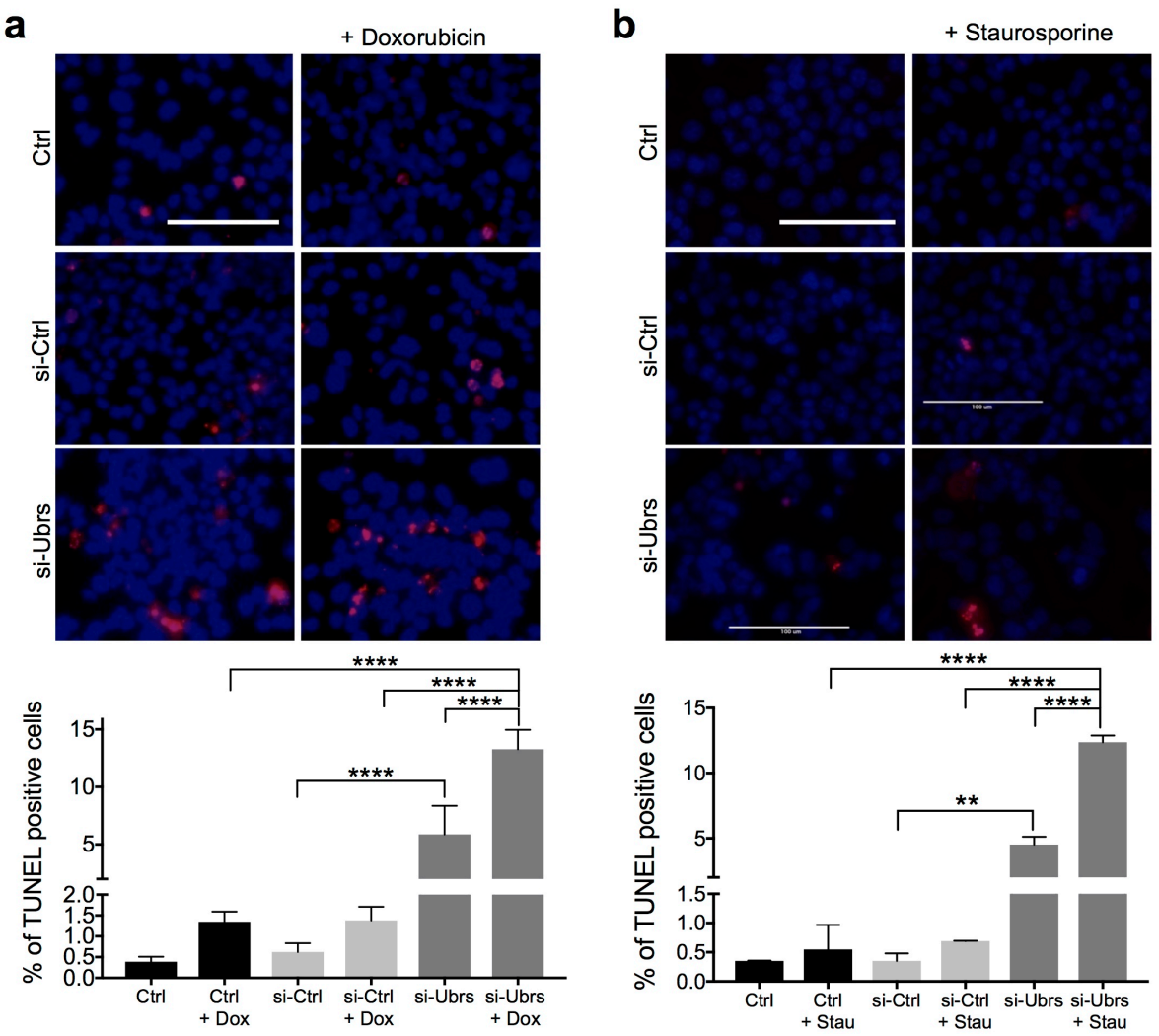

Figure 37. Knockdown of UBR-ubiquitin ligases of the N-degron pathway potentiates the action of apoptosis inducing drugs on apoptosis of cells in vitro. Analysis of cell death by TUNEL, in Hepa 1-6 cells after 72h of exposure to 1nM siRNA against UBRs and an additional 48h to doxorubicin (a) or 24h with staurosporine (b). Red nuclei represent TUNEL-positive cells. Scale bar, 100 μm. Results show mean ± SD. n= 2-4 biological replicates per condition. A minimum of 4,000 cells were counted per condition. P values were determined by a one way Anova (****P <0.0001)

Finally, the combinatorial approach was tested in the oncogene-driven mouse model of HCC. Mice with HCC were alternatively injected with LNP-siRNA at 1 mg/kg total and doxorubicin (2 or 4 mg/kg) every 3-4 days, for a total of 4 weeks, starting during the 6th week after induction of the cancer (Figure 38a). Control groups include HCC mice receiving PBS (vehicle), doxorubicin alone (2 or 4mg/kg, 1x/wk), LNP-siCtrl alone or LNP-siUBRs alone (1mg/kg, 1x/wk) (Figure 38b). Mice without HCC were also injected with doxorubicin, to test

whether the chemotherapy would affect general viability of the mice ("normal liver" on Figure 39).

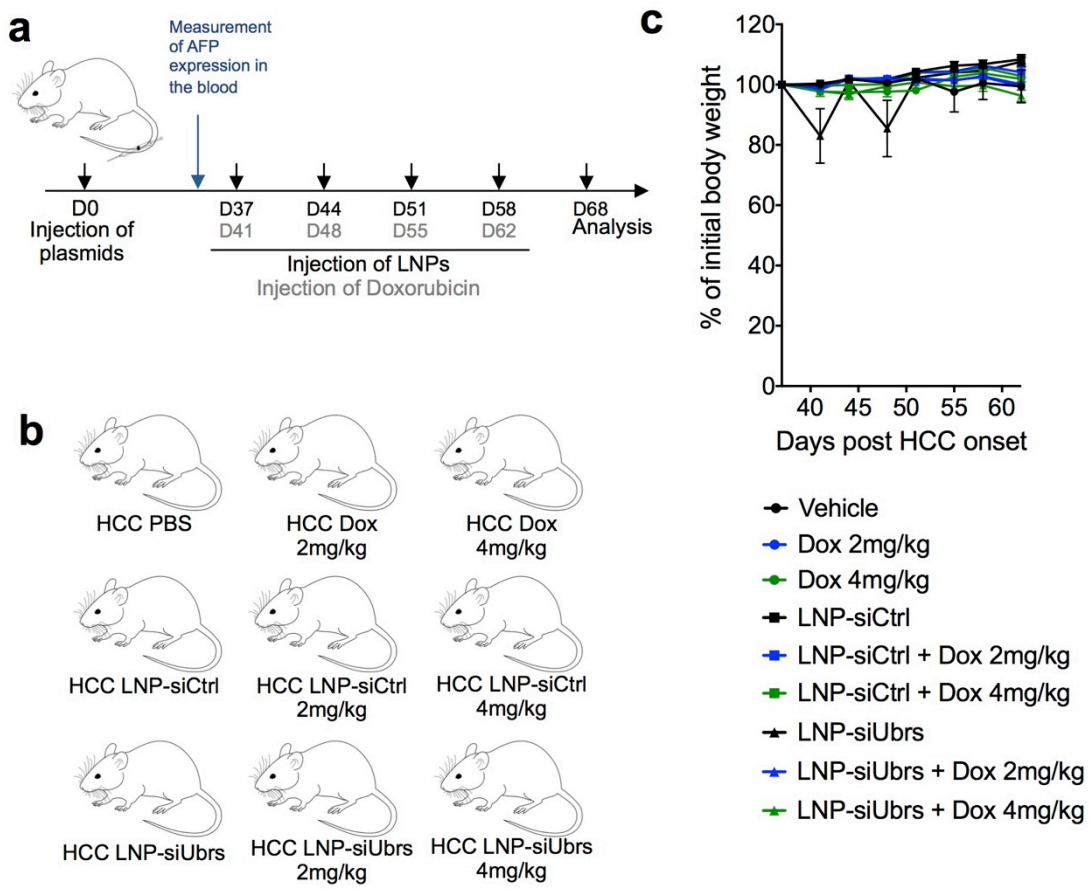

Figure 38. Combinatorial treatment of chemotherapy with LNPs is well tolerated by HCC mice. (a) Schematic representation of the experiment: timeline of tumor induction (injection of oncogene-encoding plasmids) and repeated injections of LNP-formulated siRNA (black) and Doxorubicin (grey). Tissues were collected for analysis on day 68 after tumor induction. (b) Schematic representation of the different groups of mice in the study. n=10-18 mice per group. (c) Weight curve of animals treated with LNPs, measured before each injection and averaged for the group. Measures were compared as a percentage of change from the first injection day.

We found that prolonged downregulation of the Arg/N-degron pathway combined with the use of a chemotherapeutic agent led to inhibition of HCC progression. Relative liver weights were decreased by an average of 30% compared to controls (Figures 39 and 40), and tumor load was significantly lower than that observed with doxorubicin alone, and that of the control LNP-siRNA with doxorubicin. Gross morphology and liver histology of the HCC livers treated with LNP-siUBRs and doxorubicin resembled normal liver tissue, contrarily to all other groups, indicating less proliferation and less damage to the tissue

(Figures 40 and 41). Tumor nodules were smaller, and fewer dysplastic hepatocytes were observed.

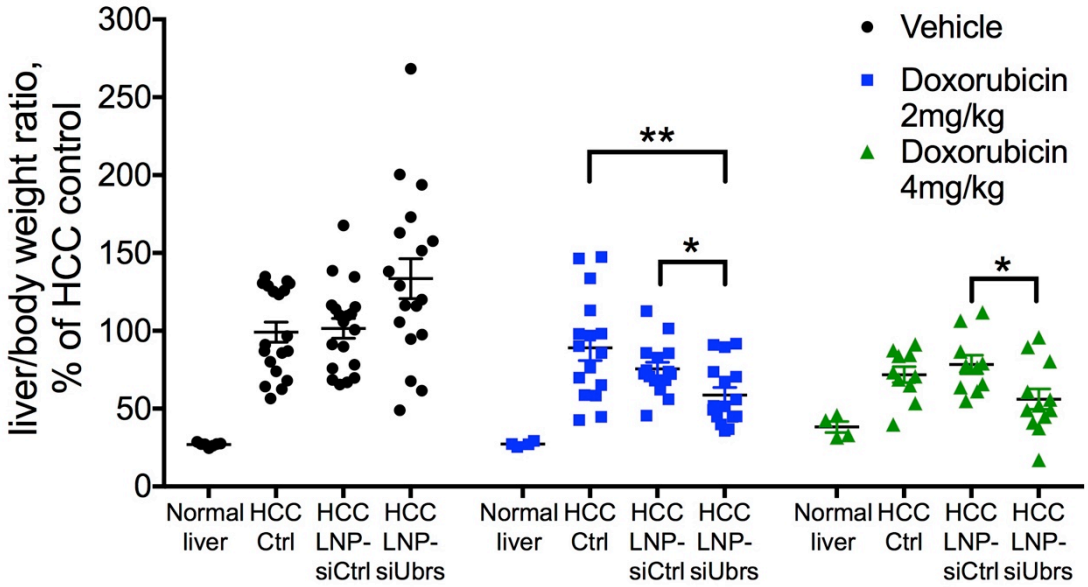

Figure 39. Chemotherapy in HCC is more efficient with downregulation of the N-degron pathway. Liver/body mass ratio analysis of mice bearing HCC treated for 4 weeks with LNPs at 1mg/kg, with or without doxorubicin treatment. n=10-18 mice per group. Results show mean ± SEM P values were determined by Mann Whitney tests (*P <0.05, **P 0.01)

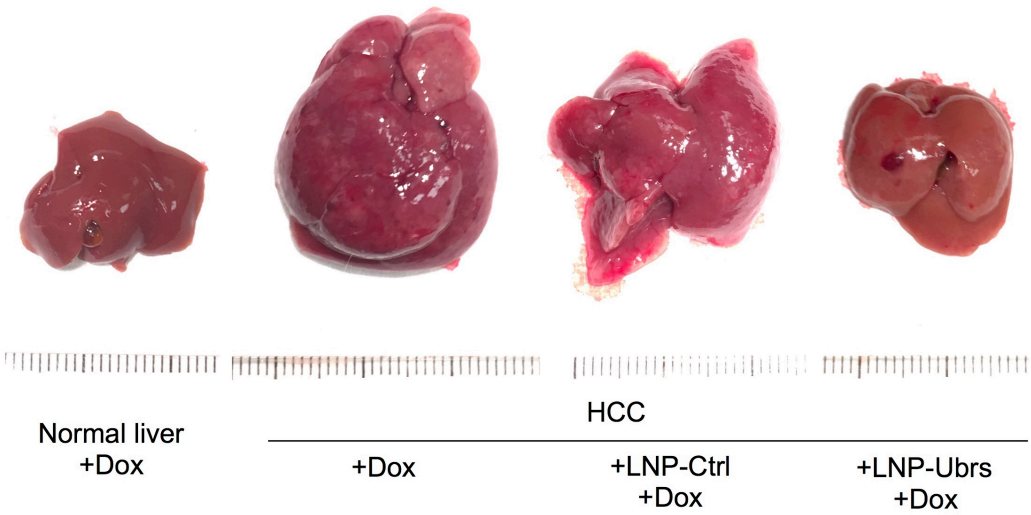

Figure 40. Representative HCC livers treated with the combinatorial therapy. Mice were treated with LNP-siRNA and Doxorubicin at 2mg/kg. Ruler = cm.

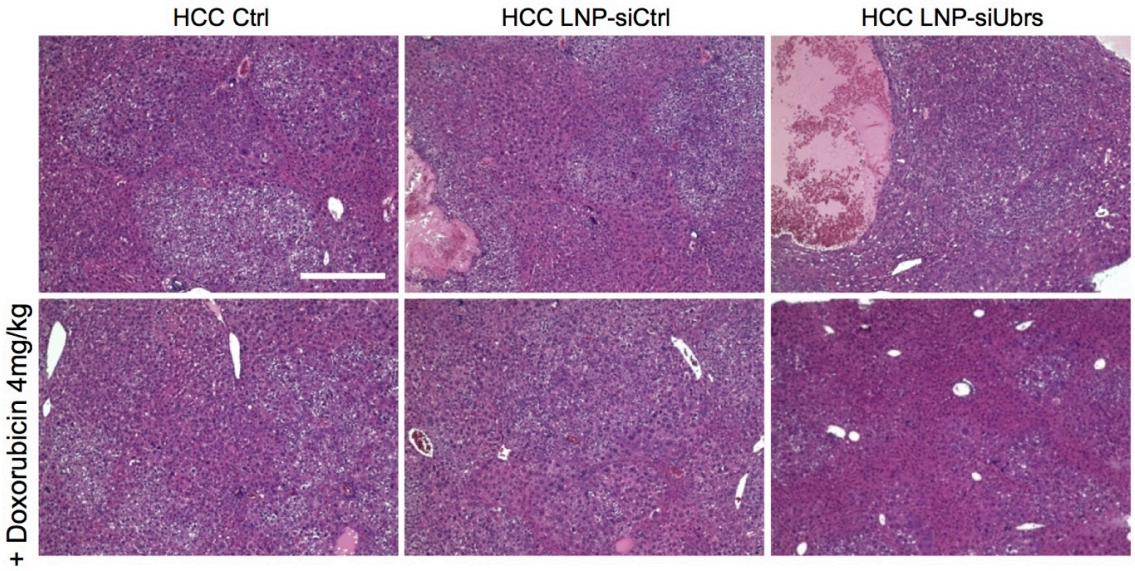

Figure 41. Histology of HCC livers treated with the combinatorial therapy. H&E staining of liver sections from HCC mice treated with LNPs and Doxorubicin. Scale bar = 100μm.

The reduced dose of LNPs used in this case allowed to avoid an increase of inflammatory immune cells, as seen by the equal number of inflammatory cells in the spleen of HCC animals of all groups (Figure 42). Additionally, doxorubicin does not have an immediate effect on inflammation, nor does it affect the viability of immune cells (Figure 42).

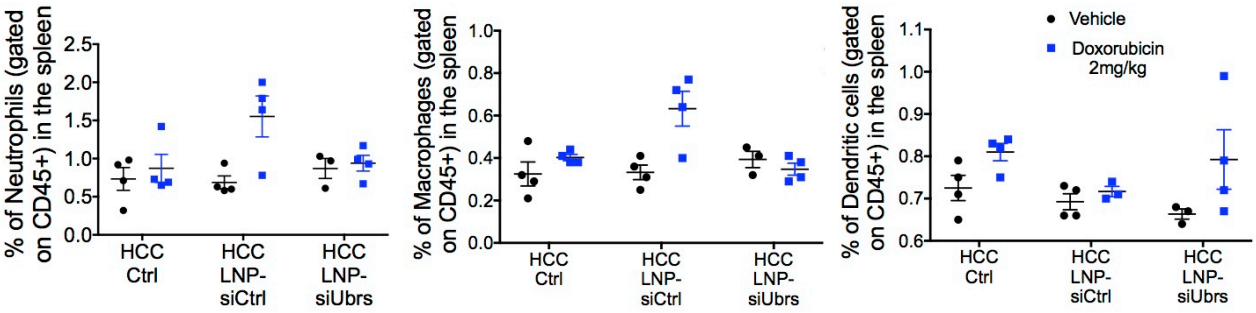

Figure 42: Doxorubicin does not affect inflammation in HCC. Analysis by flow cytometry of Neutrophils, Macrophages and Dendritic cells in the spleen of HCC mice treated with LNPs and Doxorubicin. n=4 mice per group. All differences between groups are non-significant.

To demonstrate the effect of the combinatorial treatment on tumor cell proliferation and survival, we stained fixed liver sections for Ki67, a marker of cellular proliferation (Figure

43a). In the animals treated with LNP-siUBRs, Ki67-positive cells were decreased by an average of 6% compared to controls, and the addition of doxorubicin increases the difference to 9% (p=0.0001, Mann-Whitney test). Finally, doxorubicin treatment resulted in a significant increase of TUNEL-positive staining in the liver of HCC-bearing mice treated with LNP-siUBRs. (Figure 43b). Together, these data suggest that the combined effects of the downregulation of the Arg/N-degron pathway with the use of chemotherapy on the progression of hepatocellular carcinoma is not mediated by modulation of the inflammatory response but rather by an inhibitory effect on proliferation and an increase of apoptosis.

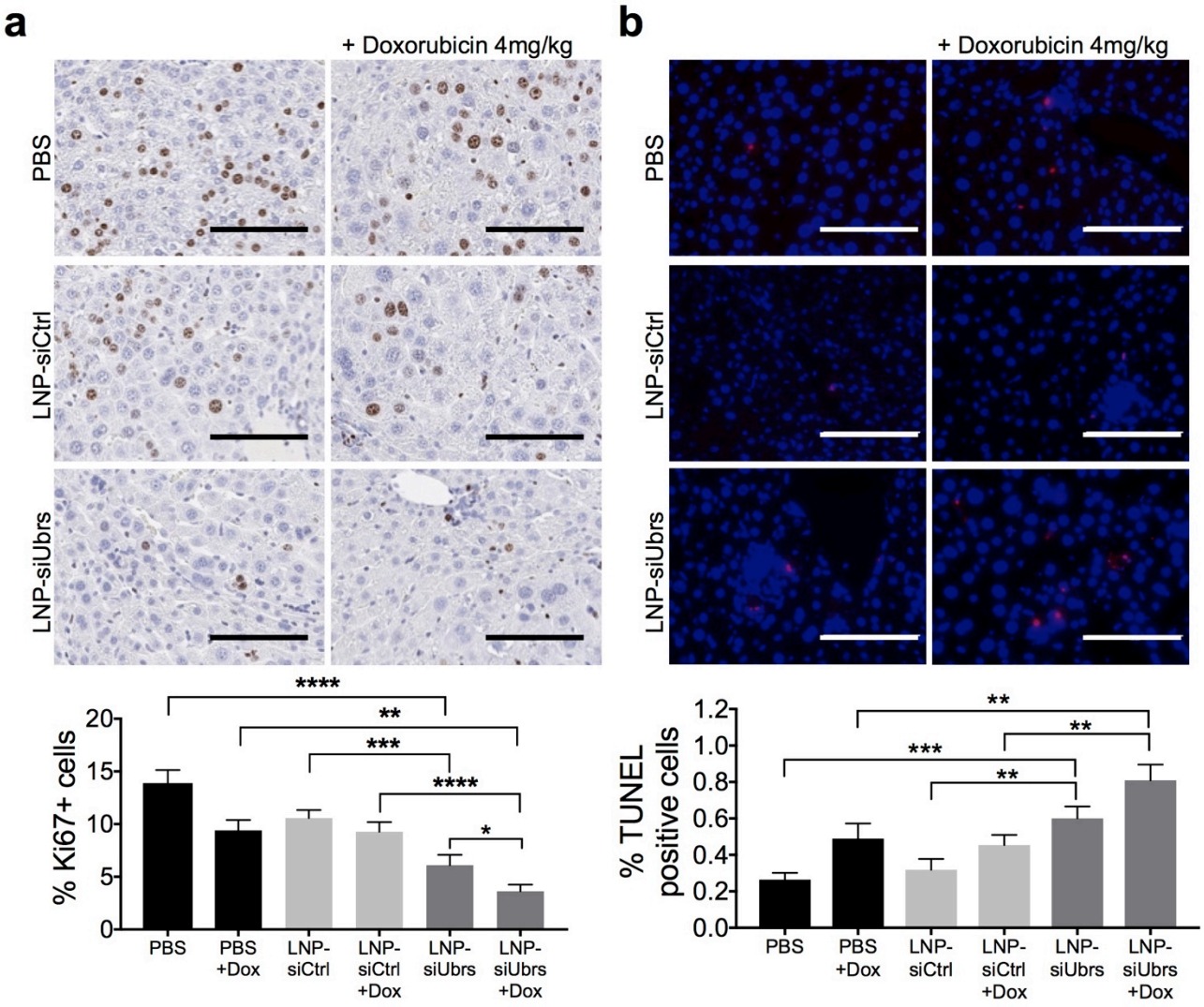

Figure 43. Downregulation of the Arg/N-degron pathway accentuates the action of doxorubicin on proliferation and apoptosis of HCC hepatocytes in vivo. (a) Liver sections stained for the expression of Ki67 as a measure of cell proliferation n=4 mice per group. (b) Analysis of cell death by TUNEL in liver sections. Red nuclei

represent TUNEL-positive cells. Scale bars, 100 μm. n=2-3 mice per group. A minimum of 10,000 cells per condition were counted. Results show mean ± SD. P values were determined by a one-way ANOVA followed by Tukey's multiple comparison's test (*P <0.05, ***P 0.001, ****P 0.0001)

Downregulation of the four UBR-ubiquitin ligases of the N-degron pathway is necessary for sensitization to doxorubicin

Finally, in an effort to improve the combinatorial treatment by further diminishing inflammation in the HCC mice caused by LNP injections, we sought to determine if downregulation of single UBR-ubiquitin ligases of the Arg/N-degron pathway would be sufficient to sensitize cells to apoptosis and decrease tumor load. This would allow to further decrease the amount of LNPs injected, reducing the inflammatory signal. We injected lipid nanoparticles loaded with siRNA against single UBR-ubiquitin ligases into HCC mice, once per week, for a total of four weeks after the appearance of alpha-fetoprotein in the serum of the mice. While downregulation of UBR1, UBR2 or UBR5 did not significantly affect tumor load, downregulation of UBR4 alone increased tumor load to levels comparable to downregulation of all four UBR-ubiquitin ligases combined (Figure 44).

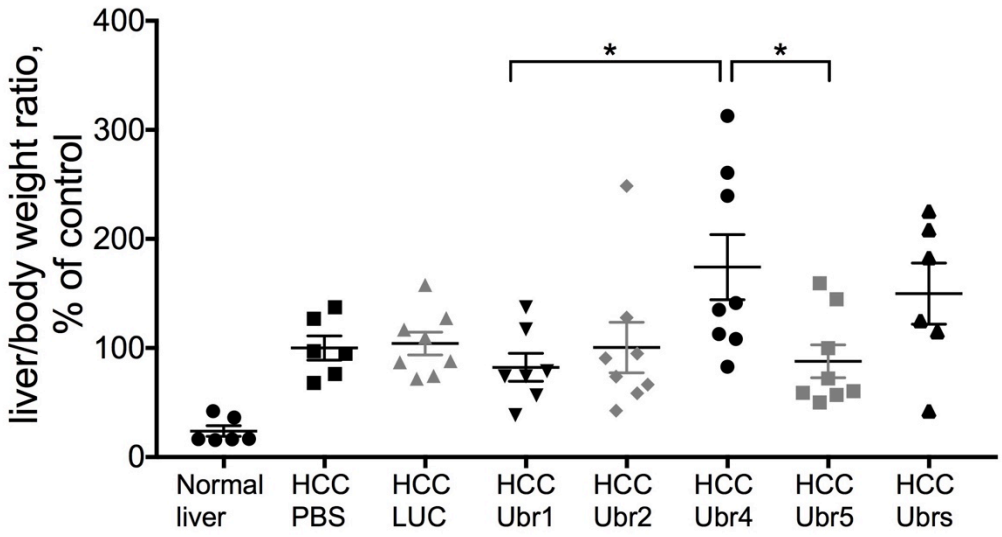

Figure 44. Effect of downregulation of individual UBR-ubiquitin ligases of the Arg/N-degron pathway on HCC tumor load. Liver/body mass ratio analysis of mice bearing HCC treated for 4 weeks with LNPs at 0.5mg/kg. n=6-9 mice per group. Results show mean ± SEM. P values were determined by a one-way ANOVA followed by Tukey's multiple comparison's test (*P <0.05)

The significant increase of tumor load in HCC mice treated with LNP-siUBR4 was accompanied by only a slight increase in neutrophils (data not shown), which in itself could not explain the increased aggressiveness of the cancer. Therefore, because of the apparent contribution of UBR4 in the control of liver cancer, we treated HCC mice using a combination of siRNA against all UBRs except UBR4, but this did not decrease tumor load, nor did it potentiate further the action of doxorubicin (Figure 45). Additionally, we could observe a mild decrease in the mean liver/body weight ration of HCC mice treated with LNP-siUBR1 or LNP-siUBR5, however this decrease was not improved with the addition of doxorubicin (Figure 45). Together, these results indicate that all four N-recognins of the Arg/N-degron pathway need to be downregulated in order to potentiate the chemotherapeutic treatment.

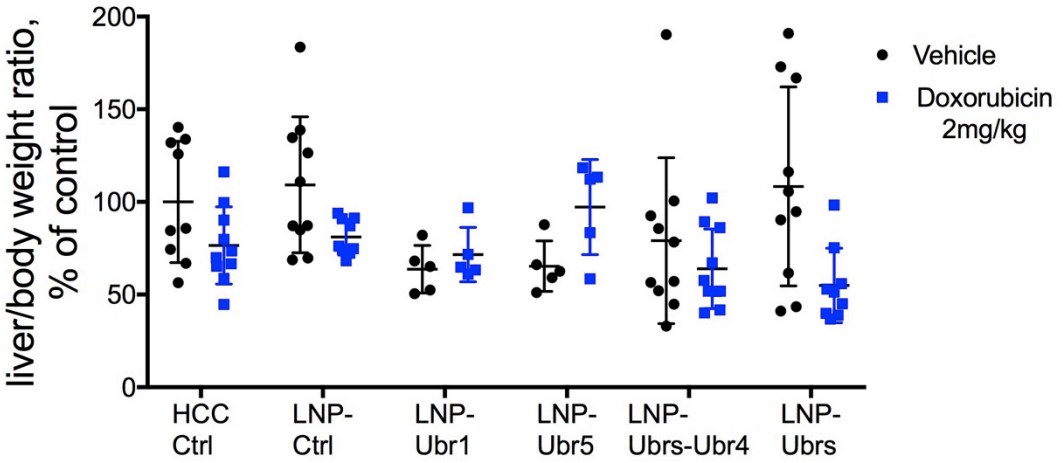

Figure 45. Effect of downregulation of individual UBR-ubiquitin ligases of the Arg/N-degron pathway on doxorubicin treatment in mice. Liver/body mass ratio analysis of mice bearing HCC treated for 4 weeks with LNPs at 1mg/kg total, with or without doxorubicin (2mg/kg). n=5-10 mice per group. Results show mean ± SEM. Statistics were determined by a one-way ANOVA followed by Tukey's multiple comparison's test. All differences between groups are non-significant.

Identification of new targets for future therapeutic applications

The last objective of this study was to propose additional target proteins that can be

used as co-therapy in combination with downregulation of the Arg/N-degron pathway, to increase sensitivity to apoptotic inducing drugs. This can be done by identifying new genes and proteins that are regulated by the Arg/N-degron pathway, which could have roles in inflammation or apoptosis. These newly identified substrates would be potential targets for the development of therapies aimed at controlling the apoptotic or inflammatory response. For this, we used two different approaches: (1) an *in silico* method to identify previously unknown important partners of the apoptotic program, based on the conservation of caspase cleavage sites, and (2) transcriptome analysis of hepatocytes treated with siRNA against UBR5. Both approaches and results will be discussed in detail below.

Study of the conservation of vertebrate caspase targets identifies novel apoptotic mediators

The apoptotic program is initiated and executed by caspases, cysteine proteases that are conserved throughout Metazoans, which selectively cut only a specific set of proteins that is also well conserved throughout evolution (Pop and Salvesen 2009). Currently, the number of known human proteins cleaved by apoptotic caspases is over 1800 (Julien and Wells 2017). Some caspase substrates are key players in the propagation of cell death, contributing to observable morphological changes and taking part in positive feedback loops that increase the efficiency or robustness of the process, and this makes them interesting targets for any therapy aiming at influencing the apoptotic program (Crawford and Wells 2011). Other caspase substrates, however, are simply by-standers of the apoptotic process (Cryns and Yuan 1998). Apoptosis is a highly conserved process; therefore, conservation of an apoptotic caspase target suggests functional significance, whereas a non-conserved target is more likely to be by-stander. Therefore, we sought to identify novel apoptotic mediators amongst all caspase substrates by conducting an *in silico* search for significant apoptotic caspase targets across different species within the Vertebrata subphylum, using different criteria of conservation combined with structural features of cleavage sites.

First, we collected all experimentally derived human apoptotic caspase targets – 3363 cleavage sites from 2040 proteins– and used their 60 amino acid sequences (30 aa on

each side of the cut site) as a query to find orthologs in vertebrates. From all vertebrate species present in non-redundant protein database, 2875 species had at least 1 caspase cleavage target orthologous to human (pBLAST e-value < $1x10^{-16}$). We chose to exclude species with poorly and unevenly represented proteomes in order to avoid false negative results, and selected 328 species with a well represented proteome (more than 8000 annotated proteins per species) for further analysis. We then elaborated five selection criteria to identify important caspase substrates in the apoptotic program

1. Aspartate residue in the P1 position.

Caspases cleave proteins at the scissile bond between P1-P1' of an octamer amino acid sequence P4-P3-P2-P1-P1'-P2'-P3'-P4', with a strict requirement for aspartate in position P1 (Figure 1A) (Schechter and Berger 1967). Indeed, our analysis shows that 92% of orthologous targets have an aspartate residue in the P1 position. Therefore, we decided to take the presence of aspartate in the P1 position as a prerequisite for cleavage conservation and as a threshold for further selection of the caspase targets most important for apoptosis.

2. Conservation of the octamer sequence

Then we estimated cleavage site similarity using the Hamming distance metrics (HD) (Hamming 1950). In this analysis, each element between two sequences are compared and attributed a value of 0 (same) or 1 (different). For 8 amino acid sequences, the HD ranges from 0 to 8, where 0 corresponds to an absolute identity of sequences and 8 to no amino acid matches. We found that unlike for the key aspartate, the whole cleavage site sequences are not well preserved in vertebrates: only 57% of orthologs have an ideal caspase cleavage site where all 8 amino acids match their human counterparts, and 18% differ in one amino acid. This finding correlates with earlier observations on smaller datasets showing that conservation of the entire cleavage site is weaker than conservation measured by the retention of aspartate in position P1 or by primary structure (Mahrus et al. 2008; Crawford et al. 2012; Seaman et al. 2016). Thus, our second selection criterion is an HD value less than 2.

3 and 4. Prevalence of coils and hydrophobicity index

Caspase substrates can also be evaluated by their secondary structure and the composition of their amino acid sequences. Structure analysis of cleavage sites in both human (Mahrus et al. 2008) and *E. coli* proteins (Timmer et al. 2009) revealed that caspases cut proteins predominantly in disordered regions or coils, in less extent in α-helices and rarely in β-sheets. We calculated secondary structures for all human 60 amino acid sequences and characterized them using Q3 accuracy symbols (α-helix (H), β-sheet (E) and coil (C)). We found that coils represent 60% of the secondary structures, 30% are α-helices and around 10% are β-sheets, in accordance with earlier observations, confirming that caspase cleavage sites are situated predominantly in unstructured regions. We then evaluated the hydrophilicity of the caspase substrates by calculating the sum of hydrophobicity indices (kilo-calories per mole for each of the twenty amino acids at a pH7) (Radzicka and Wolfenden 2002) for the central 20 amino acid sequences with P1 aspartate in the middle, for every human and orthologous sequence. This was based on the assumption that proteolysis would most likely occur within the hydrophilic portions of proteins, because these exposed parts would be more accessible for cleavage. Indeed, proteins in aqueous conditions, such as the cytosol, tend to have hydrophobic residues hidden within their structure, and hydrophilic amino acids exposed to the surface (Moelbert, Emberly, and Tang 2004). As expected, we found that most of the vertebrate caspase cleavage sites are located in a hydrophilic environment (negative values in this scale), and are likely to be exposed at the surface of the protein.

We further developed the idea that caspase cleavage sites would be situated in regions that allow for the best accessibility. This implies that the sites could be situated between two structured regions, and between less hydrophilic regions, ensuring that the cleavage site would be exposed at the surface of the protein. For each human caspase substrate, we divided the 60-amino acid long sequences into three segments of 20 amino acids, with the central part containing the cleavage site, and analyzed the difference between the lateral environment of the cleavage site and the central part. For both the secondary structure and the composition of the amino acid sequences of caspase substrates, we attributed a prevalence value to the central 20 amino acid sequences surrounding the P1 aspartate over lateral 20 amino acid sequences using the following elaborated formula:

$$\text{Prevalence value} = \frac{2c}{l+r}$$

where '*c*' is the percentage of coils or sum of hydrophobicity indices in the central 20 amino acids, '*l*' in the left, and '*r*' in the right 20 amino acids. For the secondary structure, the prevalence value should be proportional to the probability of the cleavage site to be located in an unstructured loop between structured domains. Curiously, the prevalence value for two thirds of the human caspase targets is around 1, suggesting that there is mostly no difference between the percentage of coils in regions immediately surrounding the cleavage site and in more distant sequences. For the hydrophobicity index, the prevalence value will give an indication if the localization of the cleavage site is in a hydrophilic loop between less hydrophilic segments, further exposing the cleavage site to the surface of the protein and increasing its chances of being cut. In the resultant range, a value less than 1 indicates that the cleavage site area is more hydrophilic than flanking regions. Remarkably, the distribution of these values has a peak around 1, indicating that in most human caspase targets, the cleavage site does not differ in hydrophilicity from flanking regions. And so, a coil prevalence value > 1 and a median hydrophobicity prevalence < 1 were used in further analysis as criteria to separate the most important apoptotic caspase targets from the by-standers.

5. Nature of the N-terminal amino acid, according to the N-degron pathway

It was previously shown that many important proapoptotic mediators are degraded by the N-degron pathway due to the presence of destabilizing amino acids in their nascent N-ends (Ditzel et al. 2003; Piatkov, Brower, and Varshavsky 2012; Xu, Payoe, and Fahlman 2012). Therefore, we reasoned that evolutionary conservation of destabilizing amino acid residue at the N-end of caspase cleavage products, may indicate a potential regulatory function for the protein fragment and can be used to separate caspase targets most important for cell death. We closely examined the identity of the P1' position in all human and ortholog cleavage sites and found that the distribution of amino acids in the P1' position of substrates in humans and in 328 non-human vertebrates is the same: ~30% Gly, 24% Ser, 14% Ala, and 32% are distributed among the other amino acids (Table 8).

Table 8: Distribution of amino acids in the P1' position and the nature of the amino acid according to the Arg/N-degron pathway

P'1 (amino acid)	Nature of aa[1]	Number of hits in humans	% in humans	Number of hits in Vertebrates	% in Vertebrates
G	stab	1,080	33	171,377	30
S	stab	862	26	131,638	23
A	stab	505	15	80,871	14
T	stab	92	3	20,011	4
L	destab	91	3	18,102	3
V	stab	83	3	17,729	3
F	destab	80	2	13,377	2
Y	destab	74	2	14,295	3
N	destab	65	2	18,225	3
D	destab	53	2	11,274	2
M	stab	50	2	8,552	2
E	destab	46	1	9,115	2
K	destab	41	1	7,301	1
I	destab	40	1	7,507	1
C	destab	36	1	6,986	1
H	destab	31	1	6,596	1
P	stab	28	1	9,298	2
Q	destab	22	1	3,929	1
R	destab	22	1	6,320	1
W	destab	12	0	2,754	0

[1] stab: stabilizing, destab: destabilizing, according to the Arg/N-degron pathway

This is similar to what was observed in a peptide library study (Stennicke et al. 2000) and in apoptotic Jurkat cells (Mahrus et al. 2008). Only 20 percent of caspase targets in 328 vertebrate species are destabilized after cleavage (Table 8). However, nearly 100% of these 20 percent have conservation of the destabilizing nature of the P1' residue among 328 non-human vertebrates. Curiously, among three classes of vertebrates, mammals have a lower proportion of destabilizing P1' residues compared to birds and lower vertebrates (Figure 46). Due to poor representation of the proteome, we intentionally excluded Chondrichthyes, Sarcopterygii, Amphibia and Reptilia from this particular analysis however these classes follow the same trend: the more evolved, the less destabilizing residues are found in the P1' position. In further analysis, maintenance of the destabilizing nature of P1' in more than 50% of vertebrate orthologs will be used as a criterion of target importance for apoptosis.

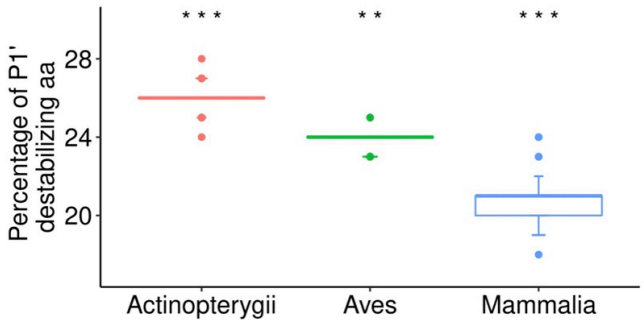

Figure 46. Distribution of P1' destabilizing amino acid residues among vertebrates. The percentage of orthologous targets with destabilizing amino acid in the P1' position was calculated for each of 328 Vertebrate species, and the distribution of these values among species was plotted for three classes: Actinopterygii, Aves and Mammals. Chondrichthyes, Sarcopterygii, Amphibia and Reptilia were excluded from this analysis because of incomparably small number of species per a class (1-20) in respect to the other classes (82-132). Evaluation of statistical significance was performed using ANOVA followed by Tukey's post-hoc test. ** $p < 0.01$. *** $p < 0.001$.

Validation of our chosen criteria

The predictive power of our chosen criteria to determine important players in the apoptotic program was evaluated by applying them to a reference set of caspase targets (24 caspase cleavage sites within 11 proteins) with known proapoptotic activity: RIPK1, TRAF1 (Piatkov, Brower, and Varshavsky 2012), CASP-2, -3, -6, -7, -8, -9, PARP1, PARP2, and ICAD (Kitazumi and Tsukahara 2011) (Table 9). The presence of aspartate in the P1 position was mandatory; therefore it is not shown in the table. Only 4 of the 24 reference targets had a conserved destabilizing P1' amino acid and because of the limited compliancy of the reference set substrates to this particular criteria, we opted not to impose it on future analysis. On the other hand, most of the reference caspase targets have well conserved cleavage sites in hydrophilic loops and in unstructured regions, which makes these three criteria predictive enough to separate the most important caspase substrates. Nonetheless, we chose to add two more criteria to refine the results: first, the presence of a caspase target in every class was considered as an additional measure of conservation; second, since there are 328 species in the filtered pBLAST output, we included having more than 96% orthologs for a caspase target as another indicator of conservation.

Table 9. Validation of conservation criteria based on the set of reference caspase targets with proven proapoptotic activity

	Criteria			
	Median Hamming distance < 2	Coil prevalence > 1	Hydrophobicity prevalence < 1	P1' destabilizing in > 50% of orthologs
# of human targets selected by threshold	2,726	1,454	1,457	554
# of reference targets selected by threshold	19	17	16	4
% of human targets selected by threshold	91.48	48.79	48.89	18.59
% of reference targets selected by threshold	79.17	70.83	66.67	16.67

The set of reference targets included 24 cleavage sites within 11 proteins: Casp2, Casp3, Casp6, Cas7, Casp8, Casp9, PARP1, PARP2, RIPK1, TRAF1, CAD.

Identification of new apoptotic mediators

Applying all five thresholds to vertebrate orthologs of human caspase targets, we generated a final list of 107 caspase targets in 99 proteins that are most conserved among vertebrates and by consequent, should be the most important in the apoptotic program (see Supplementary Table 1). Approximately 51% of the caspase targets from the list (55/107) are known to be involved in apoptosis. Some proteins, such as Caspase-7 (CASP7), Rho associated coiled-coil containing protein kinase 2 (ROCK2) and Protein Kinase N1 (PKN1) become activated upon caspase cleavage and proceed to propagate apoptosis (Lamkanfi and Kanneganti 2010; Shi and Wei 2007; Takahashi et al. 1998). Others, like aryl hydrocarbon receptor nuclear translocator (ARNT) and ubiquitin specific peptidase 19 (USP19) are anti-apoptotic regulators, which get deactivated by caspase cleavage (Shieh et al. 2014; Mei et al. 2011). These results validated our method and confirmed our hypothesis that important proteins involved in apoptosis would be conserved throughout evolution and that conversely, evolutionary conserved caspase targets would be important in apoptosis. Further pathway analysis for the 107 conserved caspase targets using the DAVID free online software (Huang da, Sherman, and Lempicki 2009) with default parameters and an EASE

threshold of 0.05%, followed by annotation using two databases: Gene Ontology (Thomas et al. 2019) and Uniprot (The UniProt 2017), allowed to highlight the more prevalent pathways where these conserved caspase targets are involved. Significantly enriched terms include nucleus-related processes such as alternative splicing and RNA processing, phosphorylation methylation and acetylation, ATP binding and protein interaction (Figure 47). The 107 caspase targets can be equally found in the cytoplasm or the nucleus, and enriched cellular locations include membranes and extracellular exosomes (Figure 47).

From the remaining targets (52/107), 22 were found to be involved in cancer, and an extensive literature search exposed 30 conserved caspase targets that have not been previously associated neither with apoptosis or cancer (Table 10). From those, many targets – ATXN2L, ESS2, QRICH1, RFC1, SF3A1 and more – are related to regulation of RNA transcription, splicing and processing, RRFM2 and SRP54 are related to protein biogenesis, ENO1 and 3 are implicated in gluconeogenesis, NAA15 participates in angiogenesis and MAP15 in microtubule organization. Another interesting caspase target is CCT5. While the exact role of this protein in apoptosis is not elucidated, recent studies indicated that this protein is significantly upregulated in several cancers (Coghlin et al. 2006; Ooe, Kato, and Noguchi 2007), can serve as a tumor associated antigen (Gao et al. 2017), and has been implicated in an anti-viral apoptotic response (Wang et al. 2019) suggesting an opportunity for the development of a new proapoptotic therapy.

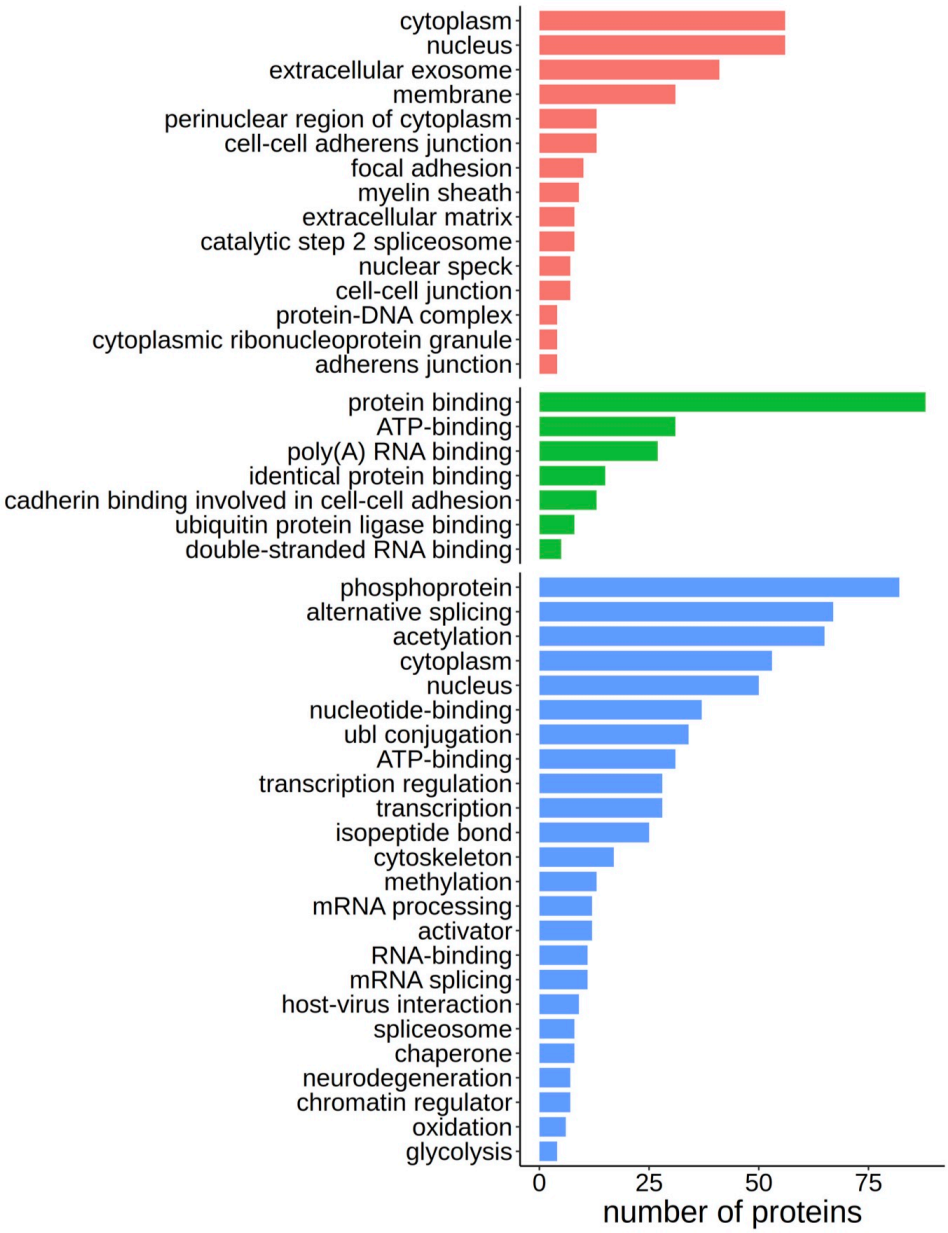

Figure 47. **Pathway enrichment for the 107 highly conserved caspase targets.** Proteins were classified in terms of Gene Ontology – Cellular Component (red), Gene Ontology – Molecular Function (green) and Uniprot Keywords (blue). P-value for annotation selection was adjusted by Benjamini-Hochberg correction. Annotations with p-value < 0.05 were considered significant and showed on the plots.

Table 10. Novel putative apoptotic mediators not previously related to cancer or apoptosis

Human gene name	Human protein symbol	Human Uniprot ID	Human cleavage site	Nature of P1' [1]
actin, beta like 2 (*ACTBL2*)	ACTBL	Q562R1	ELPDGQVI	Stab
actin gamma 1 (*ACTG1*)	ACTG	P63261	ELPDGQVI	Stab
ataxin 2 like (*ATXN2L*)	ATX2L	Q8WWM7	LESDMSNG	Stab
chaperonin containing TCP1 subunit 5 (*CCT5*)	TCPE	P48643	VDKDGDVT	Stab
EH domain containing 4 (*EHD4*)	EHD4	Q9H223	CDCDGMLD	Stab
enolase 1 (*ENO1*)	ENOA	P06733	YGKDATNV	Stab
enolase 3 (*ENO3*)	ENOB	P13929	YGKDATNV	Stab
DiGeorge syndrome critical region gene 14 (*DGCR14*)	ESS2	Q96DF8	VGPDGKEL	Stab
G elongation factor mitochondrial 2 (*GFM2*)	RRF2M	Q969S9	TVTDFMAQ	Destab
heterogeneous nuclear ribonucleoprotein A3 (*HNRNPA3*)	ROA3	P51991	SREDSVKP	Stab
heat shock protein family D (*Hsp60*) member 1 (*HSPD1*)	CH60	P10809	VGYDAMAG	Stab
microtubule associated protein 1S (*MAP1S*)	MAP1S	Q66K74	DRVDAVLV	Stab
N(alpha)-acetyltransferase 15, NatA auxiliary subunit (*NAA15*)	NAA15	Q9BXJ9	HEADTANM	Stab
asparaginyl-tRNA synthetase (*NARS*)	SYNC	O43776	KKEDGTFY	Stab
3'-phosphoadenosine 5'-phosphosulfate synthase 1 (*PAPSS1*)	PAPS1	O43252	TGIDSEYE	Stab
phosphatase and actin regulator 2 (*PHACTR2*)	PHAR2	O75167	DSPDYDRR	Destab
POTE ankyrin domain family member F (*POTEF*)	POTEF	A5A3E0	ELPDGQVI	Stab
proteasome 26S subunit, ATPase 3 (*PSMC3*)	PRS6A	P17980	QEEDGANI	Stab
proteasome 26S subunit, ATPase 3 (*PSMC3*)	PRS6A	P17980	DILDPALL	Stab
glutamine rich 1 (*QRICH1*)	QRIC1	Q2TAL8	LTVDSAHL	Stab
RNA binding motif protein 22 (*RBM22*)	RBM22	Q9NW64	SNSDGTRP	Stab
RNA binding motif protein 39 (*RBM39*)	RBM39	Q14498	ERTDASSA	Stab
replication factor C subunit 1 (*RFC1*)	RFC1	P35251	DEVDGMAG	Stab
splicing factor 3a subunit 1 (*SF3A1*)	SF3A1	Q15459	VTWDGHSG	Stab
signal recognition particle 54 (*SRP54*)	SRP54	P61011	QELDSTDG	Stab
transducin beta like 1X-linked (*TBL1X*)	TBL1X	O60907	TVFDGRPI	Stab
transducin beta like 1, Y-linked (*TBL1Y*)	TBL1Y	Q9BQ87	MEIDGDVE	Stab
tubulin alpha 3c (*TUBA3C*)	TBA3C	P0DPH7	VKCDPRHG	Stab
tubulin alpha 4a (*TUBA4A*)	TBA4A	P68366	IQPDGQMP	Stab
zinc finger CCCH-type containing 15 (*ZC3H15*)	ZC3HF	Q8WU90	VYIDARDE	Stab

[1] stab: stabilizing, destab: destabilizing, according to the Arg/N-degron pathway

Transcriptome analysis of potential UBR5-regulated genes

To identify genes that are potentially regulated by the Arg/N-degron pathway, we analyzed the transcriptome of livers of mice treated with siRNA against UBR5. We chose UBR5 because it is the most well studied of the four E3 ligases of the Arg/N-degron pathway, it is upregulated in many cancers, has known roles in various different cellular functions such as DNA damage repair, cell growth, transcription regulation and apoptosis (Shearer et al. 2015) and thus is the most promising candidate for a single gene therapy approach. Mice were injected on day 0 and 7, at 0.5mg/kg, and killed on day 14. Control groups included mice injected with PBS only (vehicle), and mice injected with LNP-siCtrl. We used two different siRNA (siUBR5-4 and siUBR5-9) to eliminate off-target genes.

A detailed description of the sample mapping can be found in the Methods section. Once the list of genes differentially expressed was established, we applied a cut-off Fold change value of 2 and -2, and the significance was established at $P<0.05$. We retained only genes that were present in both groups of mice treated with siRNA against UBR5 and then we eliminated from this list any gene that was also present in the LNP-ctrl group. This ensures to discount genes affected by the introduction of foreign material in the cell (LNPs, dsRNA) or off-target genes. After statistical analysis, we observed a total of 19 upregulated genes and 10 downregulated genes, including UBR5 itself (Figure 46 and Table 11).

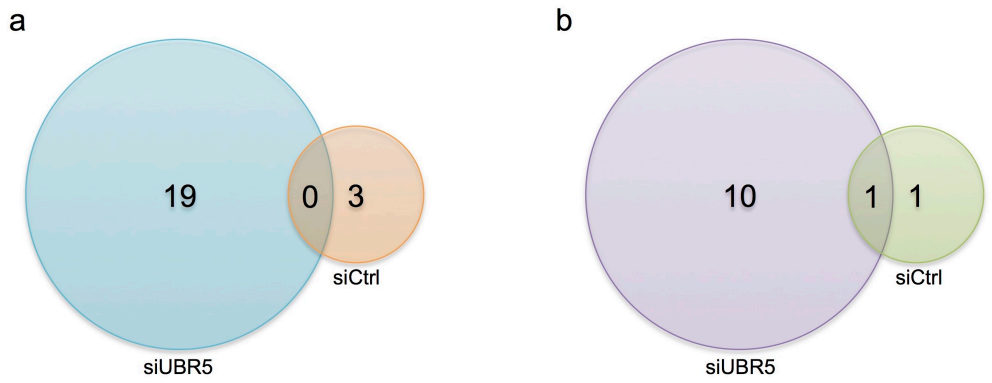

Figure 48: Venn diagrams presenting the number of upregulated (a) or downregulated (b) genes when UBR5 is downregulated. Mice were treated with LNP-siUBR5 twice, on days 0 and 7, at 0.5mg/kg, and killed on day 14.

One of the interesting downregulated genes is SerpinA12, which is an apoptosis inhibitor, suppresses inflammation and modulates insulin action (Skonieczna et al. 2019; Zieger et al. 2018). Downregulation of SerpinA12 could be a complementary mechanism by which UBR5 increases apoptosis in hepatocytes. Another observation is that a large portion of the downregulated genes are involved in bile acid elimination and drug metabolism in the liver. This could imply either a direct regulation of these genes by UBR5 or a consequence of liver damage induced by the absence of UBR5 in the liver. The genes that were upregulated have roles in various cellular functions such as transport, cell proliferation, migration and death, transcription, histone formation, actin components and formation of secondary messengers. Two of these genes, Slc28a1 and Ly6c1, are known to be upregulated as a consequence of inflammation, nonetheless their direct role is still unknown (Fernandez-Veledo et al. 2004; Lee, Wang, et al. 2013). Therefore, we dismissed increased expression of proinflammatory genes as a cause for the invasion of immune cell in the liver, although they could contribute to the maintenance of the inflammatory response.

Table 11. Differentially expressed genes after UBR5 downregulation.

	Gene name	Function	Fold change: LNP-siCtrl vs LNP-siUBR5	P value	Ref PMID (Gene ID)
Upregulated	Tmem28	Transport (calcium)	5.0	3,00E-10	-620592
	Atp2b2	Transport (calcium)	2.4	2,30E-10	7945253
	Slc28a1 (CTN1)	Transport (pyrimidine), cell cycle and cell death, tumor suppressor	2.5	0.02	23722537
	Phlda2	Cell proliferation	4.5	0.004	29861842
	Wnt11	Cell proliferation and migration	2.5	0.003	21447091
	Ripply1	Transcriptional repression	2.1	0.002	16326386
	Ly6c1	Unknown role, expressed on monocytes, neutrophils and DCs	2.4	0.02	23543767
	Miox	Catalysis of inositol to D-glucuronate	2.2	0.003	18364358
	Espnl	Actin cytoskeleton component	3.1	0.08	26926603
	Mogat1	Catalyzes the formation of DAG from 2-MG and fatty acyl-CoA	3.2	0.04	27611931
	Mogat2	Catalyzes the formation of DAG from 2-MG and fatty acyl-CoA	3.4	0.03	28943619
	Plin4	Lipid droplet protein	2.6	1,00E-13	21847662
	Orm3	Plasma protein binding	2.2	8,46E-12	31844752
	Orm2	Plasma protein binding	2.1	1,13E-16	31844752
	Cyp2d9	Cytochrome P450 unit	2.1	8,18E-12	
	Fndc10	Unknown	2.1	0.0001	-643988
	Cyp2d40	Unknown	2.1	8,00E-12	-71754
	BC049987	ncRNA	2.8	1,48E-29	N/A
	lncRNA Meg3	activates p53, tumor suppressor	3.3	0.02	26444285
Downregulated	SerpinA12 (VASPIN)	Adipokine, apoptosis inhibitor, modulates insulin action	-2.5	0.03	31511067
	Sult2a4	sulfonation of bile acids	-5.9	1.8E-10	28455387
	Sult2a1	sulfonation of bile acids	-5.1	0.001	23775849
	Sult2a5	sulfonation of bile acids	-4.8	6.9E-12	23775849
	Ugt2b37	catalyze transfer of glucuronic acid	-2.2	0.05	19131521
	Mmd2	Protein kinase	-2.1	1.1E-11	29775111
	Pkdrej	Ca2+ conducting cation channel	-2.2	0.0003	16883570
	Gria3	Glutamate receptor	-2.9	0.000002	22974439
	Gm15998	Unknown	-2.4	0.02	-100038411
	Ubr5		-2.0	2,00E-49	

Chapter 5
Discussion

In the last few years, the focus in the development of new therapies has shifted towards molecular medicine, where treatment strategies target specific molecules necessary for the growth of diseased cells, rather than hit a broad population such as all rapidly dividing cells. The bottleneck in this scenario is the identification of proper target molecules differentially expressed or malfunctioning in afflicted versus normal cells. In this sense, RNA interference could be an "all-in-one" magic bullet, serving both for discovery and therapy, as demonstrated in this project. Using siRNA against components of the Arg/N-degron pathway, we demonstrated the feasibility of such an approach and discovered how downregulation of this pathway could be beneficial for the treatment of cancer (Leboeuf et al, 2020), but could also interfere in the management of inflammation (Leboeuf, Pyatkov et al, 2020).

UBR ubiquitin ligases of the Arg/N-degron pathway are promising targets for cancer therapy

Since its discovery, the N-degron pathway has been implicated in the regulation of all major hallmarks of cancer (Hanahan and Weinberg 2011): sustained cell proliferation (Brower and Varshavsky 2009; Lee et al. 2012), evasion of tumor suppressors (Piatkov, Brower, and Varshavsky 2012; Piatkov et al. 2014), replicative immortality (Rageul et al. 2019), activated migration (Xie et al. 2009), increased angiogenesis (Lee et al. 2005) and resistance to cell death (Piatkov, Brower, and Varshavsky 2012; Ditzel et al. 2003). Additionally, the E3 ligases of the pathway each have possible individual roles in the maintenance and development of cancer, independently of their activities as N-recognins, through ubiquitylation or protein-protein interactions with oncoproteins, tumor-suppressors or tumor activators (Sultana, Theodoraki, and Caplan 2012; Akiyoshi et al. 2013; Hunt et al. 2019; Kim, Lee, Tasaki, Mun, et al. 2018; Shearer et al. 2015). UBR2 and UBR5 are upregulated in some types of cancer (O'Brien et al. 2008; Zhang et al. 2013), suggesting the importance of the N-degron pathway for cancer cells. In this work, we demonstrated that we could impair many aspects of cancer survival by tuning the expression levels of the Arg/N-degron pathway through siRNA-mediated downregulation of the ubiquitin ligases UBR1, UBR2, UBR4 and UBR5, improving the chances of overcoming the disease. Indeed, our in vitro results show that a reduced expression of the UBR-ubiquitin ligases leads to decreased proliferation and migration of hepatocellular carcinoma cells as well as increased apoptosis, in agreement with previously published roles of the N-degron pathway (Figures 18 and 19) (Varshavsky 2011). We also proved that siRNA-mediated downregulation of the Arg/N-degron pathway components efficiently reduces the functional activity of the pathway by demonstrating the accumulation of BRCA1, a known substrate of the N-degron pathway. The second set of siRNA against the four UBR-ubiquitin ligases studied allowed us to confirm that phenotypes observed after siRNA treatment were due to specific target downregulation and not off-target effects, since both sets of siRNA produced the same phenotypes. Off target effects of siRNA can emerge from sequence-dependent silencing of non-specific genes, slicer-independent translational repression of genes with similar seed-region sequences or sequence-independent effects such as immune recognition or

displacing of endogenous miRNA from the RISC complexes in the cell, resulting in dysregulation of gene expression (Sigoillot and King 2011). Therefore, validation of phenotypes using at least a second siRNA is necessary to confirm how downregulation of a gene affects the biology of a cell or organism.

Confident in our in vitro results, we proceeded to evaluate the effects of long-term downregulation of the Arg/N-degron pathway in adult tissue, using lipid nanoparticle mediated siRNA delivery. Previously published attempts to disturb the Arg/N-degron pathway in mice include total ablation of the UBR-ubiquitin ligases, which was revealed to be lethal for embryos, making it impossible to study the consequences of removing the pathway in fully formed tissue (An et al. 2006; Kwon et al. 2002; Kwon et al. 2001; Tasaki et al. 2013; Saunders et al. 2004). Our study is the first to demonstrate that sustained downregulation of the mRNA and protein levels of UBR ubiquitin ligases of the Arg/N-degron pathway can be achieved in mature adult tissue, without significant toxicity to the animal. IV injections of LNP-siRNA allowed liver-specific prolonged downregulation of UBR1, UBR2, UBR4 and UBR5 without excessive apoptosis of mature hepatocytes, indicating that slow proliferating normal adult cells can endure a dysfunctional N-degron pathway for an extended period of time (Figure 23). These findings are corroborated by the Ate1$^{-/flox}$ mouse, where partial ablation of the pathway is well tolerated by mature, adult tissue with low proliferation rates such as the kidney, brain, heart and liver (Brower and Varshavsky 2009; Leu, Kurosaka, and Kashina 2009), suggesting an opportunity for pharmacological intervention in cancer, which has a much faster proliferation rate and should be more sensitive to the loss of the N-degron pathway, even partially.

Although injections of LNP-siUBRs were well tolerated, the high dose of nanoparticles given to the mice caused infiltration of inflammatory cells such as inflammatory monocytes (Ly6C^{high}), neutrophils and eosinophils, in the liver and the spleen of LNP-siUBRs treated animals (Figure 23 and 24). Despite recent advances in designing more efficient lipids (Dong et al. 2014; Love et al. 2010), less immunogenic particles and siRNA that avoids immunostimulatory repeats (Sato et al. 2017; Broering et al. 2014; Judge et al. 2006), the LNP-siRNA itself remains a trigger for the immune system (Abrams et al. 2010; Chen, May, and Li 2013). Indeed, cationic lipids have been shown to illicit an inflammatory response in animals, particularly by increasing secretion of interferon alpha

and gamma, and activating interferon responsive genes (Kedmi, Ben-Arie, and Peer 2010). Moreover, in a pre-clinical study evaluating the effect of lipid nanoparticles containing siRNA against VEGF and kinesin spindle protein on the progression of liver cancer, the control LNP encapsulating siRNA against the Luciferase gene had the same immunostimulatory profile than the test LNP and even caused enlargement of the spleen, indicating that the inflammatory response came from the particle rather than being a target specific effect (Barros and Gollob 2012; Tabernero et al. 2013). In our case, the inflammation caused by the LNP is clearly exacerbated when the Arg/N-degron pathway is impaired, as no significant infiltration of mononuclear cells was detected in the livers of LNP-siCtrl treated mice. Increased inflammation was also observed when we treated HCC mice with LNPs containing siRNA against UBRs (Figure 27). Contrarily to our predictions, these mice showed increased liver size and tumor load compared to controls, and this was most likely due to the inflammation observed in the same animals. The slight amelioration in tumor progression seen in the LNP-Ctrl treated mice compared to the vehicle control could be attributed to acute inflammatory response following LNP injections, as short bursts of proinflammatory cytokines are beneficial to the anti-tumor response (Ni and Lu 2018; Berraondo et al. 2019). However, sustained inflammation provokes an increase in tumor proliferation, as seen in the LNP-siUbrs treated mice. These observations led us to believe that downregulation of the Arg/N-degron pathway could interfere with the inflammatory response.

Generally, the onset of inflammation involves activation of the inflammasome, a large protein complex organized around receptors, which are capable of recognizing specific cytosolic pathogen- or damage-associated molecular patterns such as dsRNA or foreign lipids (Martinon, Burns, and Tschopp 2002; Sharma and Kanneganti 2016). The Arg/N-degron pathway has been shown to regulate the activation of the NLRP1B inflammasome, which is required for the response against anthrax lethal factor (Chui et al. 2019; Xu et al. 2019). Although LNPs and siRNA most likely trigger the immune system through a different mechanism involving Toll-Like Receptors or RIG-1 receptors and their respective inflammasomes (Whitehead et al. 2011), a similar interaction with the N-degron pathway could be foreseen. Additionally, as will be discussed further in the following sections of this discussion, the Arg/N-degron pathway is involved in the degradation of

proinflammatory protein fragments and the control of the inflammatory response. As we are delivering siRNA to downregulate the Arg/N-degron pathway in the liver, we are also continuously providing an inflammatory stimulus (the lipid nanoparticles) while removing the capacity of the cells to degrade the proinflammatory fragments by shutting down their defense mechanism (the N-degron pathway). Thus, a delicate balance exists between using enough siRNA to cause sufficient downregulation of the Arg/N-degron pathway to sensitize cells to apoptosis while avoiding accumulation of proinflammatory fragments and a disproportionate inflammatory response (Figure 35). An alternative strategy would be the use of GalNAc conjugates as carriers for the siRNA, as these molecules deliver specifically to hepatocytes while avoiding immune activation (Kim et al. 2019). However, using a conjugate to deliver siRNA requires additional chemical modifications to the oligonucleotide as no protection is offered to the molecule against nucleases (Foster et al. 2018). These additional modifications can affect the efficacy of the siRNA, requiring to screen once again for the most potent conjugated siRNA. Since our siRNA are very potent and the turnover rate of the UBR-ubiquitin ligase mRNA is low, we chose to decrease the amount of LNP-siRNA injected, and to combine this treatment with the administration of a chemotherapeutic drug. The joint strategy would cause both generation and accumulation of proapoptotic fragments.

Potentialisation of chemotherapy through downregulation of the Arg/N-degron pathway

A newer approach in the treatment of cancer is to use a combination of chemotherapeutic drugs with specific pathway inhibitors (Chen and Lahav 2016). This allows harnessing the power of both strategies while overcoming therapy resistance and avoiding major side effects. In our case, using siRNA against UBRs to downregulate the Arg/N-degron pathway sensitizes cells to apoptosis and reduces proliferation, which in turn enhances the effects of the chemotherapeutic drug. First, we evaluated this strategy in vitro, and confirmed that when used in combination, lower doses of both the siRNA and doxorubicin are needed to reduce proliferation and increase apoptosis than if used as single agents. The same results were obtained in the HCC model, where downregulation of UBR-ubiquitin ligases and administration of doxorubicin synergize in controlling tumor load by

reducing proliferation and increasing apoptosis (Figure 39 and 43). Because of the lower dose of lipid nanoparticles, no extra inflammation was perceived in groups receiving LNP-siUbrs versus controls. A previous study demonstrating a synergistic antitumor effect using a UBR1 inhibitor in combination with shikonin, a necrosis inducing drug, in a colon cancer mouse model (Agarwalla and Banerjee 2016) supports our claim that downregulation of the Arg/N-degron pathway can boost chemotherapy efficacy in various cancers. However, in our liver cancer model, all four UBR-ubiquitin ligases of the Arg/N-degron need to be downregulated in order to potentiate the effect of doxorubicin. Indeed, downregulation of either UBR1 or UBR5 in HCC mice led to decreased tumor load but this decrease was not improved with the addition of doxorubicin. These contrasting results could be explained by the different levels of expression of each UBR-ubiquitin ligase in various tissues (Uhlen et al. 2015), impacting the contribution of the single E3 ligases in the overall role of the Arg/N-degron pathway.

Since the expression of Arg/N-degron pathway components is mostly confined to highly proliferating cells (Brower and Varshavsky 2009), and known to be overexpressed in some types of cancer cells, even partial downregulation of protein levels of UBRs is enough to sensitize cells to the chemotherapy, enhancing the efficiency of the drug. The net effect of combining siRNA-mediated UBR1, UBR2, UBR4 and UBR5 inhibition with doxorubicin is significant inhibition of tumor proliferation and increased tumor cell apoptosis, resulting in lower tumor load in HCC mice.

The missing link: the role of the Arg/N-degron pathway in inflammation

In this study, we set out to prove that UBR ubiquitin ligases of the Arg/N-degron pathway are promising targets for the development of new therapy, especially in the context of cancer. This assumption was based on the ability of these E3 enzymes to recognize, ubiquitylate and degrade proapoptotic fragments via the 26S proteasome. In this function, UBR1, UBR2, UBR4 and UBR5 are regulators of apoptosis, and downregulating them causes accumulation of proapoptotic fragments, making cells more susceptible to reaching the point of no return in the apoptotic program. Additionally, cancer cells are more sensitive to a partial ablation of the Arg/N-degron pathway because of their high

proliferation rate, making them more dependent on proteolysis to eliminate unwanted or damaged proteins. Therefore, we should have seen an immediate effect on proliferation and apoptosis of cancer cells when they were treated with siRNA against UBR-ubiquitin ligases. However, while examining the effects of long-term downregulation of the Arg/N-degron pathway in adult mice, we encountered a strong inflammatory response in the liver and spleen. Although we can attribute the source of the inflammatory signal to the nanoparticle itself, the difference between the livers of mice receiving LNPs with control siRNA versus siUBRs suggests that downregulation of the Arg/N-degron pathway impairs the control and resolution of the inflammatory response.

It is well known that the apoptotic and inflammatory processes are extremely similar. In fact, these cellular reactions most probably originate from a common ancestor molecular pathway, where evasion of pathogens occurred by "cell suicide" (Green and Fitzgerald 2016; Munoz-Pinedo 2012; Ameisen 2002). Interactions between host and pathogen have provided evolutionary pressure to further develop apoptosis as a defense mechanism, linking cell death programs with inflammatory responses through NF-κB induction, which in turn regulates the expression of numerous genes important for apoptosis, inflammatory responses, innate and acquired immunity (Karin and Lin 2002). Other commonalities between apoptosis and inflammation are the caspases and their essential roles in the onset of both mechanisms (Pop and Salvesen 2009; Thornberry and Lazebnik 1998). Caspase-family proteases are critical effectors of the apoptotic and the inflammatory program, and their activation leads to rapid cleavage of a variety of proteins. Once cleaved by caspases or endopeptidases activated by the apoptotic or inflammatory program, the substrates expose new N-termini (Agard, Maltby, and Wells 2010; Wensink, Hack, and Bovenschen 2015), which could be recognized by the Arg/N-degron pathway E3 ligases. Consequently, we hypothesized and proved in this study that fragments generated by activated inflammatory caspases and inflammation related endopeptidases could be Arg/N-degron substrates, positioning the Arg/N-degron pathway as a major player in the control and resolution of inflammation through targeted degradation of inflammatory protein signals (Leboeuf, Pyatkov et al, 2020).

Proteolysis through the Arg/N-degron pathway contributes to the control of inflammation

Resolution of inflammation involves complex active molecular and cellular events that ultimately lead to restoration of homeostasis, and these events begin with chemokine depletion, abrogation of neutrophil recruitment and downregulation of proinflammatory cytokines (Ortega-Gómez, Perretti, and Soehnlein 2013; Sugimoto et al. 2016). However, many of the proinflammatory chemokines and cytokines activated during the inflammatory response are proteolytically processed, and the irreversible nature of this process implies that activated fragments either need to be sequestered, inhibited or degraded through a ubiquitin related system such as the N-degron pathway in order to turn off the signal. In this study, we identified *in silico* fifteen protein fragments with experimentally confirmed inflammatory functions that contain destabilizing N-terminal amino acids, seven of which (Asn^{120}-CASP1, Gln^{81}-CASP4, Gln^{137}-CASP5, Cys^{149}-Rab39a, Asp^{10}-PDK1, Ile^{29}-GRZA and Ile^{27}-GRZM) are shown to contain N-degrons and be substrates of the Arg/N-degron pathway (Table 7). For all fragments except granzymes, the Arg/N-degron pathway is the main mechanism of degradation. Our results illustrate that one of the main strategies used by cells to eliminate proteolytically activated fragments generated during inflammation is degradation via their built-in degron, which is exposed upon activation or proteolytic cleavage. Proof of the importance of this mechanism is through strong evolutionary conservation of the destabilizing nature of N-terminal residues at the P1' position of the proinflammatory fragments, including a substitution to a destabilizing residue in higher mammals in the case of caspase-1 (Figure 28). Considering that a low percentage of caspase substrates contain residues recognized by the Arg/N-degron pathway in the P1' site (Crawford and Wells 2011), only a fitness-increasing trait could exert an evolutionary constraint of this sort and conserve a short *in vivo* half-life for these proinflammatory fragments. This stresses the importance of the Arg/N-degron pathway in the degradation of inflammatory signals that would otherwise hinder the resolution process.

Additionally, we demonstrated that unlike apoptotic caspases such as caspase-3 and 8 (Piatkov et al, 2012, and confirmed in this work), inflammatory caspase-1, and possibly other inflammatory caspases, which are also activated by LPS and subsequently activate

caspase-1 (Jimenez Fernandez and Lamkanfi 2015), do not cleave the E3 ligases of the Arg/N-degron pathway. In this case, the E3 ligases remain intact and able to target proinflammatory fragments for degradation throughout all stages of inflammation.

Downregulation of the Arg/N-degron sensitizes cells to inflammatory stimuli

One significant and obvious outcome of the Arg/N-degron pathway as a mechanism of degradation for proinflammatory protein fragments would be exaggerated inflammatory responses in cells with a malfunctioning Arg/N-degron pathway. Indeed, if substrates such as activated inflammatory caspases or granzymes were not degraded, they would constantly cleave their target proteins, generating an uninterrupted influx of inflammatory protein fragments such as cytokines of the IL-1β family. However, loss of the N-degron pathway does not necessarily translate to immediate increase in inflammation. Similarly to apoptosis, where downregulation of the Arg/N-degron pathway only led to a 1-3% increase in spontaneous apoptosis, an additional stimulus is needed to initiate the inflammatory response. We found that when the E3 ligases of the Arg/N-degron pathway are downregulated, the consequence upon inflammatory stimuli such as LPS is a much greater secretion of IL-1β even at low concentrations of the endotoxin (Figure 33). In accordance with our findings, partial ablation of the Arg/N-degron pathway in humans and animal models also leads to increased inflammation or inflammation-prone phenotypes. Patients with the Johanson-Blizzard syndrome, who have loss of function mutations in the *UBR1* gene, exhibit increased inflammatory infiltrates in the pancreas, inducing acinar cell destruction and pancreatic insufficiency (Kruger et al. 2009; Zenker et al. 2005). *UBR1*$^{-/-}$ mice are also more sensitive to induced pancreatitis as shown by increased elastase activity and an elevated systemic inflammatory response upon cerulean dosing (Kwon et al. 2001; Zenker et al. 2006). In addition, post-natal deletion of the arginyltransferase Ate1 in mice causes brain edema (Brower and Varshavsky 2009), a general indicator of inflammation. Ate1 is essential for the recognition of destabilizing N-terminal residues requiring arginylation (Figure 3), which are present in proinflammatory fragments Cys^{149}-Rab39a, Asp^{10}-PDK1, Glu^{6}-IL36β and Glu^{245}-Ataxin 3. Without arginylation, these fragments will

accumulate in cells due to lack of recognition and degradation by the Arg/N-degron pathway. Finally, results presented in this thesis indicate that partial inhibition of the Arg/N-degron pathway by downregulation of UBR1, UBR2, UBR4 and UBR5 in the mouse liver causes infiltration of neutrophils and eosinophils, known effectors of inflammation. This also elevates serum IL-1β levels upon LPS challenge in mice treated with LNP-siUBRs compared to controls (data not shown), although the interpretation of this result is complicated by the fact that most of the nanoparticles are internalized by hepatocytes, cells which under normal circumstances do not secrete IL-1β. In summary, these phenotypes indicate that ablation of the Arg/N-degron pathway not only impairs resolution of inflammation but also increases susceptibility to a stronger inflammatory response, even in presence of a weak stimulus.

The Arg/N-degron pathway as a regulator of inflammation

In light of the results presented in this study as well as recently published data, we propose a model wherein the Arg/N-degron pathway participates in the control of inflammation in two ways: a) in the generation of inflammatory signals by degradation of inhibitory anti-inflammatory domains and b) in the resolution of inflammatory states through selective degradation of inflammatory mediators or proinflammatory fragments (Figure 49).

Recently, a role for the Arg/N-degron pathway in the development of the immune response against anthrax Lethal Factor (LF) was discovered. Upon infection, the LF protease cleaves the mouse inflammasome NLRP1B and generates a destabilized neo-N terminus that is recognized by the UBR2 E3 ligase of the Arg/N-degron pathway, ubiquitylated and degraded through the 26S proteasome. Degradation of the N-terminal fragment frees the CARD domain of the NLRP1B, which can then recruit caspase-1 and initiate pyroptosis (Chui et al. 2019; Xu et al. 2019). These studies were the first to indicate a role for N-terminal degradation in the onset of an inflammatory response. Our results suggest a broader role for N-terminal degradation in the control and resolution of the same response. This dual control mechanism of the immune response by the Arg/N-degron pathway is also present in plants. Plants respond to pathogens using the innate immunity of each cell, through a series of molecular pathways involving specific transmembrane receptors that broadly relate to the vertebrate Nod-like-receptors (NLR) or Toll-like receptors (TLR), which form the

inflammasomes, the caspase-1 activation platforms (Jones and Dangl 2006; Martinon and Tschopp 2006; Hornung et al. 2009). The pathogen response initiated by binding to NLR-type receptors requires ubiquitylation and degradation of proteins that prevent initiation of the immune response (Sorel et al. 2019). Knockout of key components of the Arg/N-degron pathway in *Arabidopsis thaliana* prevents mounting an immune response to a variety of pathogens, which suggests that this pathway is involved in the degradation of proteins involved in the initiation of the immune response (de Marchi et al. 2016). Conversely, the Arg/N-degron pathway is involved in the degradation of protein fragments cleaved by the *Pseudomonas syringae* protease effector AvrRpt2, fragments whose functions have not been elucidated yet but could participate in positively regulating the immune reaction, considering the function of RIN4, the main target of AvrRpt2 (Goslin et al. 2019). Removing these fragments could help in the resolution of the immune response in the plant.

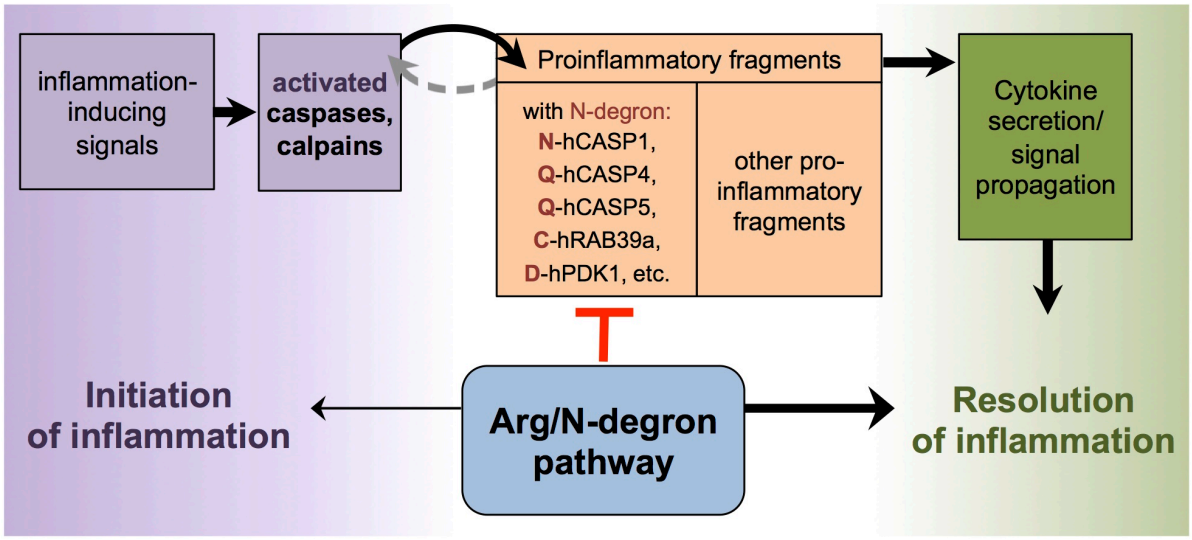

Figure 49: **Working model where the N-degron pathway regulates inflammation.** Selective degradation of proinflammatory protein fragments by the Arg/N-degron pathway could act as a control mechanism to prevent over-stimulation of the immune system and to resolve inflammation.

Additional links between the Arg/N-degron pathway and inflammation can be made through it's roles in the protein quality control mechanism (Heck, Cheung, and Hampton 2010), a cellular process present in all cells from yeast to mammals, and when impaired, is responsible for generation of inflammation in diseases such as Alzheimer's and Parkinson

(Dubnikov, Ben-Gedalya, and Cohen 2017; Currais et al. 2017). Moreover, due to the ubiquitous expression of the N-degron pathway, inflammation control mechanisms provided by this pathway are present in any cell type, acting as an on/off "switch" for the initiation of an inflammatory response, and/or as a "pro-resolving" mediator by means of degradation of proinflammatory fragments, depending on the cell type and on the source of the stimuli. Nonetheless, the Arg/N-degron pathway is now a newly identified participant in the regulation of inflammation.

Identification of new targets as potential co-therapy

Another approach to avoid inflammation and increase the sensitivity or efficacy of our combinatorial treatment involving sensitizing cells to apoptosis through downregulation of the Arg/N-degron pathway is to act on other proteins that are involved in apoptosis or inflammation. This can be done through downregulation of the mRNA using siRNA, as performed in this project, or with small molecule inhibitors, or through upregulation of the mRNA by using CRISPR activation or similar techniques (Chavez et al. 2015). However, such targets should be carefully selected. We used two different strategies: one to identify apoptotic caspase substrates and major players in the apoptotic program that could partner with the chemotherapeutic drugs to sensitize or cause apoptosis, and the second strategy is to identify genes regulated by UBR5 that could affect inflammation, and be influenced on to moderate the inflammatory response.

In order to identify potential actors that are important in the apoptotic program, we first examined all human and orthologous apoptotic caspase targets using different criteria of conservation combined with structural features of cleavage sites. We used the following parameters to refine our search: the presence of aspartate in the P1 position, cleavage site similarity, structural disordinance (having the cleavage site in an unstructured region between two structured regions), hydrophilicity of the cleavage site area, the nature of the amino acid in the P1' position according to the Arg/N-degron pathway, presence of orthologs in all seven vertebrate classes and in 96% of species studied (314 out of 328). The selected criteria allowed us to sort the 107 most relevant caspase substrates out of 3363, and identify 30 novel targets previously unknown for their role in apoptosis and cancer (Gubina et al, 2020).

When examining the predictive power of our chosen parameters against a reference set of caspase targets with known proapoptotic activity (RIPK1, TRAF1, CASP-2, -3, -6, -7, -8, -9, PARP1, PARP2, and ICAD), the only criteria that was not met by all targets was the conserved amino acid with a destabilizing nature at the P1′ position. This is because mammals have a lower proportion of destabilizing P1′ residues compared to all other vertebrates, indicating an evolutionary tendency to replace destabilizing P1′ residues with stabilizing amino acids. Similar trends were also observed for the percentage of P1 glutamate cut sites, where mammals have a lower incidence of P1 E-cut sites (3%) compared to birds (7%) and ray-finned fish (9%) (results not shown). Previous in vitro experiments have shown that caspases-3, -6, and -7 are able to cleave substrates with P1 E cut sites with the same affinity than aspartate, albeit with twofold slower efficacy, and that substitution of the P1 glutamate by aspartate rescues the higher cleavage rate (Seaman et al. 2016; Stennicke et al. 2000). Therefore, we stipulated that by switching from glutamate to aspartate in the P1 site during evolution, species ensure a faster cleavage rate for these specific caspase substrates. Moreover, a shift from a P1′ destabilizing to stabilizing amino acid in a caspase substrate would prevent the fragment from being degraded by the N-degron pathway once the new N-terminus is exposed, making it persist more and function longer. Both of these evolutionary trends make apoptosis more aggressive in higher vertebrates. Additionally, reducing the reliance on a less specific regulator of apoptosis such as the N-degron pathway can be explained by the increased complexity and redundancy of mechanisms of apoptosis regulation (Oberst, Bender, and Green 2008; Zmasek and Godzik 2013).

Of the 107 most relevant caspase substrates to the apoptotic program, 20% have a potential built-in N-degron that gets exposed upon cleavage by caspases, a number that is in line with previous results (Supplementary Table 1) (Seaman et al. 2016; Stennicke et al. 2000). All 24 of the caspase substrates containing a destabilizing residue at the P1′ position have perfect conservation of the destabilizing nature of this residue throughout vertebrates, suggesting the importance of fast degradation of these particular fragments through the N-degron pathway. This also indicates that these proteins, along with other known proapoptotic fragments that contain an N-degron (Piatkov, Brower, and Varshavsky 2012), most likely accumulate in cells where the N-degron pathway is inhibited, contributing to increasing the susceptibility to apoptosis, as seen in hepatocytes treated with siRNA against

UBR-ubiquitin ligases. Therefore, these particular caspase substrates would be interesting to further investigate as co-therapy targets in our combinatorial treatment.

Pathway analysis of the 107 conserved caspase targets indicated that these substrates are involved in a variety of cellular activities: alternative splicing and RNA processing; RNA transcription; phosphorylation; methylation; acetylation; ATP binding; protein interaction; protein biogenesis; apoptosis; and more general processes like angiogenesis; gluconeogenesis; and tumorogenesis. 55 caspase substrates in the final list were found to be involved with apoptosis, while 22 were associated with cancer and 30 have undetermined roles in apoptosis or cancer. Further studies are needed to determine how exactly these caspase substrates contribute to the apoptotic program and how best to intervene in order to boost this effect and use them in an anti-tumor treatment. Most likely many of them could be manipulated in conjunction with the Arg/N-degron pathway to increase sensitivity to apoptosis and ameliorate the response to chemotherapy.

The second set of targets examined is the list of genes that are differentially expressed after UBR5 knockdown in the liver of mice treated with LNP-siUBR5. Transcriptome analysis suggests that UBR5 may be involved in the regulation of sulfotransferase genes (from the Sult2a family) and a gene from the UDP glycosyltransferase 2 family. These genes are involved in bile acid elimination (Turgeon et al. 2001) and drug metabolism in the liver (Alnouti 2009). This could imply that UBR5 is involved in regulation of processes such as detoxification from endogenous and xenobiotic substances, although further experiments are needed to confirm direct links between UBR5, Sult2a and Ugt2b. An additional interesting observation is the decrease in the expression of SerpinA12, which could be one of the mechanisms by which the Arg/N-degron pathway affects cell death and suppresses inflammation, as these two functions have been attributed to the VASPIN protein (Skonieczna et al. 2019; Zieger et al. 2018). Upregulated genes also tell an interesting story, although it remains to be explored if their increased expression is due to the absence of UBR5. The genes that were upregulated following UBR5 have a vast variety of functions: cell proliferation, transport of calcium or nucleosides, histone proteins, cell wall components, actin components and formation of diacylglycerol. Two of these genes, Slc28a1 and Ly6c1, are generally increased following proinflammatory cytokine signaling such as TNFα and IL-6, however no direct causative role has been discovered for these

proteins in inflammation (Fernandez-Veledo et al. 2004; Lee, Wang, et al. 2013). Other genes are involved in cell proliferation, although their actions are contradictory: upregulation of Phlda2 has an antiproliferative effect (Wang et al. 2018), while Wnt11 promotes cell growth (Uysal-Onganer and Kypta 2012). Another intriguing candidate is long non-coding RNA Meg3, which activates p53 upon stimulation (Zhu et al. 2015). Nonetheless, none of the genes differentially regulated after UBR5 knockdown have a role in the initiation of inflammation, which adds to the mounting evidence that the role of the N-degron pathway in the regulation of inflammation is not through transcriptional activation. Another argument could be that the nineteen upregulated genes after UBR5 knockdown are simply a response to cellular damage inflicted by the absence of UBR5. Indeed, UBR5 is involved in the regulation of many pathways such as DNA damage repair, cell cycle control, apoptosis, calcium ion binding, cell adhesion, etc, (Shearer et al. 2015) and lack of this protein would mean a dysregulation of these pathways. More work needs to be done to fully uncover the relationship between UBR5 and the genes reported here (Table 11). Additionally, genes differentially regulated after UBR1, UBR2 or UBR4 knockdown should be examined to thoroughly appreciate the transcriptome profile after Arg/N-degron pathway downregulation.

siRNA in combinatorial treatments: the future of targeted therapies?

The term "chemotherapy" is attributed to the famous German chemist Paul Ehrlich, who defined it, in the early 1900's, as using chemicals to treat disease but it wasn't until the 60's that chemotherapy was combined to surgery and radiotherapy to treat cancer (DeVita and Chu 2008). However, despite considerable improvements of the chemical molecules, side effects and long-term sequelae of chemotherapy remain, most likely because the drugs also affect non-cancer cells (Nurgali, Jagoe, and Abalo 2018). Immune checkpoint inhibitors are new and promising treatments for cancer, but they also have challenges such as toxicity, resistance of tumors to these treatments and development of autoimmune diseases (Fares et al. 2019; Spiers, Coupe, and Payne 2019). Therefore, combinatorial treatments designed to either target multiple pathways at once, or potentiate the action of one agent with another, are the new cornerstone in cancer therapy development (Bayat Mokhtari et al.

2017; Chen and Lahav 2016; Saputra et al. 2018). Combinatorial targeted therapies allow to lower the dose of the chemotherapy or immune check-point inhibitor used, diminishing the side effects, and in some cases, helps to deliver the drug specifically to tumor cells. As stated in the beginning of this discussion, siRNA could be the "all-in-one" solution to the challenges in the development of combinatorial treatment. Indeed, siRNA can serve to identify molecular targets that will boost chemotherapy (Williams et al. 2017), can be used to downregulate these same targets directly in cancer cells in vivo (Singh, Trivedi, and Jain 2018), and finally, the carriers used for the siRNA, especially nanoparticles, can be formulated with the anti-cancer drugs inside, helping with targeted delivery of both the chemotherapeutic agent and the oligonucleotide (Mou et al. 2019). This thesis is a precise example of how siRNA can be used to identify and downregulate specific mRNA to affect a molecular pathway capable of crippling cancer cells. Much effort has already been made in this direction in the last few years and predictions can easily be made that siRNA will become an indispensable tool in targeted therapy development.

Chapter 6
Conclusion

The general aim of this PhD work was to validate the Arg/N-degron pathway as a new target for therapy. Based on the positive roles that the Arg/N-degron pathway has in favor of cancer maintenance, we hypothesized and proved in this study that downregulation of the UBR-ubiquitin ligases of the pathway can influence cancer development and increase apoptosis in tumor cells. Using an RNA interference approach in mice, we investigated the role of these proteins in the normal liver and in the context of hepatocellular carcinoma to understand (1) the consequences of long-term downregulation of UBR1, UBR2, UBR4 and UBR5 ubiquitin ligases in the normal adult liver; (2) how long-term partial ablation of the Arg/N-degron pathway would affect development and maintenance of hepatocellular carcinoma; and (3) how a combinatorial treatment for hepatocellular carcinoma could be developed based on downregulation of the Arg/N-degron pathway, with co-delivery of chemotherapy. We also investigated additional target proteins that can be used as co-therapy in combination with downregulation of the Arg/N-degron pathway, to increase sensitivity to apoptosis inducing drugs. To do so, we examined proteins that are subject to caspase cleavage once the apoptotic program is initiated, as well as cell transcriptome affected after UBR5 knockdown.

The conclusions to this study are three-fold and can be summarized as follows:

- The Arg/N-degron pathway was validated as a promising target for cancer therapy and potentiates the action of chemotherapy.
- The Arg/N-degron pathway plays an important role in the regulation of inflammation through targeted degradation of proinflammatory substrates
- This study led to the identification of potential partners for co-therapy, to further sensitize cells to apoptosis.

Our study is a proof-of-concept demonstrating that the Arg/N-degron pathway is a promising target for the development of novel cancer therapies. Long-term downregulation of UBR-ubiquitin ligases of the Arg/N-degron pathway in the liver of adult mice is well tolerated, and can be sustained for more than four weeks, provided that the chosen dose of LNP-siUbrs is low enough not to induce an inflammatory response. In the liver cancer model, downregulation of the Arg/N-degron pathway alone does not have a visible impact on proliferation or apoptosis of cancer cells. However, when co-administered with doxorubicin, we demonstrated that impairment of the Arg/N-degron pathway potentiates the action of chemotherapy, improving the outcome of the treatment. The observed reduction of tumor growth could be attributed to a decrease in cancer cell proliferation as well as an increase in apoptosis in the tumors. Furthermore, a study of the downregulation of individual UBR-ubiquitin ligases of the Arg/N-degron pathway in our mouse model of HCC demonstrated that all four E3 ligases are required to be targeted in this organ in order to synergize with the chemotherapy and increase its effects. As the N-degron pathway is involved in proliferation, migration, apoptosis and DNA damage repair, any drug or treatment that interferes with these pathways could be boosted by prior or concomitant downregulation of the N-degron pathway.

Second, during the course of this study, we uncovered the role of the Arg/N-degron pathway in the regulation of inflammation. Through degradation of proinflammatory fragments, which are conserved throughout evolution, the Arg/N-degron pathway participates in the maintenance of homeostasis, eliminating signals that would otherwise cultivate chronic inflammation in tissues. Inhibition of the Arg/N-degron pathway makes cells more sensitive to an inflammatory stimulus, and most likely would prolong the

inflammatory response in time. Taking into account the results obtained in this study as well as recently published data, we propose that the Arg/N-degron pathway participates in the control of inflammation at two levels: 1) in the generation of inflammatory signals by degradation of inhibitory anti-inflammatory domains and 2) in the resolution of inflammatory states through selective degradation of inflammatory mediators or proinflammatory fragments. The Arg/N degron pathway becomes an "off switch" through which new pharmacological interventions in inflammation are possible.

Third, we identified through two different methods, potential partners for co-therapy along with downregulation of the Arg/N-degron pathway to further increase the sensitivity to apoptosis in cells, and/or to better control inflammation. By studying the conservation of apoptotic caspase targets and sorting them according to structural and biochemical features, we isolated and identified a subset of 107 likely regulators of apoptosis and potential drug targets in cancer. 30 of the 107 identified proteins meet all criteria but have undetermined roles in apoptosis so far, which makes them intriguing substrates, but further studies are needed to determine how they can become targets of therapy. Then, by examining genes differentially expressed after UBR5 knockdown, we uncovered 29 genes potentially regulated by this E3 ligase, which could participate with UBR5 in the proliferation, apoptosis or inflammation processes. Modulating the expression of any of the proteins identified here as important actors in the apoptotic or inflammatory programs has the potential to enhance the combinatorial therapy presented in this work.

The results obtained in this PhD thesis open exciting possibilities for future studies and applications. First, since components of this pathway are ubiquitously expressed, our combinatorial therapy could have a major impact on the treatment of many other cancer types, provided that the siRNA can be delivered to the target organs. Now, existing nanoparticles can reach the spleen, lungs, skin and even the brain. These new delivery vehicles will provide opportunities to develop treatments for cancer affecting organs other than the liver. Additionally, as ligand conjugates gain in popularity, more options for oligonucleotide based targeted therapies will be available, allowing siRNA delivery to tumors in more diverse organs. Then, in order to make our combinatorial treatment suitable for translational studies, we would need to validate new siRNA against UBR-ubiquitin

ligases of the Arg/N-degron pathway in primates and human cell lines. Indeed, the sequences for the mRNA of these proteins differ slightly between species, but enough to require redesign of the oligonucleotides. Furthermore, chemical modifications applied on the oligonucleotides to increase stability against nucleases affect the efficacy of siRNA in a sequence dependent manner, thus the nature and the position of the modifications need to be verified before a translation into humans is possible. Nevertheless, this study provides the experimental data needed to foresee downregulation of the Arg/N-degron pathway as a potential cancer therapy in humans.

While we used the siRNA designed and tested in this study to validate the UBR ubiquitin ligases of the Arg/N-degron pathway as valuable targets in cancer therapy, they could also be used to further interrogate the role of this pathway in normal physiology, in inflammatory settings as well as in cancer development and progression in other organs, deepening our knowledge of the fundamental biology of the Arg/N-degron pathway. Identification of additional proinflammatory Arg/N-degron substrates would consolidate the roles of this pathway in the regulation of inflammation, and further studies in animals could also provide insight as to the consequences of N-degron pathway impairment during an acute or chronic inflammatory response. Results such as those would provide the basis for modulating the Arg/N-degron pathway as a means to influence inflammation.

Finally, dissecting the functions and roles of the newly identified caspase substrates in the apoptotic program and understanding how the transcription of specific genes are influenced by UBR5 will not only provide new probable targets for therapy but will improve our general understanding of regulation of apoptosis and the complex biology involved around the components of the Arg/N-degron pathway. Both fundamental and translational research knowledge will benefit from such studies.

Acknowlegments

Many people have contributed to the results presented in this thesis. I would like to acknowledge the following people:

- Nina Gubina and Maxim Pyatkov, for the bioinformatics analysis of the caspase substrates.
- Konstantin Piatkov for the proinflammatory fragments degradation assays (Caspases, PDK1 and Rab39a).
- Tatiana Prikazchikova, Kevin Kauffman, James Kaczmarek and Luke Rhym for the formulation of the lipid nanoparticles.
- The Skoltech Genomics Core Facility, especially Maria D. Logacheva, for the RNA sequencing
- Ilya Kurochkin, for the analysis of the RNA sequencing data.
- The Koch Institute Histology Core Facility, especially Kathy Cormier, for technical support and histology analysis.

This work was supported by the Next Generation Program – Skoltech MIT Initiatives, granted to K. Piatkov and D. Anderson.

References

Abrams, M. T., M. L. Koser, J. Seitzer, S. C. Williams, M. A. DiPietro, W. Wang, A. W. Shaw, X. Mao, V. Jadhav, J. P. Davide, P. A. Burke, A. B. Sachs, S. M. Stirdivant, and L. Sepp-Lorenzino. 2010. 'Evaluation of efficacy, biodistribution, and inflammation for a potent siRNA nanoparticle: effect of dexamethasone co-treatment', *Mol Ther*, 18: 171-80.

Afonina, I. S., C. Muller, S. J. Martin, and R. Beyaert. 2015. 'Proteolytic processing of interleukin-1 family cytokines: variations on a common theme', *Immunity*, 42: 991-1004.

Agard, N. J., D. Maltby, and J. A. Wells. 2010. 'Inflammatory stimuli regulate caspase substrate profiles', *Mol Cell Proteomics*, 9: 880-93.

Agarwalla, P. and Rajkumar B. 2016. 'N-end rule pathway inhibition assists colon tumor regression via necroptosis', *Molecular Therapy - Oncolytics*, 3.

Akinc, A., M. A. Maier, M. Manoharan, K. Fitzgerald, M. Jayaraman, S. Barros, S. Ansell, X. Du, M. J. Hope, T. D. Madden, B. L. Mui, S. C. Semple, Y. K. Tam, M. Ciufolini, D. Witzigmann, J. A. Kulkarni, R. van der Meel, and P. R. Cullis. 2019. 'The Onpattro story and the clinical translation of nanomedicines containing nucleic acid-based drugs', *Nat Nanotechnol*, 14: 1084-87.

Akinc, A., W. Querbes, S. De, J. Qin, M. Frank-Kamenetsky, K. N. Jayaprakash, M. Jayaraman, K. G. Rajeev, W. L. Cantley, J. R. Dorkin, J. S. Butler, L. Qin, T. Racie, A. Sprague, E. Fava, A. Zeigerer, M. J. Hope, M. Zerial, D. W. Sah, K. Fitzgerald, M. A. Tracy, M. Manoharan, V. Koteliansky, Ad Fougerolles, and M. A. Maier. 2010. 'Targeted delivery of RNAi therapeutics with endogenous and exogenous ligand-based mechanisms', *Mol Ther*, 18: 1357-64.

Akinc, A, Goldberg M., Qin J., Dorkin R.J., Gamba-Vitalo C., Maier M., Jayaprakash K.N., Jayaraman M., Rajeev K.G., Manoharan M., Koteliansky V., Röhl I., Leshchiner E.S., Langer R., and Anderson D.G. 2009. 'Development of lipidoid–siRNA formulations for systemic delivery to the liver', *Molecular Therapy*, 17: 872-79.

Akiyoshi, B., C. R. Nelson, N. Duggan, S. Ceto, J. A. Ranish, and S. Biggins. 2013. 'The Mub1/Ubr2 ubiquitin ligase complex regulates the conserved Dsn1 kinetochore protein', *PLoS Genet*, 9: e1003216.

Alexander-Bryant, A. A., Zhang H., Attaway C. C., Pugh W., Eggart L., Sansevere R.M., Andino L.M., Dinh L., Cantini L.P., and Jakymiw A. 2017. 'Dual peptide-mediated targeted delivery of bioactive siRNAs to oral cancer cells in vivo', *Oral Oncology*, 72: 123-31.

Alnouti, Y. 2009. 'Bile Acid sulfation: a pathway of bile acid elimination and detoxification', *Toxicol Sci*, 108: 225-46.

Altekruse, S. F., K. A. McGlynn, and M. E. Reichman. 2009. 'Hepatocellular carcinoma incidence, mortality, and survival trends in the United States from 1975 to 2005', *J Clin Oncol*, 27: 1485-91.

Alter, M. J. 2007. 'Epidemiology of hepatitis C virus infection', *World Journal of Gastroenterology*, 13: 2436-41.

Altschul, S. F., T. L. Madden, A. A. Schaffer, J. Zhang, Z. Zhang, W. Miller, and D. J. Lipman. 1997. 'Gapped BLAST and PSI-BLAST: a new generation of protein database search programs', *Nucleic Acids Res*, 25: 3389-402.

Amarzguioui, M., and H. Prydz. 2004. 'An algorithm for selection of functional siRNA sequences', *Biochem Biophys Res Commun*, 316: 1050-8.

Ameisen, J. C. 2002. 'On the origin, evolution, and nature of programmed cell death: a timeline of four billion years', *Cell Death Differ*, 9: 367-93.

Amerik, A. Y., and M. Hochstrasser. 2004. 'Mechanism and function of deubiquitinating enzymes', *Biochim Biophys Acta*, 1695: 189-207.

An, J. Y., J. W. Seo, T. Tasaki, M. J. Lee, A. Varshavsky, and Y. T. Kwon. 2006. 'Impaired neurogenesis and cardiovascular development in mice lacking the E3 ubiquitin ligases UBR1 and UBR2 of the N-end rule pathway', *PNAS*, 103: 6212-7.

An, J.Y., E. Kim, A. Zakrzewska, Y.D. Yoo, J.M. Jang, D.H. Han, M.J. Lee, J.W. Seo, Y.J. Lee, T.Y. Kim, D.G. de Rooij, B.Y. Kim, and Y.T. Kwon. 2012. 'UBR2 of the N-end rule pathway is required for chromosome stability via histone ubiquitylation in spermatocytes and somatic cells.', *PLoS One*, 7: e37414.

An, J.Y., E.-A. Kim, Y. Jiang, A. Zakrzewska, D.E. Kim, M.J. Lee, I. Mook-Jung, Y. Zhang, and Y.T. Kwon. 2010. 'UBR2 mediates transcriptional silencing during spermatogenesis via histone ubiquitination.', *Proc. Natl. Acad. Sci. USA*, 107: 1912-17.

Anderson, E. M., A. Birmingham, S. Baskerville, A. Reynolds, E. Maksimova, D. Leake, Y. Fedorov, J. Karpilow, and A. Khvorova. 2008. 'Experimental validation of the importance of seed complement frequency to siRNA specificity', *RNA*, 14: 853-61.

Anthony, D. A., D. M. Andrews, M. Chow, S. V. Watt, C. House, S. Akira, P. I. Bird, J. A. Trapani, and M. J. Smyth. 2010. 'A role for granzyme M in TLR4-driven inflammation and endotoxicosis', *Journal of Immunology*, 185: 1794-803.

Arvey, A., E. Larsson, C. Sander, C. S. Leslie, and D. S. Marks. 2010. 'Target mRNA abundance dilutes microRNA and siRNA activity', *Mol Syst Biol*, 6: 363.

Baboshina, O.V., and A.L. Haas. 1996. 'Novel multiubiquitin chain linkages catalyzed by the conjugating enzymes E2EPF and RAD6 are recognized by 26S proteasome subunit 5', *J. Biol. Chem.*, 271: 2822-31.

Bachmair, A., D. Finley, and A. Varshavsky. 1986. 'In vivo half-life of a protein is a function of its amino-terminal residue.', *Science*, 234: 179-86.

Bachmair, A., and A. Varshavsky. 1989. 'The degradation signal in a short-lived protein', *Cell*, 56: 1019-32.

Baker, R.T., and A. Varshavsky. 1991. 'Inhibition of the N-end rule pathway in living cells.', *PNAS*, 87: 2374-78.

Baranova, A., J. Bode, G. Manyam, and M. Emelianenko. 2011. 'An efficient algorithm for systematic analysis of nucleotide strings suitable for siRNA design', *BMC Res Notes*, 4: 168.

Barba, A. A., S. Bochicchio, A. Dalmoro, and G. Lamberti. 2019. 'Lipid Delivery Systems for Nucleic-Acid-Based-Drugs: From Production to Clinical Applications', *Pharmaceutics*, 11.

Barba, A. A., G. Lamberti, C. Sardo, B. Dapas, M. Abrami, M. Grassi, R. Farra, F. Tonon, G. Forte, F. Musiani, M. Licciardi, G. Pozzato, F. Zanconati, B. Scaggiante, G. Grassi, and G. Cavallaro. 2015. 'Novel lipid and polymeric materials as delivery systems for nucleic acid based drugs', *Curr Drug Metab*, 16: 427-52.

Barros, S. A., and J. A. Gollob. 2012. 'Safety profile of RNAi nanomedicines', *Adv Drug Deliv Rev*, 64: 1730-7.

Bartel, B., I. Wünning, and A. Varshavsky. 1990. 'The recognition component of the N-end rule pathway.', *EMBO J.*, 9: 3179-89.

Baschuk, N., N. Wang, S. V. Watt, H. Halse, C. House, P. I. Bird, R. Strugnell, J. A. Trapani, M. J. Smyth, and D. M. Andrews. 2014. 'NK cell intrinsic regulation of MIP-1alpha by granzyme M', *Cell Death Dis*, 5: e1115.

Bayat Mokhtari, R., T. S. Homayouni, N. Baluch, E. Morgatskaya, S. Kumar, B. Das, and H. Yeger. 2017. 'Combination therapy in combating cancer', *Oncotarget*, 8: 38022-43.

Becker, C. E., E. M. Creagh, and L. A. O'Neill. 2009. 'Rab39a binds caspase-1 and is required for caspase-1-dependent interleukin-1beta secretion', *J Biol Chem*, 284: 34531-7.

Bergsbaken, T., S. L. Fink, and B. T. Cookson. 2009. 'Pyroptosis: host cell death and inflammation', *Nat Rev Microbiol*, 7: 99-109.

Berndsen, C. E., and C. Wolberger. 2014. 'New insights into ubiquitin E3 ligase mechanism', *Nat Struct Mol Biol*, 21: 301-7.

Bernstein, E., A. A. Caudy, S. M. Hammond, and G. J. Hannon. 2001. 'Role for a bidentate ribonuclease in the initiation step of RNA interference', *Nature*, 409: 363-6.

Berraondo, P., M. F. Sanmamed, M. C. Ochoa, I. Etxeberria, M. A. Aznar, J. L. Perez-Gracia, M. E. Rodriguez-Ruiz, M. Ponz-Sarvise, E. Castanon, and I. Melero. 2019. 'Cytokines in clinical cancer immunotherapy', *British journal of cancer*, 120: 6-15.

Besin, G., J. Milton, S. Sabnis, R. Howell, C. Mihai, K. Burke, K. E. Benenato, M. Stanton, P. Smith, J. Senn, and S. Hoge. 2019. 'Accelerated Blood Clearance of Lipid Nanoparticles Entails a Biphasic Humoral Response of B-1 Followed by B-2 Lymphocytes to Distinct Antigenic Moieties', *Immunohorizons*, 3: 282-93.

Betancur, J. G., and Y. Tomari. 2012. 'Dicer is dispensable for asymmetric RISC loading in mammals', *RNA*, 18: 24-30.

Bialecki, E. S., and A. M. Di Bisceglie. 2005. 'Diagnosis of hepatocellular carcinoma', *HPB (Oxford)*, 7: 26-34.

Bogorad, R. L., H. Yin, A. Zeigerer, H. Nonaka, V. M. Ruda, M. Zerial, D. G. Anderson, and V. Koteliansky. 2014. 'Nanoparticle-formulated siRNA targeting integrins inhibits hepatocellular carcinoma progression in mice', *Nat. Commun.*, 5: 3869.

Boucher, D., M. Monteleone, R. C. Coll, K. W. Chen, C. M. Ross, J. L. Teo, G. A. Gomez, C. L. Holley, D. Bierschenk, K. J. Stacey, A. S. Yap, J. S. Bezbradica, and K. Schroder. 2018. 'Caspase-1 self-cleavage is an intrinsic mechanism to terminate inflammasome activity', *J of Exp Med*, 215: 827-40.

Bradley, A., H. Zheng, A. Ziebarth, W. Sakati, M. Branham-O'Connor, J. B. Blumer, Y. Liu, E. Kistner-Griffin, C. Rodriguez-Aguayo, G. Lopez-Berestein, A. K. Sood, C. N. Landen, Jr., and S. T. Eblen. 2014. 'EDD enhances cell survival and cisplatin resistance and is a therapeutic target for epithelial ovarian cancer', *Carcinogenesis*, 35: 1100-9.

Broering, R., C. I. Real, M. J. John, K. Jahn-Hofmann, L. M. Ickenstein, K. Kleinehr, A. Paul, K. Gibbert, U. Dittmer, G. Gerken, and J. F. Schlaak. 2014. 'Chemical modifications on siRNAs avoid Toll-like-receptor-mediated activation of the hepatic immune system in vivo and in vitro', *Int Immunol*, 26: 35-46.

Brower, C. S., K. I. Piatkov, and A. Varshavsky. 2013. 'Neurodegeneration-associated protein fragments as short-lived substrates of the N-end rule pathway', *Mol Cell*, 50: 161-71.

Brower, C. S., and A. Varshavsky. 2009. 'Ablation of arginylation in the mouse N-end rule pathway: loss of fat, higher metabolic rate, damaged spermatogenesis, and neurological perturbations', *PLoS One*, 4: e7757.

Callaghan, M. J., A. J. Russell, E. Woollatt, G. R. Sutherland, R. L. Sutherland, and C. K. Watts. 1998. 'Identification of a human HECT family protein with homology to the Drosophila tumor suppressor gene hyperplastic discs', *Oncogene*, 17: 3479-91.

Carmell, M. A., and G. J. Hannon. 2004. 'RNase III enzymes and the initiation of gene silencing', *Nat Struct Mol Biol*, 11: 214-8.

Carthew, R. W., and E. J. Sontheimer. 2009. 'Origins and Mechanisms of miRNAs and siRNAs', *Cell*, 136: 642-55.

Cedillo, I., D. Chreng, E. Engle, L. Chen, A. K. McPherson, and A. A. Rodriguez. 2017. 'Synthesis of 5'-GalNAc-conjugated oligonucleotides: a comparison of solid and solution-phase conjugation strategies', *Molecules*, 22.

Cerretti, D. P., C. J. Kozlosky, B. Mosley, N. Nelson, K. Van Ness, T. A. Greenstreet, C. J. March, S. R. Kronheim, T. Druck, L. A. Cannizzaro, and et al. 1992. 'Molecular cloning of the interleukin-1 beta converting enzyme', *Science*, 256: 97-100.

Cha-Molstad, H., J. E. Yu, Z. Feng, S. H. Lee, J. G. Kim, P. Yang, B. Han, K. W. Sung, Y. D. Yoo, J. Hwang, T. McGuire, S. M. Shim, H. D. Song, S. Ganipisetti, N. Wang, J. M. Jang, M. J. Lee, S. J. Kim, K. H. Lee, J. T. Hong, A. Ciechanover, I. Mook-Jung, K. P. Kim, X. Q. Xie, Y. T. Kwon, and B. Y. Kim. 2017. 'p62/SQSTM1/Sequestosome-1 is an N-recognin of the N-end rule pathway which modulates autophagosome biogenesis', *Nat Commun*, 8: 102.

Chau, V., J.W. Tobias, A. Bachmair, D. Marriott, D.J. Ecker, D.K. Gonda, and A. Varshavsky. 1989. 'A multiubiquitin chain is confined to specific lysine in a targeted short-lived protein.', *Science*, 243: 1576-83.

Chauhan, A. S., M. Kumar, S. Chaudhary, A. Dhiman, A. Patidar, P. Jakhar, P. Jaswal, K. Sharma, N. Sheokand, H. Malhotra, C. I. Raje, and M. Raje. 2019. 'Trafficking of a multifunctional protein

by endosomal microautophagy: linking two independent unconventional secretory pathways', *Faseb Journal*, 33: 5626-40.

Chavez, A., J. Scheiman, S. Vora, B. W. Pruitt, M. Tuttle, P. R. Iyer E, S. Lin, S. Kiani, C. D. Guzman, D. J. Wiegand, D. Ter-Ovanesyan, J. L. Braff, N. Davidsohn, B. E. Housden, N. Perrimon, R. Weiss, J. Aach, J. J. Collins, and G. M. Church. 2015. 'Highly efficient Cas9-mediated transcriptional programming', *Nat Methods*, 12: 326-8.

Chen, C., H. Mei, W. Shi, J. Deng, B. Zhang, T. Guo, H. Wang, and Y. Hu. 2013. 'EGFP-EGF1-conjugated PLGA nanoparticles for targeted delivery of siRNA into injured brain microvascular endothelial cells for efficient RNA interference', *PLoS One*, 8: e60860.

Chen, P. Y., L. Weinmann, D. Gaidatzis, Y. Pei, M. Zavolan, T. Tuschl, and G. Meister. 2008. 'Strand-specific 5'-O-methylation of siRNA duplexes controls guide strand selection and targeting specificity', *RNA*, 14: 263-74.

Chen, S. H., and G. Lahav. 2016. 'Two is better than one; toward a rational design of combinatorial therapy', *Curr Opin Struct Biol*, 41: 145-50.

Chen, S. J., X. Wu, B. Wadas, J. H. Oh, and A. Varshavsky. 2017. 'An N-end rule pathway that recognizes proline and destroys gluconeogenic enzymes', *Science*, 355.

Chen, Weihsu Claire, Jonathan P. May, and Shyh-Dar Li. 2013. 'Immune responses of therapeutic lipid nanoparticles', *Nanotech Rev*, 2.

Chen, X., and D. F. Calvisi. 2014. 'Hydrodynamic transfection for generation of novel mouse models for liver cancer research', *Am J Pathol*, 184: 912-23.

Cheng, A. L., C. Hsu, S. L. Chan, S. P. Choo, and M. Kudo. 2020. 'Challenges of combination therapy with immune checkpoint inhibitors for hepatocellular carcinoma', *J Hepatol*, 72: 307-19.

Cheng, J., B. A. Teply, I. Sherifi, J. Sung, G. Luther, F. X. Gu, E. Levy-Nissenbaum, A. F. Radovic-Moreno, R. Langer, and O. C. Farokhzad. 2007. 'Formulation of functionalized PLGA-PEG nanoparticles for in vivo targeted drug delivery', *Biomaterials*, 28: 869-76.

Cheng, X., and R. J. Lee. 2016. 'The role of helper lipids in lipid nanoparticles (LNPs) designed for oligonucleotide delivery', *Adv Drug Deliv Rev*, 99: 129-37.

Chernikov, I. V., V. V. Vlassov, and E. L. Chernolovskaya. 2019. 'Current Development of siRNA Bioconjugates: From Research to the Clinic', *Front Pharmacol*, 10: 444.

Choi, W.S., B.-C. Jeong, Y.J. Joo, M.-R. Lee, J. Kim, M.J. Eck, and H.K. Song. 2010. 'Structural basis for the recognition of N-end rule substrates by the UBR box of ubiquitin ligases.', *Nat Struct Mol Biol*, 17: 1175-81.

Choung, Sorim, Young Joo Kim, Seonhoe Kim, Han-Oh Park, and Young-Chul Choi. 2006. 'Chemical modification of siRNAs to improve serum stability without loss of efficacy', *Biochem Biophys Res Comm*, 342: 919-27.

Chui, A. J., M. C. Okondo, S. D. Rao, K. Gai, A. R. Griswold, D. C. Johnson, D. P. Ball, C. Y. Taabazuing, E. L. Orth, B. A. Vittimberga, and D. A. Bachovchin. 2019. 'N-terminal degradation activates the NLRP1B inflammasome', *Science*, 364: 82-85.

Ciechanover, A. 1994. 'The ubiquitin-proteasome proteolytic pathway.', *Cell*, 79: 13-21.

Ciechanover, A., S. Ferber, D. Ganoth, S. Elias, A. Hershko, and S. Arfin. 1988. 'Purification and characterization of arginyl-tRNA-protein transferase from rabbit reticulocytes. Its involvement in post-translational modification and degradation of acidic NH2 termini substrates of the ubiquitin pathway', *J Biol Chem*, 263: 11155-67.

Cipolla, L., F. Bertoletti, A. Maffia, C. C. Liang, A. R. Lehmann, M. A. Cohn, and S. Sabbioneda. 2019. 'UBR5 interacts with the replication fork and protects DNA replication from DNA polymerase eta toxicity', *Nucleic Acids Res*, 47: 11268-83.

Coghlin, C., B. Carpenter, S. R. Dundas, L. C. Lawrie, C. Telfer, and G. I. Murray. 2006. 'Characterization and over-expression of chaperonin t-complex proteins in colorectal cancer', *J Pathol*, 210: 351-7.

Cook, D. N. 1996. 'The role of MIP-1 alpha in inflammation and hematopoiesis', *J Leukoc Biol*, 59: 61-6.

Crawford, E. D., J. E. Seaman, N. Agard, G. W. Hsu, O. Julien, S. Mahrus, H. Nguyen, K. Shimbo, H. A. Yoshihara, M. Zhuang, R. J. Chalkley, and J. A. Wells. 2013. 'The DegraBase: a database of proteolysis in healthy and apoptotic human cells', *Mol Cell Proteomics*, 12: 813-24.

Crawford, E. D., J. E. Seaman, A. E. Barber, 2nd, D. C. David, P. C. Babbitt, A. L. Burlingame, and J. A. Wells. 2012. 'Conservation of caspase substrates across metazoans suggests hierarchical importance of signaling pathways over specific targets and cleavage site motifs in apoptosis', *Cell Death Differ*, 19: 2040-8.

Crawford, E.D., and J.A. Wells. 2011. 'Caspase substrates and cellular remodeling.', *Annu Rev Biochem*, 80: 1055-87.

Crooke, S. T., J. L. Witztum, C. F. Bennett, and B. F. Baker. 2018. 'RNA-Targeted Therapeutics', *Cell Metab*, 27: 714-39.

Cryns, V., and J. Yuan. 1998. 'Proteases to die for', *Gene Dev*, 12: 1551-70.

Cummings, James C., Haiwen Zhang, and Andrew Jakymiw. 2019. 'Peptide carriers to the rescue: overcoming the barriers to siRNA delivery for cancer treatment', *Translational Research*, 214: 92-104.

Currais, A., W. Fischer, P. Maher, and D. Schubert. 2017. 'Intraneuronal protein aggregation as a trigger for inflammation and neurodegeneration in the aging brain', *Faseb Journal*, 31: 5-10.

Czaplewski, L. G., J. McKeating, C. J. Craven, L. D. Higgins, V. Appay, A. Brown, T. Dudgeon, L. A. Howard, T. Meyers, J. Owen, S. R. Palan, P. Tan, G. Wilson, N. R. Woods, C. M. Heyworth, B. I. Lord, D. Brotherton, R. Christison, S. Craig, S. Cribbes, R. M. Edwards, S. J. Evans, R. Gilbert, P. Morgan, E. Randle, N. Schofield, P. G. Varley, J. Fisher, J. P. Waltho, and M. G. Hunter. 1999. 'Identification of amino acid residues critical for aggregation of human CC chemokines macrophage inflammatory protein (MIP)-1alpha, MIP-1beta, and RANTES. Characterization of active disaggregated chemokine variants', *J Biol Chem*, 274: 16077-84.

Dahlman, J. E., C. Barnes, O. Khan, A. Thiriot, S. Jhunjunwala, T. E. Shaw, Y. Xing, H. B. Sager, G. Sahay, L. Speciner, A. Bader, R. L. Bogorad, H. Yin, T. Racie, Y. Dong, S. Jiang, D. Seedorf,

A. Dave, K. S. Sandu, M. J. Webber, T. Novobrantseva, V. M. Ruda, A. K. R. Lytton-Jean, C. G. Levins, B. Kalish, D. K. Mudge, M. Perez, L. Abezgauz, P. Dutta, L. Smith, K. Charisse, M. W. Kieran, K. Fitzgerald, M. Nahrendorf, D. Danino, R. M. Tuder, U. H. von Andrian, A. Akinc, A. Schroeder, D. Panigrahy, V. Kotelianski, R. Langer, and D. G. Anderson. 2014. 'In vivo endothelial siRNA delivery using polymeric nanoparticles with low molecular weight', *Nat Nanotechnol*, 9: 648-55.

Dams, E. T., P. Laverman, W. J. Oyen, G. Storm, G. L. Scherphof, J. W. van Der Meer, F. H. Corstens, and O. C. Boerman. 2000. 'Accelerated blood clearance and altered biodistribution of repeated injections of sterically stabilized liposomes', *J Pharmacol Exp Ther*, 292: 1071-9.

David, Y., N. Ternette, M. J. Edelmann, T. Ziv, B. Gayer, R. Sertchook, Y. Dadon, B. M. Kessler, and A. Navon. 2011. 'E3 ligases determine ubiquitination site and conjugate type by enforcing specificity on E2 enzymes', *J Biol Chem*, 286: 44104-15.

Davydov, I. V., and A. Varshavsky. 2000. 'RGS4 is arginylated and degraded by the N-end rule pathway in vitro', *J Biol Chem*, 275: 22931-41.

Dayeh, Daniel M., Bradley C. Kruithoff, and Kotaro Nakanishi. 2018. 'Structural and functional analyses reveal the contributions of the C- and N-lobes of Argonaute protein to selectivity of RNA target cleavage', *J Biol Chem*, 293: 6308-25.

de Marchi, R., M. Sorel, B. Mooney, I. Fudal, K. Goslin, K. Kwasniewska, P. T. Ryan, M. Pfalz, J. Kroymann, S. Pollmann, A. Feechan, F. Wellmer, S. Rivas, and E. Graciet. 2016. 'The N-end rule pathway regulates pathogen responses in plants', *Sci Rep*, 6: 26020.

Denes, A., G. Lopez-Castejon, and D. Brough. 2012. 'Caspase-1: is IL-1 just the tip of the ICEberg?', *Cell Death Dis*, 3: e338.

Deshaies, R. J., and C. A. Joazeiro. 2009. 'RING domain E3 ubiquitin ligases', *Annu Rev Biochem*, 78: 399-434.

Deshayes, Sébastien, May Morris, Frédéric Heitz, and Gilles Divita. 2008. 'Delivery of proteins and nucleic acids using a non-covalent peptide-based strategy', *Adv Drug Deliv Rev*, 60: 537-47.

DeVita, V. T., Jr., and E. Chu. 2008. 'A history of cancer chemotherapy', *Cancer Res*, 68: 8643-53.

Dias, N., and C. A. Stein. 2002. 'Antisense oligonucleotides: basic concepts and mechanisms', *Mol Cancer Ther*, 1: 347-55.

Dinarello, C. A. 2018. 'Overview of the IL-1 family in innate inflammation and acquired immunity', *Immunological Reviews*, 281: 8-27.

Ditzel, M., R. Wilson, T. Tenev, A. Zachariou, A. Paul, E. Deas, and P. Meier. 2003. 'Degradation of DIAP1 by the N-end rule pathway is essential for regulating apoptosis.', *Nature Cell Biol.*, 5: 467-73.

Dobin, A., C. A. Davis, F. Schlesinger, J. Drenkow, C. Zaleski, S. Jha, P. Batut, M. Chaisson, and T. R. Gingeras. 2013. 'STAR: ultrafast universal RNA-seq aligner', *Bioinformatics*, 29: 15-21.

Dohmen, R.J., K. Madura, B. Bartel, and A. Varshavsky. 1991. 'The N-end rule is mediated by the UBC2 (RAD6) ubiquitin-conjugating enzyme.', *PNAS. USA*, 88: 7351-55.

Dong, C., H. Zhang, L. Li, W. Tempel, P. Loppnau, and J. Min. 2018. 'Molecular basis of GID4-mediated recognition of degrons for the Pro/N-end rule pathway', *Nat Chem Biol*, 14: 466-73.

Dong, Y., K. T. Love, J. R. Dorkin, S. Sirirungruang, Y. Zhang, D. Chen, R. L. Bogorad, H. Yin, Y. Chen, A. J. Vegas, C. A. Alabi, G. Sahay, K. T. Olejnik, W. Wang, A. Schroeder, A. K. Lytton-Jean, D. J. Siegwart, A. Akinc, C. Barnes, S. A. Barros, M. Carioto, K. Fitzgerald, J. Hettinger, V. Kumar, T. I. Novobrantseva, J. Qin, W. Querbes, V. Koteliansky, R. Langer, and D. G. Anderson. 2014. 'Lipopeptide nanoparticles for potent and selective siRNA delivery in rodents and nonhuman primates', *PNAS*, 111: 3955-60.

Dubnikov, T., T. Ben-Gedalya, and E. Cohen. 2017. 'Protein Quality Control in Health and Disease', *Cold Spring Harb Perspect Biol*, 9.

Eblen, S. T., and A. Bradley. 2017. 'MOAP-1, UBR5 and cisplatin resistance in ovarian cancer', *Transl Cancer Res*, 6: S18-S21.

Eckstein, F. 2014. 'Phosphorothioates, essential components of therapeutic oligonucleotides', *Nucleic Acid Ther*, 24: 374-87.

El-Serag, H. B., H. Hampel, and F. Javadi. 2006. 'The association between diabetes and hepatocellular carcinoma: a systematic review of epidemiologic evidence', *Clin Gastroenterol Hepatol*, 4: 369-80.

Elbashir, S. M., J. Harborth, W. Lendeckel, A. Yalcin, K. Weber, and T. Tuschl. 2001. 'Duplexes of 21-nucleotide RNAs mediate RNA interference in cultured mammalian cells', *Nature*, 411: 494-8.

Elbashir, S. M., W. Lendeckel, and T. Tuschl. 2001. 'RNA interference is mediated by 21-and 22-nucleotide RNAs', *Genes & Development*, 15: 188-200.

Elbashir, S. M., J. Martinez, A. Patkaniowska, W. Lendeckel, and T. Tuschl. 2001. 'Functional anatomy of siRNAs for mediating efficient RNAi in Drosophila melanogaster embryo lysate', *EMBO J*, 20: 6877-88.

Eldeeb, M. A., and R. P. Fahlman. 2014. 'The anti-apoptotic form of tyrosine kinase Lyn that is generated by proteolysis is degraded by the N-end rule pathway', *Oncotarget*, 5: 2714-22.

Elkayam, E., C. D. Kuhn, A. Tocilj, A. D. Haase, E. M. Greene, G. J. Hannon, and L. Joshua-Tor. 2012. 'The structure of human argonaute-2 in complex with miR-20a', *Cell*, 150: 100-10.

Elmore, S. 2007. 'Apoptosis: a review of programmed cell death', *Toxicol Pathol*, 35: 495-516.

Eulalio, Ana, Eric Huntzinger, and Elisa Izaurralde. 2008. 'Getting to the Root of miRNA-Mediated Gene Silencing', *Cell*, 132: 9-14.

Fabian, M. R., and N. Sonenberg. 2012. 'The mechanics of miRNA-mediated gene silencing: a look under the hood of miRISC', *Nat Struct Mol Biol*, 19: 586-93.

Faehnle, C. R., E. Elkayam, A. D. Haase, G. J. Hannon, and L. Joshua-Tor. 2013. 'The making of a slicer: activation of human Argonaute-1', *Cell Rep*, 3: 1901-9.

Fang, C., Y. Shang, and D. Xu. 2018. 'MUFOLD-SS: New deep inception-inside-inception networks for protein secondary structure prediction', *Proteins*, 86: 592-98.

Fares, C. M., E. M. Van Allen, C. G. Drake, J. P. Allison, and S. Hu-Lieskovan. 2019. 'Mechanisms of resistance to immune checkpoint blockade: why does checkpoint inhibitor immunotherapy not work for all patients?', *Am Soc Clin Oncol Educ Book*, 39: 147-64.

Fautz, R., B. Husein, and C. Hechenberger. 1991. 'Application of the neutral red assay (NR assay) to monolayer cultures of primary hepatocytes: rapid colorimetric viability determination for the unscheduled DNA synthesis test (UDS)', *Mutation research*, 253: 173-9.

Feng, G., and N. Kaplowitz. 2002. 'Mechanism of staurosporine-induced apoptosis in murine hepatocytes', *Am J Physiol Gastrointest Liver Physiol*, 282: G825-34.

Fenton, O. S., K. J. Kauffman, J. C. Kaczmarek, R. L. McClellan, S. Jhunjhunwala, M. W. Tibbitt, M. D. Zeng, E. A. Appel, J. R. Dorkin, F. F. Mir, J. H. Yang, M. A. Oberli, M. W. Heartlein, F. DeRosa, R. Langer, and D. G. Anderson. 2017. 'Synthesis and Biological Evaluation of ionizable lipid materials for the in vivo delivery of messenger RNA to B lymphocytes', *Adv Mater*, 29.

Fernandez-Veledo, S., R. Valdes, V. Wallenius, F. J. Casado, and M. Pastor-Anglada. 2004. 'Up-regulation of the high-affinity pyrimidine-preferring nucleoside transporter concentrative nucleoside transporter 1 by tumor necrosis factor-alpha and interleukin-6 in liver parenchymal cells', *J Hepatol*, 41: 538-44.

Fire, A., S. Xu, M. K. Montgomery, S. A. Kostas, S. E. Driver, and C. C. Mello. 1998. 'Potent and specific genetic interference by double-stranded RNA in Caenorhabditis elegans', *Nature*, 391: 806-11.

Flack, Joshua E., Juliusz Mieszczanek, Nikola Novcic, and Mariann Bienz. 2017. 'Wnt-dependent inactivation of the Groucho/TLE co-repressor by the HECT E3 ubiquitin ligase Hyd/UBR5', *Molecular cell*, 67: 181-93.e5.

Forstemann, K., M. D. Horwich, L. Wee, Y. Tomari, and P. D. Zamore. 2007. 'Drosophila microRNAs are sorted into functionally distinct argonaute complexes after production by dicer-1', *Cell*, 130: 287-97.

Foster, D. J., C. R. Brown, S. Shaikh, C. Trapp, M. K. Schlegel, K. Qian, A. Sehgal, K. G. Rajeev, V. Jadhav, M. Manoharan, S. Kuchimanchi, M. A. Maier, and S. Milstein. 2018. 'Advanced siRNA designs further improve in vivo performance of GalNAc-siRNA conjugates', *Mol Ther*, 26: 708-17.

Frank, F., N. Sonenberg, and B. Nagar. 2010. 'Structural basis for 5'-nucleotide base-specific recognition of guide RNA by human AGO2', *Nature*, 465: 818-22.

Frank-Kamenetsky, M., A. Grefhorst, N. N. Anderson, T. S. Racie, B. Bramlage, A. Akinc, D. Butler, K. Charisse, R. Dorkin, Y. Fan, C. Gamba-Vitalo, P. Hadwiger, M. Jayaraman, M. John, K. N. Jayaprakash, M. Maier, L. Nechev, K. G. Rajeev, T. Read, I. Rohl, J. Soutschek, P. Tan, J. Wong, G. Wang, T. Zimmermann, A. de Fougerolles, H. P. Vornlocher, R. Langer, D. G. Anderson, M. Manoharan, V. Koteliansky, J. D. Horton, and K. Fitzgerald. 2008. 'Therapeutic RNAi targeting PCSK9 acutely lowers plasma cholesterol in rodents and LDL cholesterol in nonhuman primates', *PNAS*, 105: 11915-20.

Friedman, R. C., K. K. Farh, C. B. Burge, and D. P. Bartel. 2009. 'Most mammalian mRNAs are conserved targets of microRNAs', *Genome Res*, 19: 92-105.

G. B. D. Causes of Death Collaborators. 2018. 'Global, regional, and national age-sex-specific mortality for 282 causes of death in 195 countries and territories, 1980-2017: a systematic analysis for the Global Burden of Disease Study 2017', *Lancet*, 392: 1736-88.

Ganesh, S., X. Shui, K. P. Craig, J. Park, W. Wang, B. D. Brown, and M. T. Abrams. 2018. 'RNAi-mediated beta-catenin inhibition promotes T cell infiltration and antitumor activity in combination with immune checkpoint blockade', *Mol Ther*, 26: 2567-79.

Gao, H., M. Zheng, S. Sun, H. Wang, Z. Yue, Y. Zhu, X. Han, J. Yang, Y. Zhou, Y. Cai, and W. Hu. 2017. 'Chaperonin containing TCP1 subunit 5 is a tumor associated antigen of non-small cell lung cancer', *Oncotarget*, 8: 64170-79.

Garneau, N. L., J. Wilusz, and C. J. Wilusz. 2007. 'The highways and byways of mRNA decay', *Nat Rev Mol Cell Biol*, 8: 113-26.

Geary, R. S., T. A. Watanabe, L. Truong, S. Freier, E. A. Lesnik, N. B. Sioufi, H. Sasmor, M. Manoharan, and A. A. Levin. 2001. 'Pharmacokinetic properties of 2'-O-(2-methoxyethyl)-modified oligonucleotide analogs in rats', *J Pharmacol Exp Ther*, 296: 890-7.

Gewirtz, A. M. 2007. 'On future's doorstep: RNA interference and the pharmacopeia of tomorrow', *J Clin Invest*, 117: 3612-4.

Gilleron, J., W. Querbes, A. Zeigerer, A. Borodovsky, G. Marsico, U. Schubert, K. Manygoats, S. Seifert, C. Andree, M. Stoter, H. Epstein-Barash, L. Zhang, V. Koteliansky, K. Fitzgerald, E. Fava, M. Bickle, Y. Kalaidzidis, A. Akinc, M. Maier, and M. Zerial. 2013. 'Image-based analysis of lipid nanoparticle-mediated siRNA delivery, intracellular trafficking and endosomal escape', *Nat Biotechnol*, 31: 638-46.

Global Burden of Disease Liver Cancer, Collaboration, T. Akinyemiju, S. Abera, M. Ahmed, N. Alam, M. A. Alemayohu, C. Allen, R. Al-Raddadi, N. Alvis-Guzman, Y. Amoako, A. Artaman, T. A. Ayele, A. Barac, I. Bensenor, A. Berhane, Z. Bhutta, J. Castillo-Rivas, A. Chitheer, J. Y. Choi, B. Cowie, L. Dandona, R. Dandona, S. Dey, D. Dicker, H. Phuc, D. U. Ekwueme, M. S. Zaki, F. Fischer, T. Furst, J. Hancock, S. I. Hay, P. Hotez, S. H. Jee, A. Kasaeian, Y. Khader, Y. H. Khang, A. Kumar, M. Kutz, H. Larson, A. Lopez, R. Lunevicius, R. Malekzadeh, C. McAlinden, T. Meier, W. Mendoza, A. Mokdad, M. Moradi-Lakeh, G. Nagel, Q. Nguyen, G. Nguyen, F. Ogbo, G. Patton, D. M. Pereira, F. Pourmalek, M. Qorbani, A. Radfar, G. Roshandel, J. A. Salomon, J. Sanabria, B. Sartorius, M. Satpathy, M. Sawhney, S. Sepanlou, K. Shackelford, H. Shore, J. Sun, D. T. Mengistu, R. Topor-Madry, B. Tran, K. N. Ukwaja, V. Vlassov, S. E. Vollset, T. Vos, T. Wakayo, E. Weiderpass, A. Werdecker, N. Yonemoto, M. Younis, C. Yu, Z. Zaidi, L. Zhu, C. J. L. Murray, M. Naghavi, and C. Fitzmaurice. 2017. 'The burden of primary liver cancer and underlying etiologies from 1990 to 2015 at the global, regional, and national level: results from the global burden of disease study 2015', *JAMA Oncol*, 3: 1683-91.

Golden, D. E., V. R. Gerbasi, and E. J. Sontheimer. 2008. 'An inside job for siRNAs', *Mol Cell*, 31: 309-12.

Gonda, D.K., A. Bachmair, I. Wünning, J.W. Tobias, W.S. Lane, and A. Varshavsky. 1989. 'Universality and structure of the N-end rule.', *J Biol Chem*, 264: 16700-12.

Gong, D., and J. E. Ferrell, Jr. 2004. 'Picking a winner: new mechanistic insights into the design of effective siRNAs', *Trends Biotechnol*, 22: 451-4.

Goslin, K., L. Eschen-Lippold, C. Naumann, E. Linster, M. Sorel, M. Klecker, R. de Marchi, A. Kind, M. Wirtz, J. Lee, N. Dissmeyer, and E. Graciet. 2019. 'Differential N-end rule degradation of RIN4/NOI fragments generated by the AvrRpt2 effector protease', *Plant Physiol*, 180: 2272-89.

Gracie, J. A., S. E. Robertson, and I. B. McInnes. 2003. 'Interleukin-18', *J Leukoc Biol*, 73: 213-24.

Graciet, E., and F. Wellmer. 2010. 'The plant N-end rule pathway: structure and functions.', *Trends Plant Sci.*, 15: 447-53.

Gredell, J. A., M. J. Dittmer, M. Wu, C. Chan, and S. P. Walton. 2010. 'Recognition of siRNA asymmetry by TAR RNA binding protein', *Biochemistry*, 49: 3148-55.

Green, D. R., and P. Fitzgerald. 2016. 'Just so stories about the evolution of apoptosis', *Curr. Biol.*, 26: R620-R27.

Gresnigt, M. S., and F. L. van de Veerdonk. 2013. 'Biology of IL-36 cytokines and their role in disease', *Semin Immunol*, 25: 458-65.

Gu, S., L. Jin, F. Zhang, Y. Huang, D. Grimm, J. J. Rossi, and M. A. Kay. 2011. 'Thermodynamic stability of small hairpin RNAs highly influences the loading process of different mammalian Argonautes', *PNAS. USA*, 108: 9208-13.

Gubina, N., Leboeuf D., Piatkov K., and Pyatkov M. 2020. 'Novel Apoptotic Mediators Identified by Conservation of Vertebrate Caspase Targets', *Biomolecules*, 10: 612.

Guimaraes, P. P. G., R. Zhang, R. Spektor, M. Tan, A. Chung, M. M. Billingsley, R. El-Mayta, R. S. Riley, L. Wang, J. M. Wilson, and M. J. Mitchell. 2019. 'Ionizable lipid nanoparticles encapsulating barcoded mRNA for accelerated in vivo delivery screening', *J Control Release*, 316: 404-17.

Gustafson, H. H., D. Holt-Casper, D. W. Grainger, and H. Ghandehari. 2015. 'Nanoparticle uptake: the phagocyte problem', *Nano Today*, 10: 487-510.

Habrant, D., P. Peuziat, T. Colombani, L. Dallet, J. Gehin, E. Goudeau, B. Evrard, O. Lambert, T. Haudebourg, and B. Pitard. 2016. 'Design of ionizable lipids to overcome the limiting step of endosomal escape: application in the intracellular delivery of mRNA, DNA, and siRNA', *J Med Chem*, 59: 3046-62.

Haley, B., and P. D. Zamore. 2004. 'Kinetic analysis of the RNAi enzyme complex', *Nat Struct Mol Biol*, 11: 599-606.

Hamilton, A. J., and D. C. Baulcombe. 1999. 'A species of small antisense RNA in posttranscriptional gene silencing in plants', *Science*, 286: 950-2.

Hamming, R. W. 1950. 'Error detecting and error correcting codes', *Bell Sys Tech J*, 29: 147-60.

Hammond, S. M., E. Bernstein, D. Beach, and G. J. Hannon. 2000. 'An RNA-directed nuclease mediates post-transcriptional gene silencing in Drosophila cells', *Nature*, 404: 293-6.

Han, Y., Y. Liu, H. Zhang, F. He, C. Shu, and L. Dong. 2017. 'Utilizing selected di- and trinucleotides of siRNA to predict RNAi activity', *Comput Math Methods Med*, 2017: 5043984.

Hanahan, Douglas, and Robert A Weinberg. 2011. 'Hallmarks of cancer: the next Ggneration', *Cell*, 144: 646-74.

Haraldsson, B., J. Nystrom, and W. M. Deen. 2008. 'Properties of the glomerular barrier and mechanisms of proteinuria', *Physiol Rev*, 88: 451-87.

Heck, J.W., S.K. Cheung, and R.Y. Hampton. 2010. 'Cytoplasmic protein quality control degradation mediated by parallel actions of the E3 ubiquitin ligases Ubr1 and San1.', *PNAS. USA*, 107: 1106-11.

Henderson, M. J., M. A. Munoz, D. N. Saunders, J. L. Clancy, A. J. Russell, B. Williams, D. Pappin, K. K. Khanna, S. P. Jackson, R. L. Sutherland, and C. K. Watts. 2006. 'EDD mediates DNA damage-induced activation of CHK2', *J Biol Chem*, 281: 39990-40000.

Henderson, M. J., A. J. Russell, S. Hird, M. Munoz, J. L. Clancy, G. M. Lehrbach, S. T. Calanni, D. A. Jans, R. L. Sutherland, and C. K. Watts. 2002. 'EDD, the human hyperplastic discs protein, has a role in progesterone receptor coactivation and potential involvement in DNA damage response', *J Biol Chem*, 277: 26468-78.

Henry, C. M., G. P. Sullivan, D. M. Clancy, I. S. Afonina, D. Kulms, and S. J. Martin. 2016. 'Neutrophil-derived proteases escalate inflammation through activation of IL-36 family cytokines', *Cell Rep*, 14: 708-22.

Hershko, A. 1991. 'The ubiquitin pathway for protein degradation.', *Trends Biochem Sci*, 16: 265-68.

Hershko, A., and A. Ciechanover. 1998. 'The ubiquitin system.', *Annu Rev Biochem*, 76: 425-79.

Hildebrand, D., K. A. Bode, D. Riess, D. Cerny, A. Waldhuber, F. Rommler, J. Strack, S. Korten, J. H. Orth, T. Miethke, K. Heeg, and K. F. Kubatzky. 2014. 'Granzyme A produces bioactive IL-1beta through a nonapoptotic inflammasome-independent pathway', *Cell Rep*, 9: 910-7.

Hirano, S., Q. Zhou, A. Furuyama, and S. Kanno. 2017. 'Differential regulation of IL-1beta and IL-6 release in murine macrophages', *Inflammation*, 40: 1933-43.

Hock, J., and G. Meister. 2008. 'The Argonaute protein family', *Genome Biol*, 9: 210.

Holen, T., M. Amarzguioui, M. T. Wiiger, E. Babaie, and H. Prydz. 2002. 'Positional effects of short interfering RNAs targeting the human coagulation trigger Tissue Factor', *Nucleic Acids Res*, 30: 1757-66.

Hornung, V., A. Ablasser, M. Charrel-Dennis, F. Bauernfeind, G. Horvath, D. R. Caffrey, E. Latz, and K. A. Fitzgerald. 2009. 'AIM2 recognizes cytosolic dsDNA and forms a caspase-1-activating inflammasome with ASC', *Nature*, 458: 514-8.

Hu, B., Y. Weng, X. H. Xia, X. J. Liang, and Y. Huang. 2019. 'Clinical advances of siRNA therapeutics', *J Gene Med*, 21: e3097.

Hu, R. G., C. S. Brower, H. Wang, I. V. Davydov, J. Sheng, J. Zhou, Y. T. Kwon, and A. Varshavsky. 2006. 'Arginyltransferase, Its Specificity, Putative Substrates, Bidirectional Promoter, and Splicing-derived Isoforms', *J Biol Chem*, 281: 32559-73.

Hu, R. G., H. Wang, Z. Xia, and A. Varshavsky. 2008a. 'The N-end rule pathway is a sensor of heme', *PNAS*, 105: 76-81.

Hu, R.-G., H. Wang, Z. Xia, and A Varshavsky. 2008b. 'The N-end rule pathway is a sensor of heme.', *PNAS. USA*, 105: 76-81.

Hu, Rong-Gui, Jun Sheng, Xin Qi, Zhenming Xu, Terry T. Takahashi, and Alexander Varshavsky. 2005. 'The N-end rule pathway as a nitric oxide sensor controlling the levels of multiple regulators', *Nature*, 437: 981-86.

Huang da, W., B. T. Sherman, and R. A. Lempicki. 2009. 'Bioinformatics enrichment tools: paths toward the comprehensive functional analysis of large gene lists', *Nucleic Acids Res*, 37: 1-13.

Huang, L., E. Kinnukan, G. Wang, S. Beaudenon, P.M. Howley, J.M. Huibregtse, and N.P Pavletich. 1999. 'Structure of an E6AP-UbcH7 complex: insights into ubiquitination by the E2-E3 cascade.', *Science*, 286: 1321-26.

Huang, Y. 2017. 'Preclinical and clinical advances of GalNAc-decorated nucleic acid therapeutics', *Mol Ther Nucleic Acids*, 6: 116-32.

Hunt, L. C., J. Stover, B. Haugen, T. I. Shaw, Y. Li, V. R. Pagala, D. Finkelstein, E. R. Barton, Y. Fan, M. Labelle, J. Peng, and F. Demontis. 2019. 'A key role for the ubiquitin Llgase UBR4 in myofiber hypertrophy in drosophila and mice', *Cell Rep*, 28: 1268-81 e6.

Hunter, T. 2007. 'The age of crosstalk: phosphorylation, ubiquitination, and beyond', *Mol Cell*, 28: 730-8.

Hur, J. K., M. K. Zinchenko, S. Djuranovic, and R. Green. 2013. 'Regulation of Argonaute slicer activity by guide RNA 3' end interactions with the N-terminal lobe', *J Biol Chem*, 288: 7829-40.

Hutvagner, G., and P. D. Zamore. 2002. 'A microRNA in a multiple-turnover RNAi enzyme complex', *Science*, 297: 2056-60.

Hwang, C. S., A. Shemorry, and A. Varshavsky. 2009. 'Two proteolytic pathways regulate DNA repair by cotargeting the Mgt1 alkylguanine transferase', *Proceedings of the National Academy of Sciences*, 106: 2142-47.

Hwang, C. S., M. Sukalo, O. Batygin, M. C. Addor, H. Brunner, A. P. Aytes, J. Mayerle, H. K. Song, A. Varshavsky, and M. Zenker. 2011. 'Ubiquitin ligases of the N-end rule pathway: assessment of mutations in UBR1 that cause the Johanson-Blizzard syndrome', *PLoS One*, 6: e24925.

Hwang, C.-S., A. Shemorry, and A. Varshavsky. 2010. 'N-terminal acetylation of cellular proteins creates specific degradation signals.', *Science*, 327: 973-77.

Igarashi, Y., A. Eroshkin, S. Gramatikova, K. Gramatikoff, Y. Zhang, J. W. Smith, A. L. Osterman, and A. Godzik. 2007. 'CutDB: a proteolytic event database', *Nucleic Acids Res*, 35: D546-9.

Inobe, T., S. Fishbain, S. Prakash, and A. Matouschek. 2011. 'Defining the geometry of the two-component proteasome degron', *Nat Chem Biol*, 7: 161-7.

Iribe, H., K. Miyamoto, T. Takahashi, Y. Kobayashi, J. Leo, M. Aida, and K. Ui-Tei. 2017. 'Chemical Modification of the siRNA Seed Region Suppresses Off-Target Effects by Steric Hindrance to Base-Pairing with Targets', *ACS Omega*, 2: 2055-64.

Islam, M. A., T. E. Park, B. Singh, S. Maharjan, J. Firdous, M. H. Cho, S. K. Kang, C. H. Yun, Y. J. Choi, and C. S. Cho. 2014. 'Major degradable polycations as carriers for DNA and siRNA', *J Control Release*, 193: 74-89.

Iwasaki, S., M. Kobayashi, M. Yoda, Y. Sakaguchi, S. Katsuma, T. Suzuki, and Y. Tomari. 2010. 'Hsc70/Hsp90 chaperone machinery mediates ATP-dependent RISC loading of small RNA duplexes', *Mol Cell*, 39: 292-9.

Jackson, A. L., J. Burchard, D. Leake, A. Reynolds, J. Schelter, J. Guo, J. M. Johnson, L. Lim, J. Karpilow, K. Nichols, W. Marshall, A. Khvorova, and P. S. Linsley. 2006. 'Position-specific chemical modification of siRNAs reduces "off-target" transcript silencing', *RNA*, 12: 1197-205.

Jadhav, S., N. Zilka, and M. Novak. 2013. 'Protein truncation as a common denominator of human neurodegenerative foldopathies', *Mol Neurobiol*, 48: 516-32.

Jiang, Yanxialei, Subrata Kumar Pore, Jung Hoon Lee, Shashi Sriram, Binh Khanh Mai, Dong Hoon Han, Pritha Agarwalla, Adriana Zakrzewska, Yongho Kim, Rajkumar Banerjee, Seung-Han Lee, and Min Jae Lee. 2013. 'Characterization of mammalian N-degrons and development of heterovalent inhibitors of the N-end rule pathway', *Chem Science*, 4: 3339.

Jimenez Fernandez, D., and M. Lamkanfi. 2015. 'Inflammatory caspases: key regulators of inflammation and cell death', *Biol Chem*, 396: 193-203.

Joeckel, L. T., R. Wallich, P. Martin, D. Sanchez-Martinez, F. C. Weber, S. F. Martin, C. Borner, J. Pardo, C. Froelich, and M. M. Simon. 2011. 'Mouse granzyme K has pro-inflammatory potential', *Cell Death & Diff*, 18: 1112-19.

Jones, J. D. G., and J. L. Dangl. 2006. 'The plant immune system', *Nature*, 444: 323-29.

Judge, A. D., G. Bola, A. C. Lee, and I. MacLachlan. 2006. 'Design of noninflammatory synthetic siRNA mediating potent gene silencing in vivo', *Mol Ther*, 13: 494-505.

Juliano, R. L. 2018. 'Intracellular trafficking and endosomal release of oligonucleotides: what we know and what we don't', *Nucleic Acid Ther*, 28: 166-77.

Julien, O., and J. A. Wells. 2017. 'Caspases and their substrates', *Cell Death Differ*, 24: 1380-89.

Kaeppel, C., S. G. Beattie, R. Fronza, R. van Logtenstein, F. Salmon, S. Schmidt, S. Wolf, A. Nowrouzi, H. Glimm, C. von Kalle, H. Petry, D. Gaudet, and M. Schmidt. 2013. 'A largely random AAV integration profile after LPLD gene therapy', *Nat Med*, 19: 889-91.

Kamola, P. J., Y. Nakano, T. Takahashi, P. A. Wilson, and K. Ui-Tei. 2015. 'The siRNA non-seed region and its target sequences are auxiliary determinants of off-target effects', *PLoS Comput Biol*, 11: e1004656.

Kanasty, R., J. R. Dorkin, A. Vegas, and D. Anderson. 2013. 'Delivery materials for siRNA therapeutics', *Nat Mater*, 12: 967-77.

Kanellopoulou, C., S. A. Muljo, A. L. Kung, S. Ganesan, R. Drapkin, T. Jenuwein, D. M. Livingston, and K. Rajewsky. 2005. 'Dicer-deficient mouse embryonic stem cells are defective in differentiation and centromeric silencing', *Genes Dev*, 19: 489-501.

Karin, M., and A. Lin. 2002. 'NF-kappaB at the crossroads of life and death', *Nat Immunol*, 3: 221-7.

Karki, P., G. R. Dahal, and I. S. Park. 2007. 'Both dimerization and interdomain processing are essential for caspase-4 activation', *Biochem Biophys Res Commun*, 356: 1056-61.

Kato, M. 1983. 'Heparin as an inhibitor of L-arginyl-tRNA: protein arginyltransferase', *J Biochem*, 94: 2015-22.

Kauffman, K. J., J. R. Dorkin, J. H. Yang, M. W. Heartlein, F. DeRosa, F. F. Mir, O. S. Fenton, and D. G. Anderson. 2015. 'Optimization of lipid nanoparticle formulations for mRNA delivery in vivo with fractional factorial and definitive screening designs', *Nano Lett*, 15: 7300-6.

Kechko, O. I., I. Y. Petrushanko, C. S. Brower, A. A. Adzhubei, A. A. Moskalev, K. I. Piatkov, V. A. Mitkevich, and A. A. Makarov. 2019. 'Beta-amyloid induces apoptosis of neuronal cells by inhibition of the Arg/N-end rule pathway proteolytic activity', *Aging*, 11: 6134-52.

Kedmi, R., N. Ben-Arie, and D. Peer. 2010. 'The systemic toxicity of positively charged lipid nanoparticles and the role of Toll-like receptor 4 in immune activation', *Biomaterials*, 31: 6867-75.

Keeler, A. M., and T. R. Flotte. 2019. 'Recombinant adeno-associated virus gene therapy in light of Luxturna (and Zolgensma and Glybera): where are we, and how did we get here?', *Annu Rev Virol*, 6: 601-21.

Khan, A. A., A. M. Alanazi, M. Jabeen, A. Chauhan, and M. A. Ansari. 2019. 'Therapeutic potential of functionalized siRNA nanoparticles on regression of liver cancer in experimental mice', *Sci Rep*, 9: 15825.

Khvorova, A., A. Reynolds, and S. D. Jayasena. 2003. 'Functional siRNAs and miRNAs exhibit strand bias', *Cell*, 115: 209-16.

Kim, H.-K., R.R. Kim, J.-H. Oh, H. Cho, A. Varshavsky, and C.-S. Hwang. 2014. 'The N-terminal methionine of cellular proteins as a degradation signal.', *Cell,* 156: 158-169.

Kim, J. M., O. H. Seok, S. Ju, J. E. Heo, J. Yeom, D. S. Kim, J. Y. Yoo, A. Varshavsky, C. Lee, and C. S. Hwang. 2018. 'Formyl-methionine as an N-degron of a eukaryotic N-end rule pathway', *Science*, 362.

Kim, S. T., Y. J. Lee, T. Tasaki, J. Hwang, M. J. Kang, E. C. Yi, B. Y. Kim, and Y. T. Kwon. 2018. 'The N-recognin UBR4 of the N-end rule pathway is required for neurogenesis and homeostasis of cell surface proteins', *PLoS One*, 13: e0202260.

Kim, S. T., Y. J. Lee, T. Tasaki, S. R. Mun, J. Hwang, M. J. Kang, S. Ganipisetti, E. C. Yi, B. Y. Kim, and Y. T. Kwon. 2018. 'The N-recognin UBR4 of the N-end rule pathway is targeted to and required for the biogenesis of the early endosome', *Journal of Cell Science*, 131.

Kim, S. T., T. Tasaki, A. Zakrzewska, Y. D. Yoo, K. Sa Sung, S. H. Kim, H. Cha-Molstad, J. Hwang, K. A. Kim, B. Y. Kim, and Y. T. Kwon. 2013. 'The N-end rule proteolytic system in autophagy', *Autophagy*, 9: 1100-3.

Kim, Y., M. Jo, J. Schmidt, X. Luo, T. P. Prakash, T. Zhou, S. Klein, X. Xiao, N. Post, Z. Yin, and A. R. MacLeod. 2019. 'Enhanced potency of GalNAc-conjugated antisense oligonucleotides in hepatocellular cancer models', *Mol Ther*, 27: 1547-57.

Kitamura, K. 2016. 'Inhibition of the Arg/N-end rule pathway-mediated proteolysis by dipeptide-mimetic molecules', *Amino Acids*, 48: 235-43.

Kitazumi, I., and M. Tsukahara. 2011. 'Regulation of DNA fragmentation: the role of caspases and phosphorylation', *FEBS J*, 278: 427-41.

Knodler, L. A., S. M. Crowley, H. P. Sham, H. Yang, M. Wrande, C. Ma, R. K. Ernst, O. Steele-Mortimer, J. Celli, and B. A. Vallance. 2014. 'Noncanonical inflammasome activation of caspase-4/caspase-11 mediates epithelial defenses against enteric bacterial pathogens', *Cell Host Microbe*, 16: 249-56.

Koller, E., T. M. Vincent, A. Chappell, S. De, M. Manoharan, and C. F. Bennett. 2011. 'Mechanisms of single-stranded phosphorothioate modified antisense oligonucleotide accumulation in hepatocytes', *Nucleic Acids Res*, 39: 4795-807.

Komander, D., and M. Rape. 2012. 'The ubiquitin code', *Annu Rev Biochem*, 81: 203-29.

Komarova, Y., and A. B. Malik. 2010. 'Regulation of endothelial permeability via paracellular and transcellular transport pathways', *Annu Rev Physiol*, 72: 463-93.

Koonin, E. V., and L. Aravind. 2002. 'Origin and evolution of eukaryotic apoptosis: the bacterial connection', *Cell Death Differ*, 9: 394-404.

Koyuncu, S., I. Saez, H. J. Lee, R. Gutierrez-Garcia, W. Pokrzywa, A. Fatima, T. Hoppe, and D. Vilchez. 2018. 'The ubiquitin ligase UBR5 suppresses proteostasis collapse in pluripotent stem cells from Huntington's disease patients', *Nat Commun*, 9: 2886.

Kozomara, A., and S. Griffiths-Jones. 2014. 'miRBase: annotating high confidence microRNAs using deep sequencing data', *Nucleic Acids Res*, 42: D68-73.

Kruger, B, J. Mayerle, M. Zenker, and M. M. Lerch. 2009. 'Johanson-blizzard syndrome: pathophysiology of ubiquitin ligase deficiency in pancreatic acinar cells', *Pathology*, 41: 51.

Kumar, S., B. J. van Raam, G. S. Salvesen, and P. Cieplak. 2014. 'Caspase cleavage sites in the human proteome: CaspDB, a database of predicted substrates', *PLoS One*, 9: e110539.

Kumar, V., J. Qin, Y. Jiang, R. G. Duncan, B. Brigham, S. Fishman, J. K. Nair, A. Akinc, S. A. Barros, and P. V. Kasperkovitz. 2014. 'Shielding of Lipid Nanoparticles for siRNA Delivery: Impact on Physicochemical Properties, Cytokine Induction, and Efficacy', *Mol Ther Nucleic Acids*, 3: e210.

Kwak, P. B., and Y. Tomari. 2012. 'The N domain of Argonaute drives duplex unwinding during RISC assembly', *Nat Struct Mol Biol*, 19: 145-51.

Kwon, J., Y. J. Jo, S. Namgoong, and N. H. Kim. 2019. 'Functional roles of hnRNPA2/B1 regulated by METTL3 in mammalian embryonic development', *Sci Rep*, 9: 8640.

Kwon, Y. T., Y. Reiss, V. A. Fried, A. Hershko, J. K. Yoon, D. K. Gonda, P. Sangan, N. G. Copeland, N. A. Jenkins, and A. Varshavsky. 1998. 'The mouse and human genes encoding the recognition component of the N-end rule pathway', *PNAS*, 95: 7898-903.

Kwon, Y. T., Z. Xia, J. Y. An, T. Tasaki, I. V. Davydov, J. W. Seo, J. Sheng, Y. Xie, and A. Varshavsky. 2003. 'Female lethality and apoptosis of spermatocytes in mice lacking the UBR2 ubiquitin ligase of the N-End Rule pathway', *Mol Cell Biol*, 23: 8255-71.

Kwon, Y.T., A.S. Kashina, and A. Varshavsky. 1999. 'Alternative splicing results in differential expression, activity, and localization of the two forms of arginyl-tRNA-protein transferase, a component of the N-end rule pathway.', *Mol Cell Biol*, 19: 182-93.

Kwon, Y.T., F. Levy, and A. Varshavsky. 1999. 'Bivalent inhibitor of the N-end rule pathway.', *J Biol Chem*, 274: 18135-39.

Kwon, Y.T., Z. Xia, I.V. Davydov, S.H. Lecker, and A. Varshavsky. 2001. 'Construction and analysis of mouse strains lacking the ubiquitin ligase UBR1 (E3a) of the N-end rule pathway.', *Mol Cell Biol*, 21: 8007-21.

Kwon, Yong Tae, Anna S. Kashina, Ilia V. Davydov, Rong-Gui Hu, Jee Young An, Jai Wha Seo, Fangyong Du, and Alexander Varshavsky. 2002. 'An essential role of N-terminal arginylation in cardiovascular development', *Science*, 297: 96-99.

Lamkanfi, M., M. Kalai, X. Saelens, W. Declercq, and P. Vandenabeele. 2004. 'Caspase-1 activates nuclear factor of the kappa-enhancer in B cells independently of its enzymatic activity', *J Biol Chem*, 279: 24785-93.

Lamkanfi, M., and T. D. Kanneganti. 2010. 'Caspase-7: a protease involved in apoptosis and inflammation', *Int J Biochem Cell Biol*, 42: 21-4.

Lamkanfi, M., T. D. Kanneganti, P. Van Damme, T. Vanden Berghe, I. Vanoverberghe, J. Vandekerckhove, P. Vandenabeele, K. Gevaert, and G. Nunez. 2008. 'Targeted peptidecentric proteomics reveals caspase-7 as a substrate of the caspase-1 inflammasomes', *Mol & Cell Prot*, 7: 2350-63.

Larsson, E., C. Sander, and D. Marks. 2010. 'mRNA turnover rate limits siRNA and microRNA efficacy', *Mol Syst Biol*, 6: 433.

Lau, P. W., K. Z. Guiley, N. De, C. S. Potter, B. Carragher, and I. J. MacRae. 2012. 'The molecular architecture of human Dicer', *Nat Struct Mol Biol*, 19: 436-40.

Layzer, J. M., A. P. McCaffrey, A. K. Tanner, Z. Huang, M. A. Kay, and B. A. Sullenger. 2004. 'In vivo activity of nuclease-resistant siRNAs', *RNA*, 10: 766-71.

Leboeuf, D., T. Abakumova, T. Prikazchikova, L. Rhym, D. G. Anderson, T. S. Zatsepin, and K. I. Piatkov. 2020. 'Downregulation of the Arg/N-degron Pathway Sensitizes Cancer Cells to Chemotherapy In Vivo', *Mol Ther,* 28: 1092-1104.

Leboeuf, Dominique, Maxim Pyatkov, Timofei S. Zatsepin, and Konstantin Piatkov. 2020. 'The Arg/N-Degron Pathway—A Potential Running Back in Fine-Tuning the Inflammatory Response?', *Biomolecules*, 10: 903.

Lee, H. Y., K. Zhou, A. M. Smith, C. L. Noland, and J. A. Doudna. 2013. 'Differential roles of human Dicer-binding proteins TRBP and PACT in small RNA processing', *Nucleic Acids Res*, 41: 6568-76.

Lee, M. J., K. Pal, T. Tasaki, S. Roy, Y. Jiang, J. Y. An, R. Banerjee, and Y. T. Kwon. 2008. 'Synthetic heterovalent inhibitors targeting recognition E3 components of the N-end rule pathway', *PNAS*, 105: 100-5.

Lee, M.J., D.E. Kim, A. Zakrzewska, Y.D. Yoo, S.H. Kim, S.T. Kim, J.W. Seo, Y.S. Lee, G.W. Dorn, 2nd, U. Oh, B.Y. Kim, and Y.T. Kwon. 2012. 'Characterization of arginylation branch of the N-end rule pathway in G-protein-mediated proliferation and signaling of cardiomyocytes.', *J Biol Chem*, 287: 24043-52.

Lee, Min Jae, Takafumi Tasaki, Kayoko Moroi, Jee Young An, Sadao Kimura, Ilia V. Davydov, and Yong Tae Kwon. 2005. 'RGS4 and RGS5 are in vivo substrates of the N-end rule pathway', *PNAS*, 102: 15030-35.

Lee, P. Y., J. X. Wang, E. Parisini, C. C. Dascher, and P. A. Nigrovic. 2013. 'Ly6 family proteins in neutrophil biology', *J Leukoc Biol*, 94: 585-94.

Lee, Y. S., K. Nakahara, J. W. Pham, K. Kim, Z. He, E. J. Sontheimer, and R. W. Carthew. 2004. 'Distinct roles for Drosophila Dicer-1 and Dicer-2 in the siRNA/miRNA silencing pathways', *Cell*, 117: 69-81.

Leek, J. T. 2014. 'svaseq: removing batch effects and other unwanted noise from sequencing data', *Nucleic Acids Res*, 42.

Leu, Nicolae Adrian, Satoshi Kurosaka, and Anna Kashina. 2009. 'Conditional tek promoter-driven deletion of arginyltransferase in the germ line causes defects in gametogenesis and early embryonic lethality in mice', *PLoS One*, 4: e7734.

Leuschner, F., P. Dutta, R. Gorbatov, T. I. Novobrantseva, J. S. Donahoe, G. Courties, K. M. Lee, J. I. Kim, J. F. Markmann, B. Marinelli, P. Panizzi, W. W. Lee, Y. Iwamoto, S. Milstein, H. Epstein-Barash, W. Cantley, J. Wong, V. Cortez-Retamozo, A. Newton, K. Love, P. Libby, M. J. Pittet, F. K. Swirski, V. Koteliansky, R. Langer, R. Weissleder, D. G. Anderson, and M. Nahrendorf. 2011. 'Therapeutic siRNA silencing in inflammatory monocytes in mice', *Nat Biotechnol*, 29: 1005-10.

Leuschner, P. J., S. L. Ameres, S. Kueng, and J. Martinez. 2006. 'Cleavage of the siRNA passenger strand during RISC assembly in human cells', *EMBO Rep*, 7: 314-20.

Lévy, F., N. Johnsson, T. Rumenapf, and A. Varshavsky. 1996. 'Using ubiquitin to follow the metabolic fate of a protein.', *PNAS. USA*, 93: 4907-12.

Lévy, F., J.A. Johnston, and A. Varshavsky. 1999. 'Analysis of a conditional degradation signal in yeast and mammalian cells', *Eur J of Biochem*, 259: 244-52.

Lewis, B. P., I. H. Shih, M. W. Jones-Rhoades, D. P. Bartel, and C. B. Burge. 2003. 'Prediction of mammalian microRNA targets', *Cell*, 115: 787-98.

Li, Jing, Xuling Wang, Ting Zhang, Chunling Wang, Zhenjun Huang, Xiang Luo, and Yihui Deng. 2015. 'A review on phospholipids and their main applications in drug delivery systems', *Asian J of Pharm Sci*, 10: 81-98.

Li, W., M. H. Bengtson, A. Ulbrich, A. Matsuda, V. A. Reddy, A. Orth, S. K. Chanda, S. Batalov, and C. A. Joazeiro. 2008. 'Genome-wide and functional annotation of human E3 ubiquitin ligases identifies MULAN, a mitochondrial E3 that regulates the organelle's dynamics and signaling', *PLoS One*, 3: e1487.

Liao, L., M. Song, X. Li, L. Tang, T. Zhang, L. Zhang, Y. Pan, L. Chouchane, and X. Ma. 2017. 'E3 Ubiquitin Ligase UBR5 Drives the Growth and Metastasis of Triple-Negative Breast Cancer', *Cancer Res*, 77: 2090-101.

Lin, X. Y., M. S. Choi, and A. G. Porter. 2000. 'Expression analysis of the human caspase-1 subfamily reveals specific regulation of the CASP5 gene by lipopolysaccharide and interferon-gamma', *J Biol Chem*, 275: 39920-6.

Ling, S., and W. C. Lin. 2011. 'EDD inhibits ATM-mediated phosphorylation of p53', *J Biol Chem*, 286: 14972-82.

Liu, J., M. A. Carmell, F. V. Rivas, C. G. Marsden, J. M. Thomson, J. J. Song, S. M. Hammond, L. Joshua-Tor, and G. J. Hannon. 2004. 'Argonaute2 is the catalytic engine of mammalian RNAi', *Science*, 305: 1437-41.

Liu, T., L. Zhang, D. Joo, and S. C. Sun. 2017. 'NF-kappaB signaling in inflammation', *Signal Transduct Target Ther*, 2.

Llave, C., Z. Xie, K. D. Kasschau, and J. C. Carrington. 2002. 'Cleavage of Scarecrow-like mRNA targets directed by a class of Arabidopsis miRNA', *Science*, 297: 2053-6.

Love, K. T., K. P. Mahon, C. G. Levins, K. A. Whitehead, W. Querbes, J. R. Dorkin, J. Qin, W. Cantley, L. L. Qin, T. Racie, M. Frank-Kamenetsky, K. N. Yip, R. Alvarez, D. W. Sah, A. de Fougerolles, K. Fitzgerald, V. Koteliansky, A. Akinc, R. Langer, and D. G. Anderson. 2010. 'Lipid-like materials for low-dose, in vivo gene silencing', *PNAS*, 107: 1864-9.

Love, M. I., W. Huber, and S. Anders. 2014. 'Moderated estimation of fold change and dispersion for RNA-seq data with DESeq2', *Genome Biol*, 15: 550.

Lubini, P., W. Zurcher, and M. Egli. 1994. 'Stabilizing effects of the RNA 2'-substituent: crystal structure of an oligodeoxynucleotide duplex containing 2'-O-methylated adenosines', *Chem Biol*, 1: 39-45.

Luten, J., C. F. van Nostrum, S. C. De Smedt, and W. E. Hennink. 2008. 'Biodegradable polymers as non-viral carriers for plasmid DNA delivery', *J Control Release*, 126: 97-110.

Macrae, I. J., F. Li, K. Zhou, W. Z. Cande, and J. A. Doudna. 2006. 'Structure of Dicer and mechanistic implications for RNAi', *Cold Spring Harb Symp Quant Biol*, 71: 73-80.

MacRae, I. J., K. Zhou, and J. A. Doudna. 2007. 'Structural determinants of RNA recognition and cleavage by Dicer', *Nat Struct Mol Biol*, 14: 934-40.

Mahrus, S., J. C. Trinidad, D. T. Barkan, A. Sali, A. L. Burlingame, and J. A. Wells. 2008. 'Global sequencing of proteolytic cleavage sites in apoptosis by specific labeling of protein N termini', *Cell*, 134: 866-76.

Manoharan, M., A. Akinc, R. K. Pandey, J. Qin, P. Hadwiger, M. John, K. Mills, K. Charisse, M. A. Maier, L. Nechev, E. M. Greene, P. S. Pallan, E. Rozners, K. G. Rajeev, and M. Egli. 2011. 'Unique gene-silencing and structural properties of 2'-fluoro-modified siRNAs', *Angew Chem Int Ed Engl*, 50: 2284-8.

Manoharan, Muthiah. 2004. 'RNA interference and chemically modified small interfering RNAs', *Curr Opin Chem Biol*, 8: 570-79.

Mao, J., Z. Liang, B. Zhang, H. Yang, X. Li, H. Fu, X. Zhang, Y. Yan, W. Xu, and H. Qian. 2017. 'UBR2 enriched in p53 deficient mouse bone marrow mesenchymal stem cell-exosome promoted gastric cancer progression via Wnt/beta-Catenin pathway', *Stem Cells*, 35: 2267-79.

Martinez, J., A. Patkaniowska, H. Urlaub, R. Luhrmann, and T. Tuschl. 2002. 'Single-stranded antisense siRNAs guide target RNA cleavage in RNAi', *Cell*, 110: 563-74.

Martinon, F., K. Burns, and J. Tschopp. 2002. 'The inflammasome: a molecular platform triggering activation of inflammatory caspases and processing of proIL-beta', *Mol Cell*, 10: 417-26.

Martinon, F., and J. Tschopp. 2006. 'Inflammatory caspases and inflammasomes: master switches of inflammation', *Cell Death and Diff*, 14: 10-22.

Matsuda, A., K. Ishiguro, I. K. Yan, and T. Patel. 2019. 'Extracellular vesicle-based therapeutic targeting of beta-catenin to modulate anticancer immune responses in hepatocellular cancer', *Hepatol Commun*, 3: 525-41.

Matsuura, K., N. J. Huang, K. Cocce, L. Zhang, and S. Kornbluth. 2017. 'Downregulation of the proapoptotic protein MOAP-1 by the UBR5 ubiquitin ligase and its role in ovarian cancer resistance to cisplatin', *Oncogene*, 36: 1698-706.

Matta-Camacho, E., G. Kozlov, F.F. Li, and K. Gehring. 2010. 'Structural basis of substrate recognition and specificity in the N-end rule pathway.', *Nat Struct Mol Biol*, 17: 1182-88.

Mattiroli, F., and T. K. Sixma. 2014. 'Lysine-targeting specificity in ubiquitin and ubiquitin-like modification pathways', *Nat Struct Mol Biol*, 21: 308-16.

Mazin, P., J. Xiong, X. Liu, Z. Yan, X. Zhang, M. Li, L. He, M. Somel, Y. Yuan, Y. P. Phoebe Chen, N. Li, Y. Hu, N. Fu, Z. Ning, R. Zeng, H. Yang, W. Chen, M. Gelfand, and P. Khaitovich. 2013. 'Widespread splicing changes in human brain development and aging', *Mol Syst Biol*, 9: 633.

McClorey, Graham, and Subhashis Banerjee. 2018. 'Cell-penetrating peptides to enhance delivery of oligonucleotide-based therapeutics', *Biomedicines*, 6: 51.

Meetei, A. R., J. P. de Winter, A. L. Medhurst, M. Wallisch, Q. Waisfisz, H. J. van de Vrugt, A. B. Oostra, Z. Yan, C. Ling, C. E. Bishop, M. E. Hoatlin, H. Joenje, and W. Wang. 2003. 'A novel ubiquitin ligase is deficient in Fanconi anemia', *Nature Genetics*, 35: 165-70.

Mei, Y., A. A. Hahn, S. Hu, and X. Yang. 2011. 'The USP19 deubiquitinase regulates the stability of c-IAP1 and c-IAP2', *J Biol Chem*, 286: 35380-7.

Meissner, B., R. Kridel, R. S. Lim, S. Rogic, K. Tse, D. W. Scott, R. Moore, A. J. Mungall, M. A. Marra, J. M. Connors, C. Steidl, and R. D. Gascoyne. 2013. 'The E3 ubiquitin ligase UBR5 is recurrently mutated in mantle cell lymphoma', *Blood*, 121: 3161-64.

Meister, G., M. Landthaler, A. Patkaniowska, Y. Dorsett, G. Teng, and T. Tuschl. 2004. 'Human Argonaute2 mediates RNA cleavage targeted by miRNAs and siRNAs', *Mol Cell*, 15: 185-97.

Metkar, S. S., C. Menaa, J. Pardo, B. Wang, R. Wallich, M. Freudenberg, S. Kim, S. M. Raja, L. Shi, M. M. Simon, and C. J. Froelich. 2008. 'Human and mouse granzyme A induce a proinflammatory cytokine response', *Immunity*, 29: 720-33.

Metzger, M. B., V. A. Hristova, and A. M. Weissman. 2012. 'HECT and RING finger families of E3 ubiquitin ligases at a glance', *J Cell Sci*, 125: 531-7.

Moelbert, S., E. Emberly, and C. Tang. 2004. 'Correlation between sequence hydrophobicity and surface-exposure pattern of database proteins', *Protein Sci*, 13: 752-62.

Moelling, K., F. Broecker, and J. E. Kerrigan. 2014. 'RNase H: specificity, mechanisms of action, and antiviral target', *Methods Mol Biol*, 1087: 71-84.

Mogk, A., R. Schmidt, and B. Bukau. 2007. 'The N-end rule pathway for regulated proteolysis: prokaryotic and eukaryotic strategies', *Trends Cell Biol*, 17: 165-72.

Mohamed, M., A. S. Abu Lila, T. Shimizu, E. Alaaeldin, A. Hussein, H. A. Sarhan, J. Szebeni, and T. Ishida. 2019. 'PEGylated liposomes: immunological responses', *Sci Technol Adv Mater*, 20: 710-24.

Monteith, A. J., H. A. Vincent, S. Kang, P. Li, T. M. Claiborne, Z. Rajfur, K. Jacobson, N. J. Moorman, and B. J. Vilen. 2018. 'mTORC2 activity disrupts lysosome acidification in systemic lupus erythematosus by impairing caspase-1 cleavage of Rab39a', *J of Immun*, 201: 371-82.

Montgomery, M. K., S. Xu, and A. Fire. 1998. 'RNA as a target of double-stranded RNA-mediated genetic interference in Caenorhabditis elegans', *PNAS. USA*, 95: 15502-7.

Morchikh, M., A. Cribier, R. Raffel, S. Amraoui, J. Cau, D. Severac, E. Dubois, O. Schwartz, Y. Bennasser, and M. Benkirane. 2017. 'HEXIM1 and NEAT1 long non-coding RNA form a multi-subunit complex that regulates DNA-mediated innate immune response', *Mol Cell*, 67: 387-99 e5.

Mou, Q., Y. Ma, F. Ding, X. Gao, D. Yan, X. Zhu, and C. Zhang. 2019. 'Two-in-one chemogene assembled from drug-integrated antisense oligonucleotides to reverse chemoresistance', *J Am Chem Soc*, 141: 6955-66.

Mukhopadhyay, D., and H. Riezman. 2007. 'Proteasome-independent functions of ubiquitin in endocytosis and signaling', *Science*, 315: 201-05.

Munday, N. A., J. P. Vaillancourt, A. Ali, F. J. Casano, D. K. Miller, S. M. Molineaux, T. T. Yamin, V. L. Yu, and D. W. Nicholson. 1995. 'Molecular cloning and pro-apoptotic activity of ICErelII and

ICErelIII, members of the ICE/CED-3 family of cysteine proteases', *J Biol Chem*, 270: 15870-6.

Munoz-Pinedo, C. 2012. 'Signaling pathways that regulate life and cell death: evolution of apoptosis in the context of self-defense', *Adv Exp Med Biol*, 738: 124-43.

Murchison, E. P., J. F. Partridge, O. H. Tam, S. Cheloufi, and G. J. Hannon. 2005. 'Characterization of Dicer-deficient murine embryonic stem cells', *PNAS. USA*, 102: 12135-40.

Nair, Jayaprakash K., Jennifer L. S. Willoughby, Amy Chan, Klaus Charisse, Md Rowshon Alam, Qianfan Wang, Menno Hoekstra, Pachamuthu Kandasamy, Alexander V. Kel'in, Stuart Milstein, Nate Taneja, Jonathan O'Shea, Sarfraz Shaikh, Ligang Zhang, Ronald J. van der Sluis, Michael E. Jung, Akin Akinc, Renta Hutabarat, Satya Kuchimanchi, Kevin Fitzgerald, Tracy Zimmermann, Theo J. C. van Berkel, Martin A. Maier, Kallanthottathil G. Rajeev, and Muthiah Manoharan. 2014. 'Multivalent N-Acetylgalactosamine-conjugated siRNA localizes in hepatocytes and elicits robust RNAi-mediated gene silencing', *J Am Chem Soc*, 136: 16958-61.

Nakanishi, K. 2016. 'Anatomy of RISC: how do small RNAs and chaperones activate Argonaute proteins?', *Wiley Interdiscip Rev RNA*, 7: 637-60.

Nakanishi, K., D. E. Weinberg, D. P. Bartel, and D. J. Patel. 2012. 'Structure of yeast Argonaute with guide RNA', *Nature*, 486: 368-74.

Nakayama, K. I., and K. Nakayama. 2006. 'Ubiquitin ligases: cell-cycle control and cancer', *Nat Rev Cancer*, 6: 369-81.

Nguyen, K. T., C. S. Lee, S. H. Mun, N. T. Truong, S. K. Park, and C. S. Hwang. 2019. 'N-terminal acetylation and the N-end rule pathway control degradation of the lipid droplet protein PLIN2', *J Biol Chem*, 294: 379-88.

Nguyen, K. T., S. H. Mun, C. S. Lee, and C. S. Hwang. 2018. 'Control of protein degradation by N-terminal acetylation and the N-end rule pathway', *Exp Mol Med*, 50: 91.

Ni, L., and J. Lu. 2018. 'Interferon gamma in cancer immunotherapy', *Cancer Med*, 7: 4509-16.

Noland, C. L., E. Ma, and J. A. Doudna. 2011. 'siRNA repositioning for guide strand selection by human Dicer complexes', *Mol Cell*, 43: 110-21.

Novobrantseva, T. I., A. Borodovsky, J. Wong, B. Klebanov, M. Zafari, K. Yucius, W. Querbes, P. Ge, V. M. Ruda, S. Milstein, L. Speciner, R. Duncan, S. Barros, G. Basha, P. Cullis, A. Akinc, J. S. Donahoe, K. Narayanannair Jayaprakash, M. Jayaraman, R. L. Bogorad, K. Love, K. Whitehead, C. Levins, M. Manoharan, F. K. Swirski, R. Weissleder, R. Langer, D. G. Anderson, A. de Fougerolles, M. Nahrendorf, and V. Koteliansky. 2012. 'Systemic RNAi-mediated gene silencing in nonhuman primate and rodent myeloid cells', *Mol Ther Nucleic Acids*, 1: e4.

Nurgali, K., R. T. Jagoe, and R. Abalo. 2018. 'Editorial: Adverse effects of cancer chemotherapy: anything new to improve tolerance and reduce sequelae?', *Front Pharmacol*, 9: 245.

O'Brien, P. M., M. J. Davies, J. P. Scurry, A. N. Smith, C. A. Barton, M. J. Henderson, D. N. Saunders, B. S. Gloss, K. I. Patterson, J. L. Clancy, V. A. Heinzelmann-Schwarz, R. Murali, R. A. Scolyer,

Y. Zeng, E. D. Williams, L. Scurr, A. Defazio, D. I. Quinn, C. K. Watts, N. F. Hacker, S. M. Henshall, and R. L. Sutherland. 2008. 'The E3 ubiquitin ligase EDD is an adverse prognostic factor for serous epithelial ovarian cancer and modulates cisplatin resistance in vitro', *British J Cancer*, 98: 1085-93.

Oberst, A., C. Bender, and D. R. Green. 2008. 'Living with death: the evolution of the mitochondrial pathway of apoptosis in animals', *Cell Death Differ*, 15: 1139-46.

Olejniczak, S. H., G. La Rocca, J. J. Gruber, and C. B. Thompson. 2013. 'Long-lived microRNA-Argonaute complexes in quiescent cells can be activated to regulate mitogenic responses', *PNAS. USA*, 110: 157-62.

Ong, S. S., A. N. Goktug, A. Elias, J. Wu, D. Saunders, and T. Chen. 2014. 'Stability of the human pregnane X receptor is regulated by E3 ligase UBR5 and serine/threonine kinase DYRK2', *Biochem J*, 459: 193-203.

Ooe, A., K. Kato, and S. Noguchi. 2007. 'Possible involvement of CCT5, RGS3, and YKT6 genes up-regulated in p53-mutated tumors in resistance to docetaxel in human breast cancers', *Breast Cancer Res Treat*, 101: 305-15.

Orban, T. I., and E. Izaurralde. 2005. 'Decay of mRNAs targeted by RISC requires XRN1, the Ski complex, and the exosome', *RNA*, 11: 459-69.

Ortega-Gómez, Almudena, Mauro Perretti, and Oliver Soehnlein. 2013. 'Resolution of inflammation: an integrated view', *EMBO Molecular Medicine*, 5: 661-74.

Panigrahi, B., R. K. Singh, S. Mishra, and D. Mandal. 2018. 'Cyclic peptide-based nanostructures as efficient siRNA carriers', *Artif Cells Nanomed Biotechnol*, 46: S763-S73.

Parhar, K., S. Eivemark, K. Assi, A. Gomez-Munoz, A. Yee, and B. Salh. 2007. 'Investigation of interleukin 1beta-mediated regulation of NF-kappaB activation in colonic cells reveals divergence between PKB and PDK-transduced events', *Mol Cell Biochem*, 300: 113-27.

Park, J. H., and C. Shin. 2015. 'Slicer-independent mechanism drives small-RNA strand separation during human RISC assembly', *Nucleic Acids Res*, 43: 9418-33.

Park, S. E., J. M. Kim, O. H. Seok, H. Cho, B. Wadas, S. Y. Kim, A. Varshavsky, and C. S. Hwang. 2015. 'Control of mammalian G protein signaling by N-terminal acetylation and the N-end rule pathway', *Science*, 347: 1249-52.

Parker, J. S., S. M. Roe, and D. Barford. 2005. 'Structural insights into mRNA recognition from a PIWI domain-siRNA guide complex', *Nature*, 434: 663-6.

Peacock, H., R. V. Fucini, P. Jayalath, J. M. Ibarra-Soza, H. J. Haringsma, W. M. Flanagan, A. Willingham, and P. A. Beal. 2011. 'Nucleobase and ribose modifications control immunostimulation by a microRNA-122-mimetic RNA', *J Am Chem Soc*, 133: 9200-3.

Peacock, H., A. Kannan, P. A. Beal, and C. J. Burrows. 2011. 'Chemical modification of siRNA bases to probe and enhance RNA interference', *J Org Chem*, 76: 7295-300.

Pei, Yi, and Thomas Tuschl. 2006. 'On the art of identifying effective and specific siRNAs', *Nature Methods*, 3: 670-76.

Personeni, N., T. Pressiani, A. Santoro, and L. Rimassa. 2018. 'Regorafenib in hepatocellular carcinoma: latest evidence and clinical implications', *Drugs Context*, 7: 212533.

Piatkov, K., L. Colnaghi, M. Bekes, A. Varshavsky, and T. Huang. 2012. 'The auto-generated fragment of the Usp1 deubiquitylase Is a physiological substrate of the N-end rule pathway.', *Mol Cell*, 48: 926-33.

Piatkov, K. I., C. S. Brower, and A. Varshavsky. 2012. 'The N-end rule pathway counteracts cell death by destroying proapoptotic protein fragments', *PNAS*, 109: E1839-E47.

Piatkov, K. I., J. H. Oh, Y. Liu, and A. Varshavsky. 2014. 'Calpain-generated natural protein fragments as short-lived substrates of the N-end rule pathway', *PNAS*, 111: E817-26.

Piatkov, K. I., T. T. Vu, C. S. Hwang, and A. Varshavsky. 2015. 'Formyl-methionine as a degradation signal at the N-termini of bacterial proteins', *Microb Cell*, 2: 376-93.

Pop, C., and G.S. Salvesen. 2009. 'Human caspases: activation, specificity, and regulation.', *J Biol Chem*, 284: 21777-81.

Prakash, Thazha P., Mark J. Graham, Jinghua Yu, Rick Carty, Audrey Low, Alfred Chappell, Karsten Schmidt, Chenguang Zhao, Mariam Aghajan, Heather F. Murray, Stan Riney, Sheri L. Booten, Susan F. Murray, Hans Gaus, Jeff Crosby, Walt F. Lima, Shuling Guo, Brett P. Monia, Eric E. Swayze, and Punit P. Seth. 2014. 'Targeted delivery of antisense oligonucleotides to hepatocytes using triantennaryN-acetyl galactosamine improves potency 10-fold in mice', *Nuc Acids Res*, 42: 8796-807.

R Core Team. 2013. 'R: A language and environment for statistical computing. R Foundation for Statistical Computing, Vienna, Austria.'.

Radzicka, Anna, and Richard Wolfenden. 2002. 'Comparing the polarities of the amino acids: side-chain distribution coefficients between the vapor phase, cyclohexane, 1-octanol, and neutral aqueous solution', *Biochemistry*, 27: 1664-70.

Rageul, Julie, Jennifer J. Park, Ukhyun Jo, Alexandra S. Weinheimer, Tri T. M. Vu, and Hyungjin Kim. 2019. 'Conditional degradation of SDE2 by the Arg/N-End rule pathway regulates stress response at replication forks', *Nucleic Acids Res*, 47: 3996-4010.

Rao, H., F. Uhlmann, K. Nasmyth, and A. Varshavsky. 2001. 'Degradation of a cohesin subunit by the N-end rule pathway is essential for chromosome stability', *Nature*, 410: 955-9.

Rawla, P., T. Sunkara, P. Muralidharan, and J. P. Raj. 2018. 'Update in global trends and aetiology of hepatocellular carcinoma', *Contemp Oncol (Pozn)*, 22: 141-50.

Rawlings, N. D., A. J. Barrett, and R. Finn. 2016. 'Twenty years of the MEROPS database of proteolytic enzymes, their substrates and inhibitors', *Nucleic Acids Res*, 44: D343-50.

Ray, K. K., R. S. Wright, D. Kallend, W. Koenig, L. A. Leiter, F. J. Raal, J. A. Bisch, T. Richardson, M. Jaros, P. L. J. Wijngaard, J. J. P. Kastelein, Orion, and Orion- Investigators. 2020. 'Two phase 3 trials of Inclisiran in patients with elevated LDL cholesterol', *N Eng J Med,* 382: 1507-1519.

Ree, R., S. Varland, and T. Arnesen. 2018. 'Spotlight on protein N-terminal acetylation', *Exp Mol Med*, 50: 90.

Reiss, Y., and A. Hershko. 1990. 'Affinity purification of ubiquitin-protein ligase on immobilized protein substrates. Evidence for the existence of separate NH2-terminal binding sites on a single enzyme', *J Biol Chem*, 265: 3685-90.

Reiss, Y., D. Kaim, and A. Hershko. 1988. 'Specificity of binding of N-terminal residues of proteins to ubiquitin-protein ligase. Use of amino acid derivatives to characterize specific binding sites.', *J Biol Chem*, 263: 2693-98.

Ren, M., Q. Guo, L. Guo, M. Lenz, F. Qian, R. R. Koenen, H. Xu, A. B. Schilling, C. Weber, R. D. Ye, A. R. Dinner, and W. J. Tang. 2010. 'Polymerization of MIP-1 chemokine (CCL3 and CCL4) and clearance of MIP-1 by insulin-degrading enzyme', *EMBO J*, 29: 3952-66.

Reynolds, A., D. Leake, Q. Boese, S. Scaringe, W. S. Marshall, and A. Khvorova. 2004. 'Rational siRNA design for RNA interference', *Nat Biotechnol*, 22: 326-30.

Rezvantalab, S., N. I. Drude, M. K. Moraveji, N. Guvener, E. K. Koons, Y. Shi, T. Lammers, and F. Kiessling. 2018. 'PLGA-based nanoparticles in cancer treatment', *Front Pharmacol*, 9: 1260.

Rivas, F. V., N. H. Tolia, J. J. Song, J. P. Aragon, J. Liu, G. J. Hannon, and L. Joshua-Tor. 2005. 'Purified Argonaute2 and an siRNA form recombinant human RISC', *Nat Struct Mol Biol*, 12: 340-9.

Robertson, S. E., J. D. Young, S. Kitson, A. Pitt, J. Evans, J. Roes, D. Karaoglu, L. Santora, T. Ghayur, F. Y. Liew, J. A. Gracie, and I. B. McInnes. 2006. 'Expression and alternative processing of IL-18 in human neutrophils', *Eur J Immunol*, 36: 722-31.

Ruda, V. M., R. Chandwani, A. Sehgal, R. L. Bogorad, A. Akinc, K. Charisse, A. Tarakhovsky, T. I. Novobrantseva, and V. Koteliansky. 2014. 'The roles of individual mammalian argonautes in RNA interference in vivo', *PLoS One*, 9: e101749.

Saha, S., and A. Kashina. 2011. 'Posttranslational arginylation as a global biological regulator.', *Dev. Biol.*, 358: 1-8.

Saha, S., J. Wang, B. Buckley, Q. Wang, B. Lilly, M. Chernov, and A. Kashina. 2012. 'Small molecule inhibitors of arginyltransferase regulate arginylation-dependent protein degradation, cell motility, and angiogenesis', *Biochem pharm*, 83: 866-73.

Saputra, E. C., L. Huang, Y. Chen, and L. Tucker-Kellogg. 2018. 'Combination Therapy and the Evolution of Resistance: The theoretical merits of synergism and antagonism in cancer', *Cancer Res*, 78: 2419-31.

Saraswathy, Manju, and Shaoqin Gong. 2014. 'Recent developments in the co-delivery of siRNA and small molecule anticancer drugs for cancer treatment', *Materials Today*, 17: 298-306.

Sasaki, T., H. Kojima, R. Kishimoto, A. Ikeda, H. Kunimoto, and K. Nakajima. 2006. 'Spatiotemporal regulation of c-Fos by ERK5 and the E3 ubiquitin ligase UBR1, and its biological role', *Mol Cell*, 24: 63-75.

Sato, Y., H. Matsui, N. Yamamoto, R. Sato, T. Munakata, M. Kohara, and H. Harashima. 2017. 'Highly specific delivery of siRNA to hepatocytes circumvents endothelial cell-mediated lipid nanoparticle-associated toxicity leading to the safe and efficacious decrease in the hepatitis B virus', *J Control Release*, 266: 216-25.

Saunders, D. N., S. L. Hird, S. L. Withington, S. L. Dunwoodie, M. J. Henderson, C. Biben, R. L. Sutherland, C. J. Ormandy, and C. K. Watts. 2004. 'Edd, the murine hyperplastic disc gene, is essential for yolk sac vascularization and chorioallantoic fusion', *Mol Cell Biol*, 24: 7225-34.

Schauer, S. E., S. E. Jacobsen, D. W. Meinke, and A. Ray. 2002. 'DICER-LIKE1: blind men and elephants in Arabidopsis development', *Trends Plant Sci*, 7: 487-91.

Schechter, I., and A. Berger. 1967. 'On the size of the active site in proteases. I. Papain', *Biochem Biophys Res Commun*, 27: 157-62.

Scheinman, R. I., R. Trivedi, S. Vermillion, and U. B. Kompella. 2011. 'Functionalized STAT1 siRNA nanoparticles regress rheumatoid arthritis in a mouse model', *Nanomed*, 6: 1669-82.

Schellekens, H., W. E. Hennink, and V. Brinks. 2013. 'The immunogenicity of polyethylene glycol: facts and fiction', *Pharm Res*, 30: 1729-34.

Schirle, N. T., J. Sheu-Gruttadauria, and I. J. MacRae. 2014. 'Structural basis for microRNA targeting', *Science*, 346: 608-13.

Schubert, S., A. Grunweller, V. A. Erdmann, and J. Kurreck. 2005. 'Local RNA target structure influences siRNA efficacy: systematic analysis of intentionally designed binding regions', *J Mol Biol*, 348: 883-93.

Schwarz, D. S., Y. Tomari, and P. D. Zamore. 2004. 'The RNA-induced silencing complex is a Mg2+-dependent endonuclease', *Curr. Biol.*, 14: 787-91.

Scott, D. C., J. K. Monda, E. J. Bennett, J. W. Harper, and B. A. Schulman. 2011. 'N-Terminal acetylation acts as an avidity enhancer within an interconnected multiprotein complex', *Science*, 334: 674-78.

Scott, L. J. 2020. 'Givosiran: First Approval', *Drugs*, 80: 335-39.

Seaman, J. E., O. Julien, P. S. Lee, T. J. Rettenmaier, N. D. Thomsen, and J. A. Wells. 2016. 'Cacidases: caspases can cleave after aspartate, glutamate and phosphoserine residues', *Cell Death Differ*, 23: 1717-26.

Selvam, C., D. Mutisya, S. Prakash, K. Ranganna, and R. Thilagavathi. 2017. 'Therapeutic potential of chemically modified siRNA: Recent trends', *Chem Biol Drug Des*, 90: 665-78.

Seong, H. A., H. Jung, H. S. Choi, K. T. Kim, and H. Ha. 2005. 'Regulation of transforming growth factor-beta signaling and PDK1 kinase activity by physical interaction between PDK1 and serine-threonine kinase receptor-associated protein', *J Biol Chem*, 280: 42897-908.

Seong, H. A., H. Jung, K. T. Kim, and H. Ha. 2007. '3-Phosphoinositide-dependent PDK1 negatively regulates transforming growth factor-beta-induced signaling in a kinase-dependent manner through physical interaction with Smad proteins', *J Biol Chem*, 282: 12272-89.

Shannahan, J. H., W. Bai, and J. M. Brown. 2015. 'Implications of scavenger receptors in the safe development of nanotherapeutics', *Receptors Clin Investig*, 2: e811.

Shao, W., G. Yeretssian, K. Doiron, S. N. Hussain, and M. Saleh. 2007. 'The caspase-1 digestome identifies the glycolysis pathway as a target during infection and septic shock', *J Biol Chem*, 282: 36321-9.

Sharma, D., and T. D. Kanneganti. 2016. 'The cell biology of inflammasomes: Mechanisms of inflammasome activation and regulation', *J Cell Biol*, 213: 617-29.

Sharma, V. K., M. F. Osborn, M. R. Hassler, D. Echeverria, S. Ly, E. A. Ulashchik, Y. V. Martynenko-Makaev, V. V. Shmanai, T. S. Zatsepin, A. Khvorova, and J. K. Watts. 2018. 'Novel cluster and monomer-based GalNAc structures induce effective uptake of siRNAs in vitro and in vivo', *Bioconjug Chem*, 29: 2478-88.

Shearer, R. F., M. Iconomou, C. K. Watts, and D. N. Saunders. 2015. 'Functional roles of the E3 ubiquitin ligase UBR5 in cancer', *Mol Cancer Res*, 13: 1523-32.

Shemorry, A., C.-S. Hwang, and A Varshavsky. 2013. 'Control of protein quality and stoichiometries by N-terminal acetylation and the N-end rule pathway.', *Mol Cell*, 50: 540-51.

Shen, B., and H. M. Goodman. 2004. 'Uridine addition after microRNA-directed cleavage', *Science*, 306: 997.

Shen, J., Y. Yin, J. Mai, X. Xiong, M. Pansuria, J. Liu, E. Maley, N. U. Saqib, H. Wang, and X. F. Yang. 2010. 'Caspase-1 recognizes extended cleavage sites in its natural substrates', *Atherosclerosis*, 210: 422-9.

Sheng, J., A. Kumagai, W.G. Dunphy, and A. Varshavsky. 2002. 'Dissection of c-MOS degron.', *EMBO J.*, 21: 6061-71.

Shi, J., and L. Wei. 2007. 'Rho kinase in the regulation of cell death and survival', *Arch Immunol Ther Exp (Warsz)*, 55: 61-75.

Shi, J., Y. Zhao, Y. Wang, W. Gao, J. Ding, P. Li, L. Hu, and F. Shao. 2014. 'Inflammatory caspases are innate immune receptors for intracellular LPS', *Nature*, 514: 187-92.

Shieh, J. M., C. J. Shen, W. C. Chang, H. C. Cheng, Y. Y. Chan, W. C. Huang, W. C. Chang, and B. K. Chen. 2014. 'An increase in reactive oxygen species by deregulation of ARNT enhances chemotherapeutic drug-induced cancer cell death', *PLoS One*, 9: e99242.

Shimizu, K., S. Yamasaki, M. Sakurai, N. Yumoto, M. Ikeda, C. Mishima-Tsumagari, M. Kukimoto-Niino, T. Watanabe, M. Kawamura, M. Shirouzu, and S. I. Fujii. 2019. 'Granzyme A stimulates pDCs to promote adaptive immunity via induction of type I IFN', *Front Immunol*, 10: 1450.

Shirako, Y., and J.H. Strauss. 1998. 'Requirement for an aromatic amino acid or histidine at the N terminus of Sindbis virus RNA polymerase', *Journal of Virology*, 72: 2310-5.

Sigoillot, F. D., and R. W. King. 2011. 'Vigilance and validation: Keys to success in RNAi screening', *ACS Chem Biol*, 6: 47-60.

Singh, A., P. Trivedi, and N. K. Jain. 2018. 'Advances in siRNA delivery in cancer therapy', *Artif Cells Nanomed Biotechnol*, 46: 274-83.

Singh, T., A. S. N. Murthy, H. J. Yang, and J. Im. 2018. 'Versatility of cell-penetrating peptides for intracellular delivery of siRNA', *Drug Deliv*, 25: 1996-2006.

Sioud, M. 2005. 'Induction of inflammatory cytokines and interferon responses by double-stranded and single-stranded siRNAs is sequence-dependent and requires endosomal localization', *J Mol Biol*, 348: 1079-90.

Sipa, K., E. Sochacka, J. Kazmierczak-Baranska, M. Maszewska, M. Janicka, G. Nowak, and B. Nawrot. 2007. 'Effect of base modifications on structure, thermodynamic stability, and gene silencing activity of short interfering RNA', *RNA*, 13: 1301-16.

Skonieczna, M., D. Hudy, T. Hejmo, R. J. Buldak, M. Adamiec, and M. Kukla. 2019. 'The adipokine vaspin reduces apoptosis in human hepatocellular carcinoma (Hep-3B) cells, associated with lower levels of NO and superoxide anion', *BMC Pharmacol Toxicol*, 20: 58.

Soffer, R.L. 1980. 'Biochemistry and biology of aminoacyl-tRNA-protein transferases.' in D. Söll, J. Abelson and P.R. Schimmel (eds.), *Transfer RNA: Biological Aspects.*

Sollberger, G., G. E. Strittmatter, M. Kistowska, L. E. French, and H. D. Beer. 2012. 'Caspase-4 is required for activation of inflammasomes', *J of Immun*, 188: 1992-2000.

Somoza, A., A. P. Silverman, R. M. Miller, J. Chelliserrykattil, and E. T. Kool. 2008. 'Steric effects in RNA interference: probing the influence of nucleobase size and shape', *Chemistry*, 14: 7978-87.

Song, J. J., S. K. Smith, G. J. Hannon, and L. Joshua-Tor. 2004. 'Crystal structure of Argonaute and its implications for RISC slicer activity', *Science*, 305: 1434-7.

Sorel, Maud, Brian Mooney, Rémi Marchi, and Emmanuelle Graciet. 2019. 'Ubiquitin/Proteasome System in Plant Pathogen Responses': 65-116.

Spiers, L., N. Coupe, and M. Payne. 2019. 'Toxicities associated with checkpoint inhibitors-an overview', *Rheumatology (Oxford)*, 58: vii7-vii16.

Sriram, S., J. H. Lee, B. K. Mai, Y. Jiang, Y. Kim, Y. D. Yoo, R. Banerjee, S. H. Lee, and M. J. Lee. 2013. 'Development and characterization of monomeric N-end rule inhibitors through in vitro model substrates', *J. Med. Chem.*, 56: 2540-6.

Sriram, S. M., B. Y. Kim, and Y. T. Kwon. 2011. 'The N-end rule pathway: emerging functions and molecular principles of substrate recognition', *Nat Rev Mol Cell Biol*, 12: 735-47.

Sriram, S. M., and Y. T. Kwon. 2010. 'The molecular principles of N-end rule recognition', *Nat Struct Mol Biol*, 17: 1164-5.

Steer, C. J., and G. Ashwell. 1980. 'Studies on a mammalian hepatic binding protein specific for asialoglycoproteins. Evidence for receptor recycling in isolated rat hepatocytes', *J Biol Chem*, 255: 3008-13.

Steinborn, B., I. Truebenbach, S. Morys, U. Lachelt, E. Wagner, and W. Zhang. 2018. 'Epidermal growth factor receptor targeted methotrexate and small interfering RNA co-delivery', *J Gene Med*, 20: e3041.

Stennicke, H. R., M. Renatus, M. Meldal, and G. S. Salvesen. 2000. 'Internally quenched fluorescent peptide substrates disclose the subsite preferences of human caspases 1, 3, 6, 7 and 8', *Biochem J*, 350 Pt 2: 563-8.

Stewart, M. D., T. Ritterhoff, R. E. Klevit, and P. S. Brzovic. 2016. 'E2 enzymes: more than just middle men', *Cell Res*, 26: 423-40.

Sugimoto, MA, LP Sousa, V Pinho, M Perretti, and MM Teixeira. 2016. 'Resolution of inflammation: What controls its onset?', *Front Immunol*, 7.

Sultana, R., M. A. Theodoraki, and A. J. Caplan. 2012. 'UBR1 promotes protein kinase quality control and sensitizes cells to Hsp90 inhibition', *Exp Cell Res*, 318: 53-60.

Sun, C., Y. Sun, D. Jiang, G. Bao, X. Zhu, D. Xu, Y. Wang, and Z. Cui. 2017. 'PDK1 promotes the inflammatory progress of fibroblast-like synoviocytes by phosphorylating RSK2', *Cell Immunol*, 315: 27-33.

Sun, L., and Z. J. Chen. 2004. 'The novel functions of ubiquitination in signaling', *Curr Opin Cell Biol*, 16: 119-26.

Suzuki, H. I., A. Katsura, T. Yasuda, T. Ueno, H. Mano, K. Sugimoto, and K. Miyazono. 2015. 'Small-RNA asymmetry is directly driven by mammalian Argonautes', *Nat Struct Mol Biol*, 22: 512-21.

Szalmas, A., V. Tomaic, O. Basukala, P. Massimi, S. Mittal, J. Konya, and L. Banks. 2017. 'The PTPN14 Tumor Suppressor Is a Degradation Target of Human Papillomavirus E7', *Journal of Virology*, 91.

Tabernero, J., G. I. Shapiro, P. M. LoRusso, A. Cervantes, G. K. Schwartz, G. J. Weiss, L. Paz-Ares, D. C. Cho, J. R. Infante, M. Alsina, M. M. Gounder, R. Falzone, J. Harrop, A. C. White, I. Toudjarska, D. Bumcrot, R. E. Meyers, G. Hinkle, N. Svrzikapa, R. M. Hutabarat, V. A. Clausen, J. Cehelsky, S. V. Nochur, C. Gamba-Vitalo, A. K. Vaishnaw, D. W. Sah, J. A. Gollob, and H. A. Burris, 3rd. 2013. 'First-in-humans trial of an RNA interference therapeutic targeting VEGF and KSP in cancer patients with liver involvement', *Cancer Discov*, 3: 406-17.

Takahashi, M., H. Mukai, M. Toshimori, M. Miyamoto, and Y. Ono. 1998. 'Proteolytic activation of PKN by caspase-3 or related protease during apoptosis', *PNAS. USA*, 95: 11566-71.

Takenouchi, T., M. Tsukimoto, Y. Iwamaru, S. Sugama, K. Sekiyama, M. Sato, S. Kojima, M. Hashimoto, and H. Kitani. 2015. 'Extracellular ATP induces unconventional release of glyceraldehyde-3-phosphate dehydrogenase from microglial cells', *Immunol Lett*, 167: 116-24.

Tang, X., J. Rao, S. Yin, J. Wei, C. Xia, M. Li, L. Mei, Z. Zhang, and Q. He. 2019. 'PD-L1 knockdown via hybrid micelle promotes paclitaxel induced Cancer-Immunity Cycle for melanoma treatment', *Eur J Pharm Sci*, 127: 161-74.

Tasaki, T., S. T. Kim, A. Zakrzewska, B. E. Lee, M. J. Kang, Y. D. Yoo, H. J. Cha-Molstad, J. Hwang, N. K. Soung, K. S. Sung, S. H. Kim, M. D. Nguyen, M. Sun, E. C. Yi, B. Y. Kim, and Y. T. Kwon. 2013. 'UBR box N-recognin-4 (UBR4), an N-recognin of the N-end rule pathway, and its role in yolk sac vascular development and autophagy', *PNAS*, 110: 3800-5.

Tasaki, T., and Y. T. Kwon. 2007. 'The mammalian N-end rule pathway: new insights into its components and physiological roles', *Trends in Biochemical Sciences*, 32: 520-8.

Tasaki, T., L. C. F. Mulder, A. Iwamatsu, M. J. Lee, I. V. Davydov, A. Varshavsky, M. Muesing, and Y. T. Kwon. 2005. 'A family of mammalian E3 ubiquitin ligases that contain the UBR box motif and recognize N-degrons', *Mol Cell Biol*, 25: 7120-36.

Tasaki, T., S. M. Sriram, K. S. Park, and Y. T. Kwon. 2012. 'The N-end rule pathway', *Annu Rev Biochem*, 81: 261-89.

Tasaki, T., A. Zakrzewska, D. D. Dudgeon, Y. Jiang, J. S. Lazo, and Y. T. Kwon. 2009. 'The substrate recognition domains of the N-end rule pathway', *J Biol Chem*, 284: 1884-95.

Terrazas, M., and E. T. Kool. 2009. 'RNA major groove modifications improve siRNA stability and biological activity', *Nucleic Acids Res*, 37: 346-53.

The UniProt Consortium. 2017. 'UniProt: the universal protein knowledgebase', *Nucleic Acids Res*, 45: D158-D69.

Thinon, E., R. A. Serwa, M. Broncel, J. A. Brannigan, U. Brassat, M. H. Wright, W. P. Heal, A. J. Wilkinson, D. J. Mann, and E. W. Tate. 2014. 'Global profiling of co- and post-translationally N-myristoylated proteomes in human cells', *Nat Commun*, 5: 4919.

Thomas, P. D., D. P. Hill, H. Mi, D. Osumi-Sutherland, K. Van Auken, S. Carbon, J. P. Balhoff, L. P. Albou, B. Good, P. Gaudet, S. E. Lewis, and C. J. Mungall. 2019. 'Gene Ontology Causal Activity Modeling (GO-CAM) moves beyond GO annotations to structured descriptions of biological functions and systems', *Nat Genetics*, 51: 1429-33.

Thorn, Caroline F., Connie Oshiro, Sharon Marsh, Tina Hernandez-Boussard, Howard McLeod, Teri E. Klein, and Russ B. Altman. 2011. 'Doxorubicin pathways', *Pharmacogenet and Genom*, 21: 440-46.

Thornberry, N. A., and Y. Lazebnik. 1998. 'Caspases: enemies within', *Science*, 281: 1312-6.

Timmer, J. C., W. Zhu, C. Pop, T. Regan, S. J. Snipas, A. M. Eroshkin, S. J. Riedl, and G. S. Salvesen. 2009. 'Structural and kinetic determinants of protease substrates', *Nat Struct Mol Biol*, 16: 1101-8.

Timms, R. T., Z. Zhang, D. Y. Rhee, J. W. Harper, I. Koren, and S. J. Elledge. 2019. 'A glycine-specific N-degron pathway mediates the quality control of protein N-myristoylation', *Science*, 365.

Tobias, J.W., T.E. Shrader, G. Rocap, and A. Varshavsky. 1991. 'The N-end rule in bacteria.', *Science*, 254: 1374-77.

Tomari, Y., C. Matranga, B. Haley, N. Martinez, and P. D. Zamore. 2004. 'A protein sensor for siRNA asymmetry', *Science*, 306: 1377-80.

Turgeon, D., J. S. Carrier, E. Levesque, D. W. Hum, and A. Belanger. 2001. 'Relative enzymatic activity, protein stability, and tissue distribution of human steroid-metabolizing UGT2B subfamily members', *Endocrinology*, 142: 778-87.

Tuschl, T., P. D. Zamore, R. Lehmann, D. P. Bartel, and P. A. Sharp. 1999. 'Targeted mRNA degradation by double-stranded RNA in vitro', *Genes and Development*, 13: 3191-7.

Tward, A. D., K. D. Jones, S. Yant, S. T. Cheung, S. T. Fan, X. Chen, M. A. Kay, R. Wang, and J. M. Bishop. 2007. 'Distinct pathways of genomic progression to benign and malignant tumors of the liver', *PNAS*, 104: 14771-6.

Uhlen, M., L. Fagerberg, B. M. Hallstrom, C. Lindskog, P. Oksvold, A. Mardinoglu, A. Sivertsson, C. Kampf, E. Sjostedt, A. Asplund, I. Olsson, K. Edlund, E. Lundberg, S. Navani, C. A. Szigyarto, J. Odeberg, D. Djureinovic, J. O. Takanen, S. Hober, T. Alm, P. H. Edqvist, H. Berling, H. Tegel, J. Mulder, J. Rockberg, P. Nilsson, J. M. Schwenk, M. Hamsten, K. von Feilitzen, M. Forsberg, L. Persson, F. Johansson, M. Zwahlen, G. von Heijne, J. Nielsen, and F. Ponten. 2015. 'Proteomics. Tissue-based map of the human proteome', *Science*, 347: 1260419.

Uysal-Onganer, P., and R. M. Kypta. 2012. 'Wnt11 in 2011 - the regulation and function of a non-canonical Wnt', *Acta Physiol (Oxf)*, 204: 52-64.

Valencia, C. A., W. Ju, and R. Liu. 2007. 'Matrin 3 is a Ca2+/calmodulin-binding protein cleaved by caspases', *Biochem Biophys Res Commun*, 361: 281-6.

Van Woensel, Matthias, Thomas Mathivet, Nathalie Wauthoz, Rémi Rosière, Abhishek D. Garg, Patrizia Agostinis, Véronique Mathieu, Robert Kiss, Florence Lefranc, Louis Boon, Jochen Belmans, Stefaan W. Van Gool, Holger Gerhardt, Karim Amighi, and Steven De Vleeschouwer. 2017. 'Sensitization of glioblastoma tumor micro-environment to chemo- and immunotherapy by Galectin-1 intranasal knock-down strategy', *Sci Rep*, 7.

Varshavsky, A. 1996. 'The N-end rule: functions, mysteries, uses', *PNAS. USA*, 93: 12142-9.

Varshavsky, A. 2005. 'Ubiquitin fusion technique and related methods.', *Meth. Enzymol.*, 399: 777-99.

Varshavsky, A. 2011. 'The N-end rule pathway and regulation by proteolysis', *Protein Sci*, 20: 1298-345.

Varshavsky, A. 2019. 'N-degron and C-degron pathways of protein degradation', *PNAS*, 116: 358-66.

Vigano, E., C. E. Diamond, R. Spreafico, A. Balachander, R. M. Sobota, and A. Mortellaro. 2015. 'Human caspase-4 and caspase-5 regulate the one-step non-canonical inflammasome activation in monocytes', *Nat Commun*, 6: 8761.

Vocelle, D., C. Chan, and S. P. Walton. 2020. 'Endocytosis controls siRNA efficiency: implications for siRNA delivery vehicle design and cell-specific targeting', *Nucleic Acid Ther*, 30: 22-32.

Vogel, A., and A. Saborowski. 2020. 'Current strategies for the treatment of intermediate and advanced hepatocellular carcinoma', *Cancer Treat Rev*, 82: 101946.

Wadas, B., J. Borjigin, Z. Huang, J. H. Oh, C. S. Hwang, and A. Varshavsky. 2016. 'Degradation of serotonin N-Acetyltransferase, a circadian regulator, by the N-end rule rathway', *J Biol Chem*, 291: 17178-96.

Walsh, C., K. Ou, N. M. Belliveau, T. J. Leaver, A. W. Wild, J. Huft, P. J. Lin, S. Chen, A. K. Leung, J. B. Lee, C. L. Hansen, R. J. Taylor, E. C. Ramsay, and P. R. Cullis. 2014. 'Microfluidic-based manufacture of siRNA-lipid nanoparticles for therapeutic applications', *Drug Delivery System, 2nd Edition*, 1141: 109-20.

Wang, H. W., C. Noland, B. Siridechadilok, D. W. Taylor, E. Ma, K. Felderer, J. A. Doudna, and E. Nogales. 2009. 'Structural insights into RNA processing by the human RISC-loading complex', *Nat Struct Mol Biol*, 16: 1148-53.

Wang, J., X. Zhao, L. Jin, G. Wu, and Y. Yang. 2017. 'UBR5 contributes to colorectal cancer progression by destabilizing the tumor suppressor ECRG4', *Dig Dis Sci*, 62: 2781-89.

Wang, L., H. Fu, G. Nanayakkara, Y. Li, Y. Shao, C. Johnson, J. Cheng, W. Y. Yang, F. Yang, M. Lavallee, Y. Xu, X. Cheng, H. Xi, J. Yi, J. Yu, E. T. Choi, H. Wang, and X. Yang. 2016. 'Novel extracellular and nuclear caspase-1 and inflammasomes propagate inflammation and regulate gene expression: a comprehensive database mining study', *J Hematol Oncol*, 9: 122.

Wang, Q., W. R. Huang, W. Y. Chih, K. P. Chuang, C. D. Chang, Y. Wu, Y. Huang, and H. J. Liu. 2019. 'Cdc20 and molecular chaperone CCT2 and CCT5 are required for the Muscovy duck reovirus p10.8-induced cell cycle arrest and apoptosis', *Vet Microbiol*, 235: 151-63.

Wang, X., G. Li, S. Koul, R. Ohki, M. Maurer, A. Borczuk, and B. Halmos. 2018. 'PHLDA2 is a key oncogene-induced negative feedback inhibitor of EGFR/ErbB2 signaling via interference with AKT signaling', *Oncotarget*, 9: 24914-26.

Weitzer, S., and J. Martinez. 2007. 'The human RNA kinase hClp1 is active on 3' transfer RNA exons and short interfering RNAs', *Nature*, 447: 222-6.

Weledji, E. P., G. Enow Orock, M. N. Ngowe, and D. S. Nsagha. 2014. 'How grim is hepatocellular carcinoma?', *Ann Med Surg (Lond)*, 3: 71-6.

Wellington, C. L., L. M. Ellerby, A. S. Hackam, R. L. Margolis, M. A. Trifiro, R. Singaraja, K. McCutcheon, G. S. Salvesen, S. S. Propp, M. Bromm, K. J. Rowland, T. Zhang, D. Rasper, S. Roy, N. Thornberry, L. Pinsky, A. Kakizuka, C. A. Ross, D. W. Nicholson, D. E. Bredesen, and M. R. Hayden. 1998. 'Caspase cleavage of gene products associated with triplet expansion disorders generates truncated fragments containing the polyglutamine tract', *J Biol Chem*, 273: 9158-67.

Wensink, A. C., C. E. Hack, and N. Bovenschen. 2015. 'Granzymes regulate proinflammatory cytokine responses', *J Immunol*, 194: 491-7.

Whitehead, K. A., J. E. Dahlman, R. S. Langer, and D. G. Anderson. 2011. 'Silencing or stimulation? siRNA delivery and the immune system', *Annu Rev Chem Biomol Eng*, 2: 77-96.

Whitehead, K. A., J. R. Dorkin, A. J. Vegas, P. H. Chang, O. Veiseh, J. Matthews, O. S. Fenton, Y. Zhang, K. T. Olejnik, V. Yesilyurt, D. Chen, S. Barros, B. Klebanov, T. Novobrantseva, R. Langer, and D. G. Anderson. 2014. 'Degradable lipid nanoparticles with predictable in vivo siRNA delivery activity', *Nat Commun*, 5: 4277.

Whitehead, Kathryn A., Robert Langer, and Daniel G. Anderson. 2009. 'Knocking down barriers: advances in siRNA delivery', *Nature Reviews Drug Discovery*, 8: 129-38.

Wickham, H. 2017. 'R Package "Tidyverse" for R: Easily Install and Load the "Tidyverse"', *R Package Version 1.2.1*, R Core Team: Vienna, Austria.

Williams, S. P., A. S. Barthorpe, H. Lightfoot, M. J. Garnett, and U. McDermott. 2017. 'High-throughput RNAi screen for essential genes and drug synergistic combinations in colorectal cancer', *Sci Data*, 4: 170139.

Wilson, R. C., and J. A. Doudna. 2013. 'Molecular mechanisms of RNA interference', *Annu Rev Biophys*, 42: 217-39.

Wu, S. Y., X. Yang, K. M. Gharpure, H. Hatakeyama, M. Egli, M. H. McGuire, A. S. Nagaraja, T. M. Miyake, R. Rupaimoole, C. V. Pecot, M. Taylor, S. Pradeep, M. Sierant, C. Rodriguez-Aguayo, H. J. Choi, R. A. Previs, G. N. Armaiz-Pena, L. Huang, C. Martinez, T. Hassell, C. Ivan, V. Sehgal, R. Singhania, H. D. Han, C. Su, J. H. Kim, H. J. Dalton, C. Kovvali, K. Keyomarsi, N. A. McMillan, W. W. Overwijk, J. Liu, J. S. Lee, K. A. Baggerly, G. Lopez-Berestein, P. T. Ram, B. Nawrot, and A. K. Sood. 2014. '2'-OMe-phosphorodithioate-modified siRNAs show increased loading into the RISC complex and enhanced anti-tumour activity', *Nat Commun*, 5: 3459.

Xia, J., A. Noronha, I. Toudjarska, F. Li, A. Akinc, R. Braich, M. Frank-Kamenetsky, K. G. Rajeev, M. Egli, and M. Manoharan. 2006. 'Gene silencing activity of siRNAs with a ribo-difluorotoluyl nucleotide', *ACS Chem Biol*, 1: 176-83.

Xia, Z., A. Webster, F. Du, K. Piatkov, M. Ghislain, and A. Varshavsky. 2008. 'Substrate-binding sites of UBR1, the ubiquitin ligase of the N-end rule pathway', *J Biol Chem*, 283: 24011-28.

Xie, Y., and A. Varshavsky. 1999. 'The E2-E3 interaction in the N-end rule pathway: the RING-H2 finger of E3 is required for the synthesis of multiubiquitin chain.', *EMBO J.*, 18: 6832-44.

Xie, Y., D. W. Wolff, T. Wei, B. Wang, C. Deng, J. K. Kirui, H. Jiang, J. Qin, P. W. Abel, and Y. Tu. 2009. 'Breast cancer migration and invasion depend on proteasome degradation of regulator of G-Protein Signaling 4', *Cancer Research*, 69: 5743-51.

Xie, Z. D., H. Liang, J. M. Wang, X. W. Xu, Y. Zhu, A. Z. Guo, X. Shen, F. Cao, and W. J. Chang. 2017. 'Significance of the E3 ubiquitin protein UBR5 as an oncogene and a prognostic biomarker in colorectal cancer', *Oncotarget*, 8: 108079-92.

Xu, Hao, Jianjin Shi, Hang Gao, Ying Liu, Zhenxiao Yang, Feng Shao, and Na Dong. 2019. 'The N-end rule ubiquitin ligase UBR2 mediates NLRP1B inflammasome activation by anthrax lethal toxin', *The EMBO Journal*: e101996.

Xu, Z., R. Payoe, and R. P. Fahlman. 2012. 'The C-terminal proteolytic fragment of the breast cancer susceptibility type 1 protein (BRCA1) is degraded by the N-end rule pathway', *J Biol Chem*, 287: 7495-502.

Yamazaki, T., T. Akada, O. Niizeki, T. Suzuki, H. Miyashita, and Y. Sato. 2004. 'Puromycin-insensitive leucyl-specific aminopeptidase (PILSAP) binds and catalyzes PDK1, allowing VEGF-stimulated activation of S6K for endothelial cell proliferation and angiogenesis', *Blood*, 104: 2345-52.

Yan, K. S., S. Yan, A. Farooq, A. Han, L. Zeng, and M. M. Zhou. 2003. 'Structure and conserved RNA binding of the PAZ domain', *Nature*, 426: 468-74.

Yan, X., F. Kuipers, L. M. Havekes, R. Havinga, B. Dontje, K. Poelstra, G. L. Scherphof, and J. A. Kamps. 2005. 'The role of apolipoprotein E in the elimination of liposomes from blood by hepatocytes in the mouse', *Biochem Biophys Res Commun*, 328: 57-62.

Yang, J. D., P. Hainaut, G. J. Gores, A. Amadou, A. Plymoth, and L. R. Roberts. 2019. 'A global view of hepatocellular carcinoma: trends, risk, prevention and management', *Nat Rev Gastroenterol Hepatol*, 16: 589-604.

Yang, M., N. Jiang, Q. W. Cao, M. Q. Ma, and Q. Sun. 2016. 'The E3 ligase UBR5 regulates gastric cancer cell growth by destabilizing the tumor suppressor GKN1', *Biochem Biophys Res Commun*, 478: 1624-9.

Yang, M., Y. Zhang, and J. Ren. 2018. 'Autophagic regulation of lipid homeostasis in cardiometabolic syndrome', *Front Cardiovasc Med*, 5: 38.

Yang, X., M. Sierant, M. Janicka, L. Peczek, C. Martinez, T. Hassell, N. Li, X. Li, T. Wang, and B. Nawrot. 2012. 'Gene silencing activity of siRNA molecules containing phosphorodithioate substitutions', *ACS Chem Biol*, 7: 1214-20.

Ye, Y., and M. Rape. 2009. 'Building ubiquitin chains: E2 enzymes at work', *Nat Rev Mol Cell Biol*, 10: 755-64.

Yoo, Y. D., S. R. Mun, C. H. Ji, K. W. Sung, K. Y. Kang, A. J. Heo, S. H. Lee, J. Y. An, J. Hwang, X. Q. Xie, A. Ciechanover, B. Y. Kim, and Y. T. Kwon. 2018. 'N-terminal arginylation generates a bimodal degron that modulates autophagic proteolysis', *PNAS. USA*, 115: E2716-E24.

Zamanian-Daryoush, M., J. T. Marques, M. P. Gantier, M. A. Behlke, M. John, P. Rayman, J. Finke, and B. R. Williams. 2008. 'Determinants of cytokine induction by small interfering RNA in human peripheral blood mononuclear cells', *J Interferon Cytokine Res*, 28: 221-33.

Zamaratski, E., P. I. Pradeepkumar, and J. Chattopadhyaya. 2001. 'A critical survey of the structure-function of the antisense oligo/RNA heteroduplex as substrate for RNase H', *J Biochem Biophys Methods*, 48: 189-208.

Zamore, Phillip D., Thomas Tuschl, Phillip A. Sharp, and David P. Bartel. 2000. 'RNAi: Double-stranded RNA directs the ATP-dependent cleavage of mRNA at 21 to 23 nucleotide intervals', *Cell*, 101: 25-33.

Zatsepin, T. S., Y. V. Kotelevtsev, and V. Koteliansky. 2016. 'Lipid nanoparticles for targeted siRNA delivery - going from bench to bedside', *Int J Nanomedicine*, 11: 3077-86.

Zelphati, O., and F. C. Szoka, Jr. 1996. 'Mechanism of oligonucleotide release from cationic liposomes', *Proc. Natl. Acad Sci. USA*, 93: 11493-8.

Zenker, M., J. Mayerle, M. M. Lerch, A. Tagariello, K. Zerres, P. R. Durie, M. Beier, G. Hulskamp, C. Guzman, H. Rehder, F. A. Beemer, B. Hamel, P. Vanlieferinghen, R. Gershoni-Baruch, M. W. Vieira, M. Dumic, R. Auslender, V. L. Gil-da-Silva-Lopes, S. Steinlicht, M. Rauh, S. A. Shalev, C. Thiel, A. B. Ekici, A. Winterpacht, Y. T. Kwon, A. Varshavsky, and A. Reis. 2005. 'Deficiency of UBR1, a ubiquitin ligase of the N-end rule pathway, causes pancreatic dysfunction, malformations and mental retardation (Johanson-Blizzard syndrome)', *Nature Genetics*, 37: 1345-50.

Zenker, M., J. Mayerle, A. Reis, and M. M. Lerch. 2006. 'Genetic basis and pancreatic biology of Johanson-Blizzard syndrome', *Endocrinol Metab Clin North Am*, 35: 243-53, vii-viii.

Zerial, M., and H. McBride. 2001. 'Rab proteins as membrane organizers', *Nat Rev Mol Cell Biol*, 2: 107-17.

Zhang, G., R. K. Lin, Y. T. Kwon, and Y. P. Li. 2013. 'Signaling mechanism of tumor cell-induced up-regulation of E3 ubiquitin ligase UBR2', *Faseb Journal*, 27: 2893-901.

Zhang, H., F. A. Kolb, V. Brondani, E. Billy, and W. Filipowicz. 2002. 'Human Dicer preferentially cleaves dsRNAs at their termini without a requirement for ATP', *EMBO J*, 21: 5875-85.

Zhang, H., F. A. Kolb, L. Jaskiewicz, E. Westhof, and W. Filipowicz. 2004. 'Single processing center models for human Dicer and bacterial RNase III', *Cell*, 118: 57-68.

Zhu, J., S. Liu, F. Ye, Y. Shen, Y. Tie, J. Zhu, L. Wei, Y. Jin, H. Fu, Y. Wu, and X. Zheng. 2015. 'Long noncoding RNA MEG3 interacts with p53 protein and regulates partial p53 target genes in hepatoma cells', *PLoS One*, 10: e0139790.

Zieger, K., J. Weiner, K. Krause, M. Schwarz, M. Kohn, M. Stumvoll, M. Bluher, and J. T. Heiker. 2018. 'Vaspin suppresses cytokine-induced inflammation in 3T3-L1 adipocytes via inhibition of NFkappaB pathway', *Mol Cell Endocrinol*, 460: 181-88.

Zimmermann, T. S., A. C. Lee, A. Akinc, B. Bramlage, D. Bumcrot, M. N. Fedoruk, J. Harborth, J. A. Heyes, L. B. Jeffs, M. John, A. D. Judge, K. Lam, K. McClintock, L. V. Nechev, L. R. Palmer, T. Racie, I. Rohl, S. Seiffert, S. Shanmugam, V. Sood, J. Soutschek, I. Toudjarska, A. J. Wheat, E. Yaworski, W. Zedalis, V. Koteliansky, M. Manoharan, H. P. Vornlocher, and I. MacLachlan. 2006. 'RNAi-mediated gene silencing in non-human primates', *Nature*, 441: 111-4.

Zmasek, C. M., and A. Godzik. 2013. 'Evolution of the animal apoptosis network', *Cold Spring Harb Perspect Biol*, 5: a008649.

Zwicker, S., E. Hattinger, D. Bureik, A. Batycka-Baran, A. Schmidt, P. A. Gerber, S. Rothenfusser, M. Gilliet, T. Ruzicka, and R. Wolf. 2017. 'Th17 micro-milieu regulates NLRP1-dependent caspase-5 activity in skin autoinflammation', *PLoS One*, 12: e0175153.

Supplemental Table 1: List of caspase substrates important in apoptosis

Human cleavage site	Human gene symbol	Human protein symbol	Human Uniprot ID	P1' amino acid effect	Reference (PMID)	Human gene name	GOTERM_MF_DIRECT
Associated with apoptosis							
VSSDFNSD	GAPDH	G3P	P04406	destabilizing	17072346; 25859407	glyceraldehyde-3-phosphate dehydrogenase(GAPDH)	GO:0004365~glyceraldehyde-3-phosphate dehydrogenase (NAD+) (phosphorylating) activity
DDGDGGWV	ATG3	ATG3	Q9NT62	stabilizing	22644571; 26061804	autophagy related 3(ATG3)	GO:0005515~protein binding
VTNDAATI	CCT8	TCPQ	P50990	stabilizing	26285900	chaperonin containing TCP1 subunit 8 (CCT8)	GO:0005515~protein binding
DFLDNERH	PKN1	PKN1	Q16512	destabilizing	9751706	protein kinase N1(PKN1)	GO:0003682~chromatin binding
DDVDLEQV VLSDDTCS VGYDDIGG	VCP	TERA	P55072	destabilizing	27729194; 31368616	valosin containing protein(VCP)	GO:0005515~protein binding
Associated with apoptosis and cancer							
WRVDSAAT	ACP1	PPAC	P24666	stabilizing	30582224; 15021900; 22957062	acid phosphatase 1, soluble(ACP1)	GO:0003993~acid phosphatase activity
ELPDGQVI	ACTB	ACTB	P60709	stabilizing	18613816; 23266771	actin beta(ACTB)	GO:0000978~RNA polymerase II core promoter proximal region sequence-specific DNA binding
VEVDAAVT	APP	A4	P05067	stabilizing	30470613; 10409650; 10319819	amyloid beta precursor protein(APP)	GO:0003677~DNA binding
TSTDGSYK	ARNT	ARNT	P27540	stabilizing	24921657; 26909609	aryl hydrocarbon receptor nuclear translocator (ARNT)	GO:0003677~DNA binding
DEIDHAEM	ATP2B4	AT2B4	P23634	destabilizing	30352569; 19755660; 22733819	ATPase plasma membrane Ca2+ transporting 4(ATP2B4)	GO:0005388~calcium-transporting ATPase activity
NDTDANPR IQADSGPI	CASP7	CASP7	P55210	stabilizing	19782763; 23979156	caspase 7(CASP7)	GO:0004190~aspartic-type endopeptidase activity
DLRDDPST	CDC42	CDC42	P60953	destabilizing	11278572	cell division cycle 42(CDC42)	GO:0003924~GTPase activity
HESDFSGV	CDC5L	CDC5L	Q99459	destabilizing	26490980; 31897231; 18567798	cell division cycle 5 like(CDC5L)	GO:0000981~RNA polymerase II transcription factor activity

Human cleavage site	Human gene symbol	Human protein symbol	Human Uniprot ID	P1′ amino acid effect	Reference (PMID)	Human gene name	GOTERM_MF_DIRECT
TFADGVPR EYLDATGG	CHD4	CHD4	Q14839	stabilizing	30872624; 29888111; 29599201	chromodomain helicase DNA binding protein 4(CHD4)	GO:0000978~RNA polymerase II core promoter proximal region sequence-specific DNA binding
SGVDIGVK	CNN2	CNN2	Q99439	destabilizing	29333089, 28714360; 28714360	calponin 2(CNN2)	GO:0003779~actin binding
TDLDGFPD	COMP	COMP	P49747	stabilizing	29228690	cartilage oligomeric matrix protein(COMP)	GO:0002020~protease binding
ESVDSVTD	CREB1	CREB1	P16220	stabilizing	30021350; 10493936; 17786359; 16084096	cAMP responsive element binding protein 1(CREB1)	GO:0000978~RNA polymerase II core promoter proximal region sequence-specific DNA binding
SYLDSGIH	CTNNB1	CTNB1	P35222	stabilizing	28430641; 27105607	catenin beta 1(CTNNB1)	GO:0001085~RNA polymerase II transcription factor binding
IDYDGSGS	DGKA	DGKA	P23743	destabilizing	26420856; 28316970; 30536880; 15870081	diacylglycerol kinase alpha(DGKA)	GO:0004143~diacylglycerol kinase activity
DHPDADKT	DICER1	DICER	Q9UPY3	stabilizing	27314098; 25558471; 18289125	dicer 1, ribonuclease III(DICER1)	GO:0003725~double-stranded RNA binding
YEVDGRDY	DLG1	DLG1	Q12959	stabilizing	16511562; 24142560	discs large MAGUK scaffold protein 1(DLG1)	GO:0004385~guanylate kinase activity
EIVDSFDD	EIF4A1	IF4A1	P60842	stabilizing	25611378; 28466778: 29163714	eukaryotic translation initiation factor 4A1(EIF4A1)	GO:0000339~RNA cap binding
HHGDGPGN	FUBP1	FUBP1	Q96AE4	stabilizing	31553912; 22926519; 28076379; 26925132	far upstream element binding protein 1(FUBP1)	GO:0003697~single-stranded DNA binding
NAADAFDI	GRK2	ARBK1	P25098	stabilizing	28572156; 31554835	G protein-coupled receptor kinase 2(GRK2)	GO:0004672~protein kinase activity
SREDSQRP	HNRNPA1	ROA1	P09651	stabilizing	29484423; 28791797; 22345078	heterogeneous nuclear ribonucleoprotein A1(HNRNPA1)	GO:0000166~nucleotide binding

Human cleavage site	Human gene symbol	Human protein symbol	Human Uniprot ID	P1′ amino acid effect	Reference (PMID)	Human gene name	GOTERM_MF_DIRECT
VDSDDLPL WESDSNEF VIADPRGN	HSP90B1	ENPL	P14625	destabilizing stabilizing stabilizing	19724918	heat shock protein 90 beta family member 1(HSP90B1)	GO:0003723~RNA binding
DKVDWVQC	KDM5A	KDM5A	P29375	destabilizing	22937203; 28714030	lysine demethylase 5A(KDM5A)	GO:0003677~DNA binding
ECLDGVPF	LIMD1	LIMD1	Q9UGP4	stabilizing	30854077;	LIM domains containing 1(LIMD1)	GO:0003714~transcription corepressor activity
DHMDRLPR	NOTCH1	NOTC1	P46531	destabilizing	15650752	notch 1(NOTCH1)	GO:0001047~core promoter binding
VEKDGLIL	PARK7	PARK7	Q99497	stabilizing	17015834; 19144925; 15983381	Parkinsonism associated deglycase(PARK7)	GO:0001047~core promoter binding
LPVDFVTA	PGK1	PGK1	P00558	destabilizing	28749413; 25867275; 19180641	phosphoglycerate kinase 1(PGK1)	GO:0004618~phosphoglycerate kinase activity
VICDSYVR	PHF5A	PHF5A	Q7RTV0	stabilizing	30932358; 29700004	PHD finger protein 5A (PHF5A)	GO:0003677~DNA binding
VFLDPNIL	PREP	PPCE	P48147	stabilizing	16700513; 24465166; 24936056	prolyl endopeptidase (PREP)	GO:0004252~serine-type endopeptidase activity
TELDMDDG	PRPSAP1	KPRA	Q14558	stabilizing	29541198	phosphoribosyl pyrophosphate synthetase associated protein 1 (PRPSAP1)	GO:0000287~magnesium ion binding
DLVDGRHS	PRPSAP2	KPRB	O60256	stabilizing	31956349	phosphoribosyl pyrophosphate synthetase associated protein 2(PRPSAP2)	GO:0000287~magnesium ion binding
DLRDDKDT	RAC1	RAC1	P63000	destabilizing	15226424; 12897143	ras-related C3 botulinum toxin substrate 1 (rho family, small GTP binding protein Rac1)(RAC1)	GO:0003924~GTPase activity
AIMDGTEI	RING1	RING1	Q06587	stabilizing	29187402; 26141041	ring finger protein 1(RING1)	GO:0003682~chromatin binding
AITDGLEI	RNF2	RING2	Q99496	stabilizing	23318437; 26450788; 23319651	ring finger protein 2(RNF2)	GO:0003682~chromatin binding
SDIDSSNF	ROCK2	ROCK2	O75116	stabilizing	17347801; 27921230	Rho associated coiled-coil containing protein kinase 2 (ROCK2)	GO:0004674~protein serine/threonine kinase activity
TPVDSPDD	RPS6KB1	KS6B1	P23443	stabilizing	27491285;	ribosomal protein S6 kinase B1	GO:0004672~protein kinase activity

Human cleavage site	Human gene symbol	Human protein symbol	Human Uniprot ID	P1' amino acid effect	Reference (PMID)	Human gene name	GOTERM_MF_DIRECT
					31387554	(RPS6KB1)	
DEYDYSKP	SDHA	SDHA	P31040	destabilizing	2901140	succinate dehydrogenase complex flavoprotein subunit A(SDHA)	GO:0000104~succinate dehydrogenase activity
LTVDGFTD	SMAD2	SMAD2	Q15796	stabilizing	19276350; 17960585	SMAD family member 2(SMAD2)	GO:0000978~RNA polymerase II core promoter proximal region sequence-specific DNA binding
MTVDGFTD	SMAD3	SMAD3	P84022	stabilizing	9796704; 17725494	SMAD family member 3(SMAD3)	GO:0000977~RNA polymerase II regulatory region sequence-specific DNA binding
DEVDAALD	SMC2	SMC2	O95347	stabilizing	21151026; 23319142; 24553121	structural maintenance of chromosomes 2(SMC2)	GO:0005515~protein binding
RKLDNTKF	SRSF1	SRSF1	Q07955	destabilizing	30429088; 22245967	serine and arginine rich splicing factor 1(SRSF1)	GO:0000166~nucleotide binding
ITPDGADV	USP13	UBP13	Q92995	stabilizing	31200745; 28569838	ubiquitin specific peptidase 13 (isopeptidase T-3)(USP13)	GO:0004197~cysteine-type endopeptidase activity
VDSDGRPD ETVDSDGR	USP19	UBP19	O94966	stabilizing	21849505; 25444757; 27517492; 21264218	ubiquitin specific peptidase 19 (USP19)	GO:0004843~thiol-dependent ubiquitin-specific protease activity
TSIDAHNG	VRK1	VRK1	Q99986	stabilizing	29103766; 21386980; 21346188; 30180179	vaccinia related kinase 1(VRK1)	GO:0004672~protein kinase activity
					Associated with cancer		
DIVDRGST	ADD1	ADDA	P35611	destabilizing	28476036	adducin 1(ADD1)	GO:0003779~actin binding
EGTDSYEL	ATP6V1D	VATD	Q9Y5K8	stabilizing	24155661	ATPase H+ transporting V1 subunit D(ATP6V1D)	GO:0005515~protein binding
LPYDQSTW	CHD3	CHD3	Q12873	destabilizing	25333848	chromodomain helicase DNA binding protein 3(CHD3)	GO:0003677~DNA binding
LDADGGPL	CPNE1	CPNE1	Q99829	destabilizing	29970127; 29151113; 29207139	copine 1(CPNE1)	GO:0001786~phosphatidylserine binding
IITDGVIT	CPNE3	CPNE3	O75131	stabilizing	20010870	copine 3(CPNE3)	GO:0004674~protein serine/threonine kinase activity
DEVDRKPE	CSTF3	CSTF3	Q12996	destabilizing	27758885	cleavage stimulation factor subunit 3(CSTF3)	GO:0003723~RNA binding

Human cleavage site	Human gene symbol	Human protein symbol	Human Uniprot ID	P1' amino acid effect	Reference (PMID)	Human gene name	GOTERM_MF_DIRECT
VDKDGLLD	EHD1	EHD1	Q9H4M9	stabilizing	29549343	EH domain containing 1(EHD1)	GO:0005509~calcium ion binding
SDVDGVTC	FBLN1	FBLN1	P23142	stabilizing	25234557; 17483339	fibulin 1(FBLN1)	GO:0001968~fibronectin binding
GVVDSEDL	HSP90AB1	HS90B	P08238	stabilizing	26358502; 30305727	heat shock protein 90 alpha family class B member 1(HSP90AB1)	GO:0001948~glycoprotein binding
ISPDSGGL	KHSRP	FUBP2	Q92945	stabilizing	31404541, 27644194,	KH-type splicing regulatory protein (KHSRP)	GO:0003677~DNA binding
DETDRDII	MACF1	MACF1	Q9UPN3	destabilizing	28782898	microtubule-actin crosslinking factor 1(MACF1)	GO:0003779~actin binding
FDPDDPNT	MAGI1	MAGI1	Q96QZ7	destabilizing	21666716	membrane associated guanylate kinase, WW and PDZ domain containing 1(MAGI1)	GO:0005515~protein binding
DEPDAFKE	P4HA1	P4HA1	P13674	stabilizing	30367042	prolyl 4-hydroxylase subunit alpha 1(P4HA1)	GO:0004656~procollagen-proline 4-dioxygenase activity
SHCDSDKG	RBBP7	RBBP7	Q16576	stabilizing	30546458	RB binding protein 7, chromatin remodeling factor (RBBP7)	GO:0003723~RNA binding
VMPDLYFY	RPSA	RSSA	P08865	destabilizing	30894280	ribosomal protein SA(RPSA)	GO:0001618~virus receptor activity
DLPDGGHL	SHMT2	GLYM	P34897	stabilizing	29180469	serine hydroxymethyltransferase 2(SHMT2)	GO:0003682~chromatin binding
DSTDSYIE	SUPT6H	SPT6H	Q7KZ85	stabilizing	24441044	SPT6 homolog, histone chaperone(SUPT6H)	GO:0000991~transcription factor activity
GGDDSFNT	TUBA1B	TBA1B	P68363	stabilizing	23625295	tubulin alpha 1b(TUBA1B)	GO:0003725~double-stranded RNA binding
TLPDGKQV	TARS	SYTC	P26639	stabilizing	25163878;	threonyl-tRNA synthetase (TARS)	GO:0003723~RNA binding
MEVDGDVE	TBL1XR1	TBL1R	Q9BZK7	stabilizing	26069883; 24667177	transducin beta like 1 X-linked receptor 1(TBL1XR1)	GO:0003714~transcription corepressor activity
SRYDSDGD	TLE3	TLE3	Q04726	stabilizing	27669982,	transducin like enhancer of split 3(TLE3)	GO:0005515~protein binding
DEVDSLCG	VPS4A	VPS4A	Q9UN37	stabilizing	27275493	vacuolar protein sorting 4 homolog A(VPS4A)	GO:0005515~protein binding
New candidate: unknown role in apoptosis or cancer							
TVTDFMAQ	GFM2	RRF2M	Q969S9	destabilizing		G elongation factor mitochondrial 2(GFM2)	GO:0003746~translation elongation factor activity
ELPDGQVI	ACTBL2	ACTBL	Q562R1	stabilizing	27989943;	actin, beta like 2(ACTBL2)	GO:0005515~protein binding
ELPDGQVI	ACTG1	ACTG	P63261	stabilizing		actin gamma 1(ACTG1)	GO:0005200~structural constituent of cytoskeleton

Human cleavage site	Human gene symbol	Human protein symbol	Human Uniprot ID	P1' amino acid effect	Reference (PMID)	Human gene name	GOTERM_MF_DIRECT
LESDMSNG	ATXN2L	ATX2L	Q8WWM7	stabilizing		ataxin 2 like(ATXN2L)	GO:0005515~protein binding
VDKDGDVT	CCT5	TCPE	P48643	stabilizing	16981251; 28969060; 16821082	chaperonin containing TCP1 subunit 5(CCT5)	GO:0005515~protein binding
CDCDGMLD	EHD4	EHD4	Q9H223	stabilizing		EH domain containing 4(EHD4)	GO:0003676~nucleic acid binding
YGKDATNV	ENO1	ENOA	P06733	stabilizing		enolase 1(ENO1)	GO:0000287~magnesium ion binding
YGKDATNV	ENO3	ENOB	P13929	stabilizing		enolase 3(ENO3)	GO:0000287~magnesium ion binding
VGPDGKEL	ESS2	ESS2	Q96DF8	stabilizing		DiGeorge syndrome critical region gene 14(DGCR14)	GO:0005515~protein binding
SREDSVKP	HNRNPA3	ROA3	P51991	stabilizing		heterogeneous nuclear ribonucleoprotein A3(HNRNPA3)	GO:0000166~nucleotide binding
VGYDAMAG	HSPD1	CH60	P10809	stabilizing		heat shock protein family D (Hsp60) member 1(HSPD1)	GO:0001530~lipopolysaccharide binding
DRVDAVLV	MAP1S	MAP1S	Q66K74	stabilizing		microtubule associated protein 1S(MAP1S)	GO:0003677~DNA binding
HEADTANM	NAA15	NAA15	Q9BXJ9	stabilizing		N(alpha)-acetyltransferase 15, NatA auxiliary subunit(NAA15)	GO:0004596~peptide alpha-N-acetyltransferase activity
KKEDGTFY	NARS	SYNC	O43776	stabilizing		asparaginyl-tRNA synthetase (NARS)	GO:0003676~nucleic acid binding
TGIDSEYE	PAPSS1	PAPS1	O43252	stabilizing		3'-phosphoadenosine 5'-phosphosulfate synthase 1(PAPSS1)	GO:0004020~adenylylsulfate kinase activity
DSPDYDRR	PHACTR2	PHAR2	O75167	destabilizing		phosphatase and actin regulator 2 (PHACTR2)	GO:0003779~actin binding
ELPDGQVI	POTEF	POTEF	A5A3E0	stabilizing		POTE ankyrin domain family member F (POTEF)	NA
QEEDGANI	PSMC3	PRS6A	P17980	stabilizing		proteasome 26S subunit, ATPase 3 (PSMC3)	GO:0003713~transcription coactivator activity
DILDPALL							
LTVDSAHL	QRICH1	QRIC1	Q2TAL8	stabilizing		glutamine rich 1 (QRICH1)	GO:0000981~RNA polymerase II transcription factor activity
SNSDGTRP	RBM22	RBM22	Q9NW64	stabilizing		RNA binding motif protein 22(RBM22)	GO:0000166~nucleotide binding
ERTDASSA	RBM39	RBM39	Q14498	stabilizing		RNA binding motif protein 39(RBM39)	GO:0000166~nucleotide binding
DEVDGMAG	RFC1	RFC1	P35251	stabilizing	6129478	replication factor C subunit 1(RFC1)	GO:0003677~DNA binding
VTWDGHSG	SF3A1	SF3A1	Q15459	stabilizing		splicing factor 3a subunit 1(SF3A1)	GO:0003723~RNA binding
QELDSTDG	SRP54	SRP54	P61011	stabilizing		signal recognition particle 54(SRP54)	GO:0003924~GTPase activity
VKCDPRHG	TUBA3C	TBA3C	P0DPH7	stabilizing		tubulin alpha 3c(TUBA3C)	GO:0003924~GTPase activity

Human cleavage site	Human gene symbol	Human protein symbol	Human Uniprot ID	P1′ amino acid effect	Reference (PMID)	Human gene name	GOTERM_MF_DIRECT
TVFDGRPI	TBL1X	TBL1X	O60907	stabilizing		transducin beta like 1X-linked(TBL1X)	GO:0003714~transcription corepressor activity
MEIDGDVE	TBL1Y	TBL1Y	Q9BQ87	stabilizing		transducin beta like 1, Y-linked(TBL1Y)	GO:0003714~transcription corepressor activity
IQPDGQMP	TUBA4A	TBA4A	P68366	stabilizing		tubulin alpha 4a(TUBA4A)	GO:0003924~GTPase activity
VYIDARDE	ZC3H15	ZC3HF	Q8WU90	stabilizing		zinc finger CCCH-type containing 15(ZC3H15)	GO:0005515~protein binding